Trinity College Dublin
Coláiste na Tríonóide, Baile Átha Cliath
The University of Dublin

p53-regulated SESN1 and SESN2 regulate cell proliferation and cell death through control of STAT3

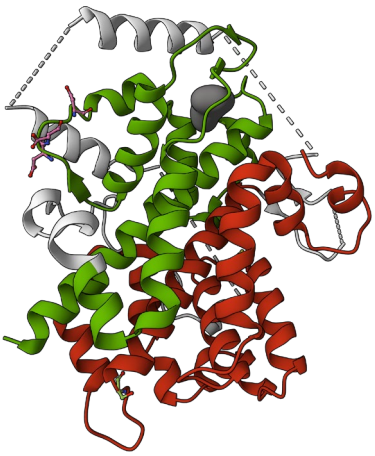

Thesis submitted to the

University of Dublin

for the degree of

Doctor in Philosophy

Alexander Haidurov

Supervisor:

Prof. Andrei Budanov

School of Biochemistry and Immunology, Trinity College Dublin

March 2024

DECLARATION

I declare that this thesis has not been submitted as an exercise for a degree at this or any other university and it is entirely my own work.

I agree to deposit this thesis in the University's open access institutional repository or allow the Library to do so on my behalf, subject to Irish Copyright Legislation and Trinity College Library conditions of use and acknowledgement.

I consent to the examiner retaining a copy of the thesis beyond the examining period, should they so wish (EU GDPR May 2018).

_____

Alexander Haidurov

March 2024

SUMMARY

Sestrins (SESN1-3), evolutionarily conserved across species from roundworms to humans, are stress-responsive proteins known for their central roles in cellular stress and homeostasis regulation. The conservation of Sestrins across the animal kingdom, from the simplicity of roundworms to the complexity of humans, testifies to their fundamental importance. Initially identified as a target of p53, a critical protein for maintaining genome stability, Sestrins have since been recognised for their response to a diverse array of stresses, including oxidative, ER, and metabolic stresses, mediated through transcription factors like FOXOs, Nrf2, ATF4, and HIF-1. Their conservation and wide-ranging response to cellular stress highlight their critical role in cellular biology.

Sestrins' three core functions are underscored by their structure. As antioxidants, they utilise a catalytic cysteine within their Sesn-A domain to neutralise oxidative stress. They also act as potent inhibitors of the mTORC1 complex. Through their Sesn-C domain, they use the 'DDYDY' motif for interactions with GATOR2, leading to mTORC1's inhibition. Additionally, Sestrins function as leucine sensors; their interaction with leucine disrupts the binding to GATOR2, thereby modulating mTORC1's activity based on leucine availability. These three functions illustrate Sestrins' versatile role in managing cellular responses to nutritional and stress signals.

Sestrins' diverse functions and widespread expression across most tissues have a complex impact on physiological processes. They counteract oxidative stress and inhibit anabolic metabolism, thus protecting against ageing and metabolic dysfunction. In contrast, within oncogenic contexts, notably lung carcinoma, Sestrins were shown to trigger cell death, serving a critical function in the removal of potentially malignant cells. This highlights the context-sensitive nature of Sestrin activity, demonstrating their capacity to maintain cellular integrity or induce apoptosis, dependent on specific cellular conditions and tissue context.

Cancer significantly impacts global health, being a significant cause of mortality. In Ireland, for example, cancer accounted for 28% of all deaths in 2021, outpacing cardiovascular diseases and respiratory issues. In 2020, it was estimated that 20% of individuals will develop cancer in their lifetime. Lung cancer, in particular, represents the most diagnosed cancer type and the leading cause of cancer deaths. Despite advances in therapeutic strategies, traditional chemotherapies remain central in cancer management, although drug resistance poses ongoing challenges. This resistance emerges through cancer's evolutionary dynamics, involving clonal expansion, diversification, and selection, complicating treatment efforts. Investigative efforts aim to understand resistance mechanisms, with one focus being p53 and

its regulated genes such as *SESN1* and *SESN2*, especially given their low expression in p53-deficient cells.

To study p53-inducible SESN1&2 and their effect on genotoxic drug resistance in the A549 epithelial cell line derived from lung adenocarcinoma, we set out to generate SESN1&2 knockouts in this line. CRISPR/Cas9 technology was instrumental in this study, providing a stable, diverse culture of SESN1&2 knockouts, enabling us to study Sestrins in cellular signalling in novel detail. Cell cytotoxicity assays were conducted under various conditions to investigate the impact of SESN1&2 on cell survival. Another method employed in this research was Western Blotting, which enabled us to study cellular signalling by examining key protein phosphorylation and expression levels. RNAseq and comparative PCR analysis were utilised to discover gene expression changes in SESN1&2 knockouts, which were used to identify critical genes in our investigation. Using molecular cloning techniques, we introduced specific genetic alterations, such as overexpression and RNA silencing, enabling the characterisation of the p53-SESN-mediated cell death pathway.

The inactivation of SESN1&2 led to increased resistance to cisplatin, indicating their critical role in apoptosis following DNA damage. This study confirms the essential function of p53 in SESN-induced apoptosis, showing that the absence of p53 conferred the same resistance as the absence of SESNs. Our findings suggest that Sestrins support DNA damage-induced apoptosis via STAT3 regulation. The inactivation of SESN1&2 results in increased STAT3 phosphorylation, suggesting a novel regulatory relationship. This modulation of STAT3 by SESN1&2 is independent of their interactions with the GATOR2 complex or antioxidative functions, suggesting an alternate mechanism. Importantly, JAK kinases were found necessary for STAT3 activity. However, JAK2 activation was not increased, unlike STAT3, highlighting that SESNs were implicated in regulating STAT3 phosphorylation downstream of JAK. Comprehensive RNAseq analysis identified the influence of SESN1 and SESN2 on genes within the JAK-STAT3 pathway, notably protein tyrosine phosphatase receptor type D (PTPRD), mapping out the following putative pathway: DNA damage triggers p53 activation, which in turn activates Sestrins. Sestrins support transcription of PTPRD, dephosphorylation of STAT3 and downregulation of MCL1, therefore supporting apoptosis.

This research demonstrates that SESN1 and SESN2 suppress cell proliferation and support apoptosis in A549 cells, revealing a regulatory axis involving p53, STAT3, and PTPRD, facilitated by SESN1&2. These insights contribute significantly to our understanding of Sestrins' role in cancer and suggest new directions for therapeutic intervention targeting the SESN-STAT3 axis in cancer treatment.

ACKNOWLEDGEMENTS

I am profoundly grateful to my parents, particularly my mother. Without their everyday support, this thesis and my time in university would be impossible.

Heartfelt thanks to my supervisor, Andrei Budanov, for his patience, guidance, time and support. I am very thankful for the independence, resources, and freedom of research Andrei granted me during my time in his lab. It was an incredible experience to have his experienced advice while also being able to have the freedom to learn new things.

Special appreciation is extended to Nicole McCabe Chu. Her everyday support made this project possible.

Special thanks must go to adjacent lab professors Derek Nolan and Gavin Davey, as our lab constantly utilised their equipment for everyday research. This research would not have been possible without their generous permission to use essential equipment. I also thank Barry Moran for his assistance and for running the TBSI Flow Cytometry Facility, which was instrumental in our research.

I thank Alanna Slater, Cormac Keegan and Conor Leahy for being great members of the Extension 3959 corner of the fifth floor of TBSI. Their hard work in maintaining the surrounding lab enabled success in this project. I wish them success in science and hope they find lab mates as diligent as themselves.

I want to thank Louisa Zielke, Andrea Muñoz Zamora and Maxim Nosenko for being supportive when I managed to leave the lab and visit our reading room. Thank you for listening to all my lab stories.

I thank past students Jane Cook and Cian Gargan for their moral support. Seeing them grow from students in the lab to developing their scientific careers has been very inspiring.

I thank Serhii Zheka, the ‘young’ intern at our lab, who is an inspiring figure and has become someone I would trust completely with any experiment.

I would like to thank Engelhardt Institute of Molecular Biology, Peter Chumakov’s lab and its members, who provided me with the starting place for my scientific journey and were crucial collaborators in this study.

Preface: All figures presented in this thesis were created by the author.

Contents

LIST OF ABBREVIATIONS

4E-BP	eIF4E-binding protein
4-OHT	4-hydroxytamoxifen
Abl	Tyrosine-protein kinase ABL1
AHPD	Alkyl hydroxyperoxidase D
AKT	Protein kinase B AKA Ak strain transforming
AMP	Adenosine monophosphate
AMPK	AMP-activated protein kinase
APRF	Acute-phase response factor
ARE	Antioxidant response elements
ATF4	Activating transcription factor 4
ATF6	Activating transcription factor 6
ATP	Adenosine triphosphate
BCA	Bicinchoninic Acid Assay
BCAA	Branched-Chain Amino Acids
BCL-xL	B-Cell Lymphoma-Extra Large
BPIFA1	Bactericidal/Permeability-Increasing Fold-Containing Family A, Member 1
BRCA	BReast CAncer susceptibility gene
CASTOR	Cellular arginine sensor for mTORC1
CMD	Carboxymuconolactone decarboxylase
CNF	Ciliary neurotrophic factor
c-Kit	Tyrosine-protein kinase KIT
CREB	Cyclic AMP response element-binding protein
Cryo-EM	Cryogenic electron microscopy
GM-CSF	Granulocyte-macrophage colony-stimulating factor
DDR	DNA damage response
DEN	Diethylnitrosamine
DEPC	Diethyl pyrocarbonate
DEPTOR	DEP-domain-containing mTOR-interacting protein
DKG	Dehydroascorbic acid
DKO	Double knockout
DMEM	Dulbecco's Modified Eagle Medium
DSS	Dextran sodium sulphate
DTT	Dithiothreitol
EBI	European Bioinformatics Institute
ECL	Enhanced chemiluminescence
EDTA	Ethylenediaminetetraacetic acid
EGF	Epidermal Growth Factor
EGFR	Epidermal Growth Factor receptor
EMBL	European Molecular Biology Laboratory
EPO	Erythropoietin
ERK	Extracellular signal-regulated kinase
FBS	Fetal bovine serum
FDR	False discovery rate
FERM	Four-point-one, ezrin, radixin, moesin
FITC	Fluorescein isothiocyanate
FL	Follicular lymphoma
FOXO	Forkhead box transcription factors
FRB	FKBP12–rapamycin binding
GAP	GTPase-activating protein
GATOR	GAP activity toward rags
GDP	Guanosine diphosphate
GFP	Green fluorescent protein

GSH	Glutathione
GSK-β	Glycogen synthase kinase-3 beta
GTP	Guanosine triphosphate
HEAT	Huntingtin, elongation factor 3, protein phosphatase 2A, yeast kinase TOR1
HIF	Hypoxia-inducible factor
IFN	Interferon
IGF	Insulin-like growth factor
IRES	Internal ribosome entry segments
IRS	Insulin receptor substrate
ISGF	Interferon-stimulated gene factor
ISR	Integrated stress response
JNK	c-Jun N-terminal kinase
KEAP1	Kelch-like ECH-associated protein 1
KICSTOR	complex comprising KPTN, ITFG2, C12orf66, and SZT2
LIF	Leukaemia inhibitory factor
LPS	Lipopolysaccharide
MAPK	Mitogen-activated protein kinase
MEF	Mouse embryonic fibroblasts
MIOS	Meiosis regulator for oocyte development
NAC	N-acetyl cysteine
NADH	Nicotinamide adenine dinucleotide + hydrogen
NADPH	Nicotinamide adenine dinucleotide phosphate
NCBI	National Center for Biotechnology Information
NPC	Nuclear pore complex
NSCLC	Non-small cell lung cancer
PDB	Protein Data Bank
PEI	Polyethyleneimine
PERK	Protein kinase R (PKR)-like endoplasmic reticulum kinase
PI	Propidium iodide
PIAS	Protein inhibitor of activated STAT
PIKK	Phosphatidylinositol 3-kinase-related kinase
PKA	Protein kinase A
PTPRB	Protein tyrosine phosphatase receptor type B
PTPRD	Protein tyrosine phosphatase receptor type D
PVDF	Polyvinylidene fluoride
RAGS	Ras-related GTP binding proteins
RAPTOR	Regulatory-Associated Protein of mTOR
RB	Retinoblastoma protein
RHEB	Ras Homolog Enriched in Brain
RICTOR	Rapamycin-Insensitive Companion of mTOR
RIPA	Radioimmunoprecipitation Assay
ROS	Reactive oxygen species
RSK	p90 ribosomal S6 kinase
RTE	Retrotransposable elements
SAM	S-Adenosylmethionine
SDS	Sodium dodecyl sulphate
SOCS	Suppressor of cytokine signalling
Src	Src kinase family
STAT	Signal Transducer and Activator of Transcription
TSC	Tuberous Sclerosis Complex
UPR	Unfolded protein response
UVRAG	UV radiation resistance-associated gene
VEGF	Vascular endothelial growth factor
WNT	WNT signalling pathway

1. CHAPTER 1: INTRODUCTION

1.1. DISCOVERY OF SESTRINS

1.1.1. SESTRIN1

In 1994, Buckbinder et al. screened for p53-responsive genes using a tetracycline system [1]. They discovered Sestrin1, which they termed clone A26 in their study. To them, it was unclear whether the A26 clone was a direct target of p53 as its induction by p53 was blocked by cycloheximide. Cycloheximide blocks protein synthesis in eukaryotes by hindering ribosomal translocation [2]. This implied that PA26 activation may have required a co-activating protein or was activated by an intermediary gene. Thus, they hypothesised that PA26 might be a direct target of p53, exhibiting activation kinetics similar to those observed with WAF1/CIP1/p21, but could not make a solid conclusion in 1994. Thus, a second publication from the same group was warranted in 1999 [3]. In their second publication, Velasco-Miguel and Buckbinder studied the PA26 in detail, providing expression kinetics and alternative splicing description. Still, most importantly, they identified that only isoforms T2 and T3 are upregulated by p53 and thus postulated that the p53-binding region is intragenic. Indeed, within intron 2 of the gene, they found a p53-binding site that required wild-type p53 to bind it, indicating that this gene is a direct target of p53.

1.1.2. SESTRIN2

In 2002, Budanov et al. identified a novel gene in a study that identified genes related to the hypoxic stress response [4]. Initially termed hypoxia-inducible gene 95 (Hi95), this gene is now known as Sestrin2 and is the most studied Sestrin to date. Budanov et al. highlighted that prolonged hypoxia induces this gene via oxidative stress and DNA damage. The latter stress insult activated *SESN2* in a p53-dependent manner. The gene induced apoptosis in HEK293T cells, sensitised MCF7 cells to DNA damage, yet protected them from ischemia and oxidative stress. Thus began the long road of studying this gene.

1.1.3. SESTRIN3

In early 2001, Peeters et al. submitted several hypothetical protein sequences reconstructed from expressed sequence tags and genomic sequences. They coined these sequences - the Sestrin family, inspired by the town of Sestri-Levante, where the authors ran a human genetics course. It was not until 2003 that their paper was published [5], which mapped the *SESN1, -2,-3* to chromosomes 10, 4 and 9, respectively. They offered Northern Blot and RT-qPCR analysis to show the ubiquitous expression of these genes and that the genes were expressed during early mouse embryogenesis. Most importantly, the authors displayed some evidence that Sestrins were disrupted in patients with heterotaxia. This study echoed that this family is

important in human health and disease and coined the concept of the Sestrin family, the pervasive stress mitigators.

1.2. CONSERVATION OF SESTRINS

The remarkable feature of Sestrins is that they are highly conserved across the animal kingdom and highly homologous from early appearances in roundworm *C. Elegans* to the latest human Sestrin such that the *C. elegans* and *Drosophila* orthologs were easily found using a homology search [4]. However, the origin of Sestrins in the evolutionary timeline remains elusive. A single Sestrin gene is found in invertebrates, whereas up to three Sestrin genes are observed in organisms of increasing complexity.

The current view is that Sestrins may have arisen from a precursor antioxidant enzyme as the Sestrin amino-terminal domain homologs are found in the Monera kingdom.

1.2.1. Why three SESTRINs?

Why are there three human Sestrins, whereas only one is found in simpler eukaryotes?

The current thinking regarding this topic is that this is for redundancy. While for invertebrates such as *D. melanogaster* and *C. elegans*, the loss of their single Sestrin is not lethal and does not affect their development [6, 7], *D. melanogaster* lacking dSesn demonstrate pronounced indicators of accelerated ageing, including the deterioration of cardiac and thoracic musculature, alongside the accumulation of lipids and carbohydrates, due to disrupted metabolic equilibrium [6, 8].

Inactivation of any of the three Sestrin family members in mammals typically does not result in noticeable developmental issues. This lack of observable defects is likely due to the overlapping functions of Sestrin proteins across various tissues, suggesting a compensatory mechanism that allows for normal development despite the absence of one Sestrin member [5, 9]. However, adult Sesn2 knockout mice that are subjected to a fasting/refeeding regimen or that are fed a high-fat diet develop glucose intolerance, insulin resistance, hepatosteatosis, increased activation of the mammalian target of rapamycin complex 1 (mTORC1), and accumulation of ROS [10, 11].

Observations indicate that mice with simultaneous knockout of *Sesn2* and *Sesn3* may exhibit glucose intolerance and insulin resistance patterns, even when fed a regular diet [9]. Subsequent research has shown that mice deficient in all three Sestrin genes (triple knockout, or TKO) are born under the anticipated Mendelian distribution. Nonetheless, a minimal fraction of these TKO mice reach maturity, presumably due to their inability to withstand the fasting period experienced by neonatal mammals between birth and the initiation of suckling [12].

The question surrounding the genomic emergence of multiple Sestrin variants remains a captivating mystery for the scientific community. The current hypothesis is that gene duplication events multiplied the number of Sestrins for redundancy of their benefits. The only evidence for this hypothesis to this date remains the fact that each Sestrin gene is found on a different chromosome. This genomic location of the three Sestrin genes is found in regions of synteny in humans and mice, suggesting that the emergence of multiple Sestrins occurred early in the metazoan evolutionary history [5]. Another reason for their duplication would be that they were likely found to be beneficial under conditions of different stressors, and duplication of this gene to recombine into the genome under a different promoter may have facilitated this evolutionary selection, as organisms which were able to express Sestrins to additional types of stresses may have displayed better evolutionary fitness.

1.2.2. Phylogenetic tree of the Sestrin proteins

While previous studies have shown the conservation of Sestrins across the model organisms *C. Elegans, D. Melanogaster, Xenopus Laevis* and *Danio Rerio* [13], a detailed phylogenetic study has not been performed. For this thesis, a protein phylogenetic tree of Sestrins was constructed using a similar approach as discussed in an earlier review [13]. Homologous protein sequences to the *C. Elegans* cSesn were selected using BLAST, attempting to collect one species of each genus that exhibits Sestrins. As a result, 805 proteins were picked across 404 species and presented on a single phylogenetic tree, as seen in Figure 1.

According to our tree, Sestrins could be traced back a long time, with one of the older homologs found in *Naegleria gruberi*, as a whole genome sequence of this organism has been published [14]. Though not a direct ancestor of the *Homo sapiens*, this organism was used to root our phylogenetic tree. It is estimated that humans and this free-living amoeboflagellate shared a common ancestor over a billion years ago.

For a long time, Sestrin was found as a single protein in the animal kingdom: protozoans, fungi, algae, sea corals, insects, nematodes and arachnids. All of these encode a single Sestrin product, which displays some homology with modern Sestrin1-3, especially in the functional motifs.

As animal evolution progressed, species developed the ability to express Sestrins via three distinct genes, each potentially encoding multiple isoforms. No studies comprehensively analysed this divergence, so only assumptions and hypotheses exist to explain and estimate when this happened. The common view is that invertebrates have one Sestrin, while vertebrate animals encode three. Our tree reinforces this.

Our tree revealed that Sestrin3 was the first Sestrin to have diverged from the single one, remaining more homologous to the progenitor Sestrin than Sestrin1 or -2. Our tree shows that Sestrin first diverged to develop into the modern Sestrin3 and a leucine-insensitive variant of Sestrin3 found in some birds and fish. Their non-leucine-sensing nature was inferred during the preparation of this tree as they were found to lack the residues recognised as leucine-binding in the Sestrin structure.

Sestrin3 seemed to have been duplicated and developed into Sestrin1 and 2, leaving three distinct protein products from three different genes in the vertebrate genomes.

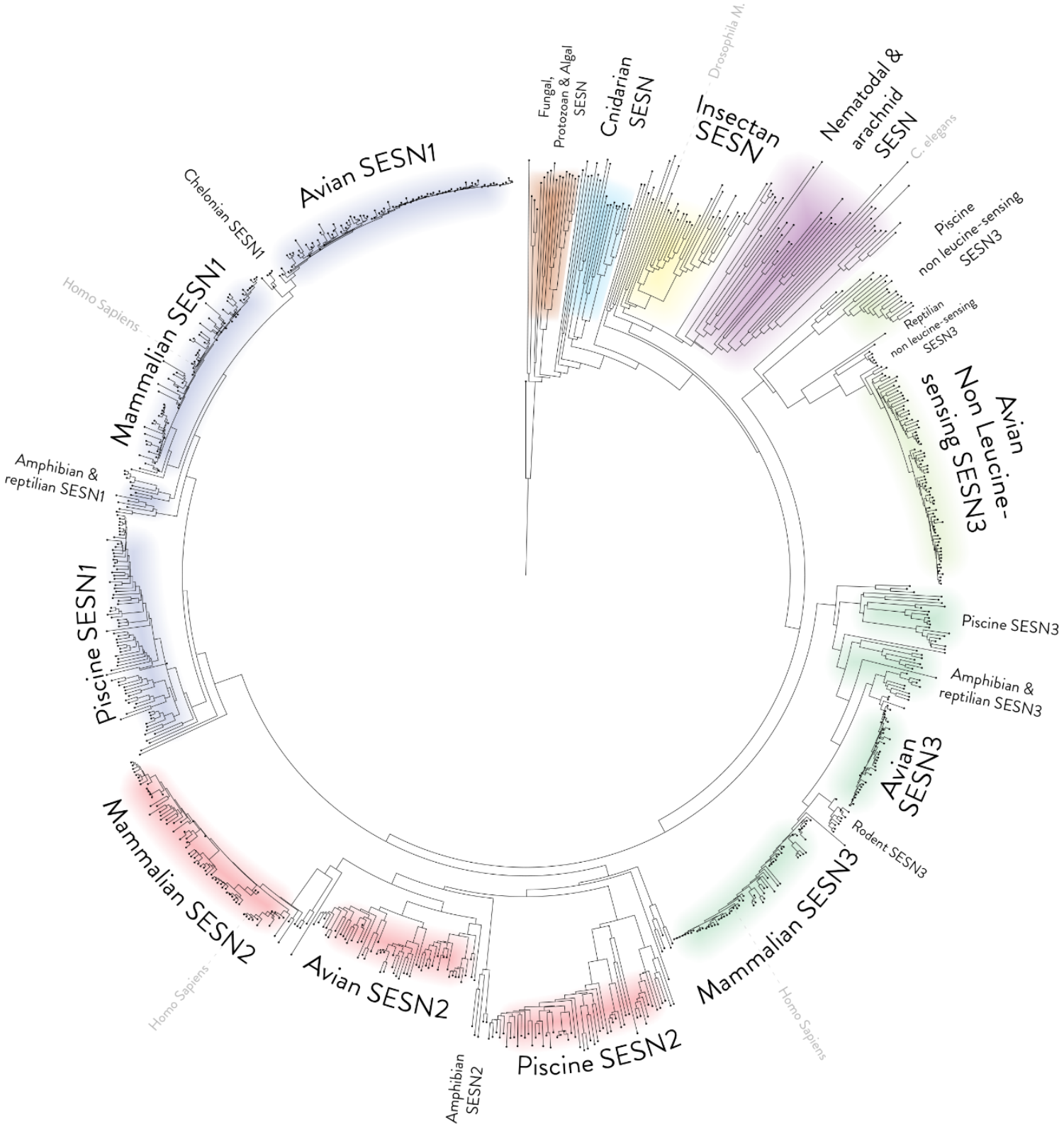

Figure 1: Phylogenetic tree based on Sestrin protein sequences
A circular phylogenetic tree based on protein alignments of Sestrin. The tree displays 805 Sestrin and Sestrin-like proteins as nodes at the tip of a leaf. Protein BLAST was used to select species with homologous proteins to the *C. Elegans* Sestrin sequence. One species of every genus was selected manually via BLAST's taxonomic display, and FASTA sequences were retrieved for each protein. A multiple sequence alignment was performed using EMBL-EBI Clustal Omega [15]. The programme was used to export the alignment as a Newick format phylogenetic tree. The file was imported into the Interactive Tree Of Life (iTOL) programme [16], and the tool was used to root the tree on the sequence of *Naegleria gruberi*, and some visual aspects of the tree were adjusted. The figure of the circular tree was exported as an image file. The tree was then annotated and coloured manually using Adobe Photoshop. As this is a protein-aligned phylogenetic tree, the distances on the tree are arbitrary. The distance from a node to the tip of a leaf represents the difference in the sequence from a previous assumed ancestor protein. E.g. all avian SESN1 seem to be highly similar, hence very close to the same line.

The antecedent Sestrins in the early animal kingdom differ substantially from each other, which is appropriate given the drastically longer time between the individual species than between vertebrate genomes. Sestrins can be neatly grouped into avian, mammalian and piscine groups. While there does not seem to be any direct function or implication to this, it is a display of divergence in evolution. This divergence of Sestrins into three distinct organisms can also be correlated with the organism's complexity. As animals evolved to be more complex, with multiple types of tissues and physiological systems, Sestrins could likely be differentially expressed.

Gene duplication is a well-described mechanism in evolutionary biology by which some organisms evolve and adapt to their environment. The mechanisms of this mode of evolution are retroposition, unequal recombination during cell division or chromosomal duplication [17]. Likely, through these mechanisms, we have inherited duplicate genes. *Homo sapiens* are claimed to have 38% of their genes in duplicate, whereas plants hold 65% duplicate genes. Bacteria range in the 17-44%. Gene duplication has been shown to be a viable mechanism for the organism to increase stress resistance, antibiotic resistance and survival [18]. For example, studies demonstrated duplication of hexose transporter in yeast in response to glucose limitation [19], gene duplication of several stress-responding genes in response to heat stress in *E. coli* [20], and that favourable agronomic qualities of domesticated crops can be attributed to gene duplication [21].

Gene duplication in mammals is a rarer event. Chromosomal duplication yields some of the worst conditions known, if not fatal [22]. Unequal recombination is a sign of genomic failure in humans, with syndromes such as Williams-Beuren Syndrome [23] and DiGeorge Syndrome [24] being examples of this. Although approximately 50% of the human genome is derived from transposable element sequences [25], these are immobile as no DNA transposons exist

in humans [26]. Retrotransposable elements (RTE) inherited by humans by millions of years of co-habitation with viral elements that target our genome are actively silenced by various genome guardians, such as p53 [27]. Long terminal repeat (LTR) RTEs of the modern human genome are highly mutated and lack replication capability. The derepression of these elements is correlated with ageing and disease [28-30].

Increased expression of Sestrin in response to different stress insults is advantageous, as Sestrins safeguard against metabolic imbalances and oxidative stress while protecting from hypoxia and DNA damage. Likely, the divergence of the single ancestral Sestrin into the three Sestrins was driven by adaptive gene duplication. Our tree displays the rapid appearance of the three Sestrins in complex animals. According to this, it is plausible that an ancestral organism, which would have derived advantages from gene duplication, appears to have been the critical evolutionary proving ground for the origination of the three distinct Sestrins. It does seem that vertebrates have inherited three distinct Sestrins from a simpler organism, but it is not clear which. The increasing complexity in organisms, along with a wider range of stressors, tissues, and physiological systems, required adaptive changes. Given the stress-mitigating nature of Sestrins, they were likely to improve evolutionary fitness; hence, the three were kept.

Considering that the first Sestrin-like protein can be traced back a billion years, the eukaryotic cell has evolved with this protein. As Sestrin pre-dates physiological systems such as the immune system and was there during the inception of animal cell signalling mechanisms, it would be appropriate to consider that this protein may be involved at the root of many cellular processes and also implicated in human diseases, such as ageing, cancer, metabolic stress and oxidative stress.

1.2.3. Sestrins' ubiquitous expression and expression outcomes

Sestrins are found to be upregulated by various stresses and are found to be differentially expressed in different tissues. Their expression is ubiquitous, with most tissues able to express Sestrins in basal conditions and in response to stress. Table 1 illustrates the levels of expression in a variety of tissues. A myriad of transcription factors governs the expression of Sestrin. Most known transcription factors that activate Sestrins are stress-response factors. While cellular stress is the primary driver of Sestrin expression, the substantial basal expression underscores the importance of Sestrins in cellular homeostasis and maintenance of cellular signalling. This is now considered due to their role as leucine-sensors.

The outcome of increased Sestrin expression in response to stress depends on whether, in that context, it would be more beneficial to support cell viability and protect tissue integrity or to activate cell death to prevent accumulation of age-related or cancer-causing damage [31, 32]. By combining these effects, Sestrins protect against age-related diseases, including cancer, by improving the overall stress tolerance of the organism [31].

	Heart	Brain	Placenta	Lung	Liver	Skeletal Muscle	Kidney	Pancreas	Spleen	Thymus	Prostate	Testis	Small Intestine	Colon	PBL
SESN1	M	MH	MH	MH	M	H	MH	MH	M	L	M	MH	L	L	L
SESN2	L	LM	M	M	M	LM	H	H	L	L	L	H	L	M	H
SESN3	L	M	M	L	LM	H	M	ND	LM	L	ND	ND	M	M	M

Table 1: Relative expression of Sestrins in various tissues.
This figure was adapted from [31], and data is from the papers [3-5]. The relative signals for each are presented as high (H), intermediate medium (MH), medium (M), intermediate low (LM), low (L), and no data (ND). PBL – peripheral blood lymphocytes.

1.2.4. Sestrins as descendants of AhpD and CMD

The first step in appreciating Sestrins' function and structure is to look back to precursor proteins. Before the dawn of Sestrins, the kingdom of monera, microbial organisms, also had stress-responsive enzymes to protect them from similar stress insults that Sestrins protect us.

If one inputs the amino terminal of Sestrin into BLAST and looks at the results, one would find high homology with enzymes alkyl hydroxyperoxidase D (AhpD) and carboxymuconolactone decarboxylase (CMD) family members.

The first efforts to understand the Sestrin function were grounded in sequence. In 2004, Budanov et al. showed that Sestrins are homologous to M. tuberculosis AhpD [33]. This high degree of homology was functionally relevant as Sestrins seemed to be a mammalian

homolog of this antioxidant enzyme and were revealed to be endogenous antioxidant stress responders.

Upon alignment (Figure 2), the authors found that a single cysteine at the end of an alpha helix was conserved and seemed crucial for the AhpD enzyme's catalytic activity. The AhpD protein plays a key role in the redox chain of tuberculosis bacillus by promoting peroxiredoxin AhpC activity [34]. Mutagenesis studies of SESN2 quickly revealed that this residue is essential for the antioxidant activity of SESN2, and hence, the first direct function of Sestrin was revealed.

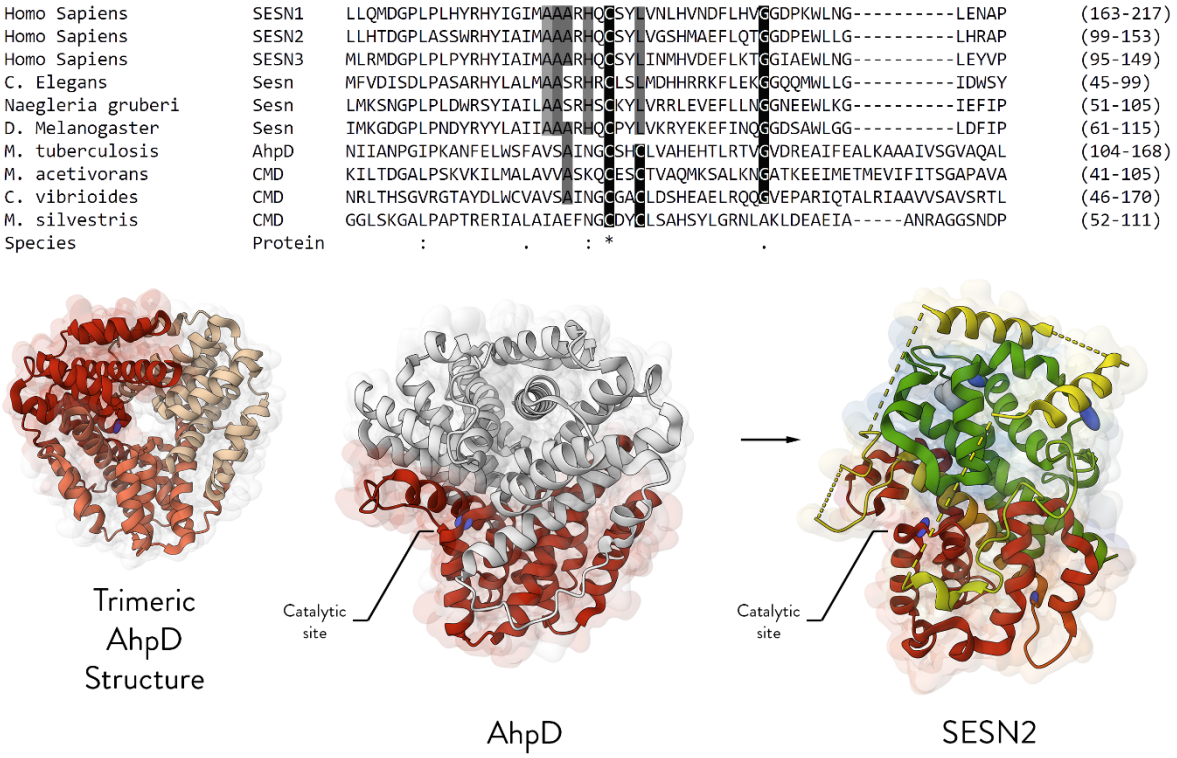

Figure 2: CLUSTAL Omega alignment of *Homo Sapiens* Sestrins and early eukaryotic Sestrins against AhpD and CMD.
Multiple sequence alignment is shown together with the structure of AhpD. The catalytic cysteine is shaded black, and other conserved residues are shaded a lighter grey according to their conservation. The trimeric AhpD structure is an artefact of crystallisation. However, AhpD is known to operate as a dimer. A monomer of AhpD is coloured red alongside the human SESN2 Sesn-A domain, which is believed to be a homolog. The catalytic site is shown.

1.2.5. Sestrin structure

Since then, elucidating more functions of Sestrins has been difficult. Although a clear mechanism was described for their antioxidant function, there was a lingering question about why a 60 kDa protein stood in for the much smaller AphD enzyme of approximately 20 kDa.

The inspiration for the structural resolution of Sestrins came from several studies that reported surprising functions. In 2008, a landmark study showed that Sestrins were potent inhibitors of mTORC1, likely acting through interaction with AMPK and TSC complexes [35]. This showed that Sestrins are not just large antioxidant enzymes; their structure still hid many secrets. Shortly after that, several studies brought Sestrins to wide attention, showing their importance in counteracting many cellular stresses and highlighting the importance of Sestrins in human diseases, such as diabetes and ageing. In 2014, the same group reported that Sestrins may inhibit mTORC1 via the GAP activity toward rags (GATOR) complexes, indicating where the search had to continue.

Out of the three Sestrin genes, only the sole protein product of *SESN2* was structurally resolved [36-38]. In 2015, Kim et al. reported a structure of the SESN2 protein produced via a selenomethionine (SeMet) substitute approach [36]. SeMet has been used to replace methionine in the human Sestrin2 protein to facilitate its structure determination via X-ray crystallography. Shortly after, in 2016, a group reported a detailed Sestrin2 structure stabilised by bound leucine, revealing a first look at this protein's 3D structure [37].

We now describe Sestrin as a multi-faceted protein. Sestrins are described to have three domains: Sesn-A (N-terminal domain), Sesn-B (linker domain) and Sesn-C (C-terminal domain).

The Sestrin protein is almost entirely made of alpha helices. Notably, the regions most conserved among the sestrin proteins fall within the α-helices. There are three highly conserved helical regions (helices α3–α8, α9–α10, and α11–α16), separated by less conserved hinge sequences. Sestrins' N-terminal sequences (Sesn-A) are less conserved [4].

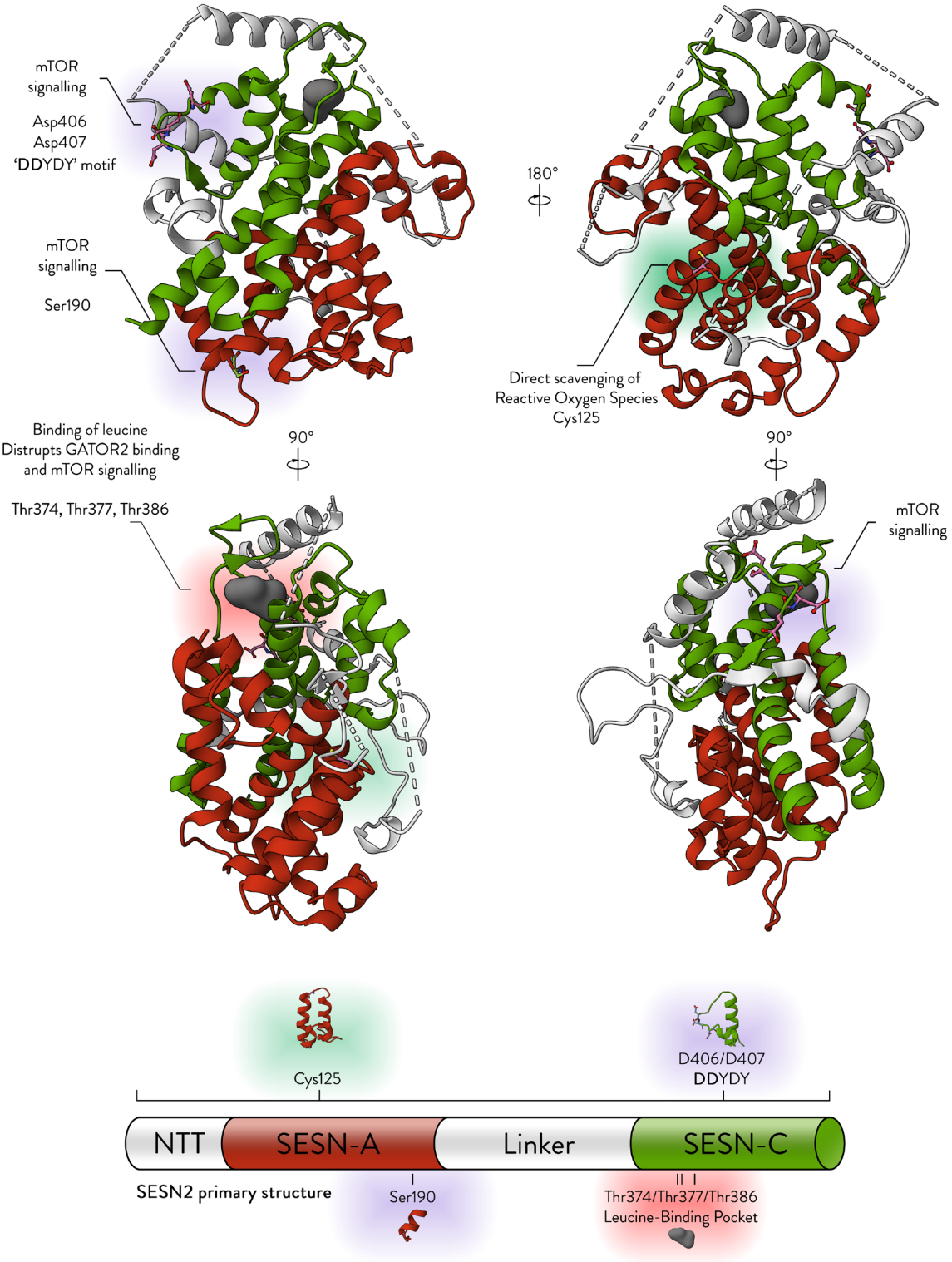

Figure 3: Ribbon structures of Sestrin2 bound to Leucine.
Sesn-A is coloured red, Sesn-B (linker) is grey, and Sesn-C is green. Several angles of the structure are shown by rotation around the Y-axis. A cartoon illustration of Sestrin primary structure, its domains and important sites are shown below the structures. Structures were drawn using Mol* (PDB ID: 5DJ4). Residues are annotated and highlighted blue. A grey space-filling element represents Leucine. Annotations and cartoon illustrations were produced for this thesis using Adobe Photoshop.

The Sesn-A domain is the homologous domain that resembles AhpD and CMD. This is the site of Sestrin's antioxidant activity. The catalytic cysteine at position 125 on SESN2 is its direct protective mechanism against ROS. Ablation of this site in SESN2 via mutagenesis has shown a complete loss of alkylhydroperoxide activity, showing its inability to reduce cumene hydroperoxide [36]. Tyrosine 127 and histidine 132 mutations were also shown to affect this ability.

While primarily associated with antioxidant properties, the Sesn-A domain holds a residue that may be key to its mTORC1-inhibiting function. Although the principal sites important for GATOR interactions are located in the Sesn-C domain, a group reported that a mutation of serine into tryptophan at position 190 prevents the binding of the GATOR subunit WDR24 and completely disrupts the Sestrin effect on mTORC1. Our alignment analysis has shown that this residue is conserved in 98.9% of Sestrin sequences analysed (Appendix B)

The Sesn-C domain has no microbial homologs and is unique to the animal kingdom.

Our alignment and analysis of 805 Sestrin proteins (Appendix B&C) has shown that one of the most conserved motifs in Sestrins is the DDYDY motif. On top of that, the Asp406 residue was shown to be conserved in 100% of Sestrin proteins. Indeed, this motif holds the Asp406 and Asp407 which is essential in binding GATOR2. Mutation of either of these residues resulted in the complete loss of WDR24 binding [36, 37]. The mutation of some proximal residues, such as Arg404, also affects the SESN effect on mTORC1. The DDYDY motif represents a highly conserved hinge just between two alpha helices.

The most recently identified function of Sestrin is to recognise and bind leucine. The leucine-bound 3D structure was resolved in an attempt to figure out this mechanism. Hence, there is strong evidence of a leucine-binding pocket in the Sesn-C domain. It is shown that Thr374-377 (sequence TYNT) and Thr386 are essential for the recognition of leucine. This leucine binding affects the protein's shape and dictates its ability to bind GATOR2. Mutations of either Thr374 or Thr386 completely abolished leucine binding and displayed constitutive binding of SESN2 to GATOR2. The authors also present evidence that distal residues are essential, as mutation of H86A also abolished leucine binding, as it was unable to form a hydrogen bond with Tyr375, thus unable to support the 'latch' of the leucine-binding pocket 'lid-latch' structure.

Domain	Mutation	Motif	Effect	Reference
N term Sesn-A	C125S	Adjacent to 'MAAAR motif'	Ablation of antioxidant function	Budanov et al., 2004 Kim et al., 2015
N term Sesn-A	S190W		Drastic loss of WDR24 binding (component of GATOR2) Unaffected leucine binding	Wolfson et al., 2016
C term Sesn-C	T374A T386A	Leucine-binding pocket	Complete loss of leucine binding ability Constitutive interaction with GATOR2 irrespective of leucine status	Saxton et al., 2016
C term Sesn-C	D406A D407A	'DDYDY motif'	Almost complete loss of WDR24 binding	Kim et al., 2015

Table 2: Table displaying the critical point mutations and the functions they have been demonstrated to affect.

These mutagenesis studies display SESN's functional domains and residues critical for its antioxidant role and GATOR2 interaction. However, it is worth noting that SESN has been described to act as a scaffold protein and interact with several important proteins, such as p62 [11]. Targeted mutagenesis does not always capture the broader effects on protein-protein interaction networks. While these studies provide robust information on how the SESN protein acts via its structure, these mutations were generated to prove known functions. It is important to note that this is not the exhaustive list of Sestrin functions and that more mutagenesis studies will shed light on how Sestrins may interact with AMPK, p62, and others.

1.2.6. The evolving dimer hypothesis

A leading hypothesis regarding the origins of Sestrins posits that a dimer formed by AhpD or a similar antioxidant enzyme underwent mutation, resulting in two distinct domains on a single protein.

This hypothesis has been explored through the structural superimposition of the Sesn-A domain onto both the Sesn-C domain and the structure of AhpD [36, 37]. Such analyses have revealed that these domains' spatial arrangement and occupation closely mirror that of an AhpD dimer, despite only a slight sequence similarity, just over 10%, between both the Sesn-

A and Sesn-C domains and AhpD. Considering AhpD is found to function as a dimer, this evidence supports the hypothesis as a leading explanation for the evolutionary origin of Sestrin.

AhpD catalyses the regeneration of the enzyme AhpC, which reduces harmful peroxides into alcohols. AhpD requires another protein called dihydrolipoamide dehydrogenase (Ldp), and together, as a cooperative unit, they achieve the transfer of electrons from NADH to AhpC. This intricate cooperation between AhpC and Ldp is crucial for AhpD's function.

Given AhpD's reliance on complex interactions, unravelling its evolutionary journey into Sestrin develops some questions. Organisms equipped with an unfunctional AhpD might struggle to adjust to prolonged stress due to the diminished regeneration of AhpC. However, this issue might not be as critical as the loss of AhpC, the primary antioxidant enzyme in this chain. Since AhpD aids in supporting another protein's activity, the possibility exists that an alternative mechanism could supplant its role. This raises intriguing questions about AhpD's direct evolutionary significance to an organism's survival and adaptation.

Gene fusion is presumably one mode of evolution that could hypothetically amplify or alter the function of an existing gene. In microbial genomes, studies have shown that gene fusion events occur, and efforts have been made to identify these gene fusions in *E. Coli* [39]. In mammalian organisms, fusion events are often associated with genomic failure and diseases like cancer; for example, the BCR-ABL1 fusion causes chronic myeloid leukaemia [40].

Whether Sestrin is a product of the fusion of an AhpD dimer and the subsequent evolution of one of the monomers into a GATOR-inhibiting unit or a fusion of AhpD with a mystery protein is a question that is difficult to answer. Despite the broad spectrum of Sestrin functions that have been identified, it is conceivable that a significant yet undiscovered role exists, potentially holding the answers to both the evolutionary origins and the pivotal biological contributions of this peptide.

Structural analysis, functional evidence and phylogeny identify that what defines a Sestrin is its GATOR2-binding motif, the DDYDY motif. As our analysis shows (Appendix B&C), it is among the most conserved domains in Sestrins. It holds the most conserved residues, Asp406 being present in all Sestrin and early eukaryote Sestrin-like proteins. Adjacent Asp407 and Tyr410 are also conserved in all of the analysed sequences. On the contrary, some Sestrin-likes presented in our analysis completely lacked the antioxidant Cys125.

If, for the definition of a Sestrin-like protein, the residues required to bind the GATOR2 complex are essential, one must examine the corresponding SESN2 binding interactors and their evolutionary prevalence to understand the evolution of Sestrins. Mutagenesis studies show

that GATOR2 is the binding target of the ‘DD’ dyad of the DDYDY motif. Studies attempting to unravel the binding site of SESN2 to GATOR2 show that subunits SEH1L and WDR24 are both required for SESN-GATOR2 interactions [41]. Large interactome studies have shown statistically significant co-immunoprecipitation of SESN2 with SEH1L and WDR24 [42]. Recent structural resolution of GATOR2 provided the putative location where SESN2 might bind both [43]. However, with this limited evidence, the exact sites of WDR24 and SEH1L that SESN2 interacts with are unclear.

WDR24 is in a class of proteins with WD40 repeats, estimates of which are found in over 260 members in humans [44]. Although SEH1L is found in the GATOR2 complex, it is also a part of the Nup107–160 complex. This complex is a part of the nuclear pore complex (NPC), constituting the ring flanking the central pore penetrating the nuclear envelope [45]. This complex was also shown to localise to kinetochores during the early stages of mitosis [46], with SEH1L shown to be essential for this localisation [47].

Therefore, the answers to the evolution of Sestrin proteins and possibly extended functions of Sestrin lay within understanding the interaction between their partners WDR24 and SEH1L and the origin and function of these proteins.

1.3. FUNCTIONS OF SESTRINs

By virtue of their unique structure and evolution, Sestrins serve as a vital link between environmental stimuli and cellular defence mechanisms, coordinating responses to a myriad of cellular stresses.

Sestrins are roadside sentinels, guarding the pathway to mTORC1, a crucial nexus where cellular signals converge, including growth factors, amino acids, energy status indicators such as ATP levels, oxygen availability, nutrient availability, glucose, lipids, and hormonal signals such as insulin. Sestrins are potent inhibitors of this complex. Through cooperation with the GATOR complexes, they can completely halter mTORC1 activity and, in this way, change the energetical mode of the cell. Their rapid inhibition of mTORC1 can bring an anabolic cell to a complete halt and initiate recycling of cellular components and support of cellular repair mechanisms.

Sestrins are also antioxidant proteins (Figure 4). Reactive Oxygen Species (ROS) are products of normal cellular metabolism. Oxidative stress leads to elevated levels of ROS. This elevation leads to DNA, protein and lipid damage and is linked to age-related pathologies. ROS can also serve as signalling molecules, regulating biological and physiological processes [48].

1.3.1. The antioxidant function of Sestrins

A conserved cysteine residue is present in the N-terminal domain across the Sestrin family. This residue, shown to be critical for SESN2's antioxidant effects, features a thiol side chain that reduces ROS accumulation through its antioxidant function, as described by Sestrin's structure [33, 36]. The mechanism of this reduction is thought to be either direct scavenging of ROS or regeneration of endogenous antioxidant products of the Prx gene. Sestrins were shown to indirectly support the regeneration peroxiredoxins (Prxs) in several cell types, including cancer cell lines and macrophages [33, 49].

However, Sestrins engage in several indirect mechanisms to mitigate cellular ROS. One proposed way this happens is via SESN's modulation of the antioxidant transcription factor Nrf2 [11]. A study has shown that SESN2 can prevent oxidative damage of the liver via autophagic degradation of Kelch-like ECH-associated protein 1 (Keap1). In the absence of oxidative stress, Nrf2 is sequestered by Keap1, facilitating its ubiquitination and subsequent proteasomal degradation through interactions with Cul3 and RBX1, components of the E3 ubiquitin ligase complex [50]. Sestrins, through their interaction with Keap1, p62, and RBX1, induce the selective degradation of Keap1, thereby activating Nrf2 [11]. This is supported by several studies demonstrating that Keap1 interacts with SESN2 [42], SESN2 co-immunoprecipitates with p62 in liver samples [11], and SESN2 facilitates the phosphorylation

of p62 through its association with Unc-51-like protein kinase 1 (ULK1) [51]. Under conditions of oxidative stress, ROS or electrophilic stress agents can modify cysteine residues on Keap1, thus altering its conformation and hindering the association with Nrf2 [52]. Serving as protectors against oxidative stress, Sestrins synergise with this action against Keap1, highlighting their role in activating Nrf2. In the absence of stress, Nrf2 accumulates in the cytoplasm, translocates into the nucleus and binds to antioxidant response elements (ARE). These genes encode for antioxidant enzymes (such as glutathione S-transferases, heme oxygenase-1, and NAD(P)H quinone dehydrogenase 1), as well as other proteins involved in the reduction of ROS and detoxification of harmful substances [53].

A study in glomerular mesangial cells has shown that SESN2 can prevent ROS accumulation by inhibiting the expression of NADPH Oxidase Nox4 [54]. The authors showed that exposure of mesangial cells to high glucose caused SESN2 activation. Given the established link between SESN2 and AMPK activation, particularly as a mechanism by which SESN2 counteracts mTORC1 activity, it is plausible that SESN2 facilitates AMPK activation in this context, thereby reducing both the levels of Nox4 protein and its production of ROS.

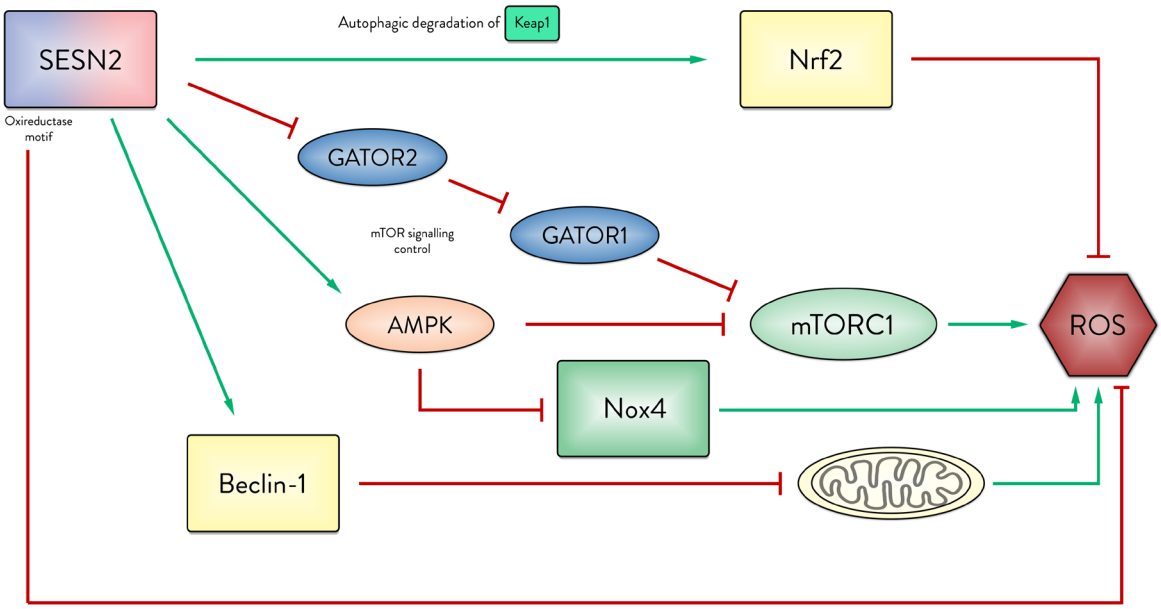

Figure 4: Sestrins protect against reactive oxidative species
Sestrins engage in direct neutralisation of ROS via their catalytic cysteine. However, indirectly, Sestrins may also influence pathways that generate ROS.

Several studies have shown evidence that Sestrins protect mitochondria from ROS-induced damage and dysfunction. This is crucial because mitochondria are a major source of ROS, which are generated as by-products of their metabolic activities. The primary ROS produced by mitochondria is superoxide (O2•−), predominantly from complex I under specific conditions,

such as high proton motive force and reduced coenzyme Q pool, or when the NADH/NAD+ ratio in the mitochondrial matrix is elevated [55]. Dysfunctional organelles lead to oxidative stress, significant damage to various macromolecules in the cell, cellular senescence, and mutagenesis [56].

Mitophagy ensures the preservation of mitochondrial function by clearing dysfunctional mitochondria or reducing surplus mitochondrial numbers to modulate mitochondrial activity in specific cell types [57]. In *D. Melanogaster*, a study showed that deleting the *dSesn* gene resulted in the accumulation of dysfunctional mitochondria [6]. A study showed that SESN2 modulates mitophagy through its interaction with p62/SQSTM1, promoting the perinuclear aggregation of impaired mitochondria in macrophages, thereby initiating the mitophagy sequence [58]. Colocalization studies have shown that a significant portion of SESN2 is located on the outer membrane of mitochondria [59], and SESN2 supports cellular resilience under glucose deprivation by modulating mitochondrial functionality and promoting energy homeostasis [60]. Finally, SESN2 has been shown to associate with ULK1 and just like with Nrf2, where it associated with ULK1 to phosphorylate p62, here SESN2 was shown to assist the phosphorylation of Beclin-1, thus promoting its interaction with Parkin [61]. The Beclin1-Parkin interaction promotes translocation of Parkin to the mitochondria, where PINK1, which accumulates at the outer membrane of damaged mitochondria, phosphorylates Parkin at several serine residues, activating Parkin and supporting its ubiquitination of mitochondrial substrates. Thus, damaged mitochondria are marked for degradation, and this process is essential in maintaining mitochondrial health.

A significant source of ROS is an anabolic cellular metabolism. Active mTORC1 facilitates a proactive metabolism, protein synthesis and lipid biosynthesis, facilitating cell growth and proliferation. The activation of anabolic processes elevates the cellular demand for ATP, increasing the metabolic rate. mTORC1 directly stimulates translation initiation, increasing protein synthesis by enhancing ribosome biogenesis and translation of mRNAs encoding ribosomal proteins and translation factors. Active mTORC1 suppresses autophagy, a catabolic process responsible for the degradation and recycling of damaged organelles and proteins, leading to the accumulation of cellular debris and damaged components. The heightened metabolic activity and reduced autophagy contribute to increased ROS production, as the mitochondrial electron transport chain, heavily involved in energy production, is a major source of ROS. Overactivated mTORC1 suppresses autophagy, supports anabolic metabolism, and contributes to cellular damage accumulation, potentially causing oxidative stress and disease.

Thus, the paramount antioxidant function of Sestrin is inhibition of mTORC1.

1.4. mTOR

1.4.1. mTORC1 structure

Mechanistic Target of Rapamycin (mTOR) is a large 289 kDa serine/threonine kinase from the PI3K-related protein kinases (PIKK) family. For comparison, the average eukaryotic protein is approximately 50 kDa [62], and a crude estimate from averaging all Uniprot entries using a statistical package like *pepstats* yields an average molecular weight of 38.2 kDa [63]. This kinase is found to be a part of two megadalton protein complexes: mTORC1 and mTORC2. These complexes are characterised by their distinct accessory proteins, differential responsiveness to rapamycin, and specific substrates and functions.

The research focus among the two complexes has been on mTORC1, attributed to its significant cellular impact upon activation. Historically, it was the first to be identified. The identification and nomenclature of mTOR stem from the investigation exploring rapamycin's mechanism, a compound recognised for its antitumor and immunosuppressive properties [64, 65], which revealed a previously unknown protein. It was quickly found that this protein was a kinase, functioning within a complex responsible for regulating protein synthesis, cell growth and proliferation, autophagy, lipid biosynthesis, and energy metabolism. Reflecting on the observations of David Sabatini, the discoverer of the mTOR pathway, as he articulated in "Twenty-five years of mTOR: Uncovering the link from nutrients to growth" [66], the mTOR pathway's broad scope of influence was unforeseen, leading to its description as “doing everything” in the realm of cellular functions.

The mTORC1 complex is inactive in isolation and may only initiate its catalytic activity after binding to its essential activator, Ras Homolog Enriched in Brain (Rheb) [67]. As seen in Figure 5, it is composed of three specific proteins - the mTOR kinase, the scaffold protein regulatory-associated protein of mTOR (RAPTOR) [68, 69] and mammalian lethal with SEC13 protein 8 (mLST8) [70].

While mLST8 contributes to the stabilization of the mTOR kinase domain in mTORC1 [71], its knockout does not impact the phosphorylation of recognised mTORC1 substrates *in vivo*. It is shown to be more critical in stabilising mTORC2, as the detrimental effects of the mLST8 knockout are attributed to mLST8 support of mTOR-RICTOR interaction [72].

RAPTOR is crucial for anchoring mTORC1 to the lysosome [73] and can facilitate the recruitment of mTORC1 substrates by binding TOR signalling motifs found on numerous canonical mTOR substrates [74, 75].

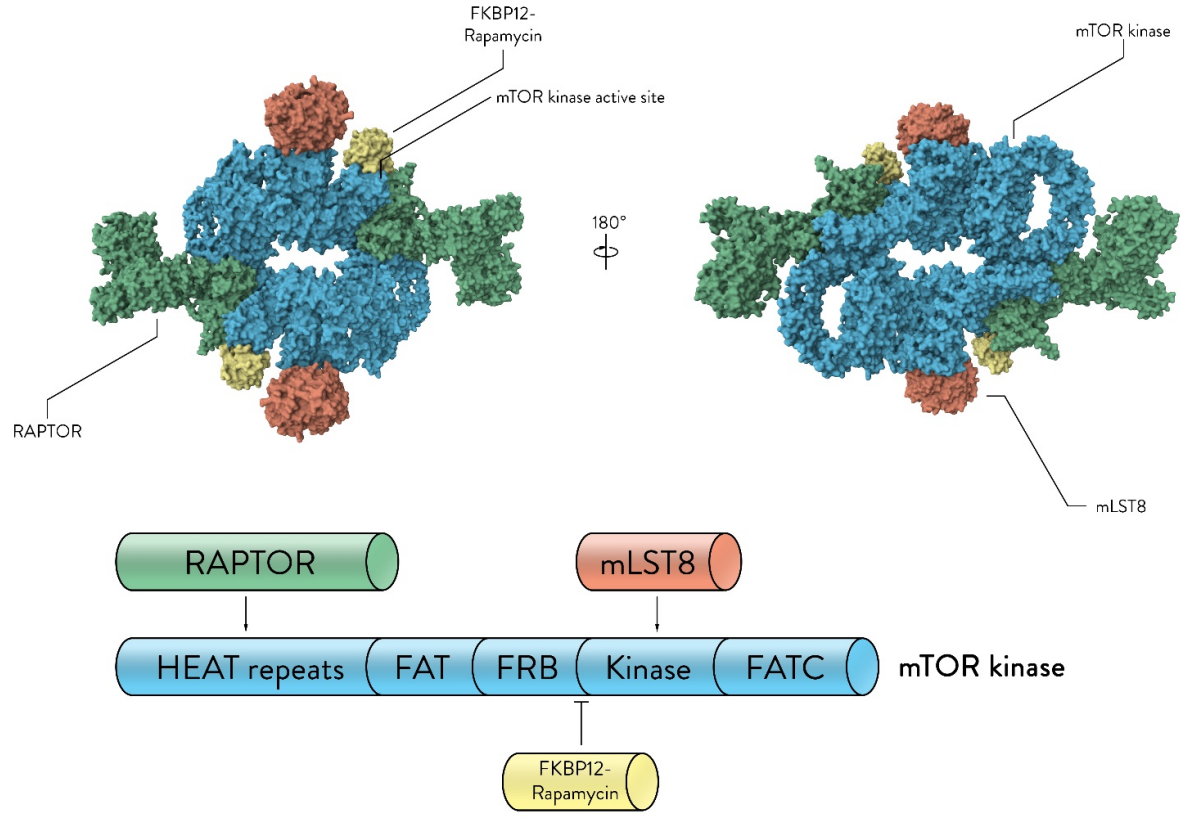

Figure 5: The mTORC1 assembles into a megadalton 'lozenge' shape complex. Gaussian surface representation of the mTORC1. The mTOR kinase is coloured blue, mLST8 orange, RAPTOR green and the FKBP12-rapamycin complex is yellow. A cartoon rendition of the primary structure of mTOR kinase, its domains, and its accessory proteins is shown below. The structure was retrieved from PDB (PDB ID: 5FLC). Annotations and cartoon illustrations were produced for this thesis using Adobe Photoshop.

Additionally, RAPTOR targets mTORC1's endogenous inhibitor proline-rich AKT substrate 40 kDa (PRAS40), which can be inhibited by Akt in response to insulin signals [76, 77]. A similar function is performed by DEP-domain-containing mTOR-interacting protein (DEPTOR), which directly inhibits the mTOR kinase, thus being an endogenous inhibitor of both mTORC1 and -2 [78]. Various factors modulate DEPTOR's inhibition, but mainly, it is inhibited through mTORC1 itself, which neutralises its inhibitor to sustain its activity [79].

Structural studies using high-resolution cryo-EM have elucidated that mTORC1, a dimeric complex characterised by a unique 'lozenge' shape, incorporates two mTOR kinases. RAPTOR binds to mTOR at its HEAT repeats, stabilizing the complex's structure and serving as a bridge between two mTOR kinases [80, 81]. Similar structural approaches have yielded

insights into the mechanism of mTORC1 inhibition by rapamycin. Rapamycin binds to a protein FKBP12, forming a complex and binding the FKBP12–rapamycin binding (FRB) domain of mTOR to partially occlude substrate entry into the kinase active site [71]. Similarly, it was shown that PRAS40 can obstruct the mTOR active site by binding the FRB domain and mLST8. This is thought to be in addition to PRAS40's ability to bind RAPTOR [67].

Cells must precisely modulate mTORC1 activity in response to swiftly varying conditions, including changes in nutrient availability or systemic cues from feeding and fasting. Given that mTORC1 triggers a resource-demanding anabolic program, its activation is contingent upon the availability of energy, growth factors, and essential macromolecules.

To accommodate these diverse inputs, mTORC1 undergoes stringent regulation through upstream signalling mechanisms mediated by two sets of small G proteins: Rheb and Rag GTPases.

Sestrins inhibit mTORC1 via these two parallel pathways: the GATOR-RAGS axis and the AMPK-TSC-Rheb axis. A visual summary of this can be seen in Figure 6, and a brief introduction of these two signalling axes will be given below.

1.4.2. mTORC1 regulation

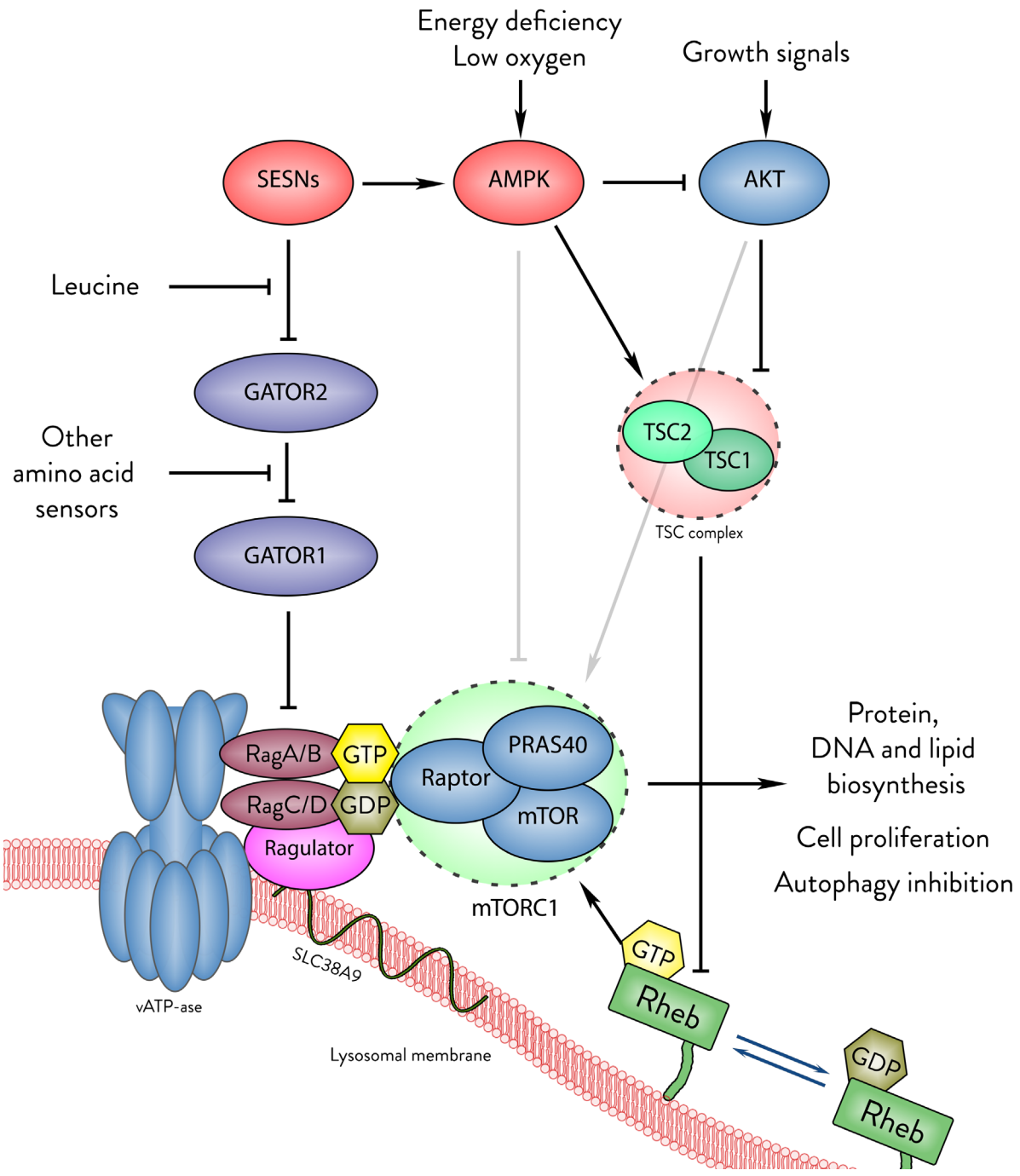

Figure 6: Sestrins inhibit mTORC1 via two parallel pathways.
The GATOR-Rags and TSC-Rheb signalling axes are displayed. Sestrins influence both signalling axes of mTORC1 regulation to inhibit this complex. Annotations and cartoons were produced for this thesis using Adobe Photoshop.

Over the last ten years, biochemical research has developed a comprehensive model wherein the specific nucleotide-binding states of the Rheb and Rag GTPases critically influence mTOR kinase function and cellular positioning, respectively. This modulation

directly impacts mTOR's role in facilitating cellular growth by altering its enzymatic activity [82, 83] and regulating its spatial distribution within the cell [84, 85].

1.4.2.1. RHEB-TSC signalling axis integrates environmental signals into mTORC1

In a cellular environment abundant with amino acids, ATP, cytokines, glucose, various growth factors, and endocrine signals, Rheb transitions to an active GTP-bound state on the lysosomal surface [86]. mTORC1, a critical convergence point for cellular signals, orchestrates protein synthesis, cell growth, proliferation, autophagy, lipid biosynthesis, and energy metabolism based on these inputs, necessitating precise regulation in response to fluctuating environmental cues.

To ensure the precise regulation of the Rheb-mTORC1 axis, this spectrum of signals from the cellular environment is channelled towards the tuberous sclerosis complex (TSC), a critical upstream trimeric complex comprising of TSC1, TSC2, and TBC1D7 [87-90].

TSC functions as a GTPase-activating protein (GAP) for Rheb on the lysosome, facilitating the transition of Rheb from its active GTP-bound form to its inactive GDP-bound state [82, 91].

The TSC2 complex mediates the incorporation of growth signals into mTORC1 activity. Following insulin stimulation, insulin/insulin-like growth factor 1 (IGF-1) triggers Akt activation, leading to the phosphorylation of TSC2 at various sites. This phosphorylation causes TSC to detach from the lysosomal surface, thus reducing its inhibitory action on Rheb and mTORC1 [88, 92-94]. Growth hormone [95], epidermal growth factor [96], platelet-derived growth factor [97], and fibroblast growth factor [98] signal to mTORC1 using the Akt-TSC axis.

As these signals can have extensive consequences for the cell through the activity of mTORC1, the signalling nexus is subject to a degree of self-negative feedback. The mTORC1 substrate S6K1 can directly phosphorylate insulin receptor substrate 1 (IRS-1), blocking insulin-mediated activation of the PI3K-Akt pathway [99, 100].

Cellular processes such as cell fate determination, migration, apoptosis, and inflammation can influence mTORC1 through the TSC. Through an unclear mechanism, Wnt and tumour necrosis factor (TNF) pathways can also repress TSC activity [101, 102]. The Ras receptor can also repress TSC inhibitory phosphorylation by ERK [103] and p90 ribosomal S6 kinase (RSK) [104].

In addition to the TSC-Rheb axis, growth factors directly influence mTORC1 activity via PRAS40, an endogenous inhibitor of the mTORC1 complex. In the absence of inhibitory signals, PRAS40 associates with RAPTOR to abolish Rheb-driven mTORC1 activation [76, 77]. However, in the presence of growth signals, Akt phosphorylates PRAS40, which results

in its binding to the cellular 14-3-3 scaffold protein, thereby alleviating the inhibition of mTORC1. Similarly, oxidative stress can suppress mTORC1 activity by inducing the upregulation of REDD1, a protein that activates TSC via 14-3-3 interactions [105, 106].

Hypoxia and metabolic stress can deplete cellular stores of ATP. The AMP-activated protein kinase (AMPK) complex is a central sensor of the AMP/ATP ratio in the cell, thus being known as a master sensor of cellular energy status. AMPK inhibits mTORC1 directly by phosphorylating RAPTOR and indirectly by activating TSC2 [107-109].

1.4.2.2. Sestrins inhibit Rheb GTPases via AMPK

The identification of Sestrins as potent inhibitors of mTORC1 marked them as key regulators of this pathway at a time when knowledge of mTORC1 regulation was confined to the TSC-Rheb axis, and the role of Rag complexes remained unidentified.

The 2008 study, which identified Sestrins as mTORC1 inhibitors, pointed to the AMPK-TSC-Rheb pathway as their likely mechanism of action [35]. The deletion of SESN2 N- or C-terminals, or expression of those terminals individually, abolished the SESN2 inhibitory effect on mTORC1. Both SESN2 domains are required; hence, the entire SESN structure is implicated in this mechanism. The redox mutant C125S of SESN2 seemed to be just as effective at inhibiting mTOR as the wild-type SESN2, underscoring this effect as a new function of this protein. The authors showed a significant decrease in activated Rheb in the presence of SESN2, and the knockdown of TSC2 dramatically compromised the SESN2-induced mTORC1 inhibition. Most importantly, evidence was shown that the TSC and AMPK co-immunoprecipitated with SESN2, suggesting that SESN2 participates in protein-protein interactions within the AMPK-TSC-Rheb signalling axis. The truncated SESN2 lacking the N-terminal could not interact with AMPK.

The precise mechanism of SESN-AMPK interaction remains unclear. Research interest significantly shifted toward the Rags complexes and their impact on mTORC1, as they were discovered around the same time the interaction between Sestrins and AMPK was identified. The discovery of Rags revealed a completely new signalling axis involving intracellular signals, redirecting the focus of mTOR research increasingly toward the Rags complexes.

The latest evidence of Sestrins in the AMPK-TSC-Rheb axis shows that Sestrin acts as the platform for the formation of a complex between AMPK and its primary activator, LKB1 (liver kinase B1), which is responsible for phosphorylation of AMPK catalytic α subunit [35, 110]. The study showed that LBK1 co-immunoprecipitated with SESN2 and that the amount of LBK1 precipitated with SESN2 correlated to the p-AMPK in a time-dependent manner in ischemic heart tissue.

The intricate regulation of mTORC1, encompassing the TSC-Rheb axis, PRAS40-mediated control, and the modulation by Sestrins via the AMPK-TSC-Rheb pathway, underscores the sophisticated adaptation of cells to environmental changes. These mechanisms ensure that mTORC1 activity is precisely calibrated to the extracellular stimuli, enabling cells to adapt to changes in nutrient availability, growth signals, and stress conditions.

However, mTORC1 co-localises with GTP-Rheb only when nutrients like amino acids and glucose are present, activating the Rag heterodimer to recruit mTORC1 to the lysosome from the cytoplasm.

1.4.2.3. Ras-related GTP binding proteins (RAGS) dock mTORC1 to the lysosome and sense intracellular stimuli

Alongside nutrients, growth factors, and various intercellular signals, mTORC1 is also subject to regulation by an intracellular amino acid-sensing axis. The observation that amino acids drive protein synthesis has been noted first by supplement industries. The development and commercialization of amino acid supplements can be traced as early as the 1970s, and research papers have shown the effects of branched amino acids (BCAA) in the 1980s [111-113] into the well-developed and researched concepts after the 1990s [114]. Nowadays, the average protein supplement boasts its BCAA percentage or leucine content straight on the label. Many of these effects were found to be related to mTORC1, with early studies reporting that leucine and arginine are essential for mTORC1 activity [115, 116].

Although the Rags were identified in 2001 [117], the 2008 discovery that Rag-GTPases regulate mTORC1 revealed an entirely novel axis of mTORC1 regulation, one shown to mediate amino acid signalling. Rags are small GTPases that are found to function as heterodimers. They are configured so that the dimer of RagA/B is bound to RagC/D, and in their active state, RagA/B is bound to GTP, while RagC/D is bound to GDP [84, 85]. The Rags are anchored to the lysosome by the Ragulator complex [105, 118, 119]. In their inactive configuration, GDP is bound to RagA/B instead, and GTP to RagC/D. This binding is highly coordinated by intercommunication between the subunits; for example, the binding of GTP to one subunit prevents GTP from associating with the other [120]. The mechanism by which the active Rags complex recruits mTORC1 has been revealed by structural studies, which postulate that the protruding shape of RAPTOR of the mTORC1 anchors to the active Rags complex [73].

Their importance in docking mTORC1 to the lysosome proves to be a major regulation necessity for mTORC1 activity. While the TSC-Rheb axis funnels all environmental signals to mTORC1, the spatial requirement of mTORC1 being docked by Rags dictates that its activation can only occur when both intracellular conditions, such as amino acid availability,

and extracellular conditions, including growth signals, are favourable to supporting sustained cell growth.

1.4.2.4. GATOR complexes are the primary regulators of RAGs

In the last few years, studies have focused on proteins that detect cytosolic cues, particularly sensors of amino acids, and relay these signals to mTORC1 by activating or inhibiting the Rag GTPases. At the core of the main regulatory mechanism of Rag GTPases are the GATOR complexes, which are divided into two main components: GATOR1 and GATOR2. The interplay between GATOR1 and GATOR2 is crucial, integrating various intracellular signals to finely adjust mTORC1 activity in response to these inputs.

GATOR1, the primary regulator of Rag GTPases, demonstrates GAP activity towards Rags mainly via its NPRL2 subunit. It consists of three subunits: DEPDC5, NPRL2, and NPRL3 [121, 122].

The KICSTOR complex, including KPTN, ITFG2, C12orf66, and SZT2, links GATOR1 to the lysosome, which is essential for responding to amino acid scarcity [123, 124]. Upon a decrease in cytosolic amino acid levels, GATOR1 activates to hydrolyse GTP on RagA/B, thereby inhibiting the mTORC1 pathway [125]. The mechanism by which GATOR1 regulates Rag GTPases remains largely unresolved. GATOR1, unlike typical GTPase-activating proteins, is hypothesised to interact with Rag GTPases through two distinct modes: a functional mode and an 'inhibitory' mode [125]. The inhibitory mode is characterised by a strong binding affinity between the GATOR1 regulatory subunit DEPDC5 and Rag GTPases but a low GAP activity. In contrast, the functional mode occurs when DEPDC5 is not bound to Rags, allowing the catalytic NPRL2 to hydrolyse GTP actively. Though recent, this dual-mode hypothesis is underpinned by limited evidence, and elucidating the exact mechanism is one of today’s scientific challenges.

The major regulator of GATOR1 is GATOR2. This complex counteracts the GATOR1 function, thereby robustly promoting mTORC1 activity. The exact molecular processes by which the GATOR2 complex antagonises GATOR1 are yet to be determined. The most recent major insight into the GATOR signalling axis is the structural resolution of the GATOR2 complex. GATOR2 is a pentameric complex of WDR59, WDR24, MIOS, SEH1L and SEC13 [121]. It is shown that it adopts a large megadalton, cage-like architecture. The subunit MIOS forms an octagon-like ring scaffold consisting of four MIOS-SEH1L dimers, two WDR59-SEC13, and two WDR24-SEH1L [43]. The MIOS-SEH1L dimers generate four inward-facing beta propellers, which are believed to stabilise the ring. The remaining dimers form outward-facing beta propellers, which are thought to mediate interactions with SESN2, CASTOR1 and GATOR1. Notably, the structure revealed that CASTOR1 and SESN2 bind different sites of

GATOR2 and can do so simultaneously [43]. Figure 7 displays the structure of GATOR2, which visually supports the earlier observations that SESN2's interaction with GATOR2 requires the availability of both SEH1L and WDR24 [41].

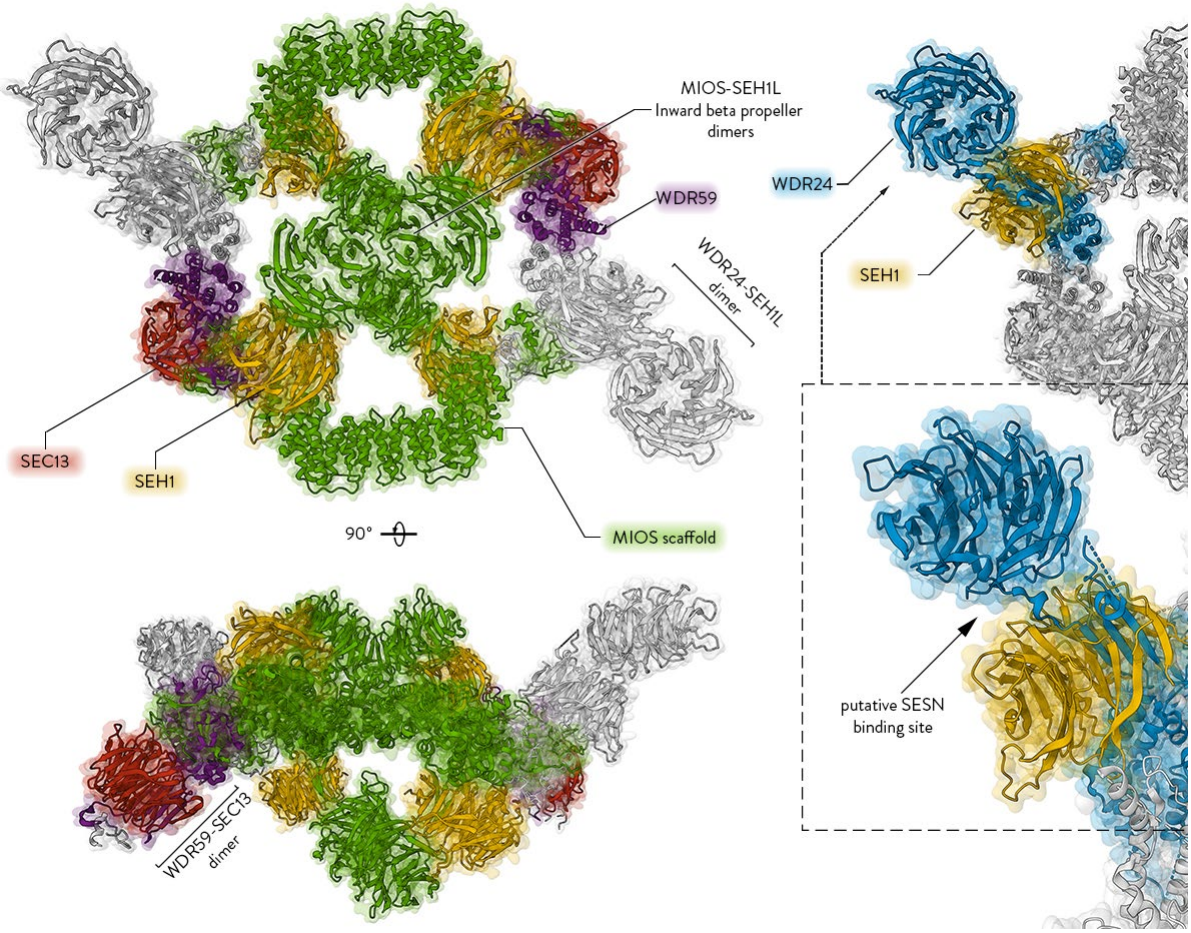

Figure 7: The structure of GATOR2.
On the left, the view from the top of the complex is provided, with a 90-degree rotation by the X axis below, to display the side elevation view. Individual subunits are coloured: MIOS – green, WDR59 – purple, SEC13 – red, SEH1L – yellow. The WDR24-SEH1L is uncoloured. On the right, top view shows the outward-facing dimer WDR24-SEH1L, which is important for SESN2 regulation of the complex. WDR24 – blue, SEH1L – yellow. The structure, boxed by a dotted rectangle, offers a zoomed-in view from the side of the dimer. As shown, this dimer forms a large pocket in which a third protein of a similar size may bind (SESN2). The structure was retrieved from PDB (PDB ID: 7UHY). Annotations were produced for this thesis using Adobe Photoshop.

1.4.2.5. Intracellular sensors utilise GATOR complexes to signal to mTORC1

Several intracellular sensors have been identified within the GATOR signalling pathway. The cellular arginine sensor for mTORC1 (CASTOR1) detects cytosolic arginine and can operate either as a homodimer or in conjunction with CASTOR2 as a heterodimer. In arginine's absence, CASTOR1 represses GATOR2, detaching from the complex upon arginine binding [126, 127]. SLC38A9, embedded in the lysosomal membrane, tracks amino acid

concentrations within the lysosome, serving as the principal sensor of the lysosomal nutrient sensing system [128, 129]. It facilitates the export of neutral amino acids from the lysosome, controlled by the presence of arginine [130]. Evidence suggests that SLC38A9 might facilitate amino acid efflux post-autophagy, with lysosomal arginine binding to its transmembrane helix, activating RagA/B through GTP loading in collaboration with Ragulator [131, 132]. Additionally, the lysosomal v-ATPase, crucial for lysosomal pH balance, was shown to interact with the Rag-Ragulator complex and affect the Rags' nucleotide-loading state [133]. The Folliculin (FLCN)–FNIP2 complex, acting as a GAP for RagC/D, further ensures mTORC1 activation in the amino acid-rich environment [134, 135]. Furthermore, SAMTOR inhibits mTORC1 under conditions of methionine or S-adenosylmethionine (SAM) scarcity by binding to GATOR1 and KICSTOR, with SAM replenishment reversing this inhibition and boosting mTORC1 activity [136].

1.4.2.6. GATOR2 is the direct binding target of SESN2

During the study of SESN2 and its effect on the AMPK complex, analysis of SESN2 complexes by mass spectrometry led to the discovery of a new AMPK-independent mechanism of mTORC1 inhibition mediated by GATOR and Rags. The follow-up to this analysis shows that Sestrins directly interact with the GATOR2 complex through WDR24 and SEH1L proteins and inhibit the suppressive effects of GATOR2 toward GATOR1 [41, 137, 138] Further research by the team that elucidated the SESN2 protein structure demonstrated that acute leucine deprivation leads to SESN2 binding and inhibiting of GATOR2, thus blocking mTORC1's lysosomal recruitment [139]. The reintroduction of leucine reverses this SESN2-induced inhibition of mTORC1, and mutations in the presumptive leucine-binding pocket of SESN2 were found to eliminate this regulatory effect [37, 139].

1.4.2.7. Sestrin inhibition of mTORC1 via GATOR2 is leucine sensitive

Sestrins are ubiquitously expressed across various tissues, raising the question of how their potent mTORC1 inhibitory effects are modulated under physiological conditions. It is suggested that Sestrins serve as a molecular rheostat, finely tuning the cellular response to leucine availability and mTORC1 inhibition [139, 140]. Under conditions where leucine is abundant and cellular growth proceeds normally, Sestrin levels are maintained at a low baseline. This ensures that even minor fluctuations in leucine levels can elicit a significant mTORC1 response through Sestrin activity.

Upon exposure to stress, cellular mechanisms significantly upregulate Sestrin expression, leading to mTORC1 inhibition independent of leucine concentrations. This regulatory model suggests an explanation for the widespread expression of Sestrins and sheds light on the tissue-specific variations in their expression levels, likely reflecting differential leucine requirements among tissues. Figure 8 below visualises this concept.

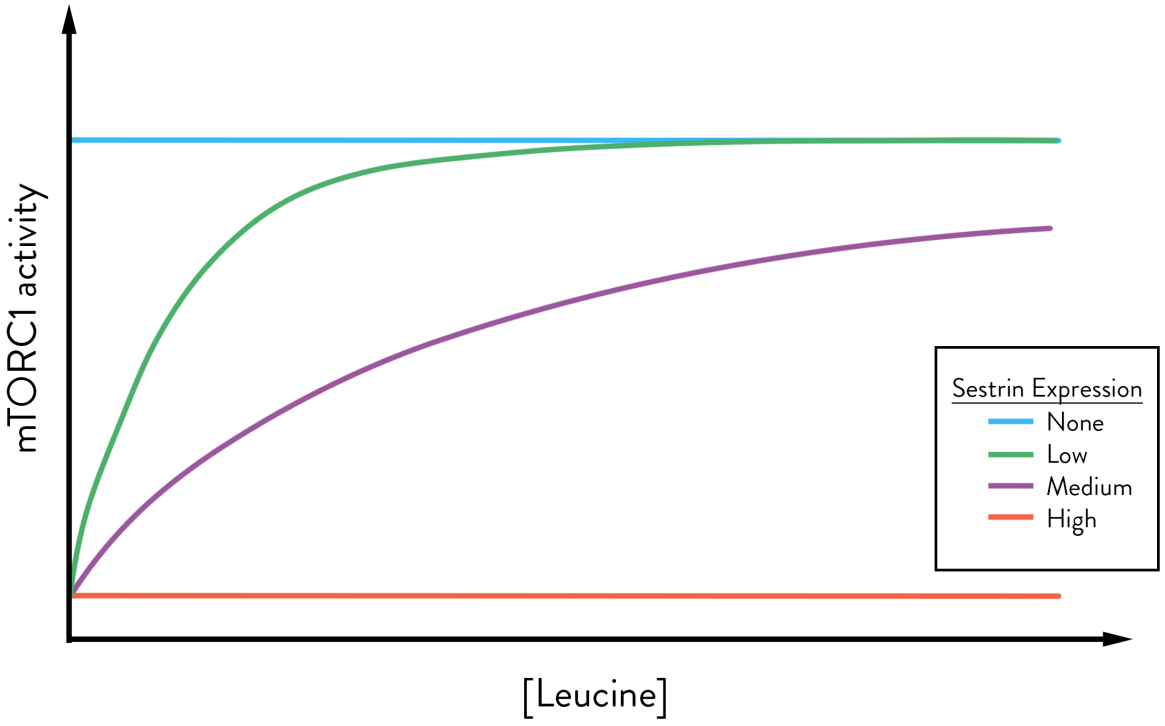

Figure 8: Modulation of mTORC1 activity by Sestrin expression in varying leucine concentrations
This graph illustrates a conceptual model where mTORC1 activity is depicted as a function of leucine concentration under varying Sestrin expression conditions. The depicted curves are arbitrary and are intended to conceptually demonstrate the hypothesised modulation of mTORC1 response by Sestrins in the presence of different leucine levels.

1.4.3. mTORC1 functions

While the prolonged effects of mTORC1 activation lead to cell growth, proliferation, biomass accumulation, lipid biosynthesis, and energy metabolism, the main direct molecular effects that mTORC1 mediates are support of protein translation and inhibition of autophagy in its inception. The most extensively researched substrates of mTORC1 that support protein synthesis are the eukaryotic translation initiation factor 4E-binding protein 1 (4E-BP1) and the ribosomal protein S6 kinase beta-1 (p70S6K). This relationship is depicted in Figure 9.

1.4.3.1. mTORC1 disables the 4E-BP mRNA translation repressor

To regulate protein synthesis, mTORC1 targets the 4E-BP family members, the extensively studied 4E-BP1, and its less-studied counterparts, 4E-BP2 and 4E-BP3. Unphosphorylated 4E-BP1 inhibits translation by sequestering eukaryotic translation initiation factor 4E (eIF4E), which is crucial for the eIF4F cap-binding complex. mTORC1 phosphorylation of 4E-BP1 disrupts its binding to eIF4E, thereby permitting the assembly of the translation initiation complex and enabling 5′ cap-dependent mRNA translation [141-143].

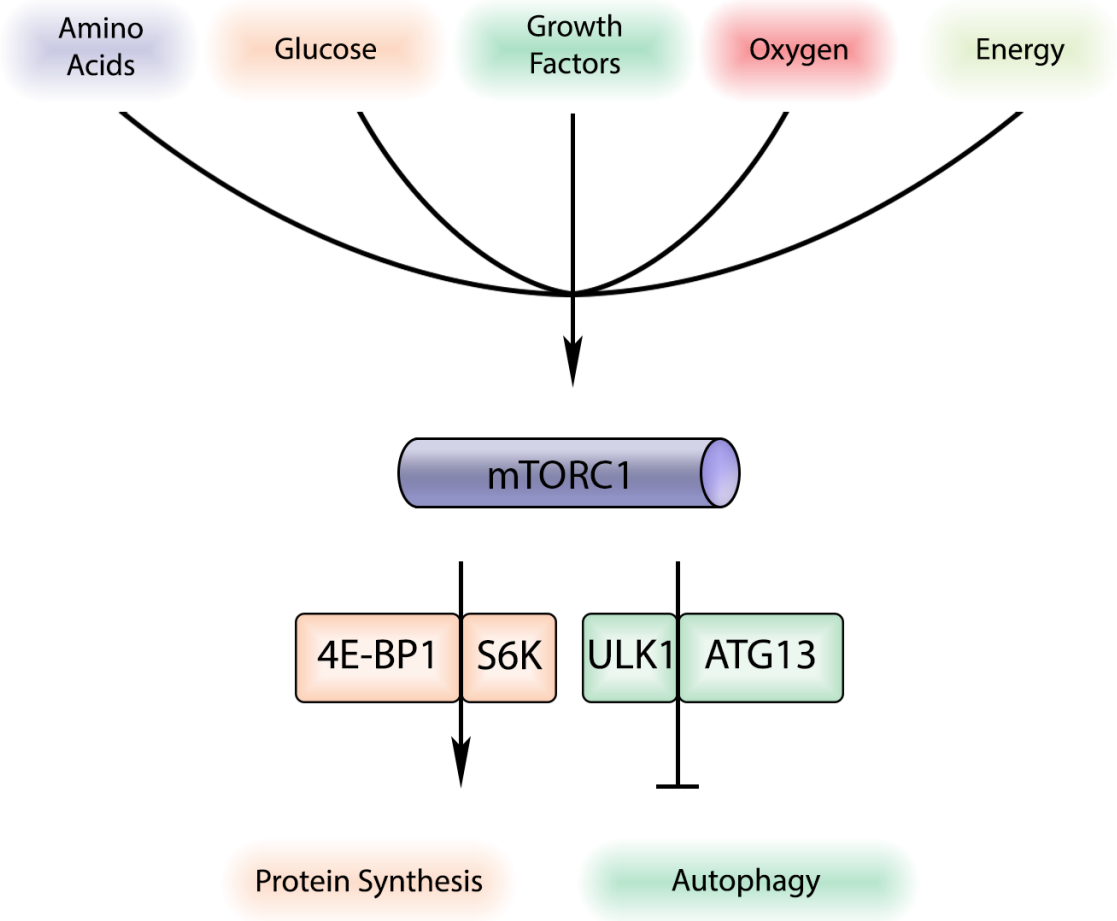

Figure 9: The downstream of mTORC1.
A simplified schematic view of the signals that mTORC1 integrates and its primary substrates by which it mediates its effects.

Furthermore, research indicates that inhibiting mTOR significantly reduces the translation of mRNAs with 5′ terminal oligopyrimidine motifs, dependent on 4E-BP. These oligopyrimidine transcripts, encoding vital components of the translation apparatus such as ribosomal proteins, highlight an additional mechanism through which mTORC1 influences protein synthesis [144, 145].

1.4.3.2. mTORC1 stimulates ribosomal biogenesis via p70S6K

Beyond phosphorylating 4E-BP1, mTORC1 also targets p70S6K1 for phosphorylation, thereby activating its kinase function [146]. While the S6 protein, a substrate of p70S6K1, often serves as a primary assay target in mTOR research, it is not directly phosphorylated by mTORC1.

The consequences of S6 phosphorylation remain less defined than those of 4E-BP, presenting a more complex picture. While mutating all five target phosphorylation sites on S6 does not detrimentally affect organism viability or translation efficiency [147], it is suggested that S6 phosphorylation's impact becomes more significant over longer durations. This extended effect is attributed to S6's potential role in enhancing the transcription of genes crucial for ribosomal biogenesis [148]. Moreover, knockout studies, such as the removal of S6K1 in mouse liver and muscle cells, have not demonstrated a decrease in global translation levels [149, 150], indicating that the immediate, notable effects of mTORC1 activity are primarily linked to 4E-BP.

1.4.3.3. mTORC1 is considered a central cellular controller of protein synthesis

While mRNA translation regulation is multifaceted, involving numerous other factors and signalling pathways beyond mTORC1, such as integrated stress response (ISR), alternative splicing, post-translational modifications of translation factors, and microRNA-mediated repression, the mTORC1 complex is still considered the major translation regulator. Cap-dependent translation is the primary mechanism of translation in eukaryotic cells. However, alternative mechanisms have been described. Cap-independent translation can occur via complicated RNA structural elements, termed internal ribosome entry segments (IRES). IRESs are located in the 5' untranslated region of an mRNA and can recruit the ribosome for translation with the help of certain factors despite being away from the cap structure. Recent findings indicate that numerous cellular mRNAs possess IRESs, with estimations suggesting that as many as 10% of all mRNAs may initiate translation via this cap-independent mechanism [151]. In addition, some unique exceptions exist. The *Hox* gene produces a subset of mRNAs which have IRE-like sites, allowing the ribosome to produce proteins independently of the cap-dependent mechanism [152]. Given that cap-dependent

translation is essential for the vast majority of mRNAs, mTORC1 stands out as a central, if not the principal, controller of protein synthesis within the cell.

1.4.3.4. mTORC1 inhibits autophagy at its inception

The principal way in which mTORC1 affects autophagy is by inhibitory phosphorylation of two key autophagy initiation proteins: unc-51-like autophagy-activating kinase 1 (ULK1) and autophagy-related 13 (ATG13) [153-155]. Both proteins are crucial components of the ULK1 complex, which also includes the 200-kDa FAK family kinase-interacting protein (FIP200) and ATG101. This complex is instrumental in the formation of the autophagosome [156]. By phosphorylating these proteins, mTORC1 effectively halts the autophagy right at its inception. The assembly of the ULK1 complex is a prerequisite for the formation of the autophagosome's encapsulating membrane around the autophagic substrate. This inhibition is similar to mTORC1's suppression of protein translation through 4E-BP1 sequestration. mTORC1 targets essential machinery necessary for these processes, making its activation a critical control point of several signalling pathways due to its significant effects on core cellular functions.

However, mTORC1 has been demonstrated to have some influence on later stages of autophagy. By phosphorylating the protein encoded by the UV Radiation Resistance-Associated Gene (UVRAG), mTORC1 was shown to inhibit autophagosome maturation and conversion of endosomes into lysosomes [157].

By simultaneously targeting key proteins such as 4E-BP1 for protein synthesis and ULK1 and ATG13 for autophagy inhibition, mTORC1 exerts robust control over essential cellular processes. The phosphorylation of 4E-BP1 and the components of the ULK1 complex allows mTORC1 to halt protein translation decisively and suppress autophagy, switching the cell from a catabolic metabolism to anabolic metabolism. These actions of mTORC1 lead to cell growth, increased production of molecules for building cell components, and higher energy generation. Therefore, the intricate regulation of mTORC1 is required, and dysregulation of this complex can lead to various cellular dysfunctions and diseases [158].

1.5. ACTIVATION OF SESTRINS

Sestrins, as a family of stress-responsive proteins, play a crucial role in preserving cellular integrity in response to a myriad of stresses. Their adamant role in mitigating stress via modulation of mTORC1 and antioxidative response is orchestrated through a network of transcription factors, each enabling the Sestrin family to respond to the specific demands of the cellular environment. These transcription factors include p53, Nrf2, HIF1α, and those implicated in the ER stress response. Figure 10 below offers a simplified schematic of SESN activation.

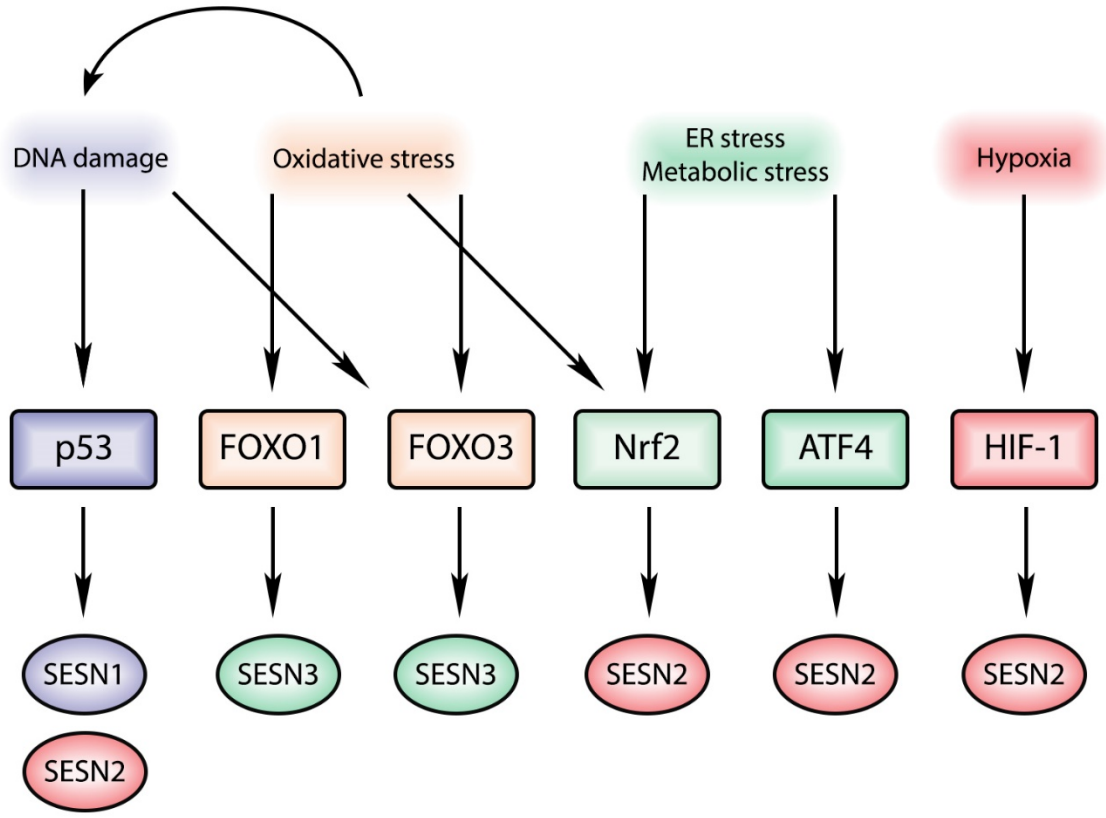

Figure 10: The activation of Sestrins in response to a diverse range of stresses.
The stress insults that activate Sestrins and the transcription factors by which they achieve this are displayed.

1.5.1. *SESN1* and *SESN2* are direct targets of p53

The initial identification of *SESN1* as a target of p53 highlighted that these proteins may be important in mediating p53's effect. After this discovery, it was shown that both *SESN1* [3] and *SESN2* [4] are activated by p53. An observation of note was that the expression of *SESN1* and *SESN2* is low in p53-deficient cells [4, 159]. A study of all p53 binding sites in the genome revealed that p53 binds to a region at a distance of 9600 bp downstream of the *SESN2* gene [160].

1.5.2. Sestrins respond to ER and oxidative stress via Nrf2

Nrf2 is a transcription factor that responds to oxidative stress. While SESN2 can activate Nrf2 via autophagic degradation of Keap1, *SESN2* was also shown to be a target of the Nrf2 transcription factor [161] in response to oxidative stress. However, Nrf2 can also be activated indirectly as a result of unfolded protein response (UPR) [60]. UPR is a potent activator of Nrf2, as PERK, an ER stress sensor located on the ER membrane, activates Nrf2 in response to unfolded protein accumulation [162]. Thus, Nrf2 can activate *SESN2* in response to oxidative and ER stress.

1.5.3. HIF1α upregulated SESN2 in response to hypoxia

HIF1α is a transcription factor involved in cellular response to hypoxia. SESN2 was initially discovered as a hypoxic gene [4]. In the context of macrophages, nitric oxide and hypoxia were shown to express SESN2 in a HIF1α-dependent manner [49]. Research on lung epithelial cells demonstrated that pre-exposure to hypoxic conditions, which activates HIF1α, led to the activation of *SESN2*, effectively reducing oxidative stress [163]. However, there may be a more complex relationship between HIF1α and SESN2, as it was shown that SESN2 can inhibit the accumulation of this transcription factor in a tumour environment, thus demonstrating tumour suppressive properties [164].

1.5.4. ER stress upregulates Sestrins via multiple transcription factors

1.5.4.1. ATF6

ATF6 is a transcription factor activated during endoplasmic reticulum (ER) stress. In the context of a human liver cancer cell line, HepG2 cells, *SESN2* was shown to be activated in a ATF6-dependent manner [165]. Silencing the ATF6 transcription factor by siRNA was demonstrated to reduce the induction of *SESN2*, providing additional evidence that the ATF6 factor is driving this expression.

1.5.4.2. PERK-XBP1

PERK-XBP1 is a part of the unfolded protein response mechanism to ER stress. A study examined the role of UPR in the activation of SESN2 in MEF cells [166]. Firstly, they showed

an upregulation of SESN2 in response to thapsigargin, an ER stress-inducing drug, and correlated it to the activation of the PERK-XBP1 axis. Knockout of PERK has shown a drastically decreased XBP1 and SESN2 expression. Similarly, knockout of XBP1 prevented SESN2 activation. Additionally, in MCF7 cells, the study demonstrated that SESN2 expression in response to the ER stress inducers brefeldin A and thapsigargin was ablated in the presence of PERK inhibitors.

1.5.4.3. ATF4

ATF4 is a transcription factor that responds to cellular stress conditions. Research involving breast and ovarian cancer cell lines, specifically MDA-MB-453 and OVCAR3, indicated that ER stress-inducing nelfinavir and proteasome inhibitor bortezomib may suppress mTORC1 activity by potentially increasing SESN2 levels [167]. However, the conclusion regarding SESN2 was strictly correlational. The study that examined the PERK-XBP1 axis in detail also alluded to the fact that ATF4 might play a role in *SESN2* activation as MCF7 cells with siRNA against ATF4 showed a decreased SESN2 response to ER inducer thapsigargin [166]. Another study demonstrated that in HeLa and RKO cells, myxothiazol—a complex III inhibitor of the mitochondrial respiratory chain—activates *SESN2*, and that silencing ATF4 with shRNA eliminated *SESN2* activation in both cell lines [168]. The study investigated this evidence and identified a potential ATF4 promoter in the 5'-UTR region of the *SESN2* gene. The team cloned this sequence into a luciferase reporter vector and then introduced both the wild-type and a mutant form of this vector into HeLa cells. Their findings demonstrated that ATF4 enhances the expression of the luciferase reporter in the presence of the wild-type sequence but not when the mutant sequence is used. Therefore, these findings substantiate that ATF4 is capable of activating SESN2 expression.

1.5.5. p38 MAPK-C/EBPβ axis may upregulate SESN2

The p38 MAPK-C/EBPβ axis plays roles in response to various stresses, including inflammation. A study has shown that under glutamine deprivation, SESN2 upregulation can be correlated with the p38 MAPK – C/EBPβ signalling axis in the context of NSCLC cell line H358. In this context, glutamine depletion is thought to trigger ROS through a reduced capacity of the endogenous glutathione (GSH). SESN2 expression was shown to subside with the addition of dehydroascorbic acid (DKG), which is thought to be reduced to ascorbic acid, contributing to the cellular endogenous antioxidant pool. Similarly, the SESN2 upregulation ceased with the treatment of a p38 MAPK inhibitor, SB202190 [169].

1.5.6. c-Jun expresses SESN2 in response to growth factor deprivation

c-Jun is a component of the AP-1 transcription factor complex, involved in cell proliferation and apoptosis. An investigation into autophagy in human nasopharyngeal carcinoma cell lines

CNE1 and CNE2 revealed that SESN2 might be upregulated by the c-Jun N-terminal kinases (JNK – c-Jun) signalling pathway. Serum deprivation triggered a dose-dependent activation of SESN2, which was associated with the activation of p-JNK and c-Jun. To investigate this further, siRNA against JNK was introduced, and the SESN2 activation was decreased, but not entirely, while c-Jun was shown to be completely inactive. Furthermore, siRNA against c-Jun specifically showed a decreased SESN2 upregulation to serum deprivation. This suggests that SESN2, at least partially, may be mediated by c-Jun [170].

1.5.7. FOXO1&3 upregulate SESN3 in response to oxidative stress

FOXO1 and FOXO3 are transcription factors that regulate gene expression in oxidative stress response. An investigation into novel ways of targeting Akt in cancer uncovered that FoxO1 upregulates SESN3. MEF cells immortalised by mutation of p53 were modified to express a genetically engineered version of FoxO1 that was fused with an oestrogen receptor. Treatment with 4-hydroxytamoxifen (4-OHT) was used to activate this chimeric protein, and SESN3 was shown to be strongly upregulated to this manipulation [171]. In a follow-up study, the same group used the same method to demonstrate that SESN3, but not SESN1 or -2, gets upregulated in this manner. To confirm this, the authors identified a promoter region in the *SESN3* gene, which FoxO1 binds, and verified it by cloning it into a luciferase reporter [172]. Similarly, a group studying the effects of FoxO3 expressed a FOXO3–ER construct in SH-EP, a human neuroblastoma cell line. Treatment with 4-OHT activated *SESN3*. Furthermore, shRNA against *SESN3* increased cell death and ROS accumulation [173].

1.6. THE JAK-STAT SIGNALLING PATHWAY

The Janus kinase-signal transducer and activator of transcription (JAK-STAT) pathway has been the primary pathway of how cells respond to interferon signals since the early 1990s. This pathway follows a general paradigm involving key components: the receptor corresponding to the signal, Janus kinase (JAK), and signal transducer and activator of transcription (STAT). Upon ligand binding to the receptor, JAKs associated with the receptor become activated, thus phosphorylating STAT molecules. These phosphorylated STATs then dimerise and translocate to the nucleus to induce the expression of a myriad of genes. This pathway was initially discovered in the context of interferon-α (IFNα)-, IFNγ- and interleukin-6 (IL-6)-mediated downstream signalling [174, 175].

The JAK/STAT pathway is composed of four JAK proteins: JAK1, JAK2, JAK3, and TYK2 [176]; and seven STAT proteins: STAT1, STAT2, STAT3, STAT4, STAT5A/B, and STAT6, which are cytoplasmatic monomers which share several conserved domains and are encoded by adjacent distinct genes [176, 177]. In addition to the seven STAT proteins, there have been described splice variants for several STAT proteins, forming isoforms such as STAT1β, STAT3β, STAT4β, and STAT5β. In some cell types, the STAT isoforms have been described to have a dominant-negative function.

The STAT proteins are responsible for several cellular processes, such as cellular differentiation, apoptosis, and cell proliferation [178].

1.6.1. JAKs

In 1991, JAK1, JAK2, and TYK2, three kinases from the family, were discovered using various cDNA-cloning methods. Their widespread expression did not immediately reveal their roles. The designation "Janus kinases," named after the two-faced Roman god, reflects their structural characteristics, while the term "JAK" (Just Another Kinase) stems from the original discoverer's nonchalant attitude towards their naming [179]. Today, we know of JAK3, and thus, the family comprises four members, each of which has a distinct expression pattern and specific sets of cytokine receptors they associate with, conferring a unique signalling specificity.

In mammals, JAK1, JAK2, and TYK2 are universally expressed, contrasting with JAK3, whose expression is more specialised, predominantly occurring in hematopoietic cells where its expression closely aligns with cell development and activation [180-182]. JAKs can be found in the cytosol when expressed in the absence of cytokine receptors. However, they are typically associated with endosomes and the plasma membrane near their specific receptors [183, 184]. The connection between JAKs and cytokine signalling was first discovered in mutant cell lines unresponsive to interferon (IFN), where reintroducing TYK2 to a deficient line

restored IFN signalling [185]. This led to the rapid identification of various receptors associated with JAKs [186-189].

Although it is challenging to attribute specific JAKs to specific types of receptors, there are some patterns to which they associate. JAK1 and JAK3 [190] associate with receptors with γ chain subunit in their cytosolic domains; some of these receptors would be the IL-2, IL-4, IL-7, IL-9, IL-15 and IL-21 receptors.

JAK1 is important for the receptor family that shares the gp130 receptor subunit [190]. These are IL-6, IL-11, oncostatin M, leukaemia inhibitory factor (LIF), ciliary neurotrophic factor (CNF).

JAK2 is important for hormone-like cytokines. Some of these are growth hormone (GH), prolactin (PRL), erythropoietin (EPO), and thrombopoietin (TPO). JAK2 also relays signals for the IL-3 receptor, the family of cytokines that signal through the IL-3 receptor, which are IL-3, IL-5 and granulocyte-macrophage colony-stimulating factor (GM-CSF). TYK2 is essential for IL-12 signalling and plays an important role in the response to lipopolysaccharide (LPS) [191].

1.6.1.1. Structure of JAKs

JAKs are relatively large proteins exceeding 1100 amino acids, with molecular masses around 120-140 kDa, and their size presented a challenge in expression and purification. While structures of JAK bound to inhibitors were available in 2009 [192, 193], the whole structure remained elusive for a long time. Structures of TYK2 FERM and SH2 domains were resolved in 2014 [194], followed by structures of the human JAK1 [195, 196] and JAK2 [197

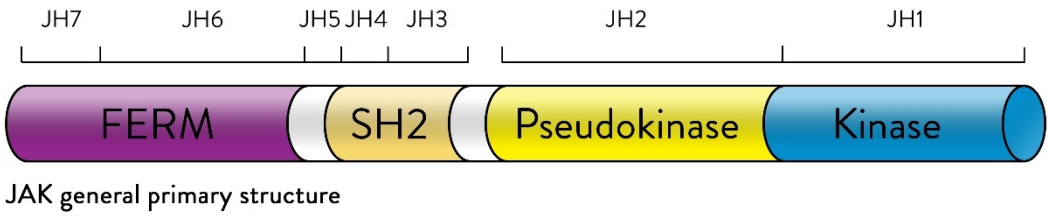

Figure 11: The primary structure of JAKs
A cartoon rendition of the primary structure of JAK. Dimensions are not representative of actual length and are only approximations. The structure is displayed from N-term to C-term, not to be confused due to the reverse nomenclature of JH1 to JH7.

The kinase domain, followed by a pseudokinase domain, is also known as JH1 and JH2. The tandem of JH1 and JH2 got JAKs their name - Janus, a two-faced god [198]. The JH1 domain displays all of the features of a typical eukaryotic kinase [199]. The JH2 domain does not display a catalytic activity but is essential in regulating JAK [200]. The importance of the JH2 domain is underscored by a single point mutation in this domain in JAK2, a valine-to-phenylalanine substitution at amino acid position 617 (V617F), which is present in the majority of patients with polycythaemia vera, as well as in a high percentage of patients with essential thrombocythemia and idiopathic myelofibrosis [201-203].

These two kinase domains are followed by the Src Homology 2 (SH2) domain, also known as – JH3 and JH4, and the four-point-one, ezrin, radixin, moesin (FERM) domain – also known as JH5 and JH6. The FERM domain consists of three subdomains, the F1, F2, and F3 domains, which form a trilobed FERM architecture observed in proteins containing FERM domains [204]. JAK FERM domains resemble canonical FERMs but feature unique adaptations for interaction with SH2. The L1 linker, longer in JAKs (29-42 residues), connects the F1 and F2 domains, enlarging the SH2 interaction surface [205]. The extended linker and slightly different chemical composition of JAK FERM domains, particularly a highly basic alpha helix in JAK F2 not found in canonical FERMs [195, 205], are believed to facilitate JAK's binding to cytokine receptors and potentially enhance interactions with the plasma membrane. The SH2 domain (JH3 and JH4) is a key domain for the JAK-STAT family. However, the specific role of SH2 in JAK is unclear. Some research shows that this domain is important for JAK1 in binding the oncostatin M receptor subunit (OSMR), which pairs with other subunits like gp130 to form the functional receptor complex for oncostatin M signalling [206]. Together with the FERM domain, the amino terminus is known to be the receptor-binding part of JAKs. The role of the SH2 domain is much more pronounced in STATs, the principal binding partners, and the next in tandem with the JAK-STAT signalling pathway.

1.6.2. STATs

The STAT family of transcription factors in mammals contains seven members: STAT1, STAT2, STAT3, STAT4, STAT5A/B and STAT6 [207-213].

The different combinations that JAKs can form with STATs create numerous potential pathways for signalling. However, there can be some generalisation of the pathway. STAT1 and STAT2 are typically associated with the response to interferons, STAT4 and STAT6 response is primarily to interleukins, and STAT3 and STAT5 promiscuously respond to a wide variety of extracellular signals, including cytokines and growth factors [214].

The first STAT to be discovered was STAT1 in 1990. These authors identified and characterised the products of a gene called the Interferon-stimulated gene factor 3 (ISGF3). This gene produces a complex of three subunits which at the time were unknown but are now STAT1, STAT2 and IRF9 [215]. The isoforms of STAT1, termed Stat1α and Stat1β, were discovered later in a subsequent article in 1992 [208]. What is known as STAT3 was discovered by another group in 1993 and termed acute-phase response factor (APRF) [216]. In 1994, the same group that identified STAT1 decided to coin the term STATs while announcing APRF as a new family member: STAT3 [213].

1.6.3. STAT3

STAT3 is made of 770 amino acids and is also characterised by the presence of six functionally conserved domains: an amino-terminal domain (NH2), the coiled-coil domain (CCD), the DNA-binding domain (DBD), the linker domain, the SRC homology 2 (SH2) domain and the carboxyl-terminal transactivation domain (TAD). SH2 is the most highly conserved STAT domain and plays a vital role in signalling via binding to specific phosphotyrosine motifs [178, 217].

The Table 3 below shows signalling molecules that utilise STAT3.

Factors to which STAT3 responds									
Group		Signalling Molecule							
IL6/gp130	cytokines	IL6	IL11	IL27	IL31	CNF	CT-1	LIF	OSM
IL2/γ chain	cytokines	IL2	IL7	IL9	IL15	IL21			
IL-10 family	cytokines	IL10	IL19	IL20	IL22	IL24	IL26	IL28	IL29
Type I and type 2 interferons		IFNα	IFNβ	IFNγ					
Receptor tyrosine kinases		EGF	FGF	FL	GH	IGF-1	M-CSF	PDGF	
Other		IL3	IL5	IL12	IL23	G-CSF	leptin	PAF	

Table 3: The signalling molecules that activate STAT3.
Abbreviations: CNF, ciliary neurotropic factor; CT-I, cardiotrophin I; EGF, epidermal growth factor; FGF, fibroblast growth factor; FL, Flt3 ligand; G-CSF, granulocyte colony-stimulating factor; GH, growth hormone; IFN, interferon; IL, interleukin; IGF-1, insulin-like growth factor I; LIF, leukemia inhibitory factor; M-CSF, macrophage colony-stimulating factor; OCM, oncostatin M; PAF, platelet-activating factor; PDGF, platelet-derived growth factor.
Sources: [218-220]

Figure 12 provides a visual representation of a STAT3 dimer bound to DNA, illustrating its structural domains.

A study showed that the NH2 domain contributes to STAT3's function as a transcription factor by enhancing its transcriptional potential through the stabilization of the enhanceosome complex [221]. Mutation of the NH2 terminal showed faster shuttling across the nuclear membrane, impeded dimerisation of unphosphorylated STAT3, and faster efflux of phosphorylated STAT3, suggesting that the NH2 is important in the correct localisation of activated STAT3 [222]. Other studies showed that the domain is important in the transcription of some specific genes [223, 224].

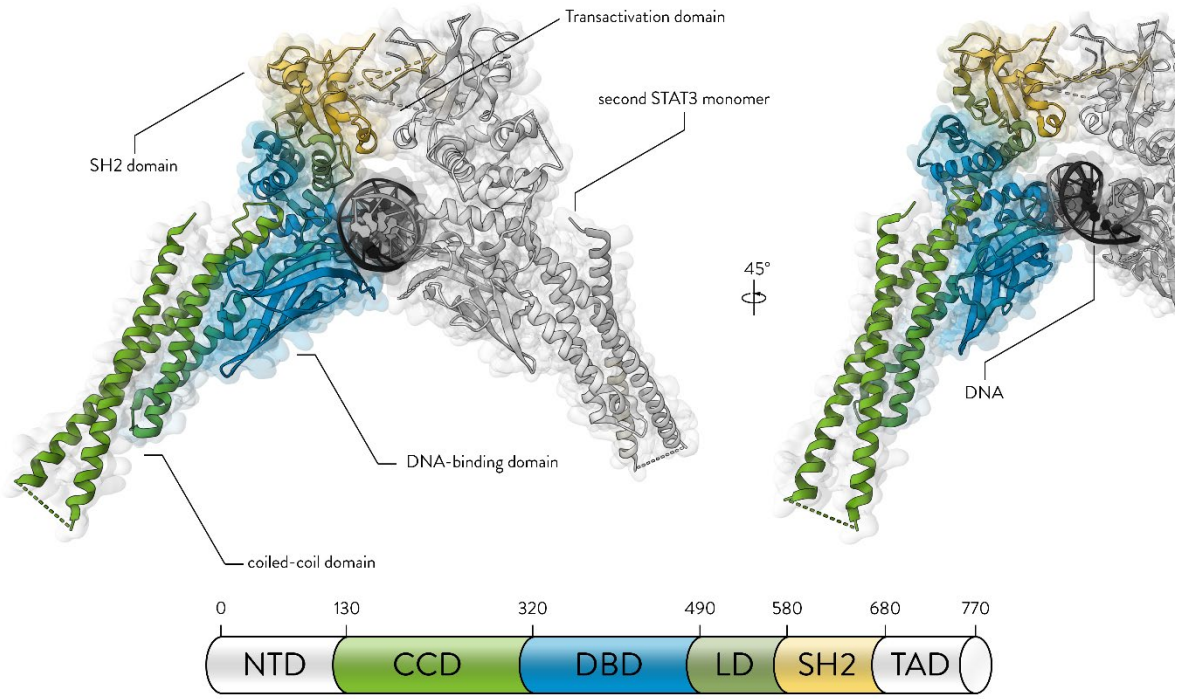

Figure 12: The structure of an activated STAT3 molecule bound to DNA.
Ribbon structure of STAT3 displayed an elevation view, with the DNA helix facing the observer. A 45-degree rotation by the Y axis is displayed to the right. Individual domains are coloured: coiled-coil domain (CCD) – green, DNA binding domain (DBD) – blue, linker domain (LD) – dark green, Src Homology 2 domain (SH2) – yellow. A cartoon rendition of the primary structure of STAT3 is shown below. The structure was retrieved from PDB (PDB ID: 6QHD). Annotations and cartoon illustrations were produced for this thesis using Adobe Photoshop.

The role of the CCD is thought to be in supporting STAT3 structure and its import into the nucleus. A study described several mutations in the CCD critical for the structure and postulated that alterations in the CCD disrupted the SH2 domain [225]. Additionally, the study that identified a mechanism for STAT3's nuclear translocation described a region in the CCD that is necessary for import by importin-α3 [226].

The transactivation domain (TAD) functions similarly to the NH2 domain in regulating STAT3 but is the principal regulatory region due to its critical phosphorylation sites. Truncation of this portion of STAT3 rendered the molecule constitutively active in the COS-7 cell line [227]. Its designation as the 'transactivation domain' stems from early reports of its crucial importance in its activation of transcription (transactivation). The TAD contains essential residues like Tyr705, the principal marker of STAT3 activation, and Ser727, crucial for enhancing STAT3's transcriptional function [228].

It was shown that the SH2 domain is crucial in STAT function. The SH2 domain of one STAT molecule binds the phosphorylated tyrosine of another STAT molecule [229], particularly

Tyr705, the marker of an activated STAT3. This interaction is the essential feature of STATs, as their dimerisation is essential for DNA binding. The reciprocal interaction between two SH2 domains of a STAT3 dimer stabilises the dimer structure. More importantly, this change in conformation is said to expose the DNA-binding domain and thus stabilise the DNA interacting elements of STATs [230].

1.6.4. The JAK-STAT signal transduction

Figure 13 depicts the JAK-STAT3 signalling transduction pathway as described in the following sections, providing a schematic for reference.

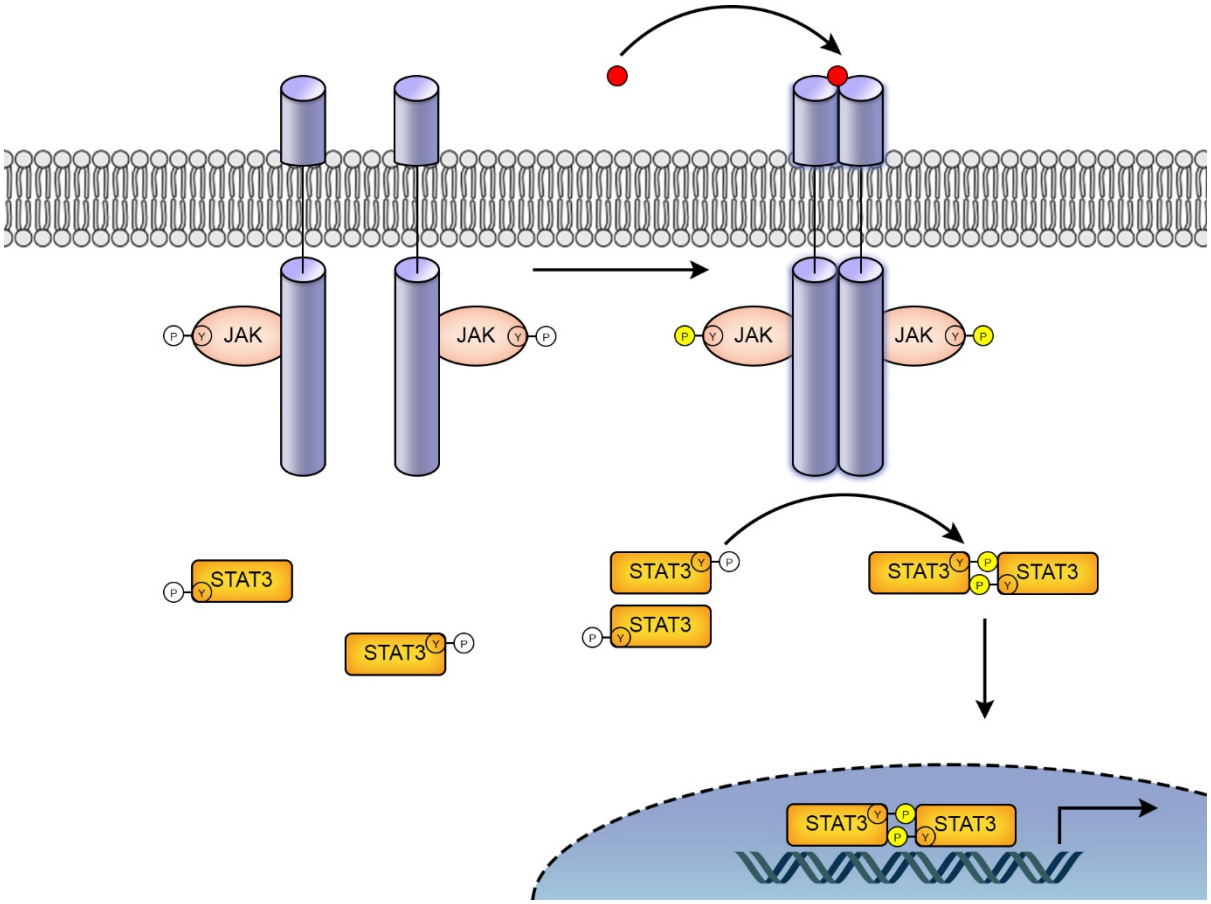

Figure 13: A simplified schematic of the JAK-STAT3 signalling pathway.
The ligand binds and promotes dimerisation of the receptor. JAKs autophosphorylate and thus phosphorylate and promote the dimerisation of STAT3. Activated STAT3 dimer is transported into the nucleus in which it upregulates transcription of pro-survival, growth and angiogenesis genes.

A specific ligand (e.g., cytokines such as interleukin-6) binds to its cognate receptor (e.g., gp130), leading to the recruitment and activation of JAK2, which is bound to the receptor's intracellular domain. JAK2 undergoes autophosphorylation on specific tyrosine residues, enhancing its kinase activity. The essential phosphorylation for JAK2's catalytic activity is the tyrosine 1007 site. Although there are two adjacent phosphotyrosine sites in JAK2, Y1007 and Y1008, mutagenesis of Y1007F, but not Y1008F, abolished all kinase activity [231]. Two regulatory autophosphorylations were shown. Autophosphorylation of Tyrosine 221 increased JAK2 kinase activity, and tyrosine 570 phosphorylation decreased the kinase activity, the latter potentially being a part of signal termination [232]. Phosphorylation of tyrosine 813 (Y813) was shown to be essential for the binding of an adaptor protein SH2-Bβ [233].

Activated JAK2 then phosphorylates STAT3 on Tyr705. This phosphorylation induces a conformational change in STAT3, promoting its dimerisation through reciprocal SH2 domain-p-Tyr705 interactions. The phosphorylation of STAT3 on Tyr705 is essential for its activity. In 1993, STAT1's Tyr701 was the first phosphorylation to be shown to be essential in STATs [234]. Two years later, mutagenesis of Tyr705 in STAT3 was shown to cease STAT3 function [235]. The study that described the mechanism of STAT3 activation in 1994 via dissociation and reassociation assays showed that dimerisation of STAT1 is mediated through SH2 domain-phosphotyrosine peptide interactions [236]. A separate study showed that mutagenesis of sites around Tyr705 in STAT3 affected its dimerisation [227].

Once phosphorylated and dimerised, STATs can be recognised by specific importins and translocated into the nucleus. For STAT1, a mechanism was described in which importin-α5 binds tyrosine-phosphorylated STAT1 dimers. Furthermore, the study showed that a point mutation of leucine 407 to alanine produced a STAT1 molecule that accurately phosphorylated and dimerised yet could not be imported into the nucleus. This demonstrated that the nuclear import of STATs is a regulated process, with dimers being recognised and transported by importins.

Upon entering the nucleus, STAT3 dimers bind to specific DNA sequences, including palindromic IFN-γ–activated sequence (GAS) elements [174], to upregulate genes involved in key cellular processes such as growth, survival, and differentiation.

Some exceptions to this paradigm have been proposed. An alternative splicing form of STAT3, known as STAT3β, is a shorter version that replaces the C-terminal 55 amino acid residues of STAT3 with 7 different residues. Thus, STAT3β lacks the transactivation domain [237]. It has been proposed that the beta isoform binds DNA slightly better yet cannot recruit co-activators needed for STAT3 transcriptional activity, thus acting as an endogenous negative factor for

the gene [238]. To further investigate this effect, a group claims to have designed a phosphorodiamidate morpholino oligomer to redirect endogenous STAT3 alternative splicing from STAT3α to STAT3β, favouring the stable production of STAT3β in MDA-MB-435. The splicing switch to favour STAT3β displayed that the isoform has antitumour properties [239].

STAT3 is unusual in nuclear import as unphosphorylated STAT3 can be imported into the nucleus [226]. However, this unphosphorylated STAT3 makes up a small portion of nuclear STAT3 and cannot bind target DNA sequences. The function of unphosphorylated STAT3 in the nucleus has been proposed to engage in alternative signalling and self-regulation. Unphosphorylated STAT3 may be able to upregulate a small subset of genes, and cancers may exploit the transcription of STAT3 to increase the levels of unphosphorylated STAT3 in the nucleus [240]. IL-6 may drive the accumulation of unphosphorylated STAT3 [241], and the study's authors show that STAT3 might compete with IκB by binding unphosphorylated NFκB, thus engaging in alternative signalling.

1.7. CANCER

Cancer stands as a leading cause of mortality in Western countries. In Ireland, for instance, 28% of all deaths in 2021 were due to cancer, surpassing other major causes of death such as cardiovascular disease at 27% and respiratory system-related issues at 9%, making cancer the foremost cause of mortality [242]. In 2020, statistics showed that about 20% of people will develop cancer during their lifespan [243].

In 2018, reports showed that lung cancer is the most commonly diagnosed cancer (11.6% of the total cases) and the leading cause of cancer death (18.4% of the total cancer deaths) [244].

Lung cancer is the primary cause of cancer-related mortality around the globe, with a 5-year survival rate not exceeding 18% [245]. About 85% of lung cancers are classified as non-small cell lung cancer (NSCLC), with adenocarcinomas being the predominant tumour type [246]. The incidence of this type of cancer is further exacerbated by the rising number of elderly individuals in the population, smoking habits, and environmental pollution, which are significant risk factors for lung carcinogenesis. Despite the introduction of various innovative strategies for cancer treatment, traditional chemotherapies that induce genotoxic stress in rapidly dividing cancer cells continue to be the primary method for managing lung cancer and other cancer types. Drug resistance continues to be a principal problem in the treatment of cancer, as cancers often develop adaptations to the chemotherapies, allowing them to survive and proliferate in their presence [247]. The mechanisms of such resistance are incredibly complex. Cancers develop through a repetitive cycle of clonal expansion, genetic diversification, and clonal selection within the adaptive landscapes shaped by tissue ecosystems and therapeutic pressures. This inherently evolutionary nature of cancer is the primary cause of therapeutic setbacks [248]. The major challenge of contemporary cancer research is understanding the mechanisms responsible for eliminating cancer cells and developing new approaches to target the pathways deregulated in cancer cells that provide resistance to chemotherapeutic drugs. Identifying key proteins susceptible to modulation by small molecules and enhancing cellular sensitivity to chemotherapeutic agents is a crucial goal. Uncovering endogenous tumour suppressor genes not only elucidates the mechanisms underlying carcinogenesis, cancer metastasis, and drug resistance but also opens new pathways for the development of innovative therapies.

The p53 protein, the product of the tumour protein *TP53* gene, plays a significant role in protecting from lung carcinogenesis, as mutations in *TP53* are found in more than 45% of human lung cancers [249]. Moreover, the inactivation of p53 in mouse models dramatically accelerates lung carcinogenesis and shortens lifespan [250]. Protein p53 works as a direct

transcriptional regulator of several hundred genes responsible for suppressing cell proliferation, induction of cell death, regulation of metabolism, and control of reactive oxygen species [32, 159, 251]. However, the precise mechanism of suppression of carcinogenesis by p53 in the lung remains elusive and requires meticulous analysis of different p53 targets. *SESN1&2* genes are direct targets of p53, and previous studies have shown that the expression of *SESN1* and *SESN2* is low in p53-deficient cells [4, 159].

The GENT2 cancer expression database reveals a widespread reduction of Sestrin expression across various cancers [252]. SESN1 levels are reduced by 28.5% across all tumours. SESN2 also experiences a decrease, with an 8.6% reduction observed consistently across all tumour types. Specifically, in lung cancer, the decrease is more pronounced for SESN1, with a 52.8% reduction in expression across lung tumours. Although the decrease in SESN2 within lung cancers is not as marked as SESN1, it still represents a notable reduction of 7.9%. This is supported by published studies which demonstrate that the expression of SESN1 and SESN2 is downregulated in human lung cancers [253, 254].

1.7.1. STATs in cancer

STAT proteins, particularly STAT3 and STAT5, are consistently overactivated across various cancers, driving tumour growth, angiogenesis, and immune suppression. Tumour dependency on STAT3 signalling offers a unique therapeutic opportunity, with evidence from cell culture and animal studies underscoring the potential of STAT3 and STAT5 as molecular targets. STAT3, a central node in numerous oncogenic pathways, is hyperactivated in cancerous and non-cancerous cells within the tumour microenvironment. In several types of cancer, STAT3 is overexpressed or constitutively activated with a high incidence in hepatocellular carcinomas, myelomas, lymphomas, breast, lung, skin, head, and neck cancers [255], and in most cases, it is correlated with a poor prognosis due to its high association with immunosuppression and tumour growth [256].

A gain-of-function mutation in STAT3 transforms cells [257]. Constitutive STAT3 activation is associated with several human tumour types, and STAT3 function is essential for transformation by several oncogenic tyrosine kinases [258, 259]. Whole-exome and targeted sequencing found that 40% of patients with large granular lymphocytic leukaemia had activating mutations in STAT3 [260].

STAT3 transcriptionally activates genes responsible for cell proliferation (Cyclin D1 and c-Myc), inhibition of cell death (MCL1 and BCL-xL), tissue remodelling (MMP2 and MMP9), inflammation (IL-6 and IL-10), and angiogenesis (VEGF and bFGF) [261, 262]. Cytokines, such as IL-6, bind and activate their corresponding receptors, which dimerise and recruit JAK2. Recruitment of JAK2 molecules to their complementary receptors induces their auto-

phosphorylation and activation, allowing them to phosphorylate STAT3 [261]. In parallel, STAT3 can also be activated by other tyrosine kinase family members, including EGFR, IGFR, and SRC [261]. In normal cellular conditions, STAT3 is tightly controlled by receptor and non-receptor tyrosine phosphatases, such as PTPRD and SHP1/2, respectively. STAT3 is also negatively regulated by the Suppressor of Cytokine Signalling (SOCS) family members, which inhibit the activity of JAK kinases through the control of their ubiquitination and degradation, and by PIAS proteins, which bind STAT3 and inhibit its transcriptional activity [261-263]. However, STAT3 is constitutively active in many cancers, supporting cell proliferation, invasiveness, and the cancer stemness phenotype [261-263]. Hyperactivity of STAT3 in NSCLCs is associated with poor prognosis, and persistent phosphorylation can be found as commonly as in 65% of NSCLCs [263]. STAT3 hyperactivation could be caused by many factors, including cytokine production by cancer and immune cells, activation of oncogenes, and inactivation of tumour suppressor proteins [261].

1.7.2. SESNs in cancer

Carcinogenesis is distinguished by critical hallmarks such as continuous cell growth, resistance to apoptosis, evasion of tumour suppressors, genomic instability, and persistent inflammation, among others [264]. Sestrins are implicated in moderating these aspects, suggesting a link between p53 activation and tumour suppression [32, 265]. However, the contribution of Sestrins to carcinogenesis regulation presents a paradox. Sestrins inhibit mTORC1 while also stimulating the AKT pathway [265], both of which are frequently activated in cancers and can have opposing effects on tumorigenesis, either supporting or suppressing it depending on the context. These parallel pathways indicate that Sestrins could inhibit tumour growth by repressing mTORC1 or promote survival and proliferation through AKT activation [266]. Additionally, their role in autophagy activation can either deter or facilitate carcinogenesis, depending on the carcinogenesis stage and type [267]. Consequently, the impact of Sestrins on cell viability may differ based on the stress type, resulting in varying effects within tumours.

1.7.2.1. Sestrins and follicular lymphomas

The 6q21 locus, which includes *SESN1*, frequently undergoes deletion in human follicular lymphomas, and SESN1 expression is notably reduced in lymphomas that express the mutant EZH2X641Y protein [268]. EZH2, a crucial component of the Polycomb Repressive Complex 2 and a histone-lysine N-methyltransferase, catalyses the methylation of histone H3 on lysine 27, effectively repressing gene expression—a process vital for lymphocyte maturation [269].

The EZH2X641Y mutation in lymphoma cells leads to mTORC1 activation via a SESN1-dependent mechanism. This activation of mTORC1 is implicated in the progression of leukaemia, as evidenced by the observation that mTORC1 inhibition suppresses stem cell proliferation and leukaemia advancement [270].

1.7.2.2. Sestrins and lung cancer

The involvement of Sestrins in lung carcinogenesis remains debated. SESN1 and SESN2 frequently exhibit reduced expression in lung tumours, with decreased SESN2 levels marking a poor prognosis for lung cancer patients [253, 254]. The loss of SESN1 and SESN2 in A549 lung adenocarcinoma cells facilitates tumour growth and enhances resistance to apoptosis [159, 254, 271]. Interestingly, *Sesn2* knockout in mice suppresses early-stage lung tumour growth, which may be linked to diminished AKT kinase activity [254]. However, in the A549 cell line obtained from advanced lung adenocarcinoma, SESN2 did not contribute to the activation of AKT and sensitised cancer cells to stress and pro-apoptotic cytokines [159, 254, 271].

1.7.2.3. Sestrins and liver cancer

Unpublished findings from Karin and Budanov suggested that *Sesn2* knockout in mice leads to reduced liver tumour growth in diethylnitrosamine (DEN)-induced liver carcinogenesis models [272]. In contrast, a later study indicated that increased expression of *Sesn3*, another member of the Sestrin family, correlates with improved survival rates in animal models of liver cancer [273]. Experiments involving mice injected with the carcinogen DEN and subsequently fed a choline-deficient high-fat diet showed that *Sesn3* knockout animals developed a greater number and larger, more metastatic tumours compared to control subjects, underscoring the tumour-suppressive role of the *Sesn3* gene [273].

1.7.2.4. Sestrins in prostate cancer

While SESN3 exhibits antiproliferative properties, it has been identified as upregulated in hormone-refractory prostate cancers [274]. This increase in SESN3 expression occurs in prostate carcinoma cells transitioning into hormone-refractory neuroendocrine prostate carcinoma. Such changes may be associated with the reduced expression of micro-RNA-708, which directly interacts with *SESN3* mRNA, thereby diminishing its expression [275].

1.7.2.5. Sestrins in skin cancer

In contrast to Sestrins' recognised tumour-suppressive function across multiple tissues, SESN2 frequently shows elevated expression in various skin cancers, including melanomas and squamous cell carcinomas, acting as an oncogene to promote skin carcinogenesis [276]. This effect may be attributed to SESN2's protective role against ultraviolet and other stressors that threaten cancer cell viability, primarily through the activation of AKT [276, 277].

1.7.2.6. Sestrins in colon cancer

Expression analysis of SESN2 in colorectal cancers revealed it is often downregulated, with its reduced levels linked to advanced tumour stages marked by vascular invasion, lymph node, and liver metastasis. Furthermore, lower SESN2 expression correlates with a poor prognosis and a reduced patient life expectancy [278]. While this pattern may suggest SESN2 inactivation primarily occurs in advanced stages of cancer—where the critical tumour suppressor p53, a significant activator of Sestrins, is frequently inactivated, implying SESN2 downregulation as a secondary effect—research by Ro et al. indicates that Sesn2 knockout in a mouse model of dextran sodium sulphate (DSS)-induced carcinogenesis leads to accelerated tumour growth. This increase is associated with heightened mTORC1 activity and elevated inflammation levels in the colon [279].

1.7.2.7. Sestrins and cancer stem cell

Tumours are recognised for their heterogeneous cell composition, mirroring the diversity seen in normal tissues. Various cell types collaborate to support the tumour with adaptive mechanisms for survival and propagation within the host. Recent research highlights that cancer growth and spread are often propelled by cancer stem cells. They are noted for their unlimited proliferative capacity, stress resistance, and ability to differentiate into various cancer cell subtypes. These cells also exhibit heightened resistance to cancer treatments [280]. Putative cancer stem cells, or so-called tumour-initiating cells with stem-like properties, have been identified in a range of cancers, including leukaemia [281], lung carcinoma [282, 283], hepatocarcinoma [284, 285], colon carcinoma [286], melanoma [287], squamous carcinoma [288], prostate carcinoma, and other types of cancer [280]. While the involvement of cancer stem cells in follicular lymphoma remains debated, tumour-initiating cells possessing stem-like qualities have been reported for these cancer types [289].

The function of Sestrins in regulating both stem cell and cancer cell activities remains unclear. However, some tumour-regulating effects of Sestrins could stem from their involvement in transforming stem cells into cancer stem cells. This transformation may occur through mutations that enable stem cells to bypass senescence and apoptosis, processes often linked with Sestrin activation, or through Sestrins' suppression of stem-like properties in "differentiated" cancer cells. This suppression allows them to continually differentiate and develop resistance to cancer treatments [280]. Nonetheless, defining specific genes of interest in certain cancer cell types is challenging due to the criteria for identifying cancer stem cells.

The activity of SESN3 in liver cancer was examined for its impact on cancer stem cell function. Tumours lacking SESN3 exhibited increased AKT and STAT3 activities and showed elevated levels of stem cell markers, including Acta2, Cd44, and Cd133 [273]. Moreover, the same

study showed that SESN3 might regulate stemness by sequestering the transcription factor Gli2 in the cytoplasm through direct protein-protein interactions. However, as the SESN3-Gli2 interaction was shown via an overexpression study in 293T cells, this hypothesis requires validation using endogenous protein from liver cells [273]. Nevertheless, the support of stemness through the regulation of Gli2, AKT and STAT3 may represent a crucial pathway through which SESN3 may counteract liver carcinogenesis.

In follicular lymphomas, mutation or inactivation of the EZH2 gene may lead to SESN1 downregulation and mTORC1 activation [268]. EZH2, often elevated in leukaemias and other cancers, may promote lymphoma stem cell proliferation and resistance to chemotherapy and radiotherapy [290], suggesting that SESN1 inhibition by EZH2 could enhance stem/progenitor cell proliferation in blood cancers and other types. Sestrins are also suggested to counteract stemness in various cancers, including lung and colon, where their anticarcinogenic roles have been noted. Studies have identified stem-like cells in adenocarcinoma A549, H2170, and colon carcinoma cells HCT116, SW480 [291, 292], suggesting that Sestrins may influence stemness potentially through TGFβ and hedgehog signalling regulation. Conversely, SESN2's role in activating AKT might protect skin stem cells from DNA damage, suggesting an intricate balance between SESN2-AKT signalling benefits and SESN2's antitumor effects. Therefore, the differential impact of Sestrin family members on various stem cells may derive from their specific environmental contexts and distinct roles in stem cell-specific signalling pathways.

1.8. Hypotheses and Aims

Previously, Sestrins have been extensively researched for their role in metabolism, antioxidative defence, and mTORC1 signalling. Overactive mTORC1 is a frequent occurrence in cancer, leading to uncontrolled cell growth and proliferation. Prior studies have demonstrated that p53-inducible Sestrins play a significant role in regulating cell death, particularly in the context of cancer [254, 271]. Furthermore, these studies suggested opposing roles for Sestrins in various stages of cancer [254]. Unpublished preliminary research suggests that SESN1&2-deficient A549 cells are resistant to cisplatin. Our investigation will aim to characterise cell death and the possible mechanisms through which SESN1 and SESN2 may influence cancer cell death and proliferation, as well as their potential implications in therapeutic resistance.

1.8.1. Hypotheses

1. *Sestrins inhibit mTORC1 signalling to suppress malignant cell proliferation*

SESN1 and SESN2 function as inhibitors of mTORC1 activity, potentially suppressing cancer cell growth and proliferation. Their interaction with the GATOR2 complex and AMPK is crucial to their effect on mTORC1, and these pathways may be deregulated in cancer.

2. *Sestrins may promote apoptosis through p53-dependent pathways*

SESN1 and SESN2 are key mediators of apoptosis in cancer cells, operating through p53-dependent pathways. Upon activation by p53, these Sestrins are hypothesised to enhance the expression of pro-apoptotic factors and reduce the survival of damaged or malignant cells, thereby contributing to the prevention of tumour growth.

3. *Sestrins may modulate chemotherapy resistance in cancer*

SESN1 and SESN2 play a crucial role in modulating the sensitivity of cancer cells to chemotherapeutic agents. The inactivation of these Sestrins is hypothesised to confer resistance to drugs like cisplatin by altering key signalling pathways involved in cell survival and DNA repair, thus posing a challenge to effective cancer treatment.

1.8.2. Aims

1. *To elucidate the role of SESN1 and SESN2 in regulating mTORC1 signalling and its impact on cell proliferation*

We aim to investigate how SESN1 and SESN2 interact with the mTORC1 signalling pathway to regulate cancer cell growth. To determine if Sestrins influence upstream or downstream signalling of mTORC1 in the context of cancer, and thus their implication for cell death and proliferation.

2. *To investigate the mechanisms by which SESN1 and SESN2 mediate cell death in cancer*

We will attempt to determine the pathways through which SESN1 and SESN2 influence cell death in cancer cells. We will also explore the involvement of p53 and other downstream effectors in SESN-mediated cell death, providing insights into how Sestrins contribute to the suppression of malignant cells.

3. *To assess the role of SESN1 and SESN2 in chemotherapy resistance and identify potential therapeutic targets*

We will examine the role of SESN1 and SESN2 in the development of resistance to chemotherapeutic agents. Investigate how the inactivation or overexpression of these Sestrins affects cancer cell survival pathways, and thus sensitivity to drugs like cisplatin, aiming to identify potential targets for combating therapeutic resistance in cancer treatment.

1.9. APPENDICES

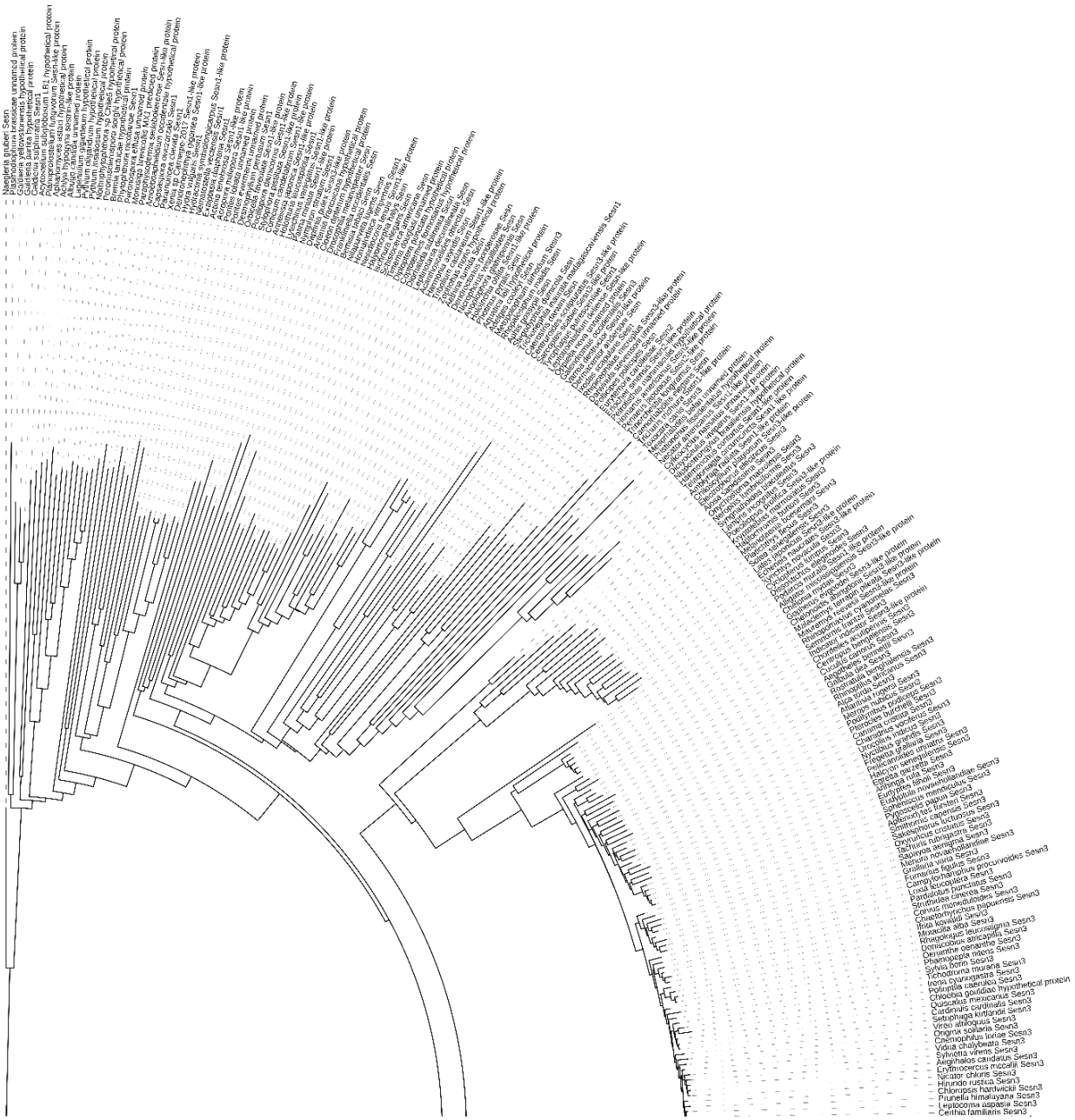

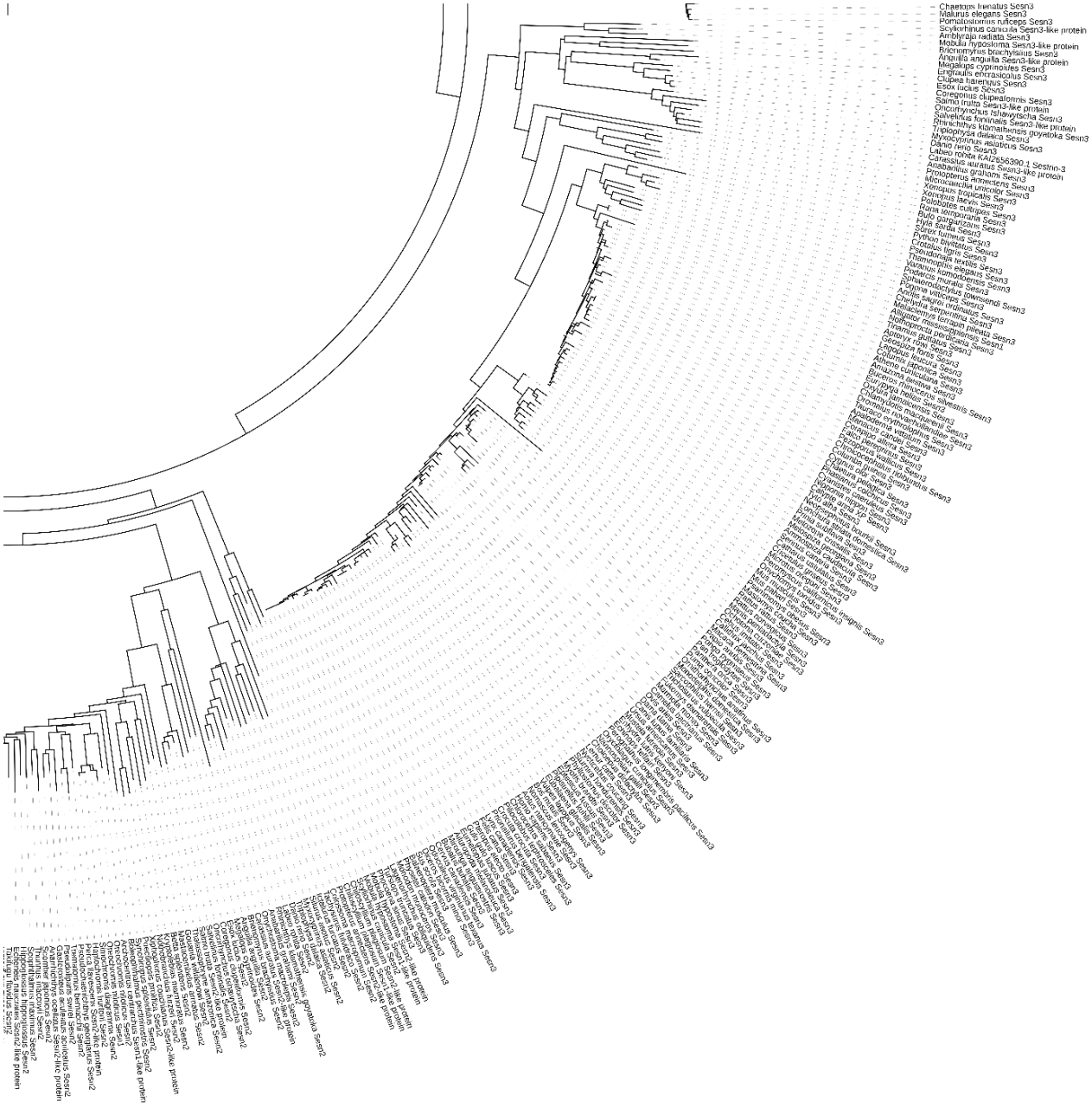
Chaetops frenatus Sesn3
Malurus elegans Sesn3
Pomatostomus ruficeps Sesn3
Scalenchinus coricula Sesn3-like protein
Amblyraja radiata Sesn3
Mobula hypostoma Sesn3-like protein
Rhinemmylus brachysalus Sesn3
Anguilla anguilla Sesn3-like protein
Megalops cyprinoides Sesn3
Engraulis ehrenbaumi Sesn3
Clupea harengus Sesn3
Esox lucius Sesn3
Coregonus clupeaformis Sesn3
Salmo trutta Sesn3-like protein
Oncorhynchus tshawytscha Sesn3
Salvelinus fontinalis Sesn3-like protein
Rhinichthys klamathensis goyatkai Sesn3
Triplophysa dalelica Sesn3
Myxocyprinus asiaticus Sesn3
Danio rerio Sesn3
Labeo rohita KAI2656390.1 Sestrin-3
Carassius auratus Sesn3-like protein
Anabarilius grahami Sesn3
Prognathus Annectens Sesn3
Microcaecilia unicolor Sesn3
Xenopus tropicalis Sesn3
Xenopus laevis Sesn3
Palobates bulrigeri Sesn3
Rana temporaria Sesn3
Bufo gargarizans Sesn3
Hyla sarda Sesn3
Sorex fumeus Sesn3
Python bivittatus Sesn3
Crotalus tigris Sesn3
Pseudonaja textilis Sesn3
Thamnophis elegans Sesn3
Varanus komodoensis Sesn3
Eublepharis macularius Sesn3
Sphaerodactylus townsendi Sesn3
Anolis vittigerus Sesn3
Chelydra serpentina Sesn3
Malaclemys terrapin Sesn3
Alligator mississippiensis Sesn3
Anseranas semipalmata Sesn3
Dendrocygna arcuata Sesn3
Anas platyrhynchos Sesn3
Gallus gallus Sesn3
Meleagris gallopavo Sesn3
Colinus virginianus Sesn3
Callipepla squamata Sesn3
Tympanuchus cupido Sesn3
Phasianus colchicus Sesn3
Chrysolophus pictus Sesn3
Numida meleagris Sesn3
Balearica regulorum Sesn3
Grus americana Sesn3
Aramus guarauna Sesn3
Rallus elegans Sesn3
Gallinula chloropus Sesn3
Fulica atra Sesn3
Haematopus ostralegus Sesn3
Recurvirostra avosetta Sesn3
Himantopus himantopus Sesn3
Glareola pratincola Sesn3
Charadrius vociferus Sesn3
Pluvialis squatarola Sesn3
Vanellus vanellus Sesn3
Calidris pugnax Sesn3
Limosa lapponica Sesn3
Numenius phaeopus Sesn3
Tringa totanus Sesn3
Actitis macularius Sesn3
Arenaria interpres Sesn3
Gallinago gallinago Sesn3
Scolopax rusticola Sesn3
Phoenicopterus ruber Sesn3
Podiceps cristatus Sesn3
Phaethon lepturus Sesn3
Sula sula Sesn3
Fregata magnificens Sesn3
Pelecanus crispus Sesn3
Nipponia nippon Sesn3
Egretta garzetta Sesn3
Ardea alba Sesn3
Nycticorax nycticorax Sesn3
Cathartes aura Sesn3
Gymnogyps californianus Sesn3
Haliaeetus leucocephalus Sesn3
Accipiter nisus Sesn3
Buteo buteo Sesn3
Aquila chrysaetos Sesn3
Falco peregrinus Sesn3
Falco cherrug Sesn3
Falco tinnunculus Sesn3
Psittacus erithacus Sesn3
Melopsittacus undulatus Sesn3
Nestor notabilis Sesn3
Cacatua galerita Sesn3
Eolophus roseicapillus Sesn3
Agapornis roseicollis Sesn3
Psittacula krameri Sesn3
Amazona aestiva Sesn3
Ara macao Sesn3
Aratinga solstitialis Sesn3
Cuculus canorus Sesn3
Tauraco erythrolophus Sesn3
Coccyzus americanus Sesn3
Geococcyx californianus Sesn3
Tyto alba Sesn3
Strix occidentalis Sesn3
Bubo bubo Sesn3
Athene cunicularia Sesn3
Strix nebulosa Sesn3
Caprimulgus carolinensis Sesn3
Chordeiles minor Sesn3
Nyctibius grandis Sesn3
Antrostomus vociferus Sesn3
Podargus strigoides Sesn3
Colius striatus Sesn3
Leptosomus discolor Sesn3
Trogon elegans Sesn3
Pharomachrus mocinno Sesn3
Merops nubicus Sesn3
Coracias garrulus Sesn3
Eurystomus orientalis Sesn3
Upupa epops Sesn3
Phoeniculus purpureus Sesn3
Buceros rhinoceros Sesn3
Bucorvus leadbeateri Sesn3
Anthracoceros albirostris Sesn3
Aceros nipalensis Sesn3
Tockus nasutus Sesn3
Ramphastos vitellinus Sesn3
Pteroglossus aracari Sesn3
Megalaima virens Sesn3
Psilopogon haemacephalus Sesn3
Jynx torquilla Sesn3
Picus canus Sesn3
Dendrocopos major Sesn3
Melanerpes formicivorus Sesn3
Sphyrapicus varius Sesn3
Colaptes auratus Sesn3
Dryocopus pileatus Sesn3
Campephilus principalis Sesn3
Picoides pubescens Sesn3
Leiothlypis peregrina Sesn3
Setophaga ruticilla Sesn3
Cardellina pusilla Sesn3
Geothlypis trichas Sesn3
Icteria virens Sesn3
Mimus polyglottos Sesn3
Toxostoma rufum Sesn3
Sturnus vulgaris Sesn3
Acridotheres tristis Sesn3
Gracula religiosa Sesn3
Corvus brachyrhynchos Sesn3
Pica pica Sesn3
Cyanocitta cristata Sesn3
Perisoreus canadensis Sesn3
Nucifraga columbiana Sesn3
Garrulus glandarius Sesn3
Pyrrhocorax pyrrhocorax Sesn3
Corvus corax Sesn3
Corvus cornix Sesn3
Corvus frugilegus Sesn3
Corvus monedula Sesn3
Corvus moneduloides Sesn3
Corvus hawaiiensis Sesn3
Corvus ossifragus Sesn3
Corvus caurinus Sesn3
Corvus imparatus Sesn3
Corvus brachyrhynchos Sesn3
Corvus corone

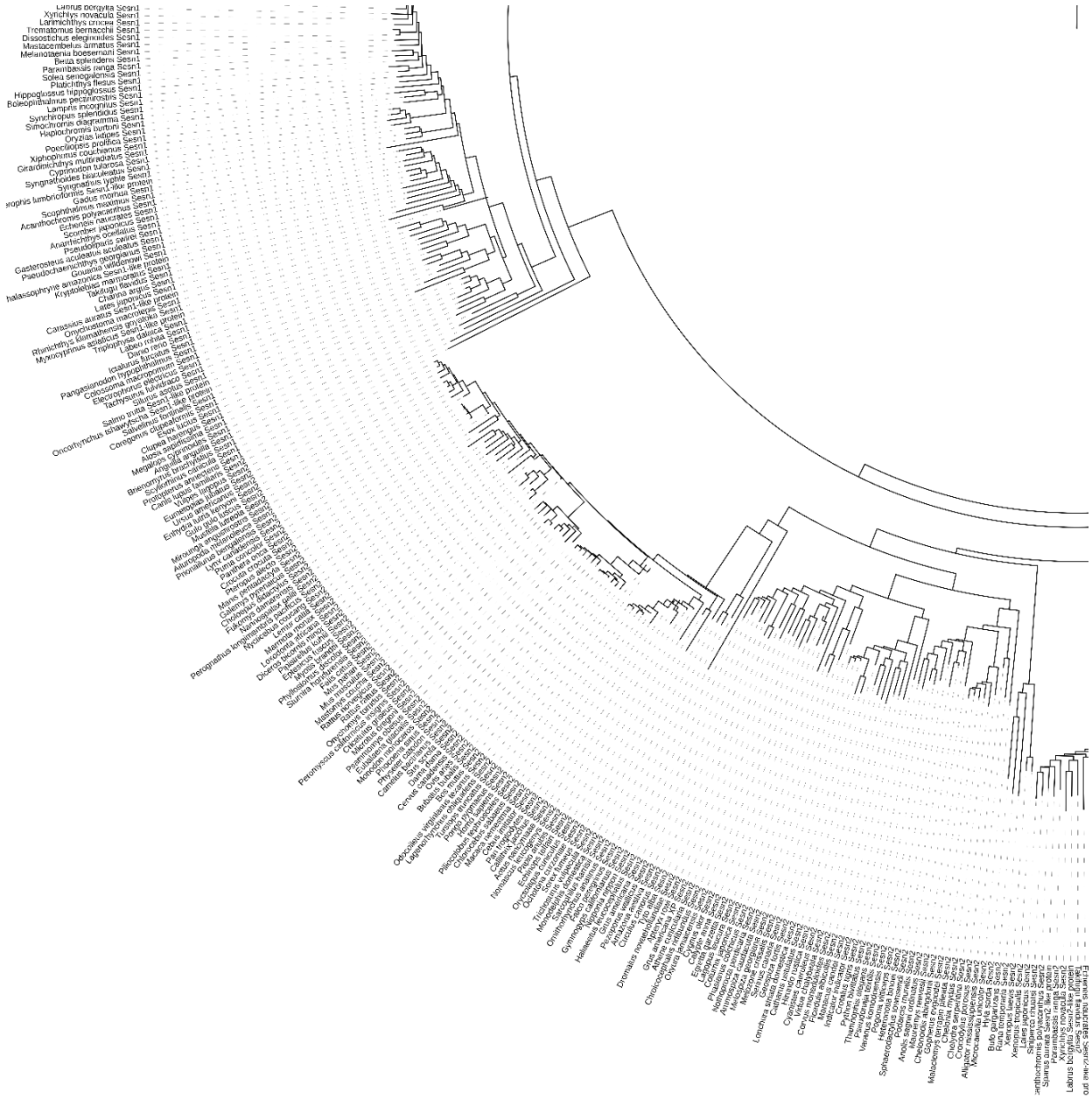
Larimichthys crocea Sesn1
Trematomus bernacchii Sesn1
Dissostichus eleginoides Sesn1
Mastacembelus armatus Sesn1
Melanotaenia boesemani Sesn1
Betta splendens Sesn1
Parambassis ranga Sesn1
Solea senegalensis Sesn1
Plectorhinchus flavomaculatus Sesn1
Hippoglossus hippoglossus Sesn1
Boleophthalmus pectinirostris Sesn1
Lampris incognitus Sesn1
Synchropus sphenidius Sesn1
Simochromis diagramma Sesn1
Haplochromis burtoni Sesn1
Oryzias latipes Sesn1
Poecilopsis prolifica Sesn1
Xiphophorus couchianus Sesn1
Girardinichthys multiradiatus Sesn1
Cyprinodon tularosa Sesn1
Myoxocephalus brandtii Sesn1
Syngnathoides biaculeatus Sesn1
Syngnathus typhle Sesn1
Hippocampus kuda Sesn1
Gadus morhua Sesn1
Scophthalmus maximus Sesn1
Acanthochromis polyacanthus Sesn1
Echeneis naucrates Sesn1
Scomber japonicus Sesn1
Anarhichthys ocellatus Sesn1
Pseudopleuronectes yokohamae Sesn1
Gasterosteus aculeatus Sesn2
Pseudochaenichthys georgianus Sesn1
Gouania willdenowi Sesn1-like protein
Takifugu flavidus Sesn1
Takifugu rubripes Sesn1
Lates japonicus Sesn1
Carassius auratus Sesn1-like protein
Onychostoma macrolepis Sesn1
Rhynchocypris lagowskii Sesn1
Myxocyprinus asiaticus Sesn1
Triplophysa dalaica Sesn1
Labeo rohita Sesn1
Danio rerio Sesn1
Ictalurus furcatus Sesn1
Pangasianodon hypophthalmus Sesn1
Colossoma macropomum Sesn1
Electrophorus electricus Sesn1
Tachysurus fulvidraco Sesn1
Silurus asotus Sesn1-like protein
Salmo trutta Sesn1-like protein
Oncorhynchus tshawytscha Sesn1
Stylephorus chordatus Sesn1
Coregonus clupeaformis Sesn1
Esox lucius Sesn1
Clupea harengus Sesn1
Ausia sp. Sesn1
Megalops cyprinoides Sesn1
Anguilla anguilla Sesn1
Brienomyrus brachyistius Sesn1
Scyphurinus ramicirris Sesn1
Protobrama ambiens Sesn1
Carlia fusca Sesn1
Vidua macroura Sesn1
Eremophila alpestris Sesn1
Ursus americanus Sesn1
Erithrura gouldiae Sesn1
Gyo gelid Sesn1
Merops nubicus Sesn1
Mirounga angustirostris Sesn1
Alligator mississippiensis Sesn1
Phrynops hilarii Sesn1
Lynx canadensis Sesn1
Panthera pardus Sesn1
Crocuta crocuta Sesn1
Phascolarctos cinereus Sesn1
Manis pentadactyla Sesn1
Callimys rhinolophus Sesn1
Chlorocebus aethiops Sesn1
Rhinopithecus roxellana Sesn1
Nomascus leucogenys Sesn1
Nannospalax galili Sesn1
Lemur catta Sesn1
Microtus ochrogaster Sesn1
Mirounga leonina Sesn1
Loxodonta africana Sesn1
Dicerorhinus sumatrensis Sesn1
Equus caballus Sesn1
Phyllostomus discolor Sesn1
Myotis lucifugus Sesn1
Sturnira hondurensis Sesn1
Felis catus Sesn1
Mus musculus Sesn1
Mastacembelus armatus Sesn1
Rattus norvegicus Sesn1
Oryctolagus cuniculus Sesn1
Peromyscus californicus Sesn1
Cricetulus griseus Sesn1
Meriones unguiculatus Sesn1
Peromyscus maniculatus Sesn1
Microtus ochrogaster Sesn1
Ictidomys tridecemlineatus Sesn1
Physeter catodon Sesn1
Camelus bactrianus Sesn1
Camelus dromedarius Sesn1
Vicugna pacos Sesn1
Bos taurus Sesn1
Cervus elaphus Sesn1
Capra hircus Sesn1
Ovis aries Sesn1
Odocoileus virginianus texanus Sesn1
Lagenorhynchus obliquidens Sesn1
Tursiops truncatus Sesn1
Orcinus orca Sesn1
Delphinapterus leucas Sesn1
Monodon monoceros Sesn1
Pteropus alecto Sesn1
Pteropus vampyrus Sesn1
Myotis davidii Sesn1
Myotis brandtii Sesn1
Myotis myotis Sesn1
Myotis lucifugus Sesn1
Sturnira hondurensis Sesn1
Ailuropoda melanoleuca Sesn1
Ursus maritimus Sesn1
Ursus americanus Sesn1
Ursus arctos horribilis Sesn1
Ursus arctos Sesn1
Ursus maritimus Sesn1
Ursus americanus Sesn1
Ursus arctos horribilis Sesn1
Ursus arctos Sesn1
Canis lupus familiaris Sesn1
Canis lupus dingo Sesn1
Canis lupus Sesn1
Canis lupus familiaris Sesn1
Canis lupus dingo Sesn1
Canis lupus Sesn1
Vulpes vulpes Sesn1
Vulpes lagopus Sesn1
Vulpes vulpes Sesn1
Vulpes lagopus Sesn1
Mustela putorius furo Sesn1
Mustela nigripes Sesn1
Mustela putorius furo Sesn1
Mustela nigripes Sesn1
Enhydra lutris kenyoni Sesn1
Enhydra lutris Sesn1
Lontra canadensis Sesn1
Aonyx capensis Sesn1
Leptonychotes weddellii Sesn1
Hydrurga leptonyx Sesn1
Mirounga leonina Sesn1
Mirounga angustirostris Sesn1
Odobenus rosmarus divergens Sesn1
Odobenus rosmarus rosmarus Sesn1
Zalophus californianus Sesn1
Eumetopias jubatus Sesn1
Callorhinus ursinus Sesn1
Neophoca cinerea Sesn1
Phoca vitulina Sesn1
Halichoerus grypus Sesn1
Pusa hispida Sesn1
Pusa caspica Sesn1
Pusa sibirica Sesn1
Mirounga leonina Sesn1
Mirounga angustirostris Sesn1
Odobenus rosmarus divergens Sesn1
Odobenus rosmarus rosmarus Sesn1
Zalophus californianus Sesn1
Eumetopias jubatus Sesn1
Callorhinus ursinus Sesn1
Neophoca cinerea Sesn1
Phoca vitulina Sesn1
Halichoerus grypus Sesn1
Pusa hispida Sesn1
Pusa caspica Sesn1
Pusa sibirica Sesn1
Dromaius novaehollandiae Sesn1
Struthio camelus Sesn1
Gallus gallus Sesn1
Meleagris gallopavo Sesn1
Anas platyrhynchos Sesn1
Chrysolophus pictus Sesn1
Coturnix japonica Sesn1
Colinus virginianus Sesn1
Callipepla squamata Sesn1
Numida meleagris Sesn1
Phasianus colchicus Sesn1
Meleagris gallopavo Sesn1
Anas platyrhynchos Sesn1
Chrysolophus pictus Sesn1
Coturnix japonica Sesn1
Colinus virginianus Sesn1
Callipepla squamata Sesn1
Numida meleagris Sesn1
Phasianus colchicus Sesn1
Gallus gallus Sesn1
Struthio camelus Sesn1
Dromaius novaehollandiae Sesn1
Corvus brachyrhynchos Sesn1
Corvus cornix cornix Sesn1
Corvus moneduloides Sesn1
Corvus hawaiiensis Sesn1
Corvus corone Sesn1
Corvus cornix cornix Sesn1
Corvus moneduloides Sesn1
Corvus hawaiiensis Sesn1
Corvus corone Sesn1
Corvus brachyrhynchos Sesn1
Alligator mississippiensis Sesn1
Chrysemys picta bellii Sesn1
Gopherus agassizii Sesn1
Chelonia mydas Sesn1
Pelodiscus sinensis Sesn1
Chelonia mydas Sesn1
Gopherus agassizii Sesn1
Chrysemys picta bellii Sesn1
Pelodiscus sinensis Sesn1
Alligator mississippiensis Sesn1
Crocodylus porosus Sesn1
Gavialis gangeticus Sesn1
Crocodylus porosus Sesn1
Gavialis gangeticus

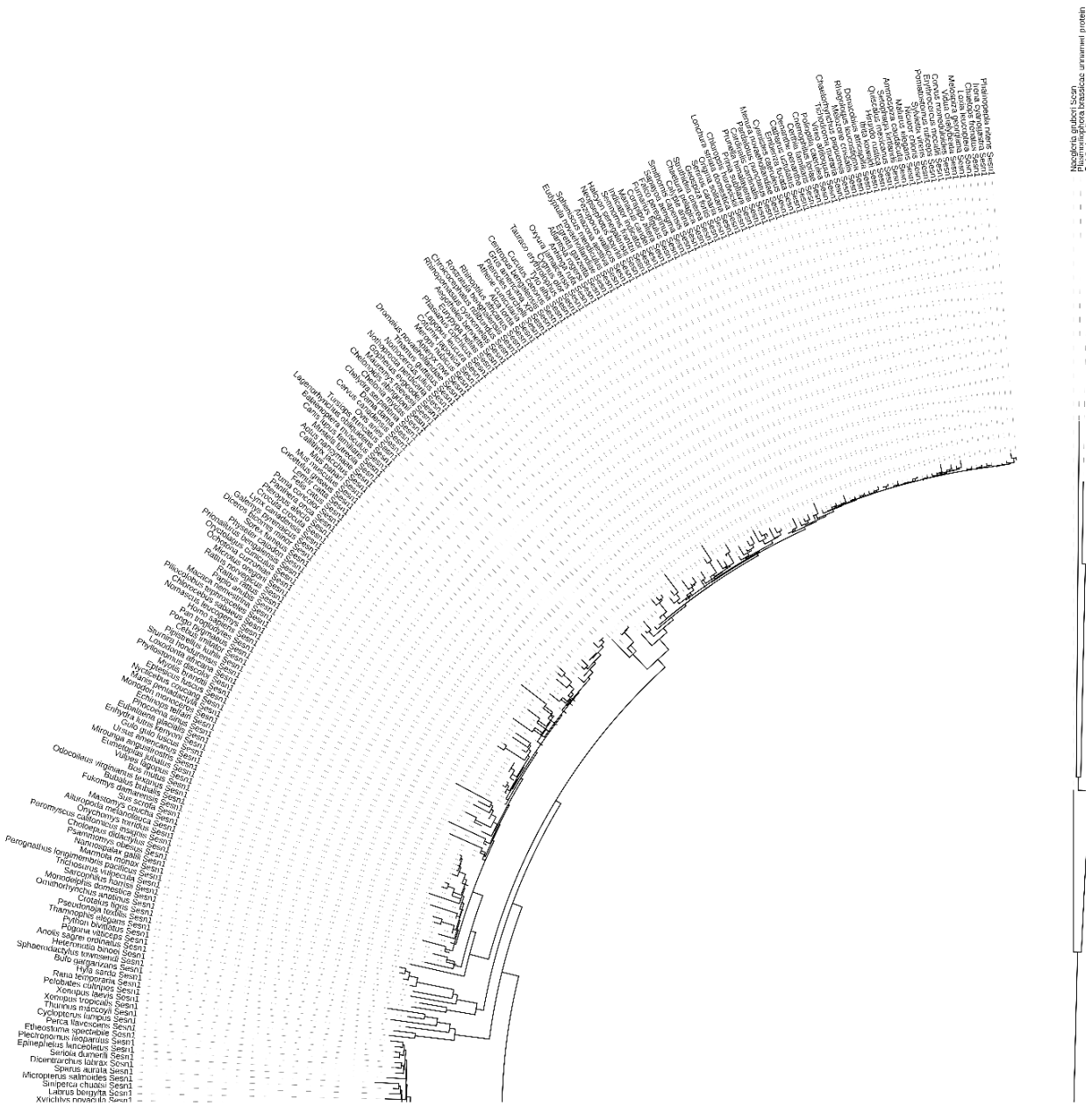

APPENDIX A: The phylogenetic tree in quarters. A closer look at the phylogenetic tree displayed in Figure 1, with individual annotations of every leaf.

POSITION	71	72	73	74	75	76	77	78	79	80	81	82	83	84	85	86
SESN2	M	S	S	G	R	V	D	N	L	A	V	V	M	G	L	H
Consens	A	T	L	G	R	L	D	N	I	T	Q	V	M	G	L	H
% of entries	29.8	26.1	36	84.1	83.2	60.7	75.9	62.4	43.5	62.1	32.3	73	91.9	44.7	37.5	98
Number of proteins	**240**	**210**	**290**	**677**	**670**	**489**	**611**	**502**	**350**	**500**	**260**	**588**	**740**	**360**	**302**	**789**

POSITION	87	88	89	90	91	92	93	94	95	96	97	98	99	100	101	102
SESN2	P	D	Y	F	T	S	F	W	R	L	H	Y	L	L	L	H
Consens	P	Q	Y	L	E	S	F	L	R	T	Q	H	Y	L	L	Q
% of entries	78.5	66.2	98.4	92.4	53.3	73.9	96.8	74.7	47	64.3	81.7	50.9	64.1	71.3	82.1	98
Number of proteins	**632**	**533**	**792**	**744**	**429**	**595**	**779**	**601**	**378**	**518**	**658**	**410**	**516**	**574**	**661**	**789**

POSITION	103	104	105	106	107	108	109	110	111	112	113	114	115	116	117	118
SESN2	T	D	G	P	L	A	S	S	W	R	H	Y	I	A	I	M
Consens	M	D	G	P	L	P	L	H	Y	R	H	Y	I	A	I	M
% of entries	69.8	93.8	98.9	96.3	98.9	79.6	53.5	46.1	49.1	98.4	93.8	95.5	96.1	63.5	90.8	96
Number of proteins	**562**	**755**	**796**	**775**	**796**	**641**	**431**	**371**	**395**	**792**	**755**	**769**	**774**	**511**	**731**	**773**

POSITION	119	120	121	122	123	124	125	126	127	128	129	130	131	132	133	134
SESN2	A	A	A	R	H	Q	C	S	Y	L	V	G	S	H	M	A
Consens	A	A	A	R	H	Q	C	S	Y	L	V	N	L	H	V	N
% of entries	98	94.8	89.6	97.1	97	81.4	99	75.9	94.5	96.8	75	62	58.6	88.7	59.1	31.6
Number of proteins	**789**	**763**	**721**	**782**	**781**	**655**	**797**	**611**	**761**	**779**	**604**	**499**	**472**	**714**	**476**	**254**

POSITION	135	136	137	138	139	140	141	142	143	144	145	146	147	148	149	150
SESN2	E	F	L	Q	T	G	G	D	P	E	W	L	L	G	L	H
Consens	E	F	L	Q	V	G	G	D	P	K	W	L	N	G	L	E
% of entries	44.1	98.8	91.4	28.6	40.7	96.3	97.6	65.7	62.1	32.9	99.6	98.3	47.6	97.8	94.5	52
Number of proteins	**355**	**795**	**736**	**230**	**328**	**775**	**786**	**529**	**500**	**265**	**802**	**791**	**383**	**787**	**761**	**419**

POSITION	151	152	153	154	155	156	157	158	159	160	161	162	163	164	165	166
SESN2	R	A	P	E	K	L	R	K	L	S	E	I	N	K	L	L
Consens	N	A	P	Q	K	L	R	N	L	N	E	I	N	K	L	L
% of entries	23.4	58.3	97	57.6	78.3	94.8	46.1	61.9	98.6	38.8	82.6	55.4	97.6	93.7	40.6	98.6
Number of proteins	**188**	**469**	**781**	**464**	**630**	**763**	**371**	**498**	**794**	**312**	**665**	**446**	**786**	**754**	**327**	**794**

POSITION	167	168	169	170	171	172	173	174	175	176	177	178	179	180	181	182
SESN2	A	H	R	P	W	L	I	T	K	E	H	I	Q	A	L	L
Consens	A	H	R	P	W	L	I	T	K	E	H	I	E	K	L	L
% of entries	98.8	99.5	90.8	99.6	99.6	96.3	75.3	84.7	82.9	76.6	95.9	94.7	56.1	32.5	98.5	65.7
Number of proteins	**795**	**801**	**731**	**802**	**802**	**775**	**606**	**682**	**667**	**617**	**772**	**762**	**452**	**262**	**793**	**529**

POSITION	183	184	185	186	187	188	189	190	191	192	193	194	195	196	197	198
SESN2	K	T	G	E	H	T	W	S	L	A	E	L	I	Q	A	L
Consens	K	T	G	E	N	S	W	S	L	A	E	L	V	H	A	V
% of entries	84.6	44.7	18.9	83.6	34	66.3	99.1	98.9	94.9	74.7	98.1	94.8	54.5	74.3	98.3	70.8
Number of proteins	**681**	**360**	**152**	**673**	**274**	**534**	**798**	**796**	**764**	**601**	**790**	**763**	**439**	**598**	**791**	**570**

POSITION	199	200	201	202	203	204	205	206	207	208	209	210	211	212	213	214
SESN2	V	L	L	T	H	C	H	S	L	S	S	F	V	F	G	C
Consens	V	L	L	T	H	Y	H	S	L	A	S	F	V	F	G	C
% of entries	92.9	87	89.6	50.8	94.9	58	98.3	63.5	96.5	77.1	97	96.1	62.1	83.7	95.4	75.9
Number of proteins	**748**	**700**	**721**	**409**	**764**	**467**	**791**	**511**	**777**	**621**	**781**	**774**	**500**	**674**	**768**	**611**

POSITION	215	216	217	218	219	220	221	222	223	224	225	226	227	228	229	230
SESN2	G	I	L	P	E	G	D	A	D	G	S	P	A	P	Q	A
Consens	G	I	N	P	E	I	D	C	D	G	G	H	T	F	R	P
% of entries	95.9	72.7	34.5	74.7	78.5	36.1	54.7	28.3	27.8	67.1	48.7	40.7	40.2	52.3	51.6	46.6
Number of proteins	**772**	**585**	**278**	**601**	**632**	**291**	**440**	**228**	**224**	**540**	**392**	**328**	**324**	**421**	**415**	**375**

POSITION	231	232	233	234	235
SESN2	P	T	P	P	S
Consens	P	S	V	S	N
% of entries	51.4	66.7	38.4	33.8	21.7
Number of proteins	**414**	**537**	**309**	**272**	**175**

POSITION	255	256	257	258	259	260	261	262	263	264	265	275	276	277	278	279
SESN2	A	R	D	V	E	A	L	M	E	R	M	D	E	G	T	S
Consens	L	S	E	V	E	A	L	M	E	R	M	E	E	E	A	S
% of entries	17	18.4	76.6	60.5	77.9	51.4	96.9	78.3	77.8	65.7	91.4	47.6	41.9	62	58.8	66.3
Number of proteins	**137**	**148**	**617**	**487**	**627**	**414**	**780**	**630**	**626**	**529**	**736**	**383**	**337**	**499**	**473**	**534**

POSITION	280	281	282	319	320	321	322	323	324	325	326	327	328	329	330	331
SESN2	Q	E	E	P	T	F	G	Y	E	D	F	T	R	R	G	A
Consens	Q	E	E	P	S	F	G	Y	K	D	F	A	R	R	G	E
% of entries	75.3	91.7	93.9	64.3	35.2	64.1	80.2	98.4	46.7	96.1	98.8	42.4	82.9	70.3	78	57
Number of proteins	**606**	**738**	**756**	**518**	**283**	**516**	**646**	**792**	**376**	**774**	**795**	**341**	**667**	**566**	**628**	**459**

POSITION	332	333	334	335	336	337	338	339	340	341	342	343	344	345	346	347
SESN2	Q	A	P	P	T	F	R	A	Q	D	Y	T	W	E	D	H
Consens	Q	A	V	P	T	F	R	A	Q	D	Y	S	W	E	D	H
% of entries	23.5	18.5	32.7	78.6	82.6	87.3	92.5	47.3	94	97	93.9	55.4	99.9	91.2	77.5	98
Number of proteins	**23.5**	**18.5**	**32.7**	**78.6**	**82.6**	**87.3**	**92.5**	**47.3**	**94**	**97**	**93.9**	**55.4**	**99.9**	**91.2**	**77.5**	**98**

POSITION	189	149	263	633	665	703	745	381	757	781	756	446	804	734	624	789
SESN2	G	Y	S	L	I	Q	R	L	Y	P	G	Q	L	L	D	E
Consens	G	F	S	L	V	N	R	L	Y	P	G	Q	L	L	D	E
% of entries	97.6	50.7	98.3	98.3	74.2	85.6	96.6	95.3	90.8	59	93	60	88	88.3	97.3	85.8
Number of proteins	**786**	**408**	**791**	**791**	**597**	**689**	**778**	**767**	**731**	**475**	**749**	**483**	**708**	**711**	**783**	**691**

POSITION	366	367	368	369	370	371	372	373	374	375	376	377	378	379	380	384
SESN2	K	F	Q	A	A	Y	S	L	T	Y	N	T	I	A	M	V
Consens	K	F	Q	M	A	Y	N	L	T	Y	N	T	M	A	M	V
% of entries	94	99.3	34.4	32.7	49.7	71.3	65	97.8	87.7	86.7	70.3	77.3	76.4	84.8	46.3	85.1
Number of proteins	**757**	**799**	**277**	**263**	**400**	**574**	**523**	**787**	**706**	**698**	**566**	**622**	**615**	**683**	**373**	**685**

POSITION	385	386	387	388	389	390	391	392	393	394	395	396	397	398	399	400
SESN2	D	T	S	V	L	R	R	A	I	W	N	Y	I	H	C	V
Consens	D	T	S	M	L	R	R	A	I	W	N	Y	I	H	C	M
% of entries	87.8	87.7	69.1	55.2	77.4	87.6	87.7	89.3	69.6	81.6	96.6	100	70.3	92.7	92.4	62.5
Number of proteins	**707**	**706**	**556**	**444**	**623**	**705**	**706**	**719**	**560**	**657**	**778**	**805**	**566**	**746**	**744**	**503**

POSITION	401	402	403	404	405	406	407	408	409	410	411	412	413	414	415	416
SESN2	F	G	I	R	Y	D	D	Y	D	Y	G	E	V	N	Q	L
Consens	F	G	I	R	Y	D	D	Y	D	Y	G	E	V	N	Q	L
% of entries	77.6	100	98.3	95	86.7	100	99.9	99.8	94.4	100	78.6	90.6	65.2	98.8	83.1	96.3
Number of proteins	**625**	**805**	**791**	**765**	**698**	**805**	**804**	**803**	**760**	**805**	**633**	**729**	**525**	**795**	**669**	**775**

POSITION	417	418	419	420	421	422	423	424	425	426	427	428	429	430	431	432
SESN2	L	E	R	N	L	K	V	Y	I	K	T	V	A	C	Y	P
Consens	L	E	R	S	L	K	V	Y	I	K	T	V	V	C	Y	P
% of entries	97.9	61.4	95.3	64.5	61.9	99.1	70.3	87.3	89.1	99.4	88.1	78.9	32.9	98.5	53	99.8
Number of proteins	**788**	**494**	**767**	**519**	**498**	**798**	**566**	**703**	**717**	**800**	**709**	**635**	**265**	**793**	**427**	**803**

POSITION	433	434	435	436	437	438	439	440	441	442	443	444	445	446	447	448
SESN2	E	K	T	T	R	R	M	Y	N	L	F	W	R	H	F	R
Consens	E	K	T	T	K	R	M	Y	D	S	F	W	R	Q	F	K
% of entries	93.3	61.2	74.7	81.9	60.1	71.6	76.5	82	53.8	52.7	68.6	87.1	78.1	63.1	92.9	51.7
Number of proteins	**751**	**493**	**601**	**659**	**484**	**576**	**616**	**660**	**433**	**424**	**552**	**701**	**629**	**508**	**748**	**416**

POSITION	449	450	451	452	453	454	455	456	457	458	459	460	461	462	463	464
SESN2	H	S	E	K	V	H	V	N	L	L	L	L	E	A	R	M
Consens	H	S	E	K	V	H	V	N	L	L	L	M	E	A	R	M
% of entries	90.1	98.5	99.9	97.5	92.7	99.3	86.8	94	96.5	87.7	71.7	39.3	99.3	97.3	99.1	82
Number of proteins	**725**	**793**	**804**	**785**	**746**	**799**	**699**	**757**	**777**	**706**	**577**	**316**	**799**	**783**	**798**	**660**

POSITION	465	466	467	468	469	470	471	472	473	474	475	476	477	478	479	480
SESN2	Q	A	A	L	L	Y	A	L	R	A	I	T	R	Y	M	T
Consens	Q	A	E	L	L	Y	A	L	R	A	I	T	R	Y	M	T
% of entries	99.5	98.5	71.9	98.9	97.1	98.6	89.4	97.1	88.1	96.5	85.8	87.8	71.4	78.3	79.1	76.5
Number of proteins	**801**	**793**	**579**	**796**	**782**	**794**	**720**	**782**	**709**	**777**	**691**	**707**	**575**	**630**	**637**	**616**

APPENDIX B: Table of residue conservation across 805 proteins used for the phylogenetic tree in Figure 1

Position – the site of the residue in the SESN2 protein.
SESN2 – the reside at that position of the SESN2 sequence.
Consens – the residue most prevalent in that position in the 805 proteins analysed.
% of entries – the percentage of proteins the consensus residue is found in.
Number of proteins – the number of proteins that this percentage corresponds to.

MEME
Multiple Em for Motif Elicitation

For further information on how to interpret these results please access https://meme-suite.org/m
To get a copy of the MEME software please access https://meme-suite.org.

If you use MEME in your research, please cite the following paper:
Timothy L. Bailey and Charles Elkan, "Fitting a mixture model by expectation maximization to discover motifs

DISCOVERED MOTIFS | MOTIF LOCATIONS | INPUTS & SETTINGS | PROGRAM INFORMATION

DISCOVERED MOTIFS

	Logo	E-value	Sites	Width	More	Submit/Download
1.		2.0e-1050	800	6	↧	⇢
2.		5.7e-1003	802	6	↧	⇢
3.		6.6e-953	797	6	↧	⇢
4.		3.3e-918	796	6	↧	⇢
5.		1.7e-905	778	6	↧	⇢
6.		1.2e-885	794	6	↧	⇢
7.		3.7e-887	800	6	↧	⇢
8.		5.4e-849	799	6	↧	⇢
9.		1.9e-840	800	6	↧	⇢
10.		2.1e-845	784	6	↧	⇢
11.		2.6e-775	707	6	↧	⇢
12.		6.7e-768	793	6	↧	⇢

APPENDIX C: MEME motif discovery using the 805 protein sequences from Figure 1.
Shown are the 6 residue conserved motifs, their statistical significance, the number of sites contributing to the construction of the motif (under Sites).
1 – The domain adjacent to the DYDDY motif, located 6 residues upstream.
2 – A highly conserved motif of unknown function.
3 – The DDYDY motif responsible for GATOR2 binding.

2. CHAPTER 2: MATERIALS AND METHODS

Antibody	Species	Typical dilution	Catalog No.
β-actin	mouse	1:5000	sc-47778
SESN1	rabbit	1:1000	Previously prepared by our group [6]
SESN2	rabbit	1:5000	10795-1-AP
γ-H2AX	rabbit	1:2500	9718
p-p53	mouse	1:2500	9286
p53	mouse	1:5000	sc-47698
p-Chk1	rabbit	1:2500	2348
p-Chk2	rabbit	1:2500	2197
p-BRCA	rabbit	1:2500	9009
DR4	rabbit	1:2500	42533
p-p70S6K	rabbit	1:2500	9234
p-4E-BP1	rabbit	1:2500	9451
p-S6	rabbit	1:5000	2211
p-ULK1	rabbit	1:1500	6888
p-AKT	rabbit	1:2500	4060
p-PDK1	rabbit	1:2500	3438
p-GSKβ	rabbit	1:2500	5558
p-PRAS40	rabbit	1:2500	2997
p-AMPK	rabbit	1:2500	2535
p-ERK	rabbit	1:2500	4695
p-JNK	rabbit	1:2500	9255
p-p38	rabbit	1:1000	9211
p-CREB	rabbit	1:1000	9198
p-β-Catenin	rabbit	1:2500	5651
p62	rabbit	1:2500	5114
p-STAT3	rabbit	1:2500	9145
STAT3	mouse	1:5000	9139
p-STAT1	rabbit	1:2500	9167
MCL1	rabbit	1:2500	5453
Cyclin D1	rabbit	1:2500	2978
p-RB	rabbit	1:1000	3590
p-CDC2	rabbit	1:2500	4539
p-JAK2	rabbit	1:1000	3771
MIOS	rabbit	1:1000	13557
Anti-mouse-HRP	goat	1:5000	sc-2005
Anti-rabbit-HRP	goat	1:5000	sc-2004

Drug	Mechanism of action	Supplier
Cisplatin	DNA-crosslinking agent and interferes with replication and transcription, culminating in apoptosis	Cayman Chemical (13119)
Etoposide	Inhibits DNA synthesis by forming a complex with topoisomerase II and DNA	Cayman Chemical (12092)
N-acetyl-cysteine	Precursor to glutathione, restores intracellular glutathione levels, supporting antioxidative processes	Thermo Fisher Scientific (11438386)
Hydrogen Peroxide	Oxidising agent, induces oxidative stress	Thermo Fisher Scientific (10386643)
Ruxolitinib	Competitive inhibition of the ATP-binding catalytic site on JAK1 and JAK2	Cayman Chemical (11609)
Erlotinib	Binds to the ATP-binding site of EGFR tyrosine kinase	Sigma-Aldrich (SML2156)
Dasatinib	Binds to the ATP-binding site of Src family kinases, specifically Src and Abl	Sigma-Aldrich (SML2589)
C188-9	Competes against pY proteins for STAT3 SH2 domain binding	Sigma-Aldrich (573128)
Actinomycin D	Interacts with DNA by intercalating between guanine-cytosine base pairs, inhibiting transcription by RNA polymerase, prevents RNA synthesis	Sigma-Aldrich (A9415)

Gene	PCR Forward primer (5'-3')	PCR Reverse primer (5'-3')
H19	ACGTGACAAGCAGGACATGA	TGAGCTGGGTAGCACCATTT
PTPRD	GTGGGGTCACCAATGCCTTA	TGCTCTCGGTCACTACAGGA
PTPRB	GCTCAACATCACTGTGGGAA	ATGTTTGACACGAAGCTGGA
HACD4	GTTCTGTGGCCACTCTTGGA	CGGATTGGCAAAGTCGCATC
BPIFA1	TGAAGCCTGGAGGAGGTACT	GAGCTTTATGCCGAGAGGGA
MCL1	TTCTTTTGGTGCCTTTGTGGCT	AAAAGCCAGCAGCACATTCCT
Cyclin D1	CAGATCATCCGCAAACACGC	AAGTTGTTGGGGCTCCTCAG

shRNA	Targeted Sequence (5'-3')
MIOS	TCTCAATGTGGTAGCAATGGC
SESN2	GAAAAGATGAGGCAGTTACAG
SESN1	GTTCAAGCACTCCTGAGAAGGT
Luciferase	CGTACGCGGAATACTTCGA
p53	GACTCCAGTGGTAATCTAC
STAT3	GCAGCAGCTGAACAACATG
MCL1	GATTGTGACTCTCATTTCT

The plasmid pCDF1-PTPRD-WT was a gift from Todd Waldman (Addgene plasmid # 25642; http://n2t.net/addgene:25642; RRID:Addgene_25642)

2.1. GENERAL METHODS

2.1.1. Reagent weighing

Measurements for reagents above 1.0g were weighed out using a Mettler Toledo B2002-S scientific balance. Measurements for reagents above 1.0g were weighed out using a Mettler k7t top-loading balance. VWR disposable weighing boats were used for weighing.

2.1.2. pH measurement and adjustment

The pH of a solution was measured using a Corning pH meter 240. Stock 10M NaOH and 3M HCl were available and used to adjust the pH of solutions. Adjustment was carried out using a Pasteur pipette and a magnetic stirrer. The Corning pH meter was calibrated before use, using pH 4, 7 and 10 standard buffer solutions.

2.1.3. Centrifugation

For the centrifugation of solutions in 1.5 mL centrifuge tubes, an Eppendorf Benchtop Centrifuge 5425 was used. For temperature-sensitive applications, the refrigerated Thermo Scientific Heraeus Fresco 21 was used.

2.2. Cell culture

2.2.1. Cell Lines

Cells were cultured in a Thermo Scientific Series 8000DH CO2 incubator at 37°C and 5% CO2. Laminar flow hoods NUAIRE and Esco Airstream Plus were used for sterile techniques. DMEM High Glucose Media was used to culture cells and as a medium for all controls. Foetal Bovine Serum (FBS) (10% v/v), L-glutamine (1% v/v) and Penicillin-Streptomycin (1% v/v) were added. DMEM with no additives was used for transfection, as serum and antibiotics can disrupt Lipofectamine or polyethyleneimine (PEI), a cationic polymer that aids transfection,

during transfection procedures. Cells were kept at 50% - 80% confluency, ensuring the cells were in the log growth phase. Volumes of DMEM used for culture: 10mL for 10cm dishes, 5 mL added for 6cm dishes, 3 mL for 6-well plates and 1 mL for 12-well plates.

A549 were obtained from the American Type Culture Collection (ATCC). The cells were cultured in DMEM supplemented with 10% FBS, 2 mM L-glutamine, and penicillin/streptomycin. To generate SESN1&2-deficient A549 cells, cells were infected with CRISPR/Cas9 & single guide (sgRNA) lentiviral constructs and selected in the medium with puromycin (1 μg/ml) as described previously [60]. The single cells were plated on a 96-well plate using a cell sorter and were allowed to form colonies 3–4 weeks after plating. The expression of *SESN1* or *SESN2* genes in the colonies was analysed by western blot, and 15 SESN1- or SESN2-negative clones were pulled together to form SESN1/2-negative multiclonal knockout cultures. Multiple clones were combined to mitigate clone-specific effects and improve the validity of our knockout model. To generate SESN1&2 double knockouts, SESN1-deficient cells were infected with recombinant lentivirus expressing sgSESN2.

The targeted sequence for sgSESN1 – 1 is 5'-CTACATTATCGTCACTACAT-3'.

The targeted sequence for sgSESN1 – 2 is 5'AATGTAGTGACGATAATGTA-3'.

The targeted sequence for sgSESN2 – 1 is 5'-CTCGGAGTCCGCCACGATCA-3'.

The targeted sequence for sgSESN2 – 2 is 5'-AGAGCCTCGAGCAGCACCTG-3'.

Human Embryonic Kidney 293 cells (HEK293T) were used to validate the effectiveness of our overexpression and shRNA constructs and lentiviral packaging. H460 was our alternative human lung cancer model, in which we attempted to generate knockouts for further studies.

The shCon(shLuc), shSESN1 (shSESN1-2), shSESN2 (shSESN2-1), and shMIOS constructs were previously described [254, 271, 293, 294]. To generate SESN1&2-silenced cells, the cells were infected with indicated lentiviral constructs and selected in the medium with puromycin (400 μg/ml) and hygromycin (400 μg/ml) described previously [254, 295]. To ectopically express SESN2, cells were infected with the SESN2-expressing lentiviral vector as previously described [293]. The plasmid pCDF1-PTPRD-WT was a gift from Todd Waldman, and PTPRD-expressing cells were generated as described [296].

2.2.2. Cell Harvesting

A549 cells are fixed to the surface of culture dishes. Trypsin-EDTA is used to cleave protein linkages to the cell culture dishes. 1mL of trypsin was used for 10cm culture dishes, 0.5mL for

6cm dishes, 0.25mL for 6-well plates, and 0.1mL for 12-well plates. The plates were incubated at 37°C with 5% CO2 for 15 minutes. 5x of DMEM volume relative to trypsin was added to neutralise trypsin activity, and cells were resuspended in this total volume. The unnecessary ratio of cells were discarded when splitting, and full DMEM was added to the remaining cells.

2.2.3. Counting Cells

All counts were performed using a Neubauer Improved Haemocytometer. Before counting, cells were thoroughly resuspended in trypsin, and an aliquot of the suspension was immediately taken. The suspension was immediately transferred into a sterile container. The aliquot was further diluted until the concentration of cells was readable under the microscope. The chambers of the haemocytometer were loaded with 8 µL of the cell dilution. Four outer corner squares and the very inner square were counted. The obtained count was divided by five to obtain a representative average. Multiple averages were collected depending on the desired accuracy of the count. A minimum of four averages was collected. After counting, the coverslip was cleaned and reloaded with the following sample. Counts were logged into an excel spreadsheet, which converted count averages into volumes needed for plating. The cell cultures were counted until the standard deviation of averages was displayed to be below 5-10%.

2.2.4. Transfection

Under a laminar flow hood, PEI or Lipofectamine was prepared in neat DMEM. One microcentrifuge tube was loaded with 1 µg/mL of plasmid in DMEM, and another was loaded with 2.5 µg/mL of PEI/Lipofectamine-3000 stock. Both tubes were incubated in DMEM for 5 minutes at room temperature, mixed into a single tube and incubated for 20 minutes more. Parallelly, cells were washed twice with PBS and covered in DMEM with FBS but without antibiotics. Then, the plasmid-PEI mix was gently applied drop by drop onto the cells and incubated for 6 hours until the medium was replaced with fully supplemented DMEM. Cells were used for an experiment 24 hours later. Transfections were performed with a GFP control to assess transfection efficiency, as transfected cells could be visualised for epifluorescence at the TBSI Microscopy and Imaging Centre.

2.3. Western Blotting

2.3.1. Cell lysis

Radioimmunoprecipitation Assay (RIPA) was the default buffer used for lysing in this project. RIPA efficiently lyses all of the cell's components, leading to the complete release of proteins from all membrane-bound compartments. RIPA: 50 mM Tris pH 8, 150 mM NaCl, 1% Triton X-100, 0.5% sodium deoxycholate, 0.1% SDS.

Preceding lysis, 10mL of RIPA lysis buffer aliquot was supplemented with cOmplete ULTRA™ Protease Inhibitor Tablets as well as 1 mM sodium orthovanadate, 1 mM β-glycerophosphate, 2.5 mM sodium pyrophosphate. RIPA with protease and phosphatase inhibitors was used for lysis.

Cell plating number for lysis: $2.5x10^5$ for a 6-well plate, $5x10^5$ for a 6 cm dish and $1x10^6$ for a 10 cm dish.

RIPA buffer volumes used: 1 mL for 15 cm dishes, 0.5 mL for 10 cm, 100 µL for 6 cm. Immediately before lysis, the cell dish was placed on ice. After washing twice with ice-cold PBS, the dish was dried entirely using an aspirator or a pipette. After removing all PBS, lysis buffer was added. Cells were scraped off the dish using a disposable cell scraper, and the cell lysates were transferred into a 1.5 mL centrifuge tube. These lysates were spun at max speed for 20 minutes at 4°C. After centrifugation, the lysates were transferred to a clean 1.5 mL centrifuge tube, and the cell pellet was discarded. The lysates were stored at -20°C or -80°C for the long term.

2.3.1. Cell Lysate Protein Quantification

Thermo Scientific™ Pierce™ BCA Protein Assay Kit was used to quantify lysate protein concentration. Fresh standards were prepared using the supplied BSA ampules. Standards and samples were set up in duplicates on a 96-well plate at 10 µL per well and then covered with 200 µL of BCA working reagent. The required volume of working reagent was prepared at a ratio of 50:1 BCA reagent A to BCA reagent B. The plate was incubated at 37°C for 30 minutes. Following incubation, absorbance was read at 562nm using a SpectraMax PLUS microplate Spectrophotometer.

2.3.2. Electrophoresis

BioRad Mini-PROTEAN Tetra Cell and SDS-PAGE tris-glycine buffer system were used to analyse protein levels. Gels were made using a 37.5:1 acrylamide mix and were prepared according to Bio-Rad General protocol for Western Blotting and a general gel recipe from Harlow and Lane [297].

Running buffer: 25 mM Tris pH 8.3, 190 mM Glycine, 0.1% SDS
Laemmi Buffer: 8% SDS, 20% 2-mercaptoethanol, 40% glycerol, 0.004% bromophenol blue. 0.25 M Tris, pH 6.8

Prior to electrophoresis, the lysate samples were diluted to 20 µg/well using x4 Laemmi buffer and RIPA. Lysates were vortexed, centrifuged and denatured at 95°C for 10 minutes. Samples were loaded into lanes in the gel. During electrophoresis, proteins were separated on an SDS-PAGE gel and later transferred from the gel to a polyvinylidene fluoride (PVDF) membrane

using a Bio-Rad PowerPac 300. The gel ran for 25 minutes at 80 volts to separate the stacking gel and then was changed to 120 volts so the resolving gel could fully resolve the proteins.

2.3.3. Immunoblotting

TBS-T Buffer: 20 mM Tris pH 7.5, 150 mM NaCl, 0.1% Polysorbate 20 (Tween 20)
Transfer buffer: 25 mM Tris pH 8.3, 190 mM Glycine, 20% methanol

The PVDF membrane was submerged in methanol to activate it, and then it was washed and left covered in dH2O. Cassette sponges and Whatman filter papers were briefly soaked in transfer buffer. The membrane was carefully applied to the gel surface and arranged between filter papers in the transfer cassette. It was rolled to eliminate air bubbles and secured in the transfer cassette. The transfer was left running at 45 V for 3 hours at 4°C or 15 V overnight at 4°C.

Following transfer, the membrane was blocked using 5% milk in TBS-T for 1hr at room temperature. The membrane was then washed in TBS-T and then transferred to a plastic container with primary antibody diluted in 5% BSA in TBS-T with 3% sodium azide and incubated overnight at 4°C on the tube roller. Membranes were washed three times in TBS-T. The membrane was transferred to a falcon tube with 5mL of primary antibody diluted in 5% BSA in TBS-T with 3% sodium azide. Membranes were incubated for 1 hour on a tube roller and were washed three times with TBS-T for 5 minutes. Pierce™ ECL Western Blotting Substrate was used for the imaging analysis. Reagent A was mixed with Reagent B in an equal ratio at approximately 300-400 µL. The membrane was incubated with ECL for 1-2 minutes and then imaged using a Bio-Rad Image GelDoc machine. ImageLab software was used to capture the chemiluminescence and a colourimetric photograph.

2.3.4. Immunoprecipitation

Lysing buffer used: NP40 buffer (50 mM Tris-HCl, 150 mM NaCl, 0.3% Igepal NP40, cOmplete ULTRA™ Protease Inhibitor, 1 mM sodium orthovanadate, 1 mM β-glycerophosphate, 2.5 mM sodium pyrophosphate, pH 7.5)

Cells were grown on 10cm culture dishes until approximately 60-80% confluence. Cells were placed on ice and washed twice with ice-cold PBS. Next, 0.5 mL of NP40 lysing buffer was added to the dish. The dish was scraped, and the collected lysate was pipetted up and down gently in the tube. The lysate was left incubating on a shaker with ice for 30 minutes. After pipetting up and down, samples were spun at max speed, 4°C. Parallelly, Protein A/G Plus Agarose beads were prepared. A mix of 11 µL beads per sample was washed with 800 µL ice-cold lysing buffer three times. Beads were spun down between washes at 3.5 thousand

rpm for 30 seconds. Finally, the washed beads were distributed evenly across the required test tubes.

After lysate was spun, a 50 µL aliquot was taken. SESN2 antibody (10 µL) was added to beads. Subsequently, the lysate was added to corresponding tubes with beads. The lysate, beads and antibody mixture was left for 4 hours at 4°C rotary agitation. After the incubation, beads were spun down as previously and washed four times with lysing buffer. Finally, all buffer was removed, and x2 Laemmi buffer was added to the beads. The beads were vortexed and then heated at 95°C for 5 minutes. The beads were briefly spun down immediately before loading onto an SDS-PAGE gel.

2.4. Plasmid Cloning

2.4.1. Transformation

For plasmid amplification, DH5α E.coli was used. Heat shock transformation was applied with the plasmid mixed in with bacteria (not more than 1/10 volume). The mix was held on ice for 20 minutes, heat shocked at 42°C for 1 minute and placed back on ice for at least one minute. Using sterile technique, bacteria were applied onto agar plates with the corresponding antibiotic for selection.

2.4.2. Amplification

Colonies were grown in 10 mL LB broth overnight, in a 50 mL falcon, at least 250 rpm spin on the Thermo Scientific Forma Orbital Shaker at 37°C. Plasmids were isolated using the QIAprep Spin Miniprep Kit.

2.4.3. DNA purification after enzymatic reactions

Restriction and other plasmid reactions were purified using the phenol:chloroform isoamyl alcohol mix (#17908). After phenol:chloroform, an additional chloroform extraction was performed. The extracted DNA was precipitated using the ethanol precipitation method, with the addition of glycogen for pelleting assistance and sodium acetate (0.3M final concentration). The ethanol-DNA mix was left overnight at -20°C or -80°C for at least one hour. Alternatively, some DNA purifications were substituted by gel-extraction by QIAquick Gel Extraction Kit if the preceding reaction could be adequately stopped, e.g. restriction enzyme heat deactivation.

2.4.4. Cloning insert into vector

All ligations were performed with the prior CIAP dephosphorylation of the vector and T4 PNK phosphorylation of the insert. 3:1 molar ratio of insert:vector was used to ligate overnight at 16°C using T4 DNA Ligase (#15224017).

2.5. Flow Cytometry

2.5.1. Propidium Iodide Cell Cytotoxicity Assay

A day before treatment, cells were plated onto 12-well plates at $1x10^5$ and grown in the presence or absence of genotoxic drugs. After incubation, plates were placed on ice immediately. The medium was extracted into 1.5 mL centrifuge tubes to collect detached dead cells. The wells were then immediately washed with 200 µL PBS, which was placed into the corresponding tube to collect dead cells from the wash. 200µL Trypsin was added into each well, and the plate was incubated for 10 minutes. Cells were resuspended before being transferred to the corresponding sample tubes. Tubes were centrifuged at 400 x g at 4°C for 10 minutes and carefully discarded supernatant. The washed pellet was resuspended in propidium iodide (100µg/mL) in PBS and stained for 20 minutes at room temperature. Flow cytometry was analysed using BD Accuri C9 with defined gates after running a control sample to measure cellular debris (Figure 1).

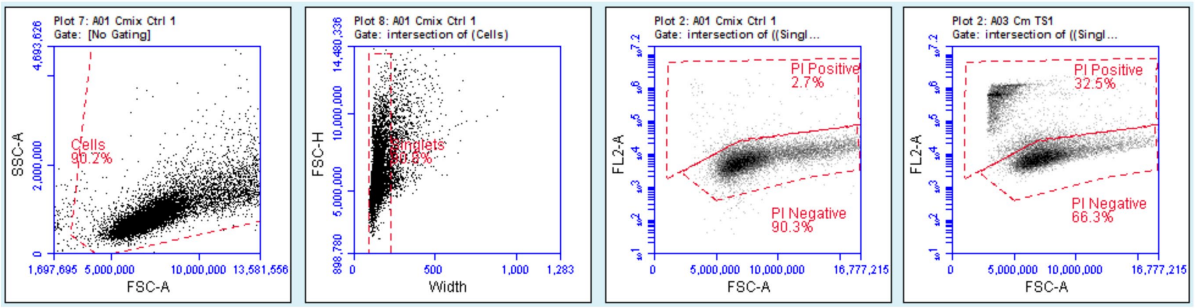

Figure 1: Analysis of cell death by propidium iodide
Left to right, gate over cells using side scatter vs forward scatter, gate over singlets forwards scatter height vs width. Two right panels show a negative death result and a positive death result. FL2-A is the filter for propidium iodide vs forward scatter, which allows for differentiation by PI alone.

2.5.2. Apoptosis (Annexin V; PI) analysis

Cells were harvested as previously described. After harvesting, the cells were washed two times in the Annexin V-binding buffer (AVBB, 10 mM HEPES, 150 mM NaCl, 5 mM KCl, 1 mM MgCl2, 1.8 mM CaCl2, pH 7.4). The cells were then stained in 50 µL AVBB containing 2 µg/mL Annexin V-FITC, left to stain at room temperature in the dark for 15 minutes, and were centrifuged and washed twice in AVBB. Finally, each sample was resuspended in 500 µL AVBB. Immediately before being analysed with BD Accuri C9, the cells were counterstained with propidium iodide (100 µg/mL). BD Accuri C9 software was used to analyse the data (Figure 2).

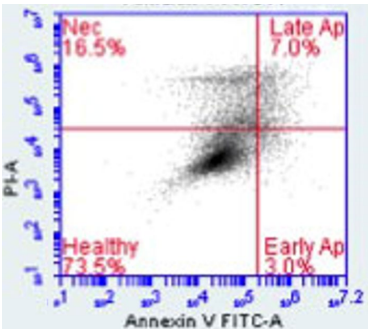

Figure 2: Annexin gate
For annexin V; PI analysis, the gating strategy was to separate the graph into four qudrants. Healthy aka Viable (Annexin V- ; PI-), Necrotic (Annexin V- ; PI+), Early Apoptotic (Annexin V+ ; PI-) and Late Apoptotic (Annexin V+ ; PI+).

2.5.3. Cell cycle analysis

A day before treatment, $1x10^5$ cells per well were plated on 12-well plates. The cells were washed with PBS before treatment, and 1 mL of glucose-free medium was used to replace the culture medium. Cells were incubated in a humidified 37°C, 5% CO2 incubator. After 24 hours of incubation, the glucose-free medium was extracted into 1.5 mL centrifuge tubes. Immediately after, cells were washed with 200 µL PBS, and the PBS was transferred to the corresponding 1.5 mL tubes. After the wash, 200 µL of trypsin-EDTA was placed into each well, and the plates were left in the incubator for up to 10 minutes. Subsequently, the cells were resuspended in trypsin and transferred into corresponding 1.5 mL tubes. The tubes were centrifuged at 300 g at 4°C for 15 minutes. After centrifugation, the supernatant was discarded, and the cellular pellet was resuspended to cold PBS. After two washes and centrifugations with PBS, the washed cellular pellet was resuspended in 400 µL PBS. 800 µL of ice-cold 100% ethanol was slowly added. Cells were left in this mix at 4°C for at least 2 hours. The ethanol-treated cells were resuspended, centrifuged at 1000 × g for 5 minutes, and washed with PBS. Finally, the cellular pellet was resuspended in 200 µL PBS containing 50 µg/mL of PI and 50 µg/mL of RNAse and incubated in this solution at 37°C in the dark for 30 minutes. The samples were then analysed using BD Accuri C9. Samples were thoroughly resuspended prior to analysis to avoid aggregates. BD Accuri C9 software was used to analyse the data.

2.6. Colony Formation Assay

Protocol for the colony formation assay was adapted from Franken et al. [298]. After cell counting, cells were plated on 6-well plates at a density of 500 cells per well. Cells were then left in DMEM overnight to adhere. PBS was used twice, and the cells were then incubated in DMEM, either with or without genotoxic drugs. They were left to grow for 6 hours, after which the drugged medium was aspirated, and cells were left to grow for two weeks until the formation of visible colonies. Cells were then stained with methylene blue for 30 minutes and rinsed with water. They were left to air-dry and then imaged and counted.

2.7. Analysis of cell proliferation/ growth curves

For analysis of cell proliferation, cells were plated onto 6 cm culture dishes at 50,000 cells/dish and counted every 24 h for 5 days. $5x10^4$ cells were plated onto several 6 cm dishes. On the following day (Day 0), the cells were counted and treated with varying drug concentrations or left untreated. Day 1 marks the first 24 hours after treatment with a drug. Cells were counted using a Neubauer Improved Haemocytometer. Four outer corner squares on the haemocytometer were counted. The obtained count was divided by four to obtain a representative average. A minimum of six averages were collected per condition. Three dishes per condition were counted to obtain three biological repeats (n=2). Counts were converted to the number of cells x 10^6. The counts were performed every 24 hours for five days.

2.8. Analysis of gene expression by RNA seq, RNA library preparation, and sequencing

Total RNA was isolated from control and SESN1&2 KO A549 cells (all in triplicate), using the MagNA Pure Compact RNA Isolation Kit (Roche, Switzerland) on a MagNA Pure Compact Instrument (Roche) according to the manufacturer's instructions. Isolated RNA was quantified with a Qubit 2.0 Fluorometer (Thermo Fisher Scientific, USA); the quality of samples was assessed on an Agilent 2100 Bioanalyzer (Agilent Technologies, USA) with the RNA Integrity Number (RIN) measurement. Samples with RIN > 7 were only used for library preparation. Transcriptome libraries were prepared using the TruSeq Stranded mRNA Library Prep Kit (Illumina, USA) following the manufacturer's protocol. cDNA quality and concentration were assessed on Qubit 2.0 Fluorometer and Agilent 2100 Bioanalyzer, respectively. Cluster densities were optimised by quantitative PCR using a Rotor-Gene Q 5 plex HRM instrument (Qiagen, Netherlands). Obtained cDNA libraries were sequenced on a NextSeq 500 System (Illumina) under the 76 bp single-end mode. Quality control of raw sequencing reads was carried out using FastQC. Trimming and filtering of reads, removal of adapters were done with Trimmomatic [299]. PolyA extraction efficacy was assessed by mapping the reads to human rRNA sequences using Bowtie2 [300]. STAR was used for splice-aware mapping reads to the reference human genome GRCh38.p12 (Ensemble annotation, release 102) [301]. Next, mapped reads can be quantified per gene using featureCounts tool from Subread package [302]. The subsequent analysis was performed in R environment. Differential expression analysis was carried out using edgeR Bioconductor package [303]. GO, KEGG and Reactome gene set enrichment analyses were performed using clusterProfiler and topGO tools [304].

2.1. RNA extraction for PCR

TRIzol reagent was used to lyse cells directly in culture dishes for RNA extraction. TRIzol volumes used: 1 mL for 6 cm culture dish, 3 mL for 10 cm dish, 11 mL for 15 cm dish. To a 1

mL volume of TRIzol lysate, 250 µL of chloroform was added, and the mixture was inverted several times gently. The chloroform-TRIzol mixture was left at room temperature until visible phase separation appeared. The mixture was spun at 10,000 rpm for 5 minutes to achieve a clear aqueous phase on the surface. The clear aqueous phase was transferred to another tube carefully, leaving 2-4 mm of phase behind to avoid pipetting the organic phase. Isopropanol, 550 µL, was added to the transferred aqueous phase and vigorously inverted. The mixture was spun at max speed for 20 minutes to pellet the nucleic acid precipitate. After the spin, isopropanol was carefully taken off using a pipette and 75% ethanol in diethylpyrocarbonate (DEPC)-treated water was added to wash salts off the nucleic acids. The washed pellet was spun at 9,500 rpm for 5 minutes, and then the ethanol was carefully taken off as much as possible with a pipette. The pellet was left to air-dry, and when a tiny meniscus covering the pellet was left, 25 µL of DEPC water was added to resuspend the pellet. The purified RNA is immediately checked on a 1% native agarose gel and nanodrop. Absorbance ratios displayed by nanodrop machines can help assess the isolation quality. A260/280 ratio of ~2 is expected for RNA, and A260/230 of more than 2 is expected for pure RNA isolation. Isolations were checked for 28S and 18S ribosomal RNA bands on the agarose gel. If both analyses suggest pure RNA, then the purification is immediately followed by a reverse transcription reaction. DNAse treatment step could be omitted due to our design of qPCR primers around an exon-exon junction, meaning genomic DNA would be amplified much later in PCR. Primer design was performed using Primer3 and BLAST combination tool available from NCBI.

2.2. RT and comparative PCR

Following RNA isolation, 1 µg of RNA was combined with 500 ng of Oligo(dT)20, 250 ng of Random hexamers and 1 µL 10 mM dNTP Mix. The mixture was then incubated at 65°C for 5 minutes, then ice for at least 1 minute. First-Strand Buffer, 5 mM of DTT, and 200 units of SuperScript III reverse transcriptase were added, and DEPC-treated H20 was used to bring the reaction mix up to 20 µL. The mixture was briefly spun and mixed with gentle pipetting before leaving the reaction at 25°C for 5 minutes, followed by 1 hour at 50°C. The reaction was finally inactivated by heating to 70°C for 15 minutes. No RT controls were prepared in parallel without adding the SuperScript III RT enzyme. The cDNA product was aliquoted and frozen or immediately used for qPCR analysis.

Comparative PCR using an Mx3000P Agilent qPCR system was performed to analyse cDNA content. The cDNA templates were mixed into a master mix with x2 Power Syber qPCR mix. Primers were diluted to a primer mix of 2 µM per primer. All mixtures were mixed using gentle pipetting, and then 18 µL of cDNA template mix was combined with 2 µL of primer mix to make up a 20 µL reaction, 0.2 µM final concentration of each primer. The reaction was consolidated

into two mixes as such to minimise pipetting error. The annealing temperature was chosen to suit each primer in the comparative analysis. As our primers were designed to give 200 bp amplicons, annealing and extension times were limited to 30 seconds to minimise non-specific amplification.

Following PCR, no-RT controls were compared to experimental wells. As genome DNA was present in our RNA isolation, we observed amplification in some no-RT controls. Results were accepted as valid only if amplification in the no-RT control starts ten cycles or more later than the experimental wells. The amplicons were also inspected on 1% agarose gel, and no-RT controls were expected to show no bands or a faint non-specific band at a different molecular weight than the experimental band, for example, primer dimer <100 bp.

2.3. Statistical Analysis

Statistical analyses were performed using GraphPad Prism 8. Two-tailed Student's t-tests ($\alpha = 0.05$) were performed as described in figure legends. Significance was defined as * ($P \leq 0.05$), ** ($P \leq 0.01$), *** ($P \leq 0.001$).

3. CHAPTER 3: p53-regulated SESN1 and SESN2 regulate cell proliferation and cell death through control of STAT3

3.1. Introduction

Sestrin1 and Sestrin2 (SESN1&2) are evolutionary conserved, stress-responsive proteins responsible for regulating cell growth and viability. Notably, SESN1&2 are *bona fide* targets of the p53 tumour suppressor. Being p53-activated genes and regulators of cell viability [4], SESN1&2 may be responsible for the pro-apoptotic effects of chemotherapy on cancer cells. Therefore, we examined the role of Sestrins in DNA damage response in the context of cisplatin, a common chemotherapeutic agent used in the treatment of various cancers. We found that the inactivation of SESN1&2 confers resistance to cisplatin and aimed to investigate the cause of this phenomenon.

The best-established target of Sestrins is the mechanical target of rapamycin complex 1 protein kinase (mTORC1), which acts as an activator of anabolic processes and an autophagy inhibitor. In our previous studies, we demonstrated that inactivation of SESN1&2 in lung adenocarcinoma A549 cells accelerates cell proliferation and confers resistance to cell death while not influencing mTORC1 activity [254], indicating that SESN1&2 modulate cellular processes via mTORC1-independent mechanisms.

In this study, we describe a new mechanism of cell proliferation and cell death regulation by SESN1&2 through the regulation of STAT3. STAT3 is a transcription factor that is activated in response to stress and inflammation and is responsible for the activation of many pro-proliferative and anti-apoptotic genes. STAT3 is often activated in human cancers, where its activity can drive cancer progression. This work demonstrates that SESN1&2 inactivation leads to activation of STAT3 via downregulation of the protein tyrosine phosphatase receptor delta (PTPRD) phosphatase, which is responsible for STAT3 dephosphorylation. Therefore, STAT3 activity induced by the deficiency of SESN1&2 genes can facilitate carcinogenesis and may lead to drug resistance in lung cancers. Activation of SESN1&2 is a potential strategy for prophylactics and treatment of human cancers.

3.2. Inactivation of SESN1&2 using CRISPR/Cas9

To study the role of the p53-inducible Sestrins in the context of cancer and chemotherapy, we sought to prepare total knockouts of SESN1 and SESN2 in A549 epithelial cell line derived from lung adenocarcinoma, using the CRISPR/Cas9 method. Previous studies on Sestrins studied these proteins in the context of overexpression by exogenous constructs or RNA silencing.

To prepare double knockouts (DKO) of SESN1&2, repeated rounds of CRISPR were performed, followed by the selection of clones via flow cytometry. The flow cytometer method involved the dispersion of single cells into a 96-well plate and the subsequent outgrowing of these clones so that they could be analysed by western blot for their presence of SESN1 or -2. This approach facilitated an accurate selection of total protein knockouts. It allowed for fewer antibiotic selections, kept the choice of antibiotic resistance cassettes plentiful, and permitted the future introduction of manipulations such as shRNA or ectopic expression. Figure 1 displays the control (Con), SESN1, SESN2 and SESN1&2 cell lines and the absence of corresponding Sestrin proteins.

A significant strength of our A549 Sestrin knockouts lies in their composition, comprising over 15 distinct clones. Each clone was validated through western blotting prior to integration into a singular knockout culture. A prominent feature of cancer is the heterogenicity of the tumour, where a single cell can be markedly genetically different from the rest of the tumour. Employing a single clone for studies could result in data that reflect isolated clonal aberrations rather than broader tumorigenic patterns. By combining multiple clones, our approach seeks to mitigate the impact of clonal variations, thereby enhancing the validity of the model as a representation of tumour complexity *in vitro*.

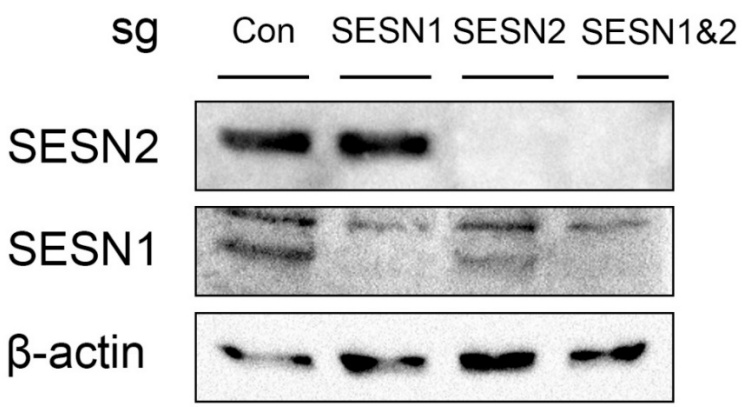

Figure 1: Inactivation of SESN1&2 using CRISPR/Cas9
A549 cells were lentivirally infected with CRISPR/Cas9 machinery and single guide (sg) against SESN1, -2, generating complete knockouts. A second single guide was introduced to generate a double knockout. The figure displays immunoblot analysis of the generated cell lines, displaying the presence or absence of SESN proteins.

3.3. Inactivation of SESN1&2 provides resistance to cisplatin

Our previous data indicate that SESN2 supports cell death in response to genotoxic chemotherapeutic drugs [4], and inactivation of SESN1&2 in cancer cells potentially provides resistance to cell death induced by DNA damage. SESN1&2 are direct targets of p53 and are strongly upregulated in response to genotoxic stress in a p53-dependent manner. Platinum-based drugs, such as cisplatin, are amongst the most widely used medications to treat lung cancers.

To study the impact of SESN1&2 in the regulation of long-term viability and propagation of A549 cells, we performed colony formation assays with control and SESN1&2-null cells treated with cisplatin. Inactivation of either SESN1 or SESN2 strongly increases the number of colonies grown after cisplatin treatment, and double SESN1&2 KO cells produce the largest number of colonies (Figure 2B). To confirm that the inactivation of SESN1&2 provides resistance to genotoxic stress and not specifically to cisplatin, we also treated cells with etoposide and observed a dramatic increase in colony formation in the cells with inactivation of SESN1 and/or SESN2 (Figure 2A).

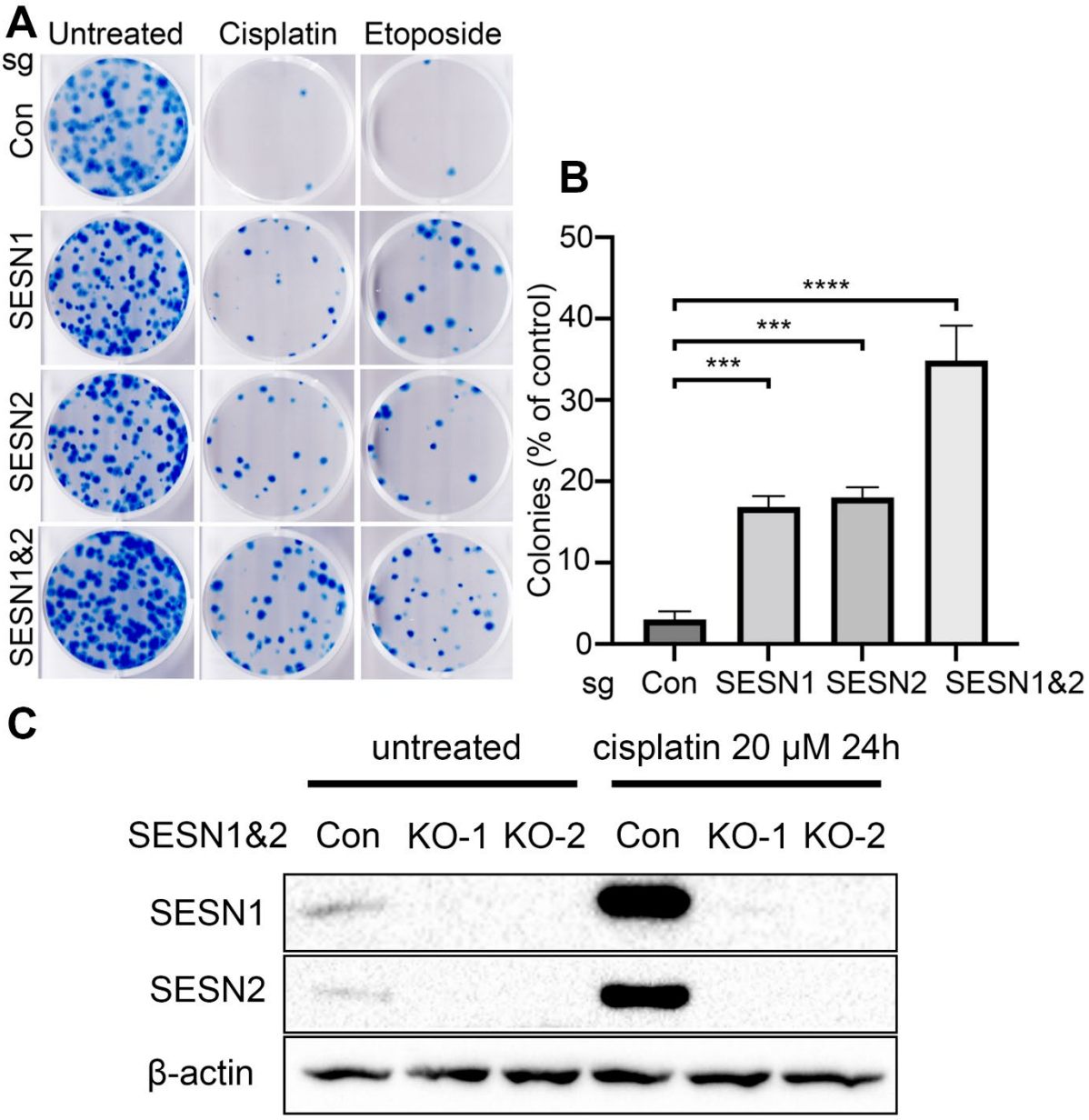

Figure 2: Inactivation of SESN1&2 provides resistance to cisplatin
A) A549 knockouts of SESN1, -2, or 1&2 were subjected to treatment with cisplatin (20 μM) or etoposide (20 μM) for 6 hours. 500 cells per well were plated onto a 6-well plate, treated with chemotherapeutic drugs and the medium was swapped. Cell colonies grew for two weeks, stained with methylene blue, and counted. Bar chart **(B)** represents data from cisplatin-treated colony formation experiments. The data are presented as mean ±S.D. P values were calculated using one-way ANOVA, followed by Tukey's post-test comparison (n=3). **C)** Western blot analysis of two independent double knockouts in response to cisplatin (20 μM; 24 hours). The upregulation of SESN1&2 in response to the genotoxic insult and the absence of this effect in knockouts are shown.

To determine whether SESN1&2 are responsible for the induction of cell death in response to cisplatin, we analysed apoptosis in cells treated with cisplatin by AnnexinV;PI staining followed by flow cytometry analysis.

Annexin V conjugated to a fluorescent dye such as fluorescein isothiocyanate (FITC) allows for the detection of apoptotic cells by flow cytometry. Annexin V is a cellular protein that binds to phosphatidylserine in the presence of calcium ions. Phosphatidylserine is a lipid that normally resides on the inner leaflet of the cell membrane and flips to the outer leaflet, thus becoming exposed. This is a hallmark of early apoptosis, and this mechanism allows macrophages to recognise and phagocytose apoptotic cells. However, it also enables researchers to use a modified Annexin V to quantify apoptosis. Annexin V is typically counterstained with propidium iodide (PI), a molecule that fluoresces when it intercalates into DNA. Hence, propidium iodide can identify cells with ruptured membranes. These cells are typically found in the late apoptotic stages or during cell necrosis.

As shown in Figure 3A, inactivation of SESN1&2 strongly suppresses apoptotic cell death in response to cisplatin, supporting our hypothesis that Sestrins play an important role in cell death activation in response to genotoxic stress. After 24 hours of cisplatin treatment, we see a significant difference in early apoptotic cells and some in the late apoptotic cohort.

We extended the experiment to include etoposide and measured apoptosis similarly (Figure 3B). Our SESN1&2 KO cells also displayed apoptotic resistance in response to etoposide treatment, further indicating the involvement of SESN1&2 in mediating apoptosis triggered by DNA damage.

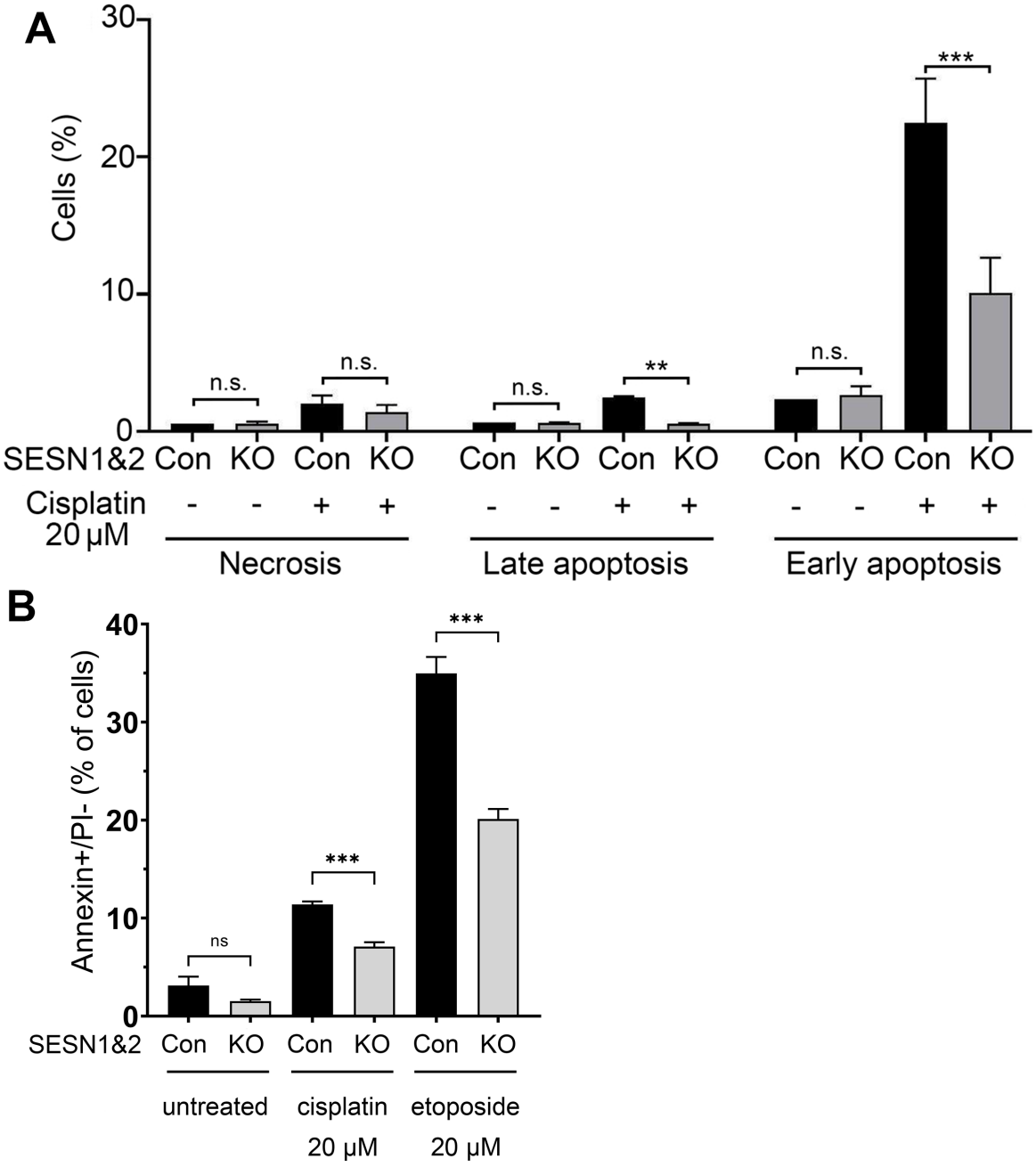

Figure 3: SESN1&2 inactivation in A549 cells confers resistance against DNA-damage-induced apoptosis

Cells were treated with genotoxic drugs, stained by AnnexinV;PI, and analysed by flow cytometry. Bar chart separates Necrosis (PI+;AnnexinV-), Late Apoptosis (PI+;AnnexinV+), and Early Apoptosis (PI-;AnnexinV+) to show a difference in cell death between SESN1&2 KO and control cells. **A)** Treatment with cisplatin (20 µM) for 24h. The data are presented as mean ±S.D. (n=4). **B)** Treatment with cisplatin (20 µM) or etoposide (20 µM) for 24h. The data are presented as mean ±S.D. (n=4). P values were calculated using two-way ANOVA, followed by Tukey's post-test comparison. Not significant, ns; p**≤0.01; p***≤0.001.

3.4. P53 is essential for SESN-mediated cell death

The principal mediator of DNA damage-induced apoptosis is the tumour suppressor protein p53. This protein is critical in preserving genomic integrity by responding to various cellular stress signals, including DNA damage. Upon DNA damage recognition, p53 becomes activated and can induce cell cycle arrest, allowing DNA repair mechanisms to correct the damage [305]. Among its responses to irreparable DNA damage, p53 can initiate apoptosis [306], a programmed cell death process, to prevent the propagation of cells with potentially oncogenic mutations.

The principal mediator of DNA damage apoptosis is p53. We tested whether SESN1&2 mediate p53's role in triggering cell death due to DNA damage. To analyse p53's influence, we knocked down p53 by shRNA in both control and SESN1&2 KO cells (Figure 4B) and compared the levels of cell death. Knockdown of p53 confers resistance to cisplatin in SESN1&2-proficient cells and eliminates the disparity in cell death levels between control and SESN1&2 KO cells in response to cisplatin (Figure 4A). This indicates a significant involvement of p53 in the apoptosis mediated by SESN1&2, underscoring its essential role as a mediator in triggering this apoptotic effect in response to DNA damage.

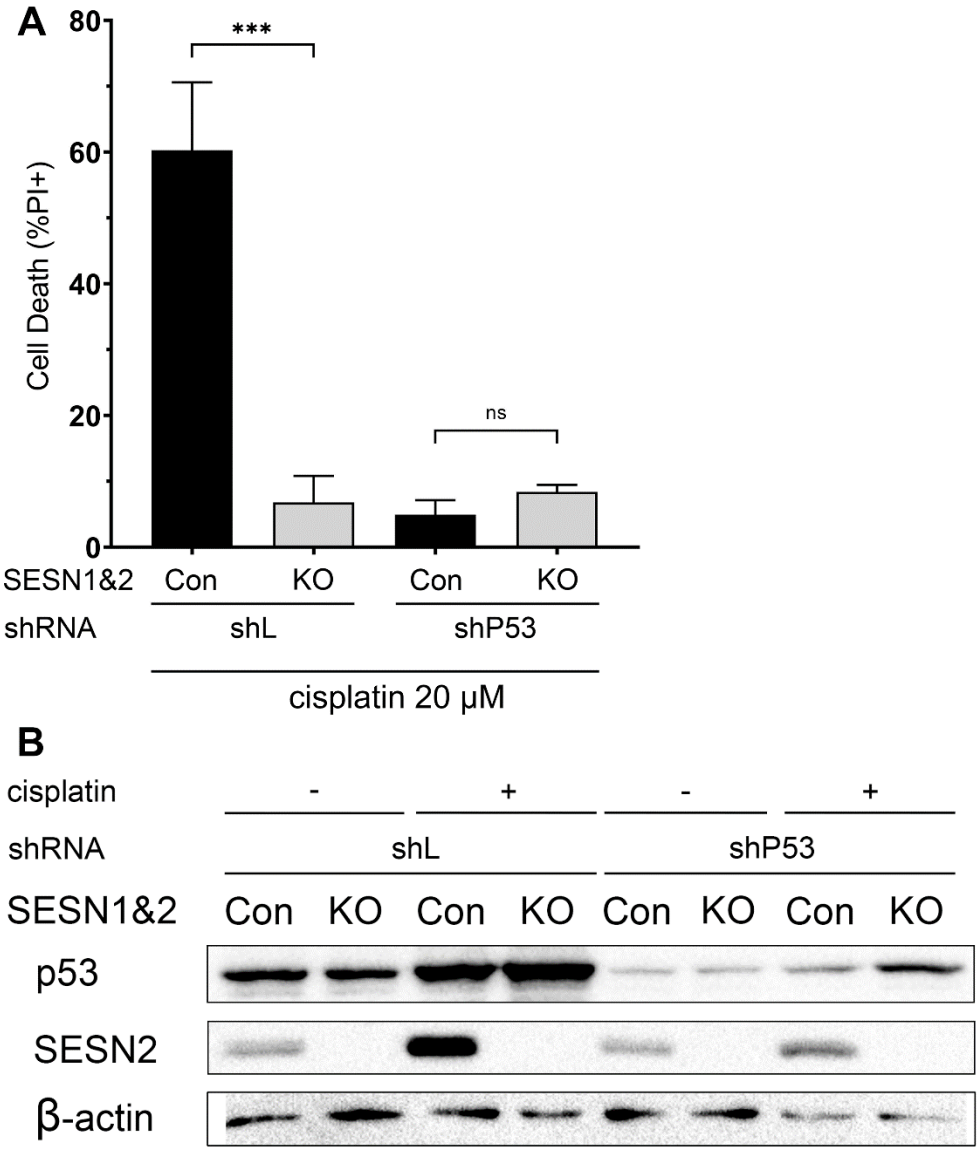

Figure 4: SESN1&2-regulated cell death is p53-dependent
Silencing of p53 by shRNA strongly inhibits cisplatin-induced cell death and eliminates the difference in cell death between the control and SESN1&2 KO. **A)** Control and SESN1&2 KO cells expressing shLuciferase (shL) or shP53 were treated with cisplatin (20 µM), stained with propidium iodide, and analysed by flow cytometry. The data represent the mean of two independent experiments ± SEM (n=2), where each experiment consisted of four replicates, whose means ± S.D. (n=4) were calculated and used for SEM calculation. P values were calculated using one-way ANOVA, followed by Tukey's post-test comparison. Not significant, ns; p***≤0.001. **B)** Western blot analysis of control and SESN1&2 KO expressing shP53. Cells were treated with cisplatin (20 µM) for 24 hours and indicated proteins were analysed subsequently.

The mechanism of cell death regulation by Sestrins remains unknown and may involve the modulation of the activity or stability of some proteins regulating the DNA damage response (DDR). To determine whether Sestrins regulate cell death by affecting the DDR pathway, we analysed the phosphorylation and expression of key proteins in this pathway. We found that SESN1&2 is strongly upregulated by cisplatin in control cells, but neither SESN1 nor SESN2 were detected in the knockout cells (Figure 5). Comparing phosphorylation and expression of the proteins involved in the DDR in control and SESN1&2 KO cells, we observed a slight increase in the phosphorylation of DDR regulators: Chk1, Chk2 and BRCA [307]. However, we found no difference in the phosphorylation of H2AX (a marker of DNA damage) or p53 between control and SESN1&2 KO cells. Moreover, no difference was observed between total p53 levels and expression of pro-apoptotic DR4 protein regulated in a p53-dependent manner (Figure 5) [308]. These data indicate that SESN1&2 presumably do not play a critical role in regulating DDR and p53 activity but might be responsible for controlling cell death downstream of p53 (Figure 5).

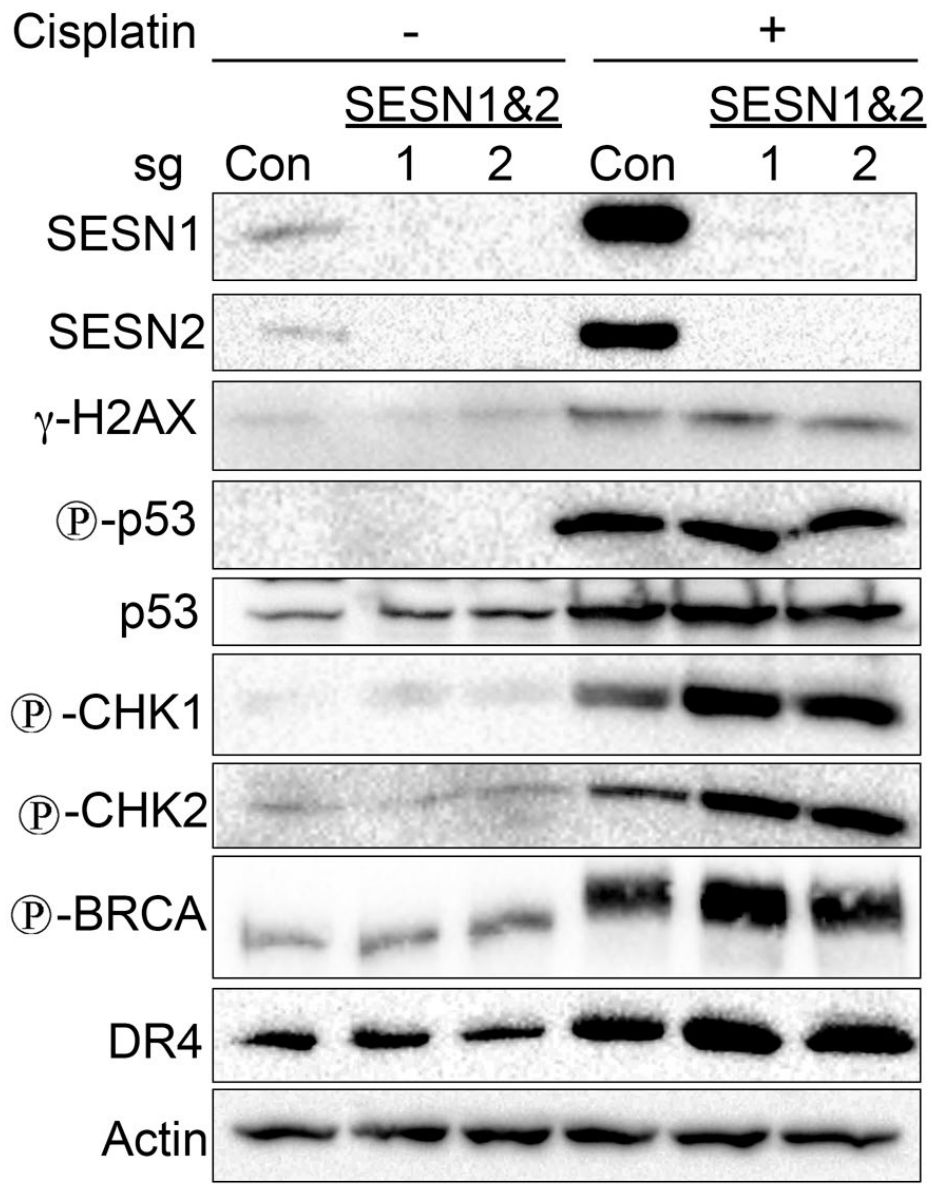

Figure 5: SESN1&2 do not affect the regulation of the DDR pathway
A549 Control (Con) and two different SESN1&2 KO (SESN1&2) cell lines were treated with cisplatin (20 μM) for 24 hours, and the expression and phosphorylation of the indicated proteins were analysed by immunoblotting.

3.5. Knockout of SESN1 and/or SESN2 activate STAT3

To study the potential role of the SESN1 and SESN2 in the regulation of cell proliferation and cell death, we analysed several signalling pathways that Sestrins can regulate in accordance with previous studies. To investigate Sestrins' inhibitory effect on mTORC1 [294], we analysed phosphorylation of mTORC1 targets (p70S6K, S6, 4EBP1, and ULK1) in control and two distinct SESN1&2 knockout A549 cell lines. We could not detect any significant difference in phosphorylation of any of these proteins, indicating that SESN1&2 does not affect mTORC1 activity in these cells in a nutrient and growth factor repleted cell culture medium (Figure 6A). To measure the activity of the mTORC2-AKT signalling pathway, which Sestrins can positively regulate, we analysed the phosphorylation of AKT, its targets (GSK-β and PRAS40), and an upstream AKT regulator PDK1. However, we did not see any notable difference in the regulation of any of these proteins. We noticed a slight decrease in the phosphorylation of the negative regulator of mTORC1, the PRAS40 protein. However, it did not affect mTORC1 activity (Figure 6A) according to the phosphorylation of mTORC1 targets. It was also reported that Sestrins might regulate AMPK, MAPK, WNT/β-Catenin and PKA-CREB signalling pathways [309-311]. Considering these possibilities, we analysed the phosphorylation of AMPK, the MAPK family members ERK, JNK and p38, β-Catenin and CREB, and we did not detect any notable difference in phosphorylation of any of these proteins between control and SESN1&2 KO cells (Figure 6A). Sestrins can also regulate cellular processes by influencing the degradation of p62, which facilitates autophagy and supports carcinogenesis [58]. However, there is no difference in the levels of p62 expression in control and SESN1&2 KO cells (Figure 6A).

The STAT3 transcription factor is often overactivated in cancers and plays an essential role in the control of cell proliferation and cell death. Strikingly, we observed higher levels of STAT3 phosphorylation in SESN1&2-deficient cells compared to control cells, but SESN1&2 inactivation did not affect the phosphorylation of STAT1, another member of the STAT family (Figure 6B). We also found that the expression of two STAT3 targets, the cell cycle activator Cyclin D1 and the suppressor of apoptotic cell death myeloid leukaemia cell differentiation protein (MCL1), were upregulated. We also observed increased phosphorylation of the retinoblastoma protein (RB), the major inhibitor of G1-S cell cycle transition, and cell division cycle protein 2 (CDC2/CDK1) – the essential driver of the G2-M cell cycle transition (Figure 6B).

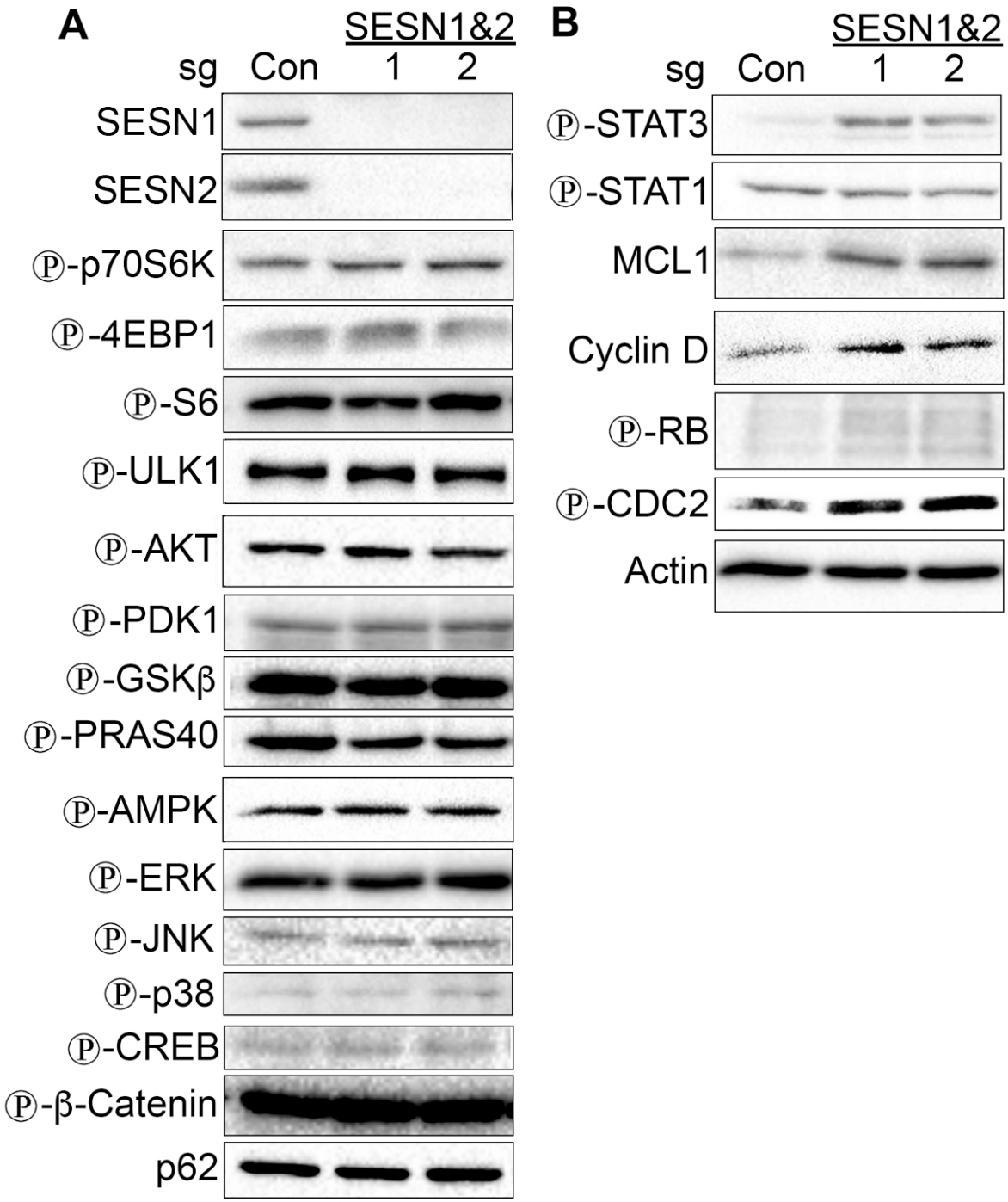

Figure 6: Analysis of signalling pathways reveals activated STAT3 in SESN1&2 KO
A) Immunoblot analysis of phosphorylation and expression of the components of several signalling pathways controlling cell growth and proliferation in control (Con) and two different SESN1&2 KO (SESN1&2) cell lines. **B)** Inactivation of SESN1&2 increases STAT3 phosphorylation, MCL1 and Cyclin D1 expression, and phosphorylation of RB and CDC2 proteins.

To study the impact of each Sestrin gene on the regulation of STAT3, we analysed its phosphorylation in single SESN1 or -2 and double SESN1&2 KO cells. Inactivation of either SESN1 or -2 displays intermediate levels of STAT3 phosphorylation between control and double KO cell lines (Figure 7A), demonstrating that both genes contribute equally to the negative regulation of phosphorylation. We also analysed the phosphorylation of upstream STAT3 kinase JAK2 but did not observe any difference in JAK2 phosphorylation between control and SESN1- or SESN2-deficient cell lines, indicating that STAT3 phosphorylation is controlled downstream of JAK2.

To rule out the potential non-specific activity of the CRISPR constructs and confirm that SESN1&2 proteins regulate STAT3, we also silenced the expression of both SESN1 and SESN2 genes in A549 cell lines by lentiviral vectors expressing corresponding shRNAs [294]. We demonstrated increased STAT3 phosphorylation in SESN1&2 knockdown cells (Figure 7B).

In parallel, we ectopically expressed SESN2 in SESN1&2 KO cells. We observed that SESN2 reconstitution restored the levels of STAT3 phosphorylation to the levels observed in control cells (Figure 7C).

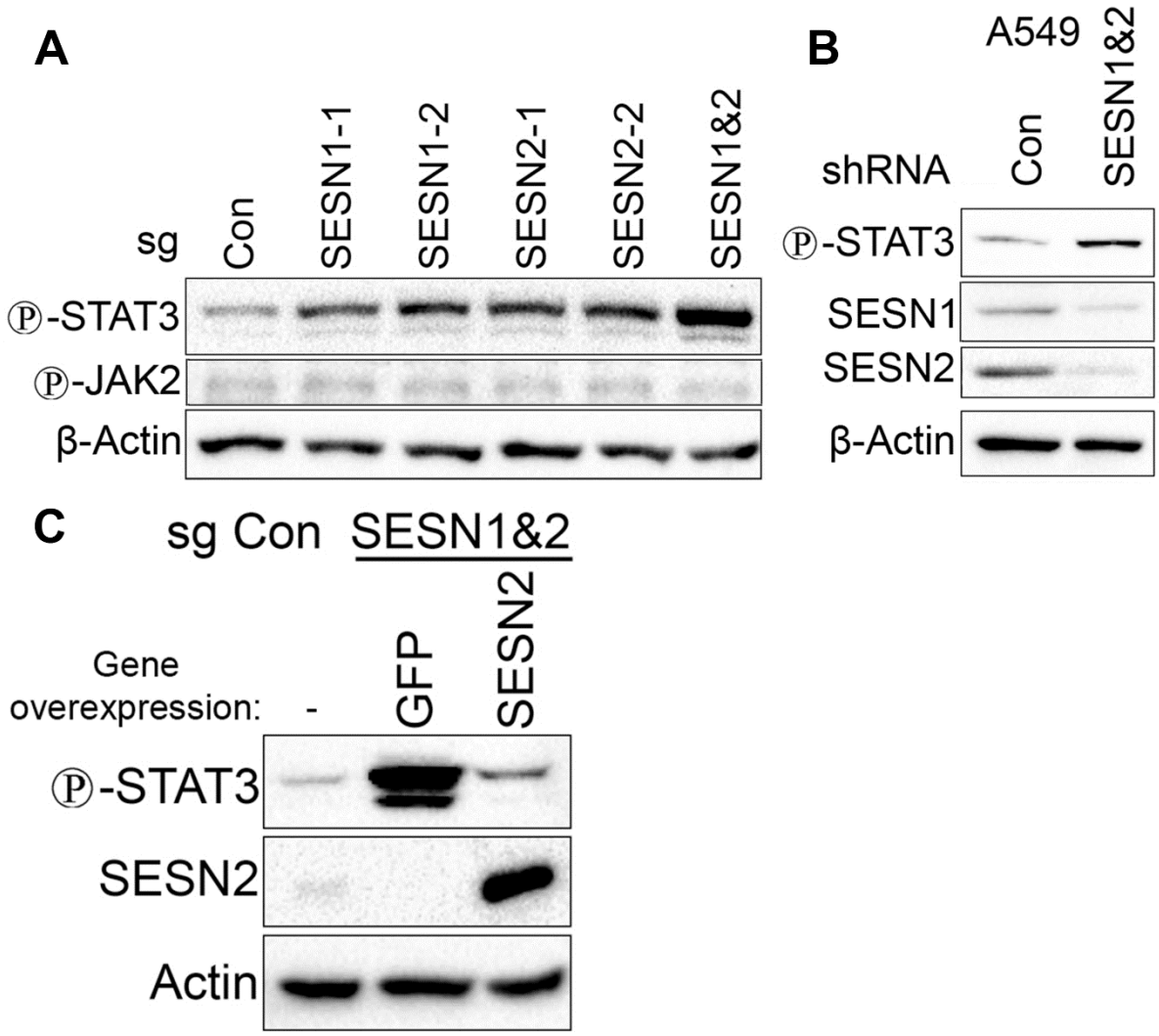

Figure 7: STAT3 activation is dependent on the expression of Sestrins
Analysis of phosphorylation of STAT3 in cell lines with different genetic manipulation mechanisms shows that STAT3 is activated independent of the mode of SESN removal. **A)** Inactivation of either SESN1 (sgSESN1) or SESN2 (sgSESN2) gene has an intermediate effect on STAT3 phosphorylation comparatively to inactivation of both SESN1&2 genes (sgSESN1&2); inactivation of SESN1, SESN2, or both genes does not affect JAK2 phosphorylation. **B)** Cells with knockdown of SESN1&2 (shRNA SESN1&2) demonstrate increased STAT3 phosphorylation levels comparatively to control cells (shRNA Con). **C)** Ectopic expression of GFP and SESN2 displays that SESN2 overexpression restores STAT3 phosphorylation in SESN1&2 KO cells to the levels observed in control cells.

3.6. Regulation of STAT3 phosphorylation by SESN1&2 is independent of GATOR2

In an attempt to determine the role of SESN1&2 in the control of STAT3 phosphorylation, we proposed that Sestrins may directly interact with the STAT3 protein, suppressing its phosphorylation by upstream kinases or activating dephosphorylation by phosphatases. To validate this assumption, we performed immunoprecipitation analysis using an approach we previously used to analyse the interactions between SESN2 and the GATOR2 protein complex, the major Sestrin interactor [293, 312]. SESN2 protein was immunoprecipitated with anti-SESN2 antibodies, and the presence of STAT3 and GATOR2 complex component MIOS was analysed using an immunoblot. We did not observe any co-precipitation of STAT3 with SESN2, while MIOS was presented in the complex (Figure 8A).

SESN2 is known for its suppression of inflammation and antioxidant activity [33, 58], so we determined if STAT3 phosphorylation in SESN1&2 KO cells may have been mediated by the secretion of growth factors or cytokines into the medium or elevation of ROS. To define whether SESN1&2 regulate STAT3 via an indirect mechanism mediated by elevated production of secreted factors, we replaced the medium of the control cells with the medium collected from the SESN1&2 KO cells. We did not observe any increase in STAT3 phosphorylation in control cells incubated with medium from SESN1&2 KO cells, ruling out the impact of secreted factors in the regulation of STAT3 phosphorylation by Sestrins (Figure 8B).

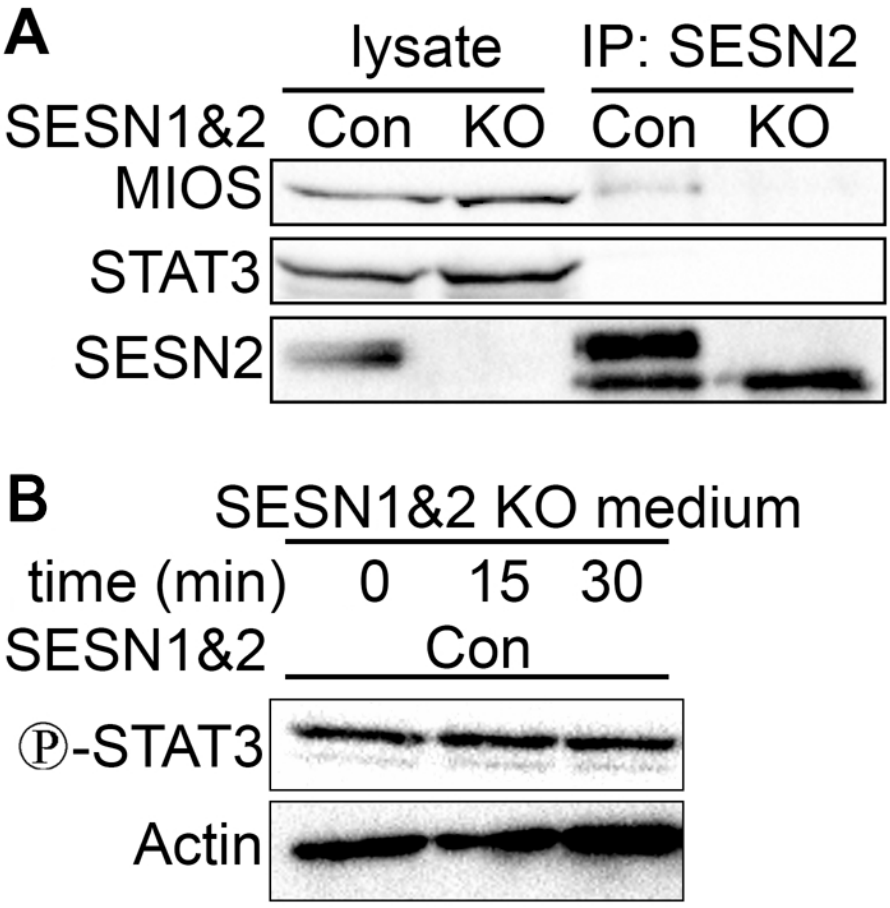

Figure 8: Sestrin does not directly interact with STAT3, and secreted factors do not contribute to STAT3 phosphorylation
A) SESN2 does not interact with STAT3. SESN2 was immunoprecipitated (IP) with an anti-SESN2 antibody, and expression of the indicated proteins was analysed by immunoblotting.
B) SESN1&2 does not regulate STAT3 phosphorylation through secreted factors. Control A549 cells (Con) were incubated with media from SESN1&2 KO cells for the indicated time intervals and analysed by immunoblotting.

We also analysed whether GATOR2 mediates the suppression of STAT3 phosphorylation by SESN1&2 and contributes to cell death. To examine this possibility, we silenced MIOS in the control and SESN1&2 KO cells by using shRNA and analysed cell death in response to cisplatin treatment with flow cytometry (Figure 9A). The knockdown of MIOS did not change cell death in either the control or SESN1&2 KO, leading us to conclude that SESNs mediate cell death via a mechanism different from their binding to GATOR2. Concurrent with these findings, western blot analysis did not reveal any observable effects on STAT3 phosphorylation in both control and SESN1&2 KO cells (Figure 9B).

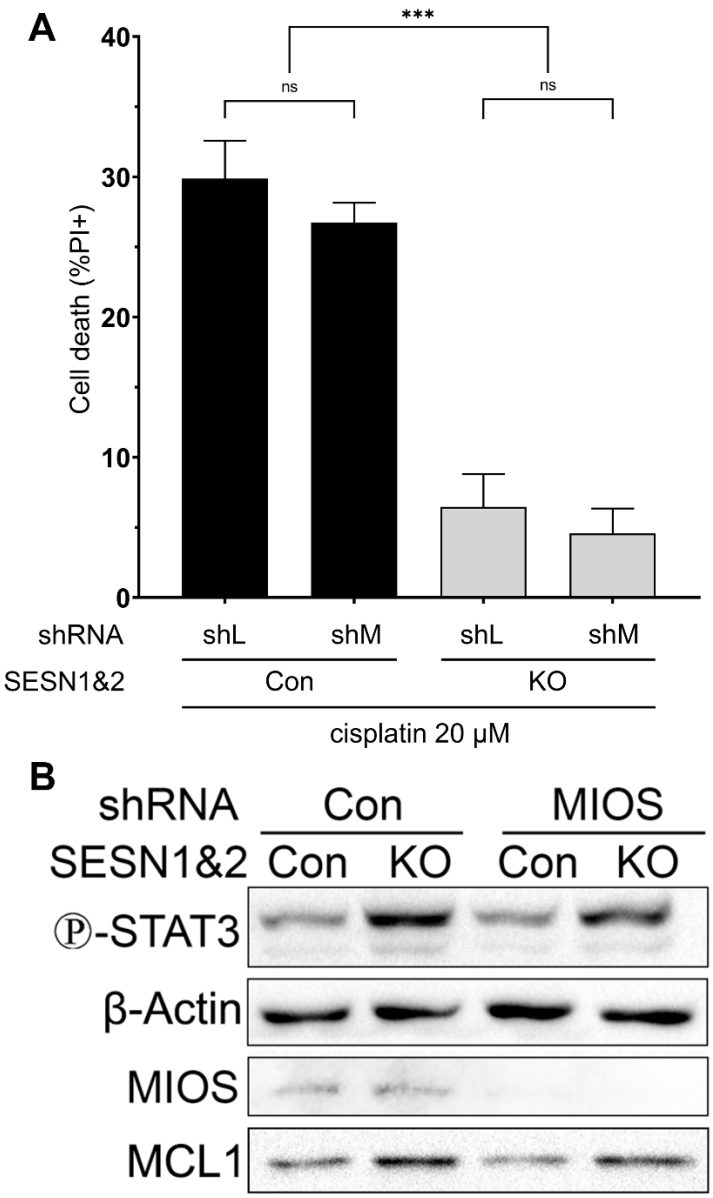

Figure 9: Resistance to cell death and activated STAT3 is independent of SESN2-GATOR2 interaction

SESN1&2-regulated cell death is GATOR2-independent. **A)** Silencing the MIOS component of GATOR2 by shRNA does not affect cisplatin-induced cell death. Cells still significantly differ in cell death between the control and SESN1&2 KO. Control and SESN1&2 KO cells expressing shLuciferase or shCon were treated with cisplatin (20 µM; 48 hours), stained with propidium iodide, and analysed by flow cytometry. The data represent the mean of two independent experiments ± SEM (n=2), where each experiment consisted of five replicates, whose means ± S.D. (n=5) were calculated and used for SEM calculation. P values were calculated using two-way ANOVA, followed by Tukey's post-test comparison. Not significant, ns; p***≤0.001. **B)** Regulation of STAT3 by SESN1&2 does not involve GATOR2. MIOS was silenced by shRNA in control and SESN1&2 KO cells, and phosphorylation and expression of the indicated proteins were analysed by immunoblotting.

3.7. Regulation of STAT3 phosphorylation by SESN1&2 is independent of their antioxidative function

To assess the influence of reactive oxygen species (ROS) on STAT3 phosphorylation in SESN1&2 knockout cells, we administered varying ROS scavenger N-acetyl cysteine (NAC) concentrations to these cells. Analysis of STAT3 phosphorylation revealed no change following NAC treatment, as depicted in Figure 10A. Considering the possibility that the duration of NAC exposure might be critical, we conducted a further experiment using the highest previously tested concentration of NAC with extended treatment periods focusing on the SESN1&2 knockout (Figure 10B). Anticipating that the absence of Sestrins, known for their antioxidant functions, could compromise the cellular oxidative stress response, we observed no decrease in STAT3 phosphorylation, even after six hours of NAC treatment. Contrary to our expectations, a slight increase in p-STAT3 levels was noted at the five and six-hour marks. This outcome led us to conclude that the antioxidative capabilities of NAC and Sestrins do not significantly impact STAT3 phosphorylation in this context.

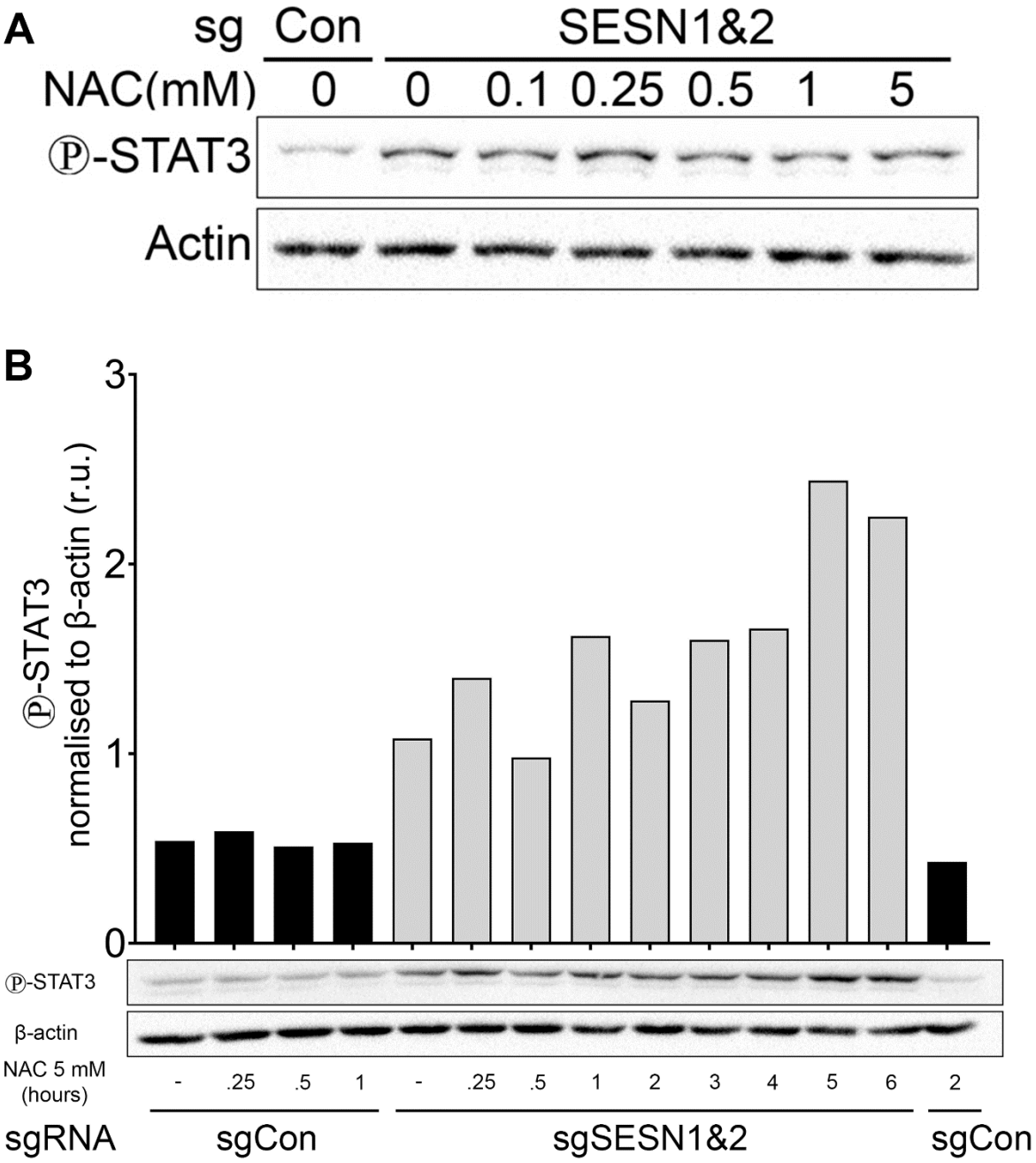

Figure 10: Treatment with ROS scavenger n-acetyl-cysteine (NAC) does not restore control STAT3 phosphorylation

Activation of STAT3 phosphorylation in SESN1&2 KO cells does not depend on the antioxidant activity of Sestrins. **A)** SESN1&2 KO cells were treated with different concentrations of a ROS scavenger NAC for 3 hours. STAT3 phosphorylation was analysed by immunoblotting and compared to control (Con). **B)** Control and SESN1&2 cells were treated with 5 mM of NAC across six hours, and STAT3 phosphorylation was analysed by immunoblotting. Bar chart shows the densitometry analysis of p-STAT3 normalised to β-actin. Bars represent their corresponding lanes shown in western blot directly below.

To examine if the STAT3 phosphorylation could be induced by the introduction of exogenous ROS, A549 control and SESN1&2 knockout cells were subjected to various treatments with hydrogen peroxide over durations ranging from 15 minutes to 24 hours and across a range of concentrations. Given the unstable nature of H_2O_2 and its use in cell culture conditions, effective concentrations that provoked a biological response varied slightly across experiments. However, concentrations between 50-100 μM were the approximate range in which we expect cell death and effects on cell morphology. Figure 11A displays cell death analysis after 24 hours of treatment with H_2O_2. We found that our knockout cells diminished resilience to exogenous ROS. This aligns with the established role of Sestrins as antioxidants.

Employing the same concentrations observed to impact cell viability, we conducted a western blot analysis one hour after treatment (Figure 11B). We considered this an adequate time interval for cellular kinases and phosphatases to be affected by the oxidative insult. No difference was observed between untreated cells and their treatment with H_2O_2; the control and SESN1&2 KO displayed the same STAT3 phosphorylation regardless of this treatment. This concluded our investigation into the role of oxidative species on STAT3 phosphorylation, as neither mitigating ROS with NAC nor inducing it with H_2O_2 yielded any discernible effect on STAT3 activity.

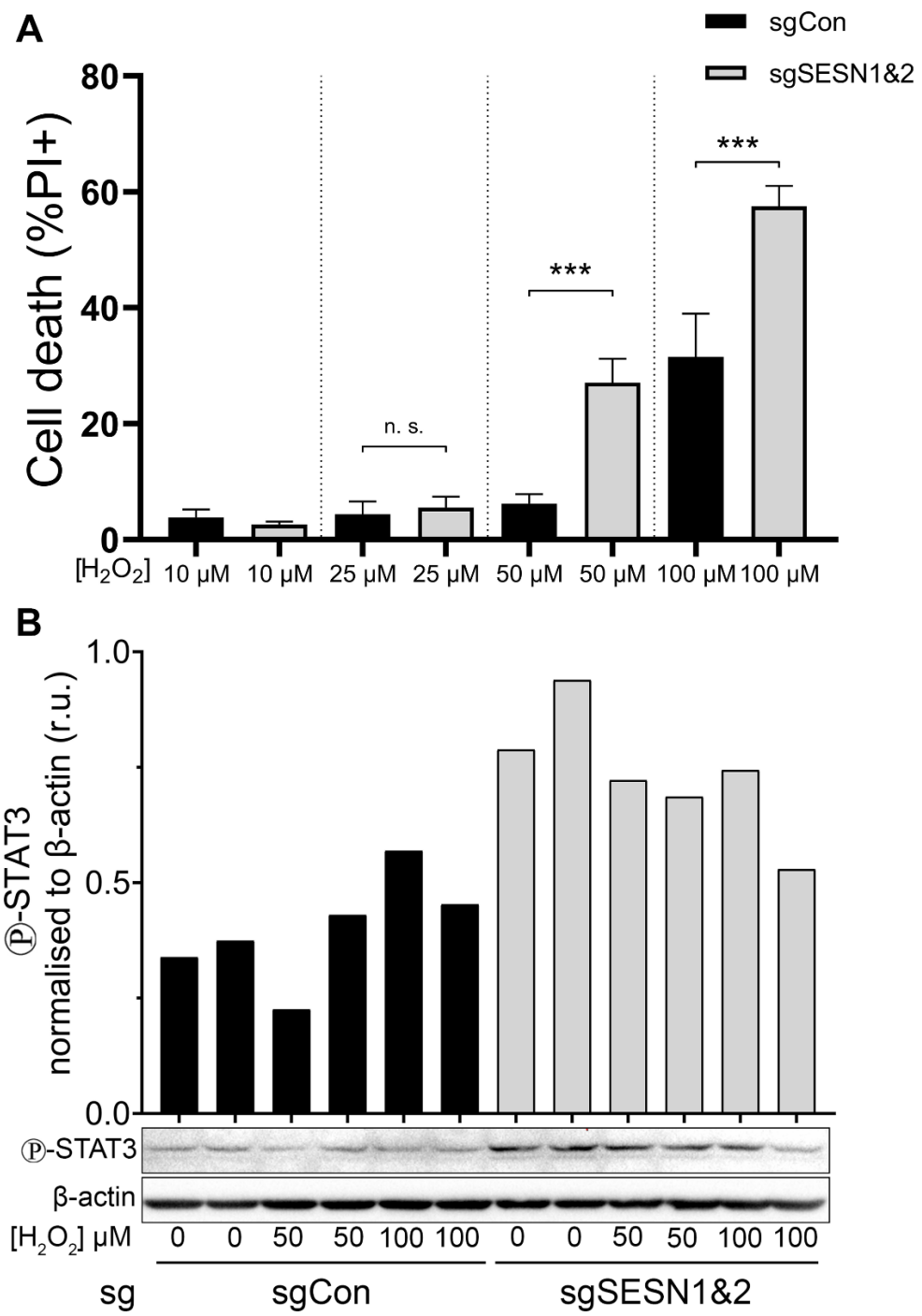

Figure 11: Treatment with hydrogen peroxide does not induce change in STAT3 phosphorylation

STAT3 phosphorylation is not sensitive to additional oxygen species introduced by H_2O_2. **A)** Control and SESN1&2 KO were treated with a range of H_2O_2 concentrations, and cell death was measured using propidium iodide and flow cytometry after 24 hours of treatment. The data are presented as mean ±S.D. (n=4). P values were calculated using one-way ANOVA, followed by Tukey's post-test comparison. Not significant, ns; p***≤0.001. **B)** Control and SESN1&2 KO cells were treated with different concentrations of H_2O_2 for 1 hour. STAT3 phosphorylation was analysed by immunoblotting. Bar chart shows the densitometry analysis of p-STAT3 normalised to β-actin. Bars represent their corresponding lanes above.

3.8. JAKs are essential for STAT3 phosphorylation in this context

Pursuing the goal of understanding the impact of SESN2 in better detail, we tested if the regulation of STAT3 phosphorylation by SESN1&2 requires JAK kinases, which are activated by cytokines and several growth factors through activation of the cognate receptors.

We employed the JAK inhibitor ruxolitinib to determine the importance of JAKs in STAT3 regulation in control and SESN1&2 KO cells. To investigate whether the resistance to cell death of the SESN1&2 KO would be affected by complete inhibition of JAKs, we co-treated control and SESN1&2 KO with cisplatin and ruxolitinib. The apoptotic cell death was measured via AnnexinV;PI staining, and flow cytometry (Figure 12A). We found that the resistance to apoptosis reversed to control levels in the presence of the JAK inhibitor, suggesting that the STAT3 activation by JAKs is essential for STAT3-mediated cell death resistance.

We observed that STAT3 was completely dephosphorylated in both control and SESN1&2 KO cells, indicating that JAKs are required for the phosphorylation of STAT3 in both control and SESN1&2 KO A549 cells (Figure 12B).

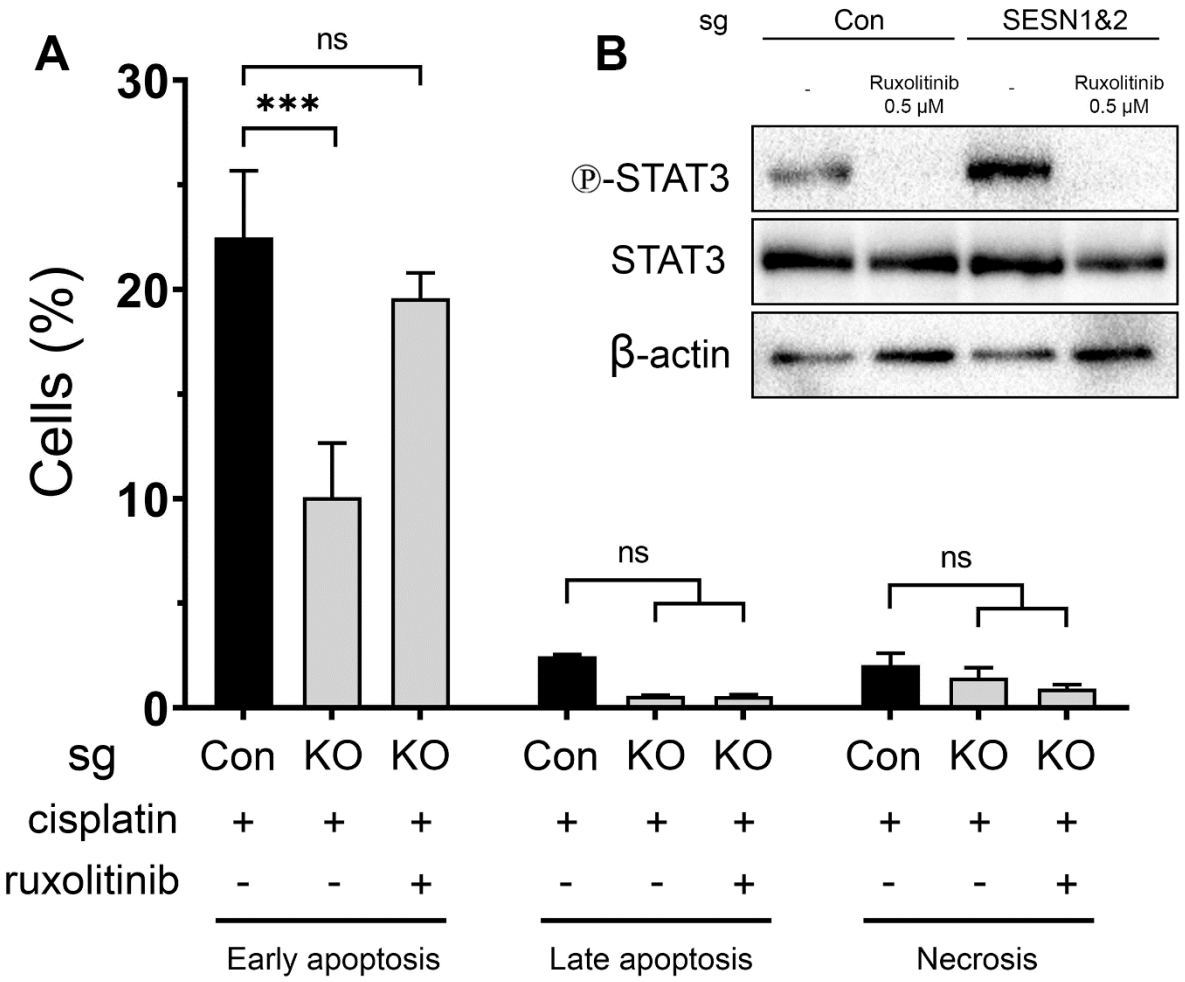

Figure 12: JAK inhibitor ruxolitinib completely inhibits phosphorylated STAT3
A) Cells were treated with cisplatin (20 μM; 24 hours) in or without the presence of ruxolitinib (0.5 μM; 24 hours) and then stained by AnnexinV;PI and analysed by flow cytometry. Bar chart separates necrosis, late apoptosis, and early apoptosis to show a difference in early apoptotic death between SESN1&2 KO and control cells. The data are presented as mean ±S.D. (n=4). P values were calculated using two-way ANOVA, followed by Tukey's post-test comparison. Not significant, ns; p***≤0.001. **B)** Immunoblot showing that treatment with JAK inhibitor ruxolitinib (0.5 μM; 6 hours) is enough to completely eliminate STAT3 phosphorylation in both control (Con) and SESN1&2 KO cells.

Epidermal growth factor receptor (EGFR), a key driver of carcinogenesis in lung adenocarcinoma cells, may also be responsible for STAT3 phosphorylation in this context. EGFR is often overactivated in lung cancer cells [313]. Mutations in the EGFR kinase domain were shown to activate STAT3 [314]. EGFR was shown to interact with SESN2 in 293T cells. In this study, EGFR-GFP was transfected into HEK293 cells. After stimulation with epidermal growth factor (EGF) for 5 min, EGFR was precipitated by an anti-GFP antibody and subject to mass spectrometry (MS) analysis [315]. However, this is an overexpression study and may be an artefact of the method. SESN2 fragment MIVADSECR, which are the first nine amino acids specific to SESN2, was detected by MS in EGFR fraction.

To check if EGFR is implicated in STAT3 regulation, we treated control and SESN1&2 KO cells with the EGFR inhibitor erlotinib and analysed STAT3 phosphorylation. Erlotinib is an EGFR inhibitor with an IC50 of 2 nM [316]. Erlotinib competitively inhibits EGFR tyrosine kinase by binding to the receptor's ATP-binding site. However, erlotinib did not affect STAT3 phosphorylation in control or SESN1&2 KO cells, ruling out the potential impact of EGFR in this process (Figure 13).

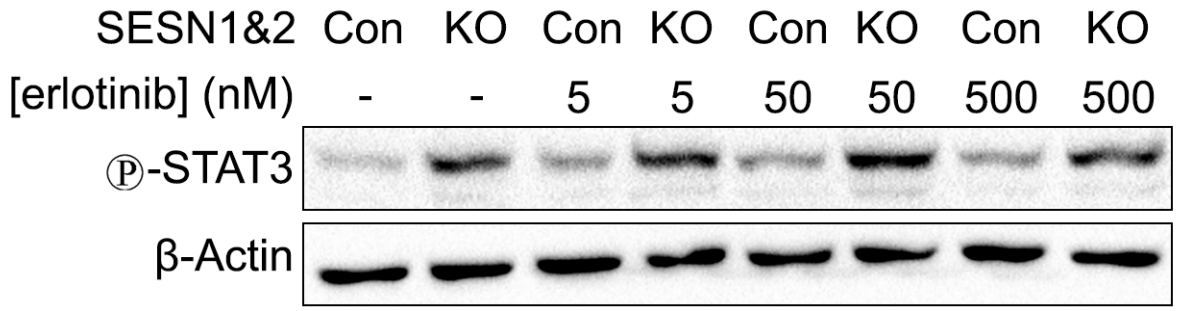

Figure 13: EGFR inhibitor erlotinib does not affect STAT3 phosphorylation
A549 control (Con) and SESN1&2 KO were treated with the EGFR inhibitor erlotinib (5-500 nM; 6 hours). Erlotinib IC50 was previously shown to be 2 nM. Phosphorylation of STAT3 was analysed by immunoblot.

To investigate the involvement of non-receptor protein-tyrosine kinases Abl, Src, and c-Kit, we used dasatinib, a potent inhibitor with IC50 values of 0.6 nM and 0.8 nM for Abl and Src, respectively [317], and 79 nM for c-Kit [318]. Treatment with concentrations well above these IC50s showed no effect on p-STAT3 levels (Figure 14A). Furthermore, concurrent treatment with dasatinib and cisplatin did not eliminate the difference in cell death between control and SESN1&2 KO (Figure 14B).

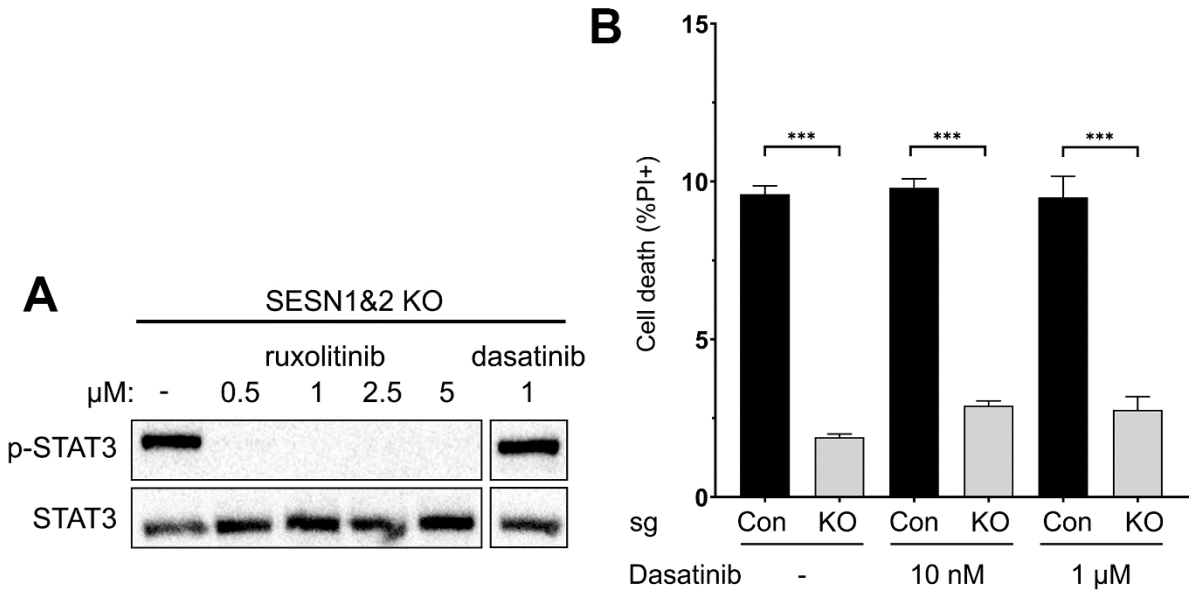

Figure 14: Dasatinib, an Abl, Src, and c-Kit inhibitor, does not affect STAT3 phosphorylation

A) A549 SESN1&2 KO was treated with ruxolitinib (0.5-5 μM; 6 hours) and dasatinib (1 μM; 6 hours). Dasatinib IC50 against its targets was shown to be 0.6 nM - 80 nM. Phosphorylation of STAT3 was analysed by immunoblot. **B)** Control and SESN1&2 KO cells were treated with cisplatin (20 μM; 48 hours) without or with dasatinib (10 nM - 1 μM), stained with propidium iodide, and analysed by flow cytometry. The data are presented as mean ±S.D. (n=4). P values were calculated using two-way ANOVA, followed by Tukey's post-test comparison. Not significant, ns; p***≤0.001.

3.9. Regulation of cell proliferation and cell death by SESN1&2 is mediated by STAT3

STAT3 plays a crucial role in cell proliferation and suppression of cell death in many tumour cells. SESN1&2 KO cells demonstrate higher proliferation rates and greater resistance to cell death than control cells.

To examine the role of STAT3 in the regulation of cell proliferation and cell death, we analysed STAT3 phosphorylation in the SESN1&2 KO cells treated with different concentrations of STAT3 inhibitor C188-9. This small molecule selectively targets the pY-peptide binding site within the STAT3 SH2 domain, blocking its phosphorylation [319]. Treatment with 20 μM of C188-9 decreased STAT3 phosphorylation to the levels observed in control cells, and incubation with 30 μM of C188-9 almost eliminated STAT3 phosphorylation (Figure 15A).

To study whether the activation of STAT3 in SESN1&2 KO cells is responsible for controlling cell death, we treated cells with cisplatin in the presence of different concentrations of C188-9. We demonstrated that treatment of SESN1&2 KO cells with 20 μM of C188-9 induced cell death to similar levels observed in the control cells (Figure 15B).

We determined proliferation rates in control cells and SESN1&2 KO cells after treating them with different concentrations of C188-9. As previously shown [254], SESN1&2 KO cells grow faster than control cells, and treatment with 20 μM of C188-9 slows down proliferation of SESN1&2 KO cells to the rate observed in the control cells. Moreover, the treatment with 30 μM of C188-9 decreases the cell proliferation rate even further (Figure 15C).

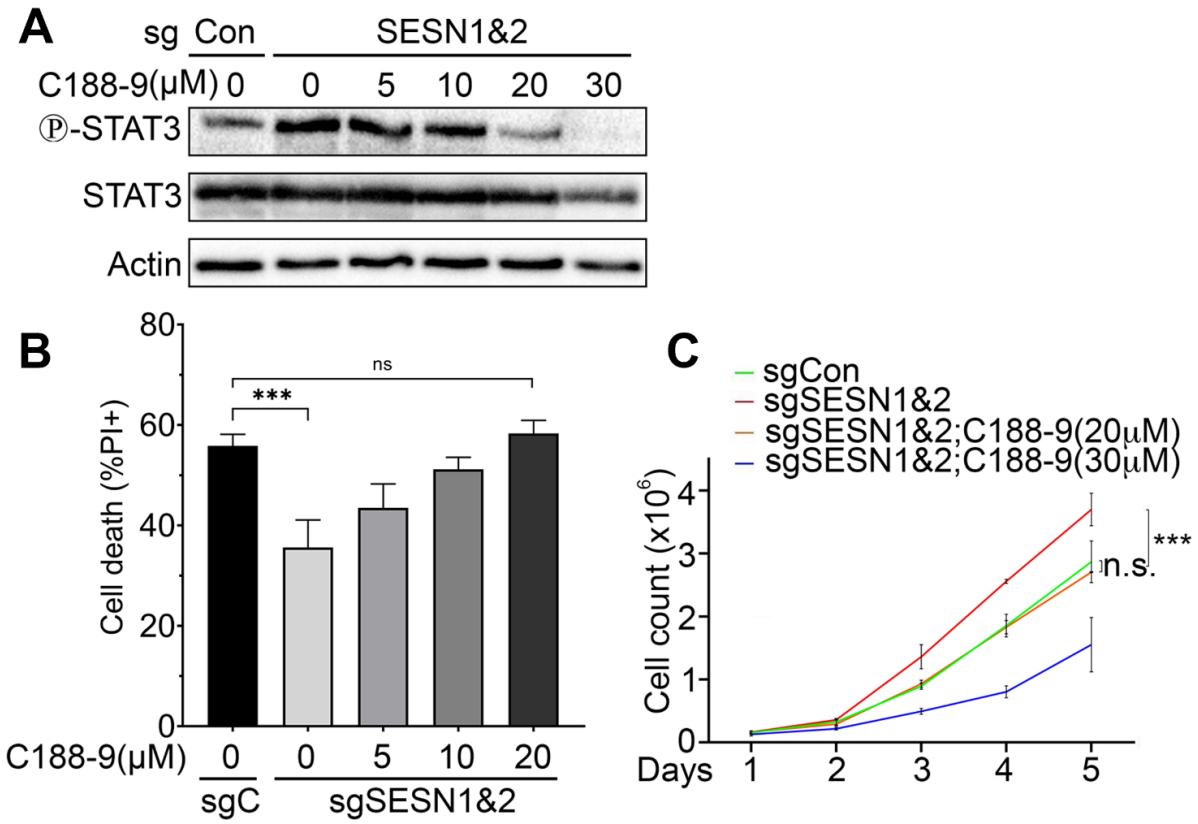

Figure 15: Small molecule inhibition of STAT3 phosphorylation suggests that SESN1&2 regulate cell proliferation and death via a STAT3-dependent mechanism
A) Analysis of STAT3 phosphorylation in response to different concentrations of STAT3 inhibitor C188-9. SESN1&2 KO (sgSESN1&2) cells were treated for 24 h with corresponding concentrations of C188-9, and phosphorylation and expression of STAT3 were determined by immunoblotting. **B)** Treatment of SESN1&2 KO cells with C188-9 reverses cell death to the levels observed in control cells. Cells were co-treated with cisplatin (20 μM) and varying concentrations of C188-9 for 24 hours. The levels of cell death were analysed by propidium iodide staining followed by flow cytometry. The data are presented as mean ±S.D. (n=4). **C)** Treatment of SESN1&2 KO cells with C188-9 reverses the proliferation rate to the levels observed in control cells. 50000 cells were plated on 6-cm culture dishes, and the number of cells was calculated every 24 hours using a haemocytometer. The data are presented as mean ±S.D. (n=2). P values were calculated using two-way ANOVA, followed by Tukey's post-test comparison. Not significant, ns; p***≤0.001. For C), day 5 of the curve was used for the statistical test.

To rule out any non-specific activity of the STAT3 inhibitor, we silenced STAT3 with shRNA and generated an almost complete knockdown of STAT3 in the control and SESN1&2 KO cells (Figure 16A). Similarly to the results based on STAT3 inhibition with C188-9, SESN1&2 KO cells with STAT3 knockdown demonstrated a decreased proliferation rate compared to control cells, indicating that STAT3 plays an important role in support of cell proliferation in A549 cells (Figure 16B). To determine if silencing of STAT3 alleviates resistance of SESN1&2 KO cells to cisplatin, we treated control and SESN1&2 KO cells expressing either control or STAT3 shRNA. While we observed a remarkable difference in the levels of cell death between control and SESN1&2 KO cells expressing control shRNA, higher levels of cell death were observed in both control and SESN1&2 KO cells expressing shSTAT3. Moreover, the difference in cell death between control and SESN1&2 KO was eliminated, underpinning the important role of STAT3 in Sestrin-regulated cell death following genotoxic stress (Figure 16C-D).

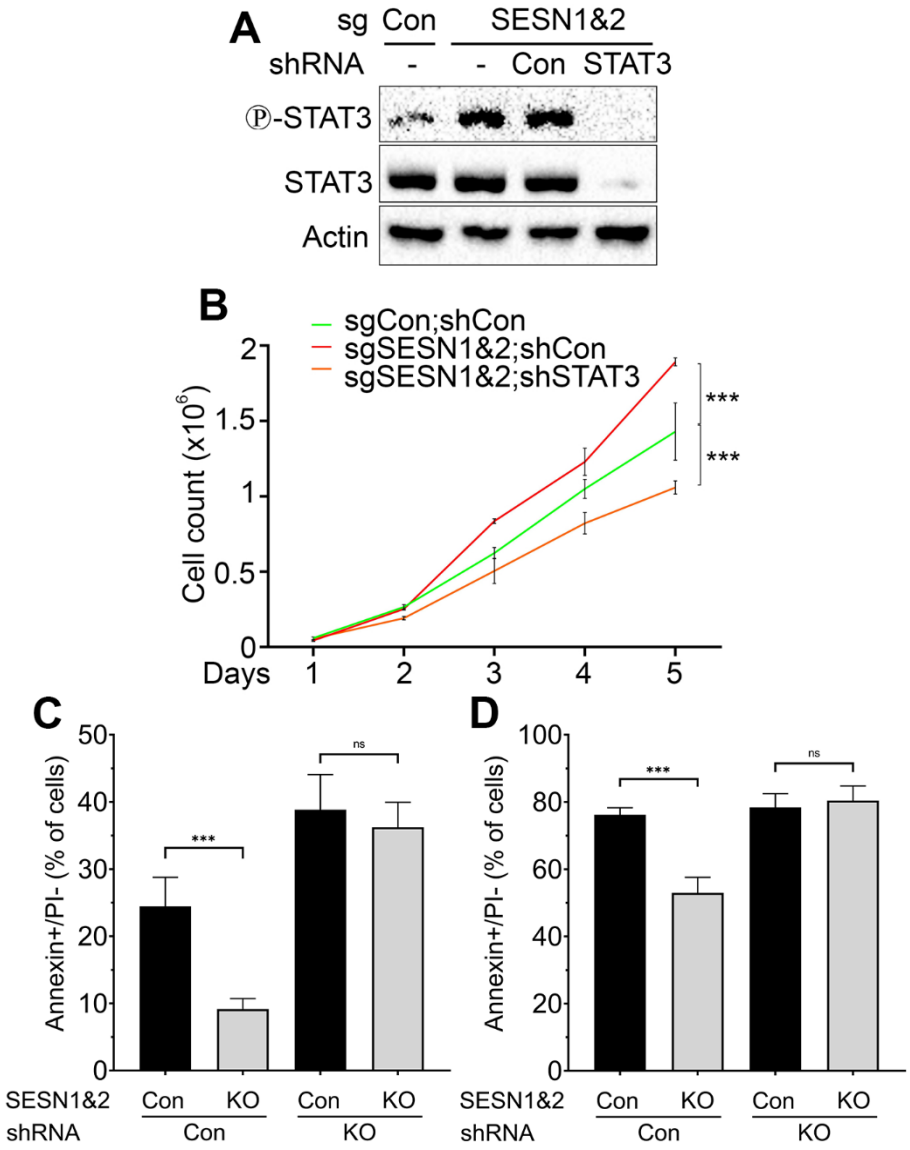

Figure 16: Short hairpin RNA silencing of STAT3 suggests that SESN1&2 regulate cell proliferation and death via a STAT3-dependent mechanism

A) Silencing of STAT3 by shRNA (shSTAT3) effectively inhibits its expression in SESN1&2 KO cells. Cells were infected with a shSTAT3-expressing lentiviral construct, selected on hygromycin, and the levels of STAT3 phosphorylation and expression were analysed by immunoblotting. **B)** STAT3 silencing suppresses the proliferation of SESN1&2 KO cells. Growth curve was obtained as in Figure 15C (n=2). **C-D)** STAT3 silencing attenuates SESN1&2 KO resistance to cisplatin to the levels observed in control cells. Control and STAT3-silenced cells were treated with cisplatin (20 μM) for 24h (Figure 16C) and 48h (Figure 16D), and the levels of apoptosis were analysed by AnnexinV;PI and flow cytometry. Bar charts represent Early Apoptosis (PI-;AnnexinV+) to show a difference in early apoptotic death between SESN1&2 KO and control cells. The data in C&D are presented as mean ±S.D. P values were calculated using one-way and two-way ANOVA, followed by Tukey's post-test comparison. Not significant, ns; p***≤0.001.

To investigate STAT3 downstream targets, we analysed the expression levels of MCL1 and Cyclin D1, which were found to be upregulated in our western blot analyses (Figure 6B).

MCL1 is an inhibitor of apoptosis from the BCL2 protein family of apoptotic regulators [320]. This anti-apoptotic protein is often overexpressed in different human cancers due to gene amplification or other mechanisms [320, 321]. Elevated expression of MCL1 suppresses cell death in response to anticancer drugs. MCL1 showed consistent upregulation, evidenced by increased detection in western blot analyses (Figure 17A) and qPCR, confirming approximately two-fold higher transcription levels than control (Figure 17B).

Employing a lentiviral vector for shRNA-mediated knockdown, we achieved stable knockdown of MCL1 expression (Figure 17C). Cell death analysis via propidium iodide staining and flow cytometry indicated a normalisation of cell death rates between control and SESN1&2 KO, alongside an overall increase in cell death in cells subjected to shMCL1 (Figure 17D). This suggests that this anti-apoptotic protein is essential in the SESN-STAT3-mediated apoptosis.

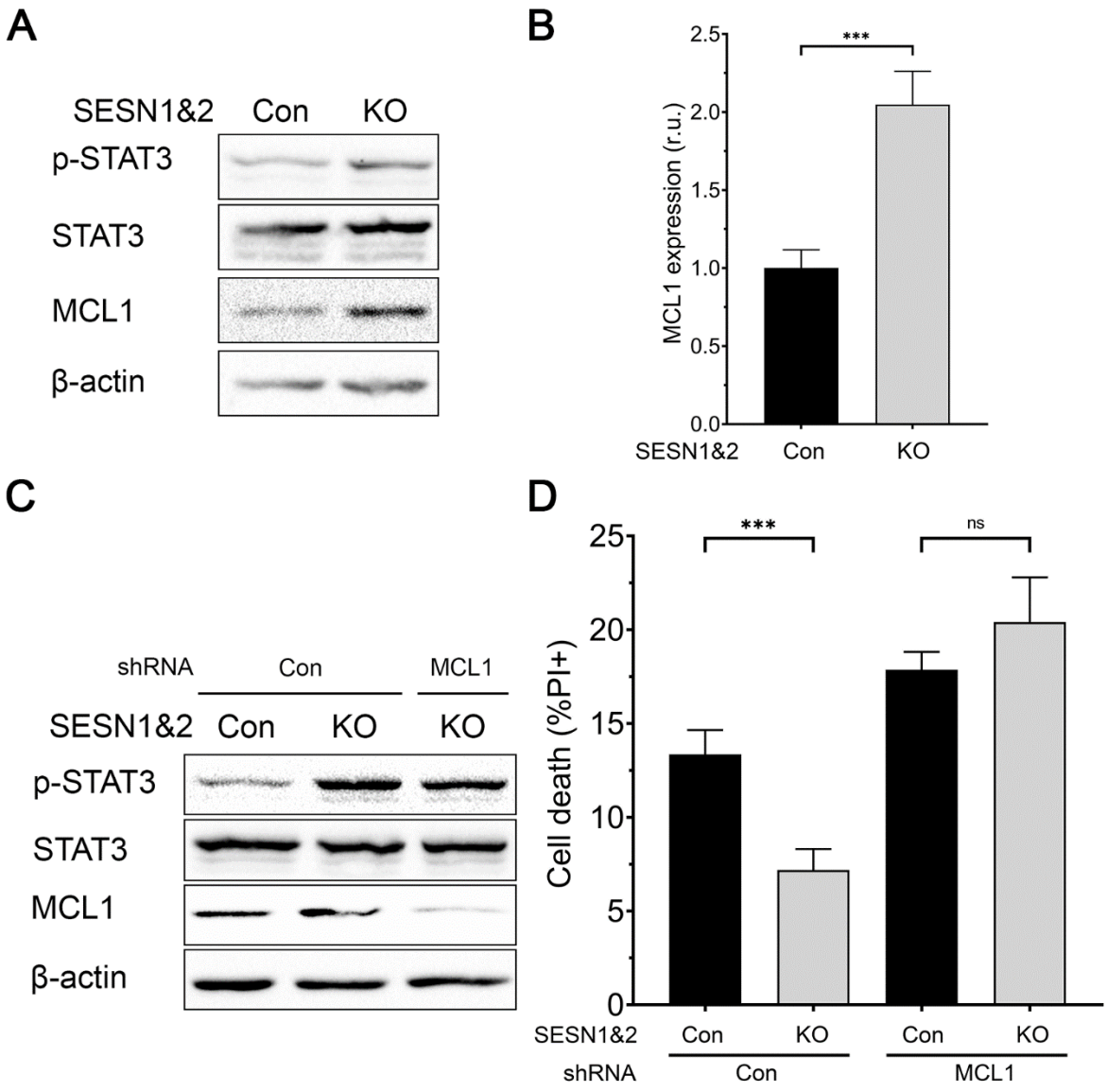

Figure 17: MCL1 mediates the anti-apoptotic effect of overactivated STAT3 in SESN1&2 KO

A) Western blot analysis of control and SESN1&2 exhibits a higher activation of STAT3 and MCL1. **B)** qPCR analysis of MCL1. The bar chart displays the mean relative MCL1 expression ±S.D. in SESN1&2 KO vs control cells (n=2). Cells were plated with the same density, cDNA was synthesised and analysed by SYBR-green-based qPCR.
C) Silencing of MCL1 by shRNA (shMCL1) inhibits its expression in SESN1&2 KO cells. Cells were infected with a shMCL1-expressing lentiviral construct, selected on hygromycin, and the levels of MCL1 expression were analysed by immunoblotting. **D)** MCL1 silencing attenuates SESN1&2 KO resistance to cisplatin to the levels observed in control cells. Control and MCL1-silenced cells were treated with cisplatin (20 μM) for 48h, and cell death was analysed by propidium iodide staining and flow cytometry. Bars represent mean ±S.D (n=4). P values were calculated using one-way ANOVA, followed by Tukey's post-test comparison. Not significant, ns; p***≤0.001.

Similarly, we examined Cyclin D1. Cyclin D1 is a regulatory protein essential for the cell cycle's progression, specifically by enabling the transition from the G1 phase to the S phase, where DNA replication occurs. While on western blot, we saw a difference in the expression of this protein (Figure 18B), we could not see a difference in its expression through qPCR analysis (Figure 18C). Additionally, we performed a basic cell cycle analysis using propidium iodide, which involves fixing cells with EtOH and staining with propidium iodide (Figure 18A). This analysis categorises cells into phases based on DNA content: cells in the G0/G1 phase with one genome copy, cells in the S phase exhibiting intermediate DNA content, and cells in the G2/M phase with two genome copies, indicating readiness for mitosis. While this approach provides a preliminary overview, it lacks the precision of more sophisticated methods like BrdU incorporation assays. However, given our limited resources and the scope of our investigation, we were constrained to this level of analysis.

Our analysis indicated an increase in SESN1&2 knockout cells in the G0/G1 phase by 10% and a decrease in the G2/M phase by 10%. Given Cyclin D1's role in facilitating the G1 to S phase transition, we anticipated an increase in cells within the S phase. Therefore, the observed discrepancy between Cyclin D1's protein levels and qPCR results, combined with the limitations of our cell cycle analysis method, leaves our findings regarding Cyclin D1's impact inconclusive.

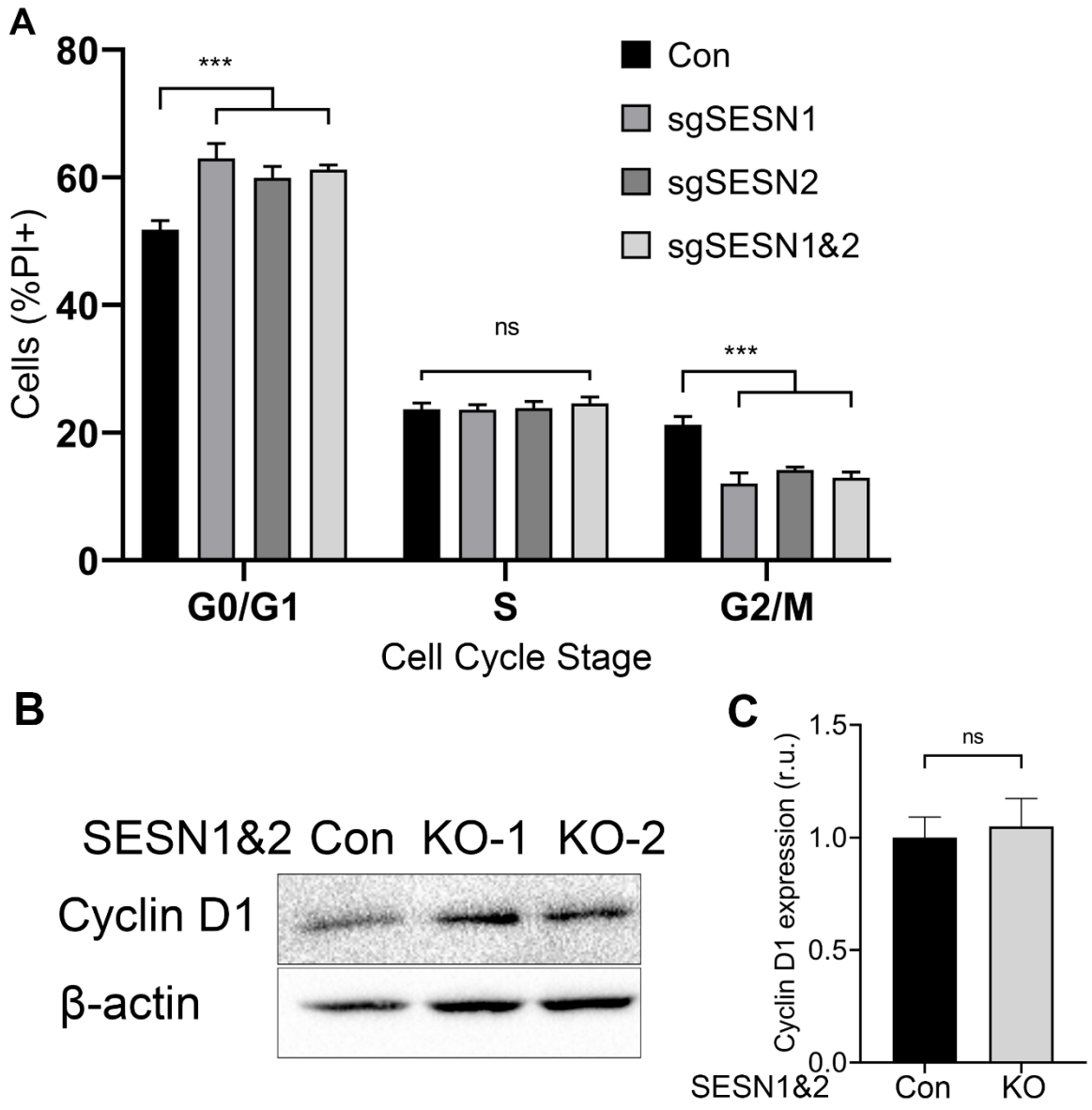

Figure 18: Cyclin D1 is marginally higher, but SESN1&2 KO arrest in G0/G1
Cyclin D1 upregulation is not reproducible, and the cell cycle analysis does not show the effects of higher Cyclin D1.
A) Flow cytometry cell cycle analysis using EtOH fixation and propidium iodide staining. Data represents the mean percentage of the corresponding cells in the population ±SD (n=6). **B)** Western blot demonstrated higher Cyclin D1 in two independent knockouts of SESN1&2. **C)** qPCR analysis of Cyclin D1. The bar chart displays the mean relative Cyclin D1 expression ±S.D. in control vs SESN1&2 KO cells (n=2).

3.10. SESN1&2 regulate the expression of genes involved in the regulation of the JAK-STAT3 pathway

The task of identifying STAT3 regulators remains a challenge of this research. Although we have investigated choice regulators of STAT3, such as EGFR, JAK kinases and non-receptor PTKs, these efforts were dictated by hints that Sestrins may be involved with these proteins. An investigation of every possible receptor, regulator or STAT3 partner was impossible for us due to resource limitations.

We collaborated with a bioinformatics-focused lab and performed an RNA-sequencing analysis comparing A549 controls against SESN1&2 knockouts. Figure 19A displays the format of the information we received: an Excel file with the list of genes upregulated or downregulated significantly. Four biological controls were compared to five distinct SESN1&2 knockouts, which comprised two completely distinct single-guide RNA sequences used to knock out SESN1&2.

Manually, we sought out potential STAT3 regulators in this list and selected five potential regulators to investigate. These were H19, PTPRD, PTPRB, HACD4/PTPLAD2, and BPIFA1. Figure 19B displays their Log2FC as seen in the RNAseq Excel file provided to us. PTPRD was one of the highest downregulated genes and also seemed to have the most research that pointed towards its involvement with STAT3.

A

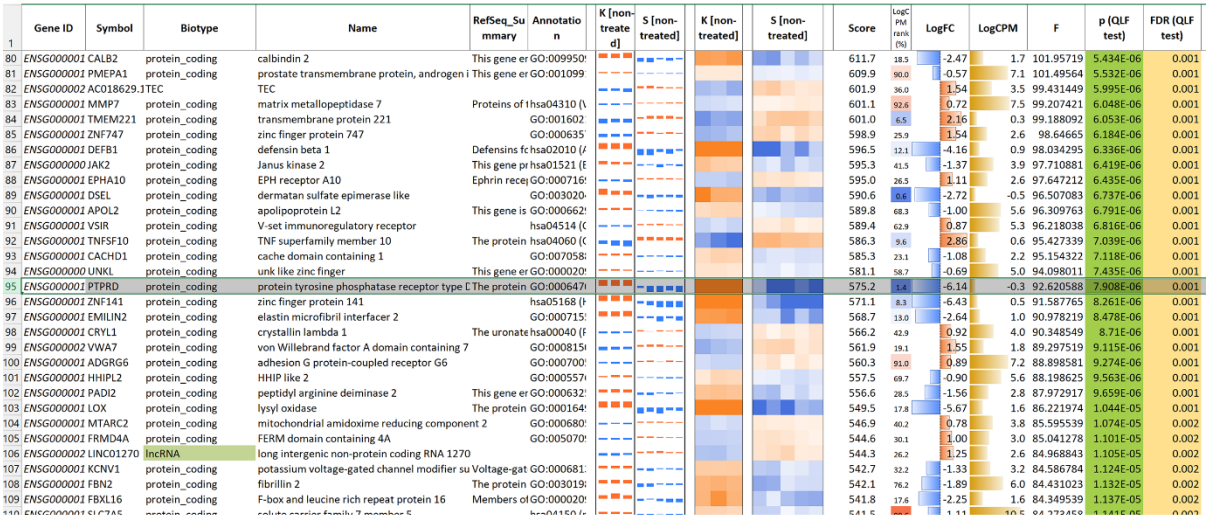

	Gene ID	Symbol	Biotype	Name	RefSeq_Summary	Annotation	K [non-treated]	S [non-treated]	K [non-treated]	S [non-treated]	Score	LogCPM rank (%)	LogFC	LogCPM	F	p (QLF test)	FDR (QLF test)
80	ENSG00000	CALB2	protein_coding	calbindin 2	This gene er	GO:009950					611.7	18.5	-2.47	1.7	101.95719	5.434E-06	0.001
81	ENSG00000	PMEPA1	protein_coding	prostate transmembrane protein, androgen i	This gene er	GO:001099					609.9	90.0	-0.57	7.1	101.49564	5.532E-06	0.001
82	ENSG00000	AC018629.1	TEC	TEC							601.9	36.0	1.54	3.5	99.431449	5.995E-06	0.001
83	ENSG00000	MMP7	protein_coding	matrix metallopeptidase 7	Proteins of t	hsa04310 (\					601.1	92.6	0.72	7.5	99.207421	6.048E-06	0.001
84	ENSG00000	TMEM221	protein_coding	transmembrane protein 221		GO:001602					601.0	6.5	2.16	0.3	99.188092	6.053E-06	0.001
85	ENSG00000	ZNF747	protein_coding	zinc finger protein 747		GO:000635					598.9	25.9	1.54	2.6	98.64665	6.184E-06	0.001
86	ENSG00000	DEFB1	protein_coding	defensin beta 1	Defensins fc	hsa02010 (/					596.5	12.1	-4.16	0.9	98.034295	6.336E-06	0.001
87	ENSG00000	JAK2	protein_coding	Janus kinase 2	This gene pr	hsa01521 (E					595.3	41.5	-1.37	3.9	97.710881	6.419E-06	0.001
88	ENSG00000	EPHA10	protein_coding	EPH receptor A10	Ephrin recej	GO:000716					595.0	26.5	1.11	2.6	97.647212	6.435E-06	0.001
89	ENSG00000	DSEL	protein_coding	dermatan sulfate epimerase like		GO:003020					590.6	0.6	-2.72	-0.5	96.507083	6.737E-06	0.001
90	ENSG00000	APOL2	protein_coding	apolipoprotein L2	This gene is	GO:000662					589.8	68.3	-1.00	5.6	96.309763	6.791E-06	0.001
91	ENSG00000	VSIR	protein_coding	V-set immunoregulatory receptor		hsa04514 (C					589.4	62.9	0.87	5.3	96.218038	6.816E-06	0.001
92	ENSG00000	TNFSF10	protein_coding	TNF superfamily member 10	The protein	hsa04060 (C					586.3	9.6	2.86	0.6	95.427339	7.039E-06	0.001
93	ENSG00000	CACHD1	protein_coding	cache domain containing 1		GO:007058					585.3	23.1	-1.08	2.2	95.154322	7.118E-06	0.001
94	ENSG00000	UNKL	protein_coding	unk like zinc finger	This gene er	GO:000020					581.1	58.7	-0.69	5.0	94.098011	7.435E-06	0.001
95	ENSG00000	PTPRD	protein_coding	protein tyrosine phosphatase receptor type D	The protein	GO:000647					575.2	1.4	-6.14	-0.3	92.620588	7.908E-06	0.001
96	ENSG00000	ZNF141	protein_coding	zinc finger protein 141		hsa05168 (H					571.1	8.3	-6.43	0.5	91.587765	8.261E-06	0.001
97	ENSG00000	EMILIN2	protein_coding	elastin microfibril interfacer 2		GO:000715					568.7	13.0	-2.64	1.0	90.978219	8.478E-06	0.001
98	ENSG00000	CRYL1	protein_coding	crystallin lambda 1	The uronate	hsa00040 (F					566.2	42.9	0.92	4.0	90.348549	8.71E-06	0.001
99	ENSG00000	VWA7	protein_coding	von Willebrand factor A domain containing 7		GO:000815					561.9	19.1	1.55	1.8	89.297519	9.115E-06	0.001
100	ENSG00000	ADGRG6	protein_coding	adhesion G protein-coupled receptor G6		GO:000700					560.3	91.0	0.89	7.2	88.898581	9.274E-06	0.001
101	ENSG00000	HHIPL2	protein_coding	HHIP like 2		GO:000557					557.5	69.7	-0.90	5.6	88.198625	9.563E-06	0.001
102	ENSG00000	PADI2	protein_coding	peptidyl arginine deiminase 2	This gene er	GO:000632					556.6	28.5	-1.56	2.8	87.972917	9.659E-06	0.001
103	ENSG00000	LOX	protein_coding	lysyl oxidase	The protein	GO:000164					549.5	17.8	-5.67	1.6	86.221974	1.044E-05	0.001
104	ENSG00000	MTARC2	protein_coding	mitochondrial amidoxime reducing component 2		GO:000680					546.9	40.2	0.78	3.8	85.595539	1.074E-05	0.002
105	ENSG00000	FRMD4A	protein_coding	FERM domain containing 4A		GO:005070					544.6	30.1	1.00	3.0	85.041278	1.101E-05	0.002
106	ENSG00000	LINC01270	lncRNA	long intergenic non-protein coding RNA 1270							544.3	26.2	1.25	2.6	84.968843	1.105E-05	0.002
107	ENSG00000	KCNV1	protein_coding	potassium voltage-gated channel modifier su	Voltage-gat	GO:000681					542.7	32.2	-1.33	3.2	84.586784	1.124E-05	0.002
108	ENSG00000	FBN2	protein_coding	fibrillin 2	The protein	GO:003019					542.1	76.2	-1.89	6.0	84.431023	1.132E-05	0.002
109	ENSG00000	FBXL16	protein_coding	F-box and leucine rich repeat protein 16	Members of	GO:000020					541.8	17.6	-2.25	1.6	84.349539	1.137E-05	0.002

B

Gene	Name	Log2 Fold Change	Mechanism	Reference
H19	H19 imprinted maternally expressed transcript	-5.28	Dephosphorylation, miRNA regulation	(Chan et al. 2009)
PTPRD	protein tyrosine phosphatase receptor type Delta	-6.14	Dephosphorylation	(Hofmann et al. 2019)
PTPRB	Protein tyrosine phosphatase receptor type B	-2.98	Unconfirmed – likely dephosphorylation	N/A
HACD4/ PTPLAD2	3-hydroxyacyl-CoA dehydratase 4/ protein tyrosine kinaselike A domain-containing protein 2	-2.60	Dephosphorylation	(Zhu et al. 2014)
BPIFA1	BPI fold containing family A member 1	-6.80	Downregulates IL-6 dependent pathways of STAT3 activation	(Saferali et al. 2020)

Figure 19: RNAseq analysis of control vs SESN1&2 KO reveals potential STAT3 regulators
Potential STAT3 regulators are downregulated in SESN1&2 KO cells**.**
A) A collaborating group performed RNAseq, and the analysis compares four biological controls (column K[non-treated]) with five different SESN1&2 KO (column S[non-treated], amongst which two different CRISPR single guides were used to generate these knockouts. A screenshot of the Excel file used for the manual identification of potential STAT3 regulators is displayed. **B)** The results of the RNAseq analysis show the genes whose expression is downregulated in SESN1&2 KO cells compared to those in the control group. Genes were identified based on false discovery rate (FDR<0.05). The table displays values of base 2-fold-change in mRNA expression in SESN1&2 KO vs control cells.

While the RNAseq analysis provided statistically significant data, we sought verification by qPCR in our lab conditions. Downregulation of the five identified genes in SESN1&2 KO cells comparatively to control cells was confirmed by qPCR (Figure 20A-B). The downregulation was as follows: H19 ~5.5 times lower, PTPRD ~17.5 times lower, ~4.9 times lower, HACD4/PTPLAD2 ~2.16 times lower, BPIFA1 ~45.25 times lower.

While most of these genes' precise role in regulating STAT3 is not well-defined, it was shown that PTPRD is a tyrosine phosphatase that can directly dephosphorylate STAT3 in

cancer cells [322]. To confirm that the downregulation of PTPRD in SESN1&2 KO cells is the consequence of the inactivation of *SESN1* and *SESN2* genes, we analysed PTPRD expression in A549 cells where *SESN1* and *SESN2* were silenced by shRNA. Our findings revealed a significant decrease in PTPRD mRNA levels in cells with SESN1&2 knockdown (Figure 20C), approximately 6.5-fold lower than in control cells, suggesting that silencing SESN1&2 does not reduce PTPRD expression to the same extent as a complete knockout.

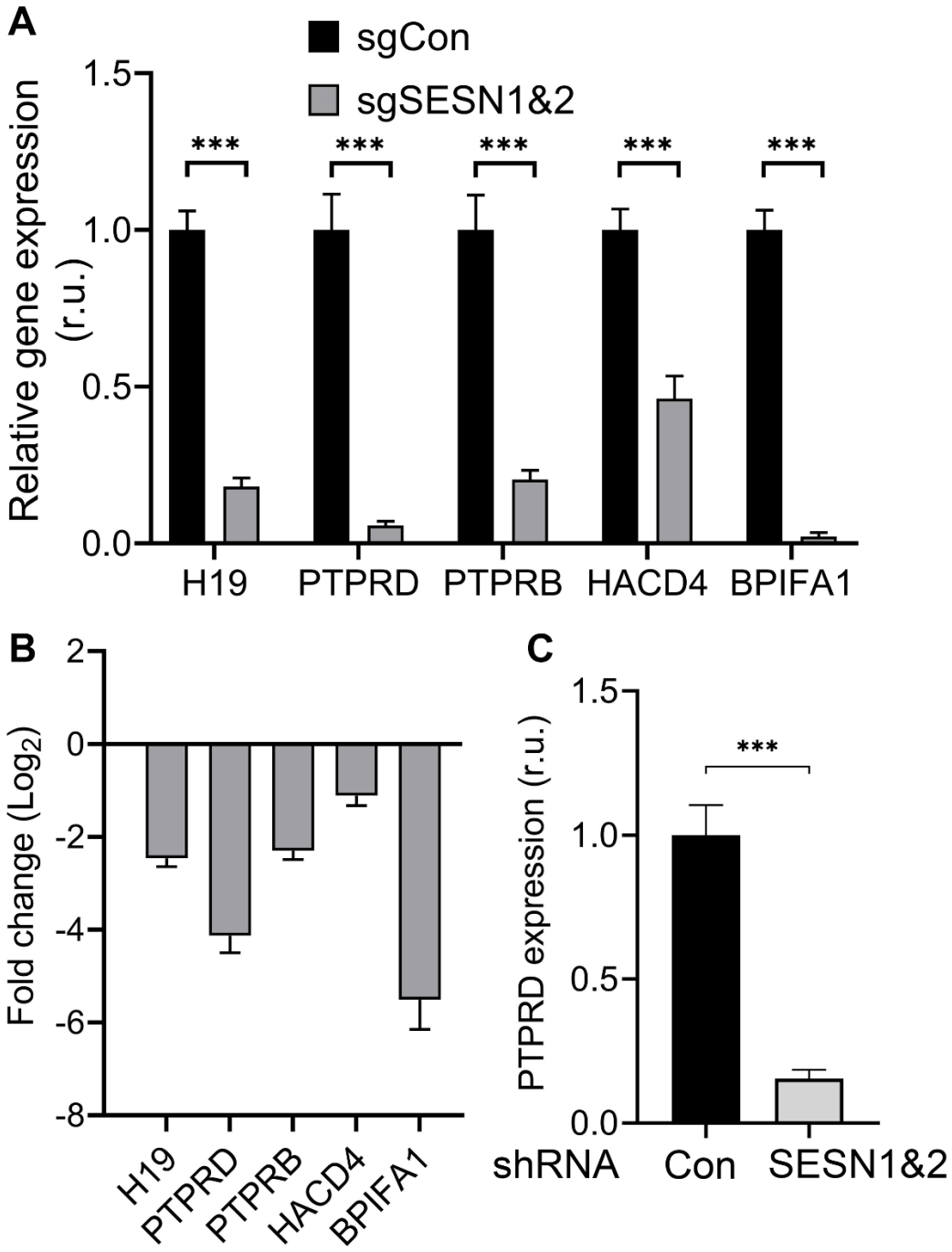

Figure 20: Validation of RNAseq data using RT-qPCR
A) qPCR validation of downregulation of the genes mentioned in Figure 19. A549 CRISPR/Cas9 control (sgCon) cells were compared to SESN1&2 KO (sgSESN1&2). The

bar chart displays the mean relative gene expression ±S.D. (n=2). **B)** A second bar chart displaying the same as A but represented as mean Log2FC ±S.D. Cells were plated with the same density, cDNA was synthesised and analysed by SYBR-green-based qPCR.
C) Special attention was given to PTPRD, and its downregulation was checked in A549 cells where SESN1&2 were silenced by shRNA rather than knockout by CRISPR. The bar chart displays the mean relative gene expression ±S.D. in control vs SESN1&2 KO cells (n=2).

To determine whether PTPRD mediates the negative regulation of STAT3 phosphorylation by SESN1&2, we ectopically overexpressed PTPRD in the SESN1&2 KO cells. Our measurement of PTPRD expression via lentiviral vector revealed an approximate 2500-fold increase in expression levels compared to control (Figure 21A).

A stable cell line expressing PTPRD enabled the assessment of its impact on STAT3 phosphorylation. By performing several independent immunoblots, we observed a partial restoration of p-STAT3 levels to control (Figure 21B). Densitometric analysis from six separate blots indicated that p-STAT3 activation was 2.8-fold higher in SESN1&2 KO cells compared to control. The introduction of the PTPRD vector moderated this increase, reducing it to 2-fold above control levels (Figure 21C).

Although this restoration of control levels of STAT3 phosphorylation was partial, it demonstrates that PTPRD can dephosphorylate STAT3 in this context. The partial nature of p-STAT3 restoration may be attributed to potential misfolding issues associated with the extensive overexpression of the protein. Additionally, the overexpression vector introduces only a single isoform of PTPRD despite the gene's capacity to potentially splice over 40 isoforms due to its extensive size (2.3 million nucleotides). Therefore, the complex nature of PTPRD expression cannot be fully mimicked by vector introduction alone, suggesting that genomic methods like gene silencing might offer a more accurate approach to studying this effect.

Attempts to generate shRNA targeting PTPRD encountered several challenges. The lack of compatible templates published led us to develop shRNA *de novo* using computational tools. Despite introducing several designed shRNA vectors into cells, PTPRD expression remained unaffected. Sequencing analysis of these vectors identified mutations within the hairpin structures, and vectors with intact hairpins failed to elicit the desired inhibitory effect. Resource and time constraints ultimately led to the indefinite suspension of efforts to develop shRNA against PTPRD in this project.

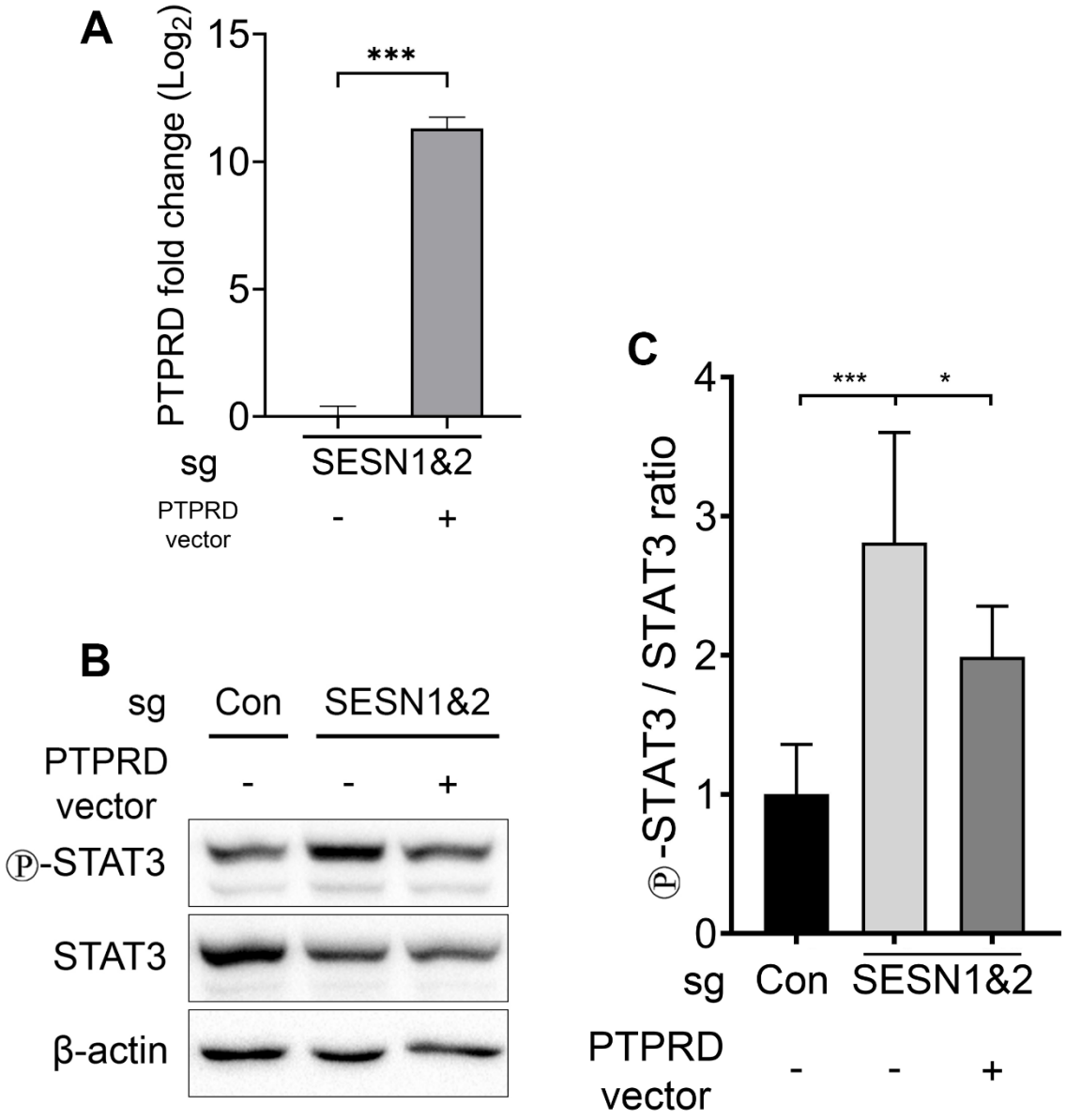

Figure 21: Ectopic expression of PTPRD lowers STAT3 phosphorylation
A) Cells were infected with a PTPRD-expressing lentiviral construct, selected on hygromycin and PTPRD expression was validated using qPCR. The bar chart displays the mean Log2FC ±S.D in control vs SESN1&2 KO cells (n=2). **B)** PTPRD expression in SESN1&2 KO cells restores STAT3 phosphorylation levels in SESN1&2 KO cells to the levels observed in control cells according to immunoblotting. **C)** Densitometry on immunoblots with ectopic expression of PTPRD was performed using Bio-Rad Image Lab Software. The bar chart represents STAT3's mean phosphorylation:expression ratio ±S.D. P values were calculated using one-way ANOVA followed by Tukey's post-test comparison (n=6). p*≤0.05; p***≤0.001.

We assessed the biological impact of ectopic PTPRD expression on cell survival and proliferation. The reintroduction of PTPRD notably mitigated cell death to levels comparable with control cells and normalised the growth rates of SESN1&2 cells with PTPRD overexpression to those of control cells (Figure 22).

However, it is crucial to recognise that these findings stem from an overexpression context. Despite observing a moderate correction in STAT3 activity, the cellular stress induced by vector introduction could potentially trigger the unfolded protein response due to ER stress, affecting cell death and growth. We did not directly measure the impact of vector-induced ER stress on cell health, yet the cells, by visual inspection, seemed robust and proliferated similarly to controls. This led us to conclude that PTPRD is vital in mediating the effects of the putative SESN-STAT3 relationship.

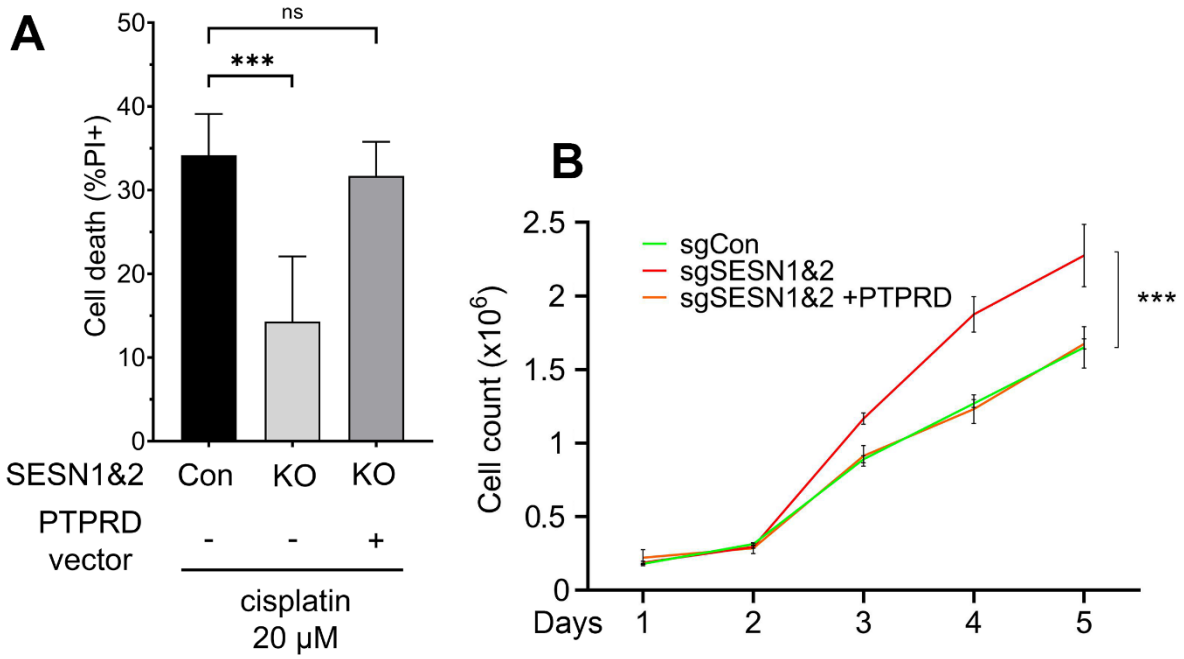

Figure 22: Ectopic expression of PTPRD attenuates cell death and proliferation
A) Ectopic PTPRD expression restores cell death to control levels according to propidium iodide staining and flow cytometry analysis. Cells were treated with cisplatin (20 µM; 48h). The bar chart represents the mean of two independent experiments ± SEM (n=2), where each experiment consisted of five replicates, whose means ± S.D. (n=5) were calculated and used for SEM calculation. P values were calculated using one-way ANOVA, followed by Tukey's post-test comparison. Not significant, ns; p***≤0.001. **B)** Ectopic PTPRD expression restores cell proliferation to control rates. 50000 cells were plated on 6-cm culture dishes, and the number of cells was calculated every 24 hours using a haemocytometer. The data is presented as mean ±S.D (n=2). P values were calculated using one-way ANOVA, followed by Tukey's post-test comparison. Not significant, ns; p***≤0.001. Day 5 of the curve was used for the statistical test.

As our ectopic SESN2 expression has shown, STAT3 phosphorylation is restored to control levels with the overexpression of SESN2 (Figure 23). We aimed to analyse whether this happens with the expression of PTPRD. We used RT-qPCR to analyse PTPRD expression in SESN1&2 KO cells ectopically expressing SESN2. While we have seen the usual reduction of PTPRD in the SESN1&2 KO, this time approximately 10.84 times lower, the levels of PTPRD in SESN1&2 KO expressing SESN2 was approximately 1.9 times lower than control. This demonstrated that the expression of SESN2 can restore, at least partially, the levels of PTPRD to control levels. Although SESN2 expression did not fully revert PTPRD levels to those of control cells, this partial restoration might be attributed to potential misfolding associated with exogenous overexpression of SESN2 or the concurrent absence of SESN1, which was not reintroduced in this experiment.

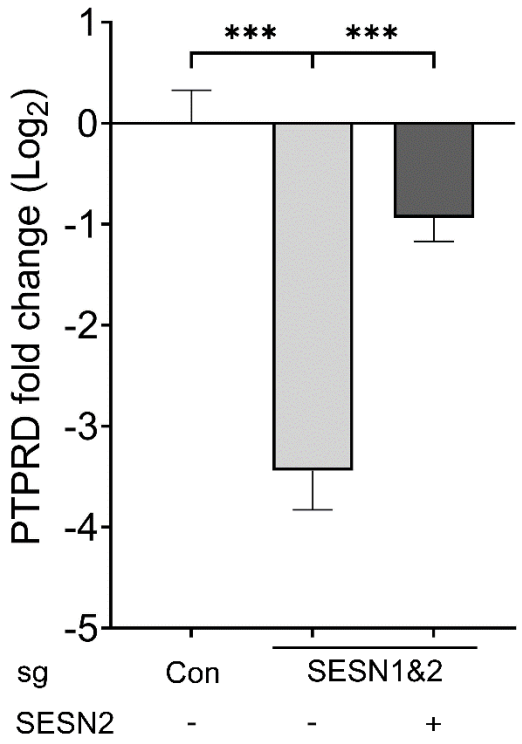

Figure 23: Reconstitution of SESN2 in SESN1&2 KO partially restores PTPRD expression

Ectopic SESN2 expression restores PTPRD expression according to qPCR analysis. The bar chart displays the mean Log2FC ±S.D in SESN1&2 KO with or without SESN2 expression vs control cells. P values were calculated using one-way ANOVA followed by Tukey's post-test comparison (n=2). p***≤0.001.

mRNA expression can be regulated by controlling its transcription or degradation. To discriminate between these two possibilities, we treated cells with Actinomycin D, the inhibitor of RNA synthesis, and measured RNA levels during the treatment. PTPRD has a half-life of approximately 35 hours, according to our analysis. Using a similar approach, a study showed that the half-life of beta-actin is 6.6 hours in the human leukaemia cell line Nalm-6 [323]. The size of PTPRD mRNA transcripts may explain this, with PTPRD isoform 5 being 8221 base pairs, whereas beta-actin is 1821 bp, according to NCBI. We observed no difference in the reduction rate of the PTPRD mRNA levels with our Actinomycin D treatment intervals of 48, 60 and 72 hours. The rate of RNA degradation was comparable between control and SESN1&2 KO cells (Figure 24).

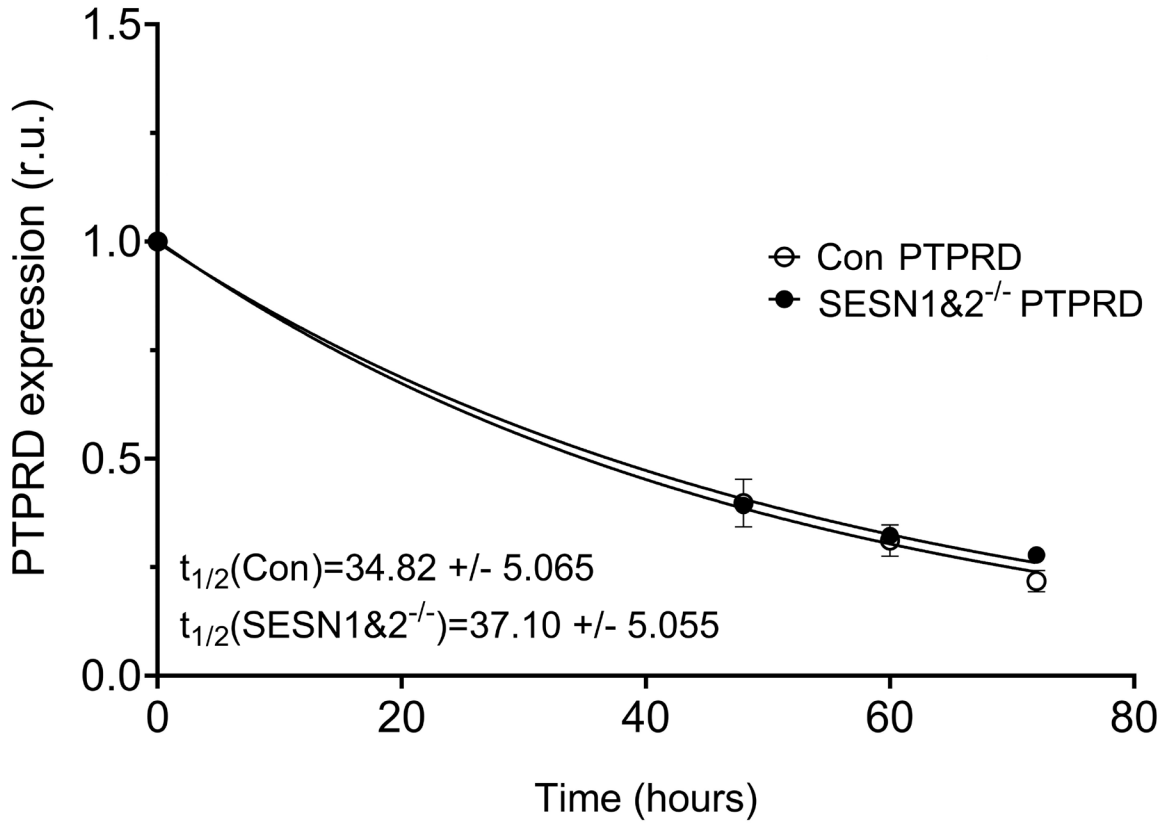

Figure 24: SESN1&2 are not involved in the stabilisation of PTPRD mRNA
Control and SESN1&2 KO cells were treated with Actinomycin D (10 µg/ml) for indicated time intervals, and the relative mRNA expression levels were analysed by qPCR. Non-linear regression of one phase exponential decay was applied to the data and the half-lives ($t_{1/2}$) were calculated for control (Con) and SESN1&2 KO. Individual points represent mean relative gene expression ±S.D. (n=2).

Although the effects of SESN1&2 on STAT3 phosphorylation have been highly reproducible in A549 cells, our research has faced a challenge in showing these results in other cell lines.

We found success in the introduction of shRNA against Sestrins in the human non-small cell lung carcinoma cell line H460, and this effect was correlated with increased STAT3 phosphorylation (Figure 25A). This warranted the selection of this cell line as another SESN knockout candidate to study this effect with the stable knockout of SESN1&2. However, technical difficulties were encountered using the same flow cytometry dispersion method for single-cell cloning. In our observations, H460 human non-small cell lung carcinoma cells exhibit a distinctive island-like growth pattern when cultured *in vitro*. This clustering behaviour could be a requirement for the growth of this cell line; hence, H460 show a low survival rate in this cloning method. Out of the several attempts, we have seen roughly a 3% survival of cells and progression into stable growing colonies derived from single cells. This severely limited our ability to select stable knockouts for this cell line. Recently, we successfully generated three distinct clones of SESN2 knockout in H460. However, the STAT3 phosphorylation seemed to be very similar to control levels, and we currently have one experiment with this cell line, shown in Figure 25B. Further experimentation or generation of double SESN1&2 knockouts using these clones could illustrate the SESN-STAT3 relationship further in this cell line.

We successfully generated a single clone stable knockout of SESN2 in 293T cells. While initially, this cell line displayed a higher phosphorylation of STAT3 (Figure 25C), this difference was challenging to replicate, and several experiments have not shown any difference in STAT3 (Figure 25D). This inconsistency may arise from variations in culturing conditions or the cell line's inherent sensitivities to standard protocols. While this study is not conclusive, there is the possibility that knockout of SESN1 is required for this effect to manifest reproducibly in this cell line. Consequently, culturing conditions should be optimised to identify differences in analysis or more experiments could confirm or deny the correlation of higher p-STAT3 with SESN expression in these cells.

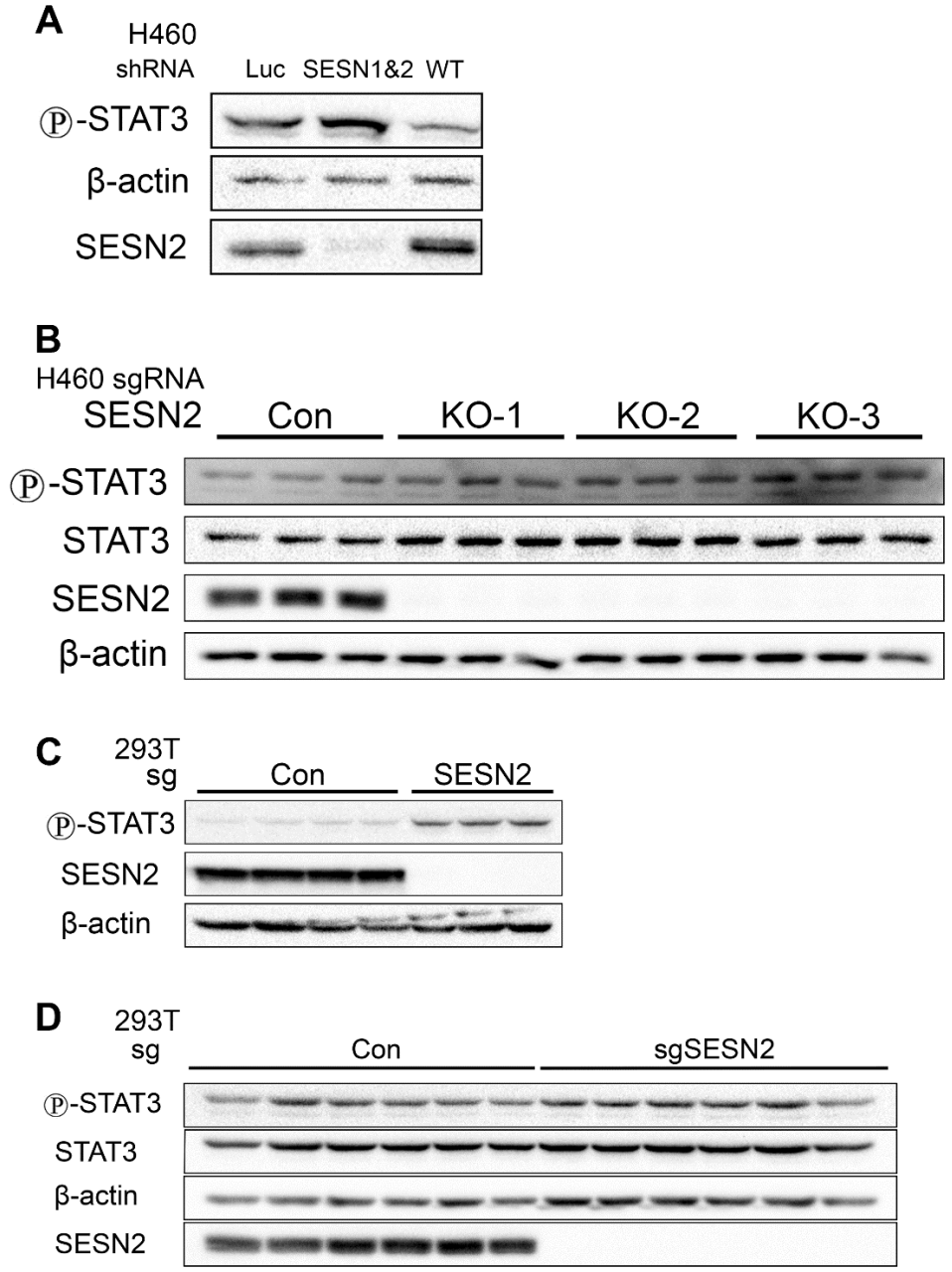

Figure 25: SESN1&2 effect on STAT3 has been difficult to replicate in cell lines other than A549

A) H460 cells with knockdown of SESN1&2 (shSESN1&2) demonstrate increased STAT3 phosphorylation levels comparatively to control cells (shLuciferase) and wild-type H460 cells (WT).

B) H460 cells with CRISPR/Cas9 knockout of just SESN2 demonstrate slightly increased STAT3 activity compared to the control single guide (Con). Multiple lanes under the same label designate biological repeats.

C-D) Two independent experiments of CRISPR/Cas9 knockout of SESN2 in 293T cells. While our initial analysis displayed a visible difference in p-STAT3, several subsequent experiments showed p-STAT3 as seen in D.

3.11. Discussion

SESN1 and SESN2 might play an ambiguous role in lung carcinogenesis, supporting tumour growth at an early stage of carcinogenesis but suppressing cell proliferation and facilitating cell death of tumour cells at an advanced stage [254]. Therefore, the deficiency of SESN1 or SESN2 supports the growth of tumour xenografts and potentially contributes to cancer progression [254, 324]. However, the mechanisms responsible for regulating carcinogenesis through Sestrins are poorly understood. Drug resistance poses a significant challenge in cancer treatment, as cancers often adapt to chemotherapies, allowing them to survive and proliferate despite treatment [247]. These resistance mechanisms are incredibly complex, characterised by cancer's continuous evolution to overcome therapeutic challenges, making successive treatments progressively more difficult [248]. Utilising CRISPR/Cas9 technology, we knocked out SESN1&2 in the A549 cell line derived from lung adenocarcinoma (Figure 1). This model, enhanced by the development of a multiclonal knockout culture, serves as a robust framework for investigating Sestrins' response to DNA damage and their involvement in cancer drug resistance.

3.11.1. Role of SESN1&2 in p53-mediated apoptosis and DNA Damage Response

Being p53-activated genes and regulators of cell viability [4], SESN1&2 may be responsible for the pro-apoptotic effects of chemotherapy on cancer cells. Therefore, we examined the role of Sestrins in the DNA damage response. Our findings show that cisplatin treatment significantly upregulates SESN1 and SESN2 expression in A549 cells via p53 activation (Figure 5) [4]. Furthermore, we demonstrated that SESN1&2 strongly contribute to cisplatin-induced cell death in A549 cells as SESN1&2-null cells have an increased resistance to apoptotic cell death and form substantially more colonies in a long-term colony-forming assay (Figure 2-3). Altogether, these data indicate that Sestrins' role in supporting p53-induced cell death may be downstream of p53. The importance of Sestrins in the control of cell death is not specific to cisplatin and is also observed upon treatment of cells with the topoisomerase inhibitor etoposide (Figure 3B). Tumour suppressor p53, the master activator of SESN1 and SESN2 transcription, plays a critical role in the induction of cell death in response to genotoxic stress, and Sestrins do not contribute to the regulation of cell death in response to cisplatin treatment in the absence of p53 (Figure 4). Being close associates of p53 in the regulation of cell viability in response to stress, Sestrins could also contribute to the control of the DDR. However, SESN1&2 do not substantially affect the expression and phosphorylation of the major regulators of the DDR and the activity of p53, as can be monitored by phosphorylation of p53 and upregulation of its target - DR4 (Figure 5).

Sestrins are well-established mTORC1 inhibitors that could prevent the growth and proliferation of cancer cells through mTORC1-dependent mechanisms. However, in this study, we were not able to demonstrate any effects of SESN1&2 inactivation on the activity of mTORC1 upon cultivating cells in nutrient-rich conditions, although that does not entirely rule out suppression of mTORC1 by Sestrins in the conditions of nutrient and oxygen deficiency [254]. Sestrins are also potential activators of the AKT kinase [325], the major regulator of metabolism and cell viability. However, inactivation of SESN1&2 does not affect the phosphorylation of an upstream AKT kinase – PDK1, or phosphorylation of AKT targets, GSKβ and PRAS40 (Figure 6). Therefore, we postulated that some alternative mechanisms might be involved in the control of cell proliferation and cell death by Sestrins in lung adenocarcinoma cells.

3.11.2. Investigating SESN1&2 influence on cell survival pathways – STAT3 may be the link between SESNs and cell death

To gain insight into the potential role of SESN1&2 in lung carcinogenesis, we searched for other Sestrin targets that might be responsible for controlling cell proliferation and cell death [264]. Our search was informed by various studies illustrating the role of Sestrins in modulating signalling pathways that govern cell growth and apoptosis across diverse cellular contexts. For example, the members of the Sestrin family were shown to activate the AMPK-MAPK signalling pathway in T-lymphocytes [309]. The MAPK family members - ERK, JNK, and p38 play essential roles in the control of cell division and viability in different cell types and may be targets of Sestrins in lung adenocarcinoma cells. However, we did not observe any difference in the phosphorylation of AMPK and any MAPK proteins in control and SESN1&2 KO cells. Sestrins might also regulate the PKA-CREB pathway via interaction with the AKAP1 protein [310], yet no effect of Sestrins' inactivation on phospho-CREB was observed. SESN2 was recently reported to be an inhibitor of the WNT-β-Catenin signalling pathway, the major regulator of cell stemness and proliferation in colon carcinoma cells [311]. However, we could not detect any effects of SESN1&2 inactivation on the phosphorylation of β-Catenin in lung adenocarcinoma cells. Finally, SESN2 was shown to be a partner of SQSTM1/p62 protein and a regulator of its stability and activity [326]. p62 is known for its role as a cargo protein in the delivery of cellular constituents into autophagosomes and, according to recent studies, stimulates hepatocarcinogenesis through control of the viability of preneoplastic cells [327]. We could not detect any difference in p62 levels between control and SESN1&2 KO cells, therefore ruling out the importance of this protein in the control of cell proliferation and cell death by Sestrins in A549 cells (Figure 6).

Analysing the expression and phosphorylation of different proteins that potentially contribute to carcinogenesis, we found that phosphorylation of STAT3 was notably increased

in single and double SESN1 and/or SESN2 KO cells compared to controls (Figure 7). Surprisingly, no difference in phosphorylation was detected for STAT1, another member of the STAT family, demonstrating that the effects of SESN1&2 inactivation were STAT3-specific (Figure 6B). Interestingly, we could not detect any consequence of Sestrin inactivation on the phosphorylation of the JAK2 kinase, an upstream regulator of STAT3 (Figure 7A). It indicates that Sestrins regulate STAT3 phosphorylation downstream of JAK2, potentially via regulation of some other STAT3 upstream kinases or phosphatases. In subsequent studies, we determined that JAK kinases are essential for STAT3 phosphorylation in both control and SESN1&2 KO A549 cells (Figure 12). Therefore, it implies that phosphatases might be key in mediating the regulation of STAT3 phosphorylation by Sestrins. The activation of STAT3 in SESN1&2 KO cells also leads to the activation of two crucial STAT3 targets: Cyclin D1 and MCL1, which are critical in supporting cell proliferation and cell viability. Cyclin D1 forms a complex with Cdk4/6 that drives the G0/G1-S phase cell cycle transition through retinoblastoma (RB) protein phosphorylation. In its hypophosphorylated form, RB binds to and inhibits the activity of E2-promoter binding protein dimerisation partner (E2F-DP1) dimers. E2F-DP1 is a transcription factor that drives cells into the S phase, and RB binding prevents cell cycle progression from G1 to S phase [328]. Accordingly, RB is hyperphosphorylated in SESN1&2 KO cells, potentially promoting cell cycle progression. Elevated RB phosphorylation is followed by phosphorylation of CDC2, a downstream driver of the cell cycle that works in complex with cyclin B to drive the M-phase transition. In agreement with these data, we have demonstrated previously that ectopic expression of SESN2 leads to downregulation of Cyclin D1 in breast carcinoma MCF7 cells, which in turn leads to suppression of colony growth [294, 329]. Cyclin D1 is a well-established oncogene found to be overexpressed in many tumours, and its overexpression stimulates unrestricted proliferation of tumour cells [330]. MCL1, a cell death inhibitor belonging to the BCL2 protein family of apoptotic regulators [320], is often overexpressed in different human cancers due to gene amplification or other mechanisms [320, 321]. Elevated expression of MCL1 suppresses cell death in response to anticancer drugs, rendering cancer cells resistant to anticancer therapies, and MCL1 targeting is a new promising strategy for the development of new anticancer drugs aiming to dismantle cancer-protecting mechanisms [320].

3.11.3. SESN1&2-mediated regulation of STAT3 phosphorylation is independent of known Sestrin functions

To understand how Sestrins regulate STAT3 phosphorylation, we examined several possibilities. These include a potential direct interaction between Sestrins and STAT3, suppression of STAT3 phosphorylation by non-receptor kinase(s), negative regulation of cytokine secretion involved in STAT3 activation, or suppression of ROS production by

Sestrins, taking into consideration the well-established antioxidant activity of Sestrins [32, 33, 54, 326]. Our immunoprecipitation refuted the hypothesis that Sestrins might interact with STAT3 (Figure 8). Additionally, our experiments to determine if SESN1&2 knockouts could elevate STAT3 phosphorylation through autocrine signalling found no supporting evidence, challenging this hypothesis (Figure 8). We also ruled out any potential impact of GATOR2 in STAT3 regulation by Sestrins as the knockdown of a critical GATOR2 compound – MIOS does not affect STAT3 phosphorylation or resistance to cell death (Figure 9). Many protein tyrosine phosphatases are redox-dependent proteins that may be inactivated by the excess ROS produced in SESN1&2-null cells [331]. To investigate these hypotheses, we performed experiments to modulate ROS levels: introducing exogenous ROS with hydrogen peroxide treatment and reducing ROS production via the antioxidant N-acetylcysteine. However, the outcomes of these treatments did not confirm the hypothesis that such mechanisms significantly influence STAT3 phosphorylation in this context (Figures 10-11). While the regulation of STAT3 phosphorylation is yet to be understood, we demonstrated that it depends on the JAK activation but not EGFR (Figure 13); the former is often overactivated in lung cancer cells [313]. We have also confirmed that the increased STAT3 phosphorylation is not a result of non-receptor PTKs (Figure 14), such as Abl or Src, which were shown to phosphorylate STAT3 in chronic myeloid leukaemia [332] and melanomas [258], respectively.

3.11.4. The implications of hyperactivated STAT3 on cell death and proliferation

STAT3 is a potential target for anticancer therapy that, when targeted in combination with chemotherapeutic or immunotherapeutic drugs, may dramatically improve the outcome for cancer patients, suppressing cell proliferation and sensitising cancer to cell death [333].

Presumably, Sestrins contribute to p53-dependent processes by modulating some collateral signalling pathways involved in the control of proliferation and cell death. STAT3 showed up in our studies as a strong candidate in the control of cell proliferation and cell death by Sestrins. Verifying the impact of STAT3 in the modulation of cell proliferation and cell death by SESN1&2, we demonstrated that inhibition of STAT3 in SESN1&2 KO cells considerably reduced cell proliferation rate and restored the levels of cell death in response to cisplatin to those observed in control cells (Figure 15-16). Furthermore, we studied two of STAT3's crucial downstream targets implicated in cell cycle and apoptosis, Cyclin D1 and MCL1, which we found upregulated on western blot (Figure 6B). Our Cyclin D1 analysis remains inconclusive. Despite observing increased SESN1&2 KO cell proliferation, which suggests accelerated cell cycle progression, propidium iodide staining indicated a shift from G2/M to G0/G1 phase, contradicting expected outcomes (Figure 18A). Nonetheless, this was a basic investigation and more precise methods, such as BrdU assay, are warranted for a comprehensive analysis.

Moreover, although Cyclin D1 upregulation was evident in western blot analyses, this increase was not mirrored in qPCR expression results (Figure 18B-C). We knocked down the anti-apoptotic protein MCL1 and found it essential for conferring cisplatin resistance in A549 cells. The silencing of this protein normalised the levels of cell death in SESN1&2 KO to control (Figure 17). Therefore, restoration of Sestrin activity or STAT3 inhibition in SESN1&2-deficient cancer cells may be a potential strategy to improve the treatment outcome for patients with cancers bearing mutations in *SESN1* or *SESN2* genes.

3.11.5. The search for potential regulators of STAT3 that link STAT3 to SESN1&2 – PTPRD may be an essential regulator

Therefore, searching for the regulation mechanism of STAT3 by Sestrins, we compared gene expression in control and SESN1&2 KO cells to find potential regulators of STAT3 activity. According to our analysis, transcripts of PTPRD, H19, HACD4/PTPLAD2, PTPRB, and BPIFA genes were downregulated in SESN1&2 KO cells (Figures 19-20). The most prominent candidate on the role in the regulation of STAT3 phosphorylation by Sestrins that appeared in our search was the protein tyrosine phosphatase receptor delta (PTPRD), whose inhibitory effect on STAT3 phosphorylation in different cancer types was demonstrated in several studies [322, 334]. PTPRD is inactivated in many human cancers and potentially plays a role as a tumour suppressor through STAT3 inhibition [335]. PTPRD also provides sensitivity to radiotherapy in nasopharyngeal carcinoma cells [336]. It was also demonstrated that PTPRD regulates PD-L1 expression in human hepatocellular carcinoma, and, accordingly, STAT3 activation leads to higher resistance of tumour cells to the anti-tumour effects of immune cells [337]. PTPRB, another member of the PTPR family, may also inhibit STAT3; however, its role in the dephosphorylation of STAT3 has not yet been proven. Non-coding H19 RNA is another STAT1&2 target that might be involved in STAT3 regulation. As demonstrated in endothelial cells, knockdown of H19 leads to STAT3 phosphorylation, and therefore, downregulation of H19 in response to SESN1&2 inactivation might cause STAT3 dephosphorylation. However, other studies show contrary effects of H19 on the regulation of STAT3 in other cell types [338]. Protein tyrosine phosphatase-like A domain-containing 2 (HACD4/PTPLAD2) is a potential tumour suppressor in squamous carcinoma that inhibits STAT3 phosphorylation [339]. Lipid-binding antimicrobial Bactericidal/permeability-increasing fold containing family A (BPIFA1) is a negative regulator of pro-inflammatory response in the lung and might inhibit STAT3 through the downregulation of IL-6, the potent activator of the JAK2-STAT3 pathway [340]. Focusing on PTPRD, we demonstrated that ectopic expression of PTPRD decreases STAT3 phosphorylation in A549 SESN1&2 KO cells (Figure 21). Moreover, overexpressing PTPRD normalised both cell death rates and proliferation to those observed in control (Figure 22). Therefore, PTPRD may play a major role in the STAT3

regulation by Sestrins. However, we cannot rule out the potential cooperation between several genes identified in our study in the Sestrin-mediated regulation of STAT3 phosphorylation in lung tumours.

The regulatory mechanism by which Sestrins influence gene expression is not fully understood. We have demonstrated that the downregulation of the PTPRD gene in SESN1&2 KO cells is not caused by accelerated degradation of its mRNA (Figure 24). Introducing SESN2 back into the double knockout cells significantly increased PTPRD levels, demonstrating a direct correlation between Sestrin presence and PTPRD gene transcription (Figure 23). Therefore, Sestrins should be responsible for the regulation of PTPRD transcription. However, the mechanism of transcriptional regulation by SESN1&2 is obscure, as most Sestrin activities occur in the cytoplasm or on the mitochondrial surface [33, 293, 341]. It was reported that SESN2 may regulate the activity of the NRF2 transcription factor by supporting KEAP1 degradation via specific autophagy that leads to the release of NRF2 followed by transcriptional activation of many genes involved in the antioxidant response [326]. Alternatively, SESN2 might directly support NRF2 transcriptional activity [342]. A549 cells bear mutations in the KEAP1 gene [343], and the regulation of NRF2 by means of KEAP1 degradation in these cells is unlikely. The regulation of gene expression by Sestrins may be mediated by a direct influence on the transcriptional activity of NRF2 or other transcription factors that have yet to be identified.

The findings of this investigation are summarised visually in Figure A on the next page.

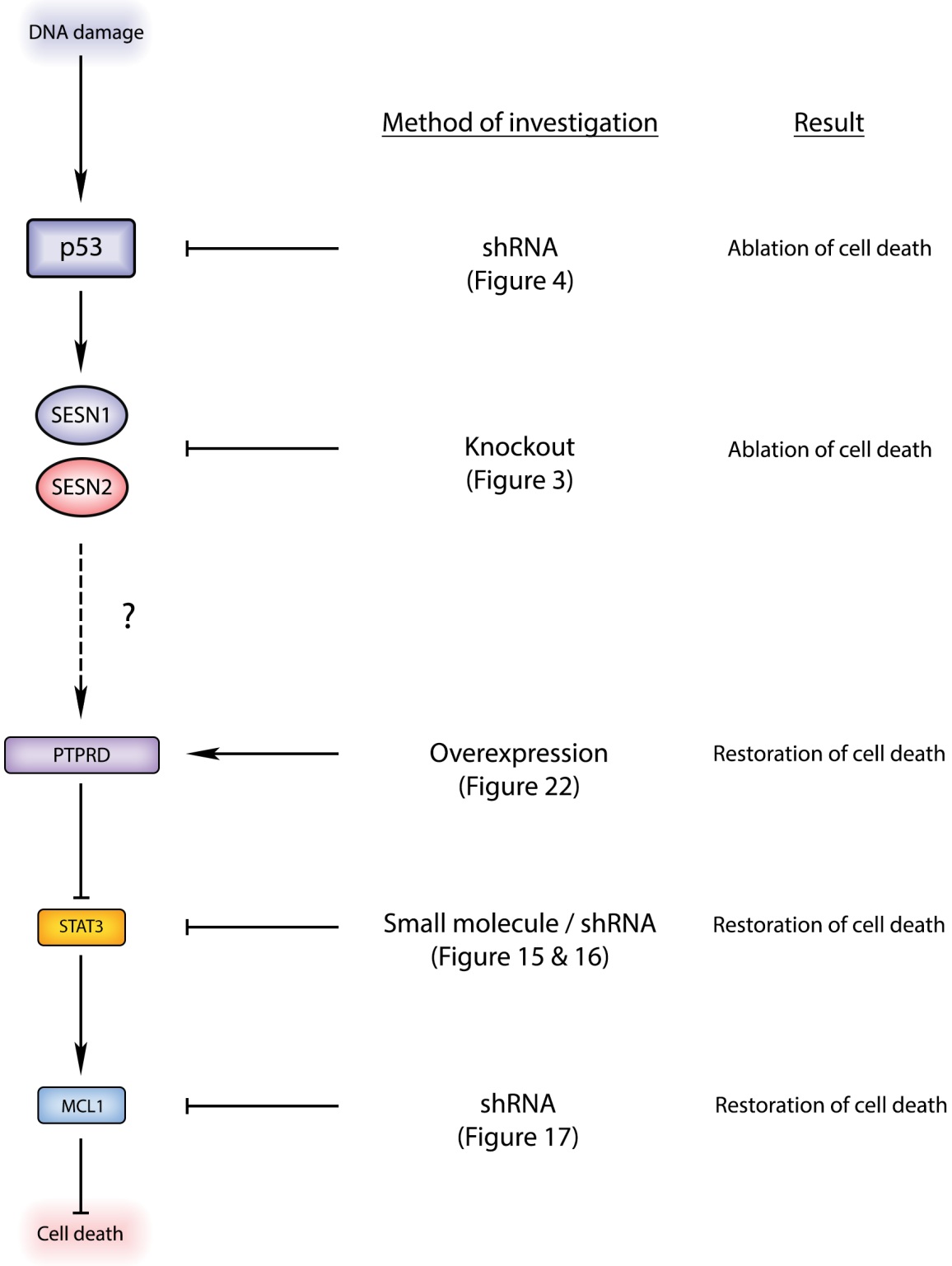

Figure A: The summary of our investigation into the p53-regulated SESN1 and SESN2 and their role in DNA-damage-induced cell death
A visual summary of our investigation into the roles of p53-regulated SESN1 and SESN2 in DNA-damage-induced cell death. It illustrates the experimental approaches taken to manipulate these pathways and the impact of these manipulations on DNA-induced cell death.

3.11.6. The implications of STAT3-SESN relationship for future cancer research

STAT3 is upregulated and activated in many human cancers, including NSCLC, prostate cancers, and melanomas [261, 263]. STAT3 promotes carcinogenesis in NSCLC and other cancer types by inhibiting cell death, activating angiogenesis, and supporting cancer cell stemness [344]. STAT3 also provides resistance to radiotherapy and chemotherapeutic drugs, such as cisplatin [345, 346]. Increased STAT3 activity in lung cancers is responsible for cisplatin resistance and poor patient survival [346]. STAT3 also contributes to the pro-tumorigenic inflammatory phenotype in cancer cells by upregulating pro-inflammatory cytokines but inhibiting anti-tumour immune response through suppression of activation and maturation of dendritic cells, tolerance to T-cell mediated cell death, and upregulation of checkpoint inhibitors [262, 347]. Here, we described a new mechanism of STAT3 activation in cancers mediated by the downregulation of p53-inducible SESN1 and SESN2 genes. Unfortunately, a major challenge faced by our study is mixed results in other cell lines. Our findings on STAT3 phosphorylation showed poor reproducibility in 293T and H460 cell lines (Figure 25). Future investigations, including the knockout of additional *SESN* genes in these cells or adjusting experimental conditions, may consistently display altered STAT3 phosphorylation. According to the GENT2 cancer expression database, Sestrins are notably suppressed across various cancers [252]. Given the pronounced impact of Sestrins on cell death and proliferation displayed by this study, future research must focus on cell lines and primary tumours where Sestrin downregulation is particularly prevalent in order to investigate this effect further. Our results highlight the significant role of STAT3 in promoting cell growth and preventing cell death caused by SESN1&2. To fully understand the role of these proteins in cancer, future research should examine their effects on other processes controlled by STAT3 using *in vivo* models. In future studies, it would also be important to evaluate the crosstalk between STAT3 and mTORC1 pathways in greater detail. Although SESN1&2 inactivation does not affect mTORC1 activity in nutrient-rich conditions, Sestrins might be crucially important for inhibiting mTORC1 under the nutrient and oxygen scarcity conditions commonly observed in tumours. mTORC1 is a well-known nutrient and oxygen sensor responsible for the control of cell proliferation and cell death [348], and the potential inhibition of mTORC1 by Sestrins in tumours adds another level of complexity in the control of carcinogenesis that needs to be evaluated in future studies.

Besides NSCLC, STAT3 activation is often observed in non-Hodgkin lymphomas, including follicular lymphomas (FL). Our previous studies demonstrated that FL are often characterised by the inactivation of SESN1 [268]. STAT3 inhibition imparts sensitivity of

lymphoma cells to chemotherapeutic drugs [349], and activation of Sestrins might be a potential mechanism to improve the outcome of anticancer therapies. Likewise, SESN2 is found to be downregulated in colon cancer [279], where STAT3 is often hyperactivated and contributes to carcinogenesis [350]. As SESN1 or SESN2 expression is often downregulated in different tumours due to the inactivation of p53 or chromatin modifications, activation of SESN1&2 expression via alternative mechanisms such as treatment with metformin or other inhibitors of metabolic pathways [295] may restore Sestrin function and intensify the therapeutic effects of the conventional as well as emerging anticancer therapies. Furthermore, Sestrins can also be potentially activated by small molecules that can interact with the leucine binding pocket of the Sestrins, enhancing their activity [351]. Additionally, activating Sestrins in healthy individuals may slow ageing and prevent the development of cancer and other age-related diseases.

3.12. Future work

3.12.1. Generation of Sestrin double knockouts in other cell lines

The primary limitation of this research is its restriction to several cell lines, and the observed effects on STAT3 are not consistently replicable across other cell lines. Currently, we have only single knockouts of SESN2 in 293T and H460 cells, and the p53-responsive SESN1 remains present in these cells. Generation of double knockouts may provide more reproducible results. SESN1 is the Sestrin found most severely downregulated across all cancers (28.5% lower), and specifically downregulated in lung cancer (52.8% lower), according to GENT2 [252]. This is compared to the SESN2 downregulation of 8.6% across all tumours and 7.9% in lung cancer. Although we have shown that SESN1 and SESN2 exert an equal effect on STAT3 (Figure 7), it is possible that SESN1 may compensate for the absence of SESN2 in these single knockout cell lines.

3.12.2. Identifying novel interactions using BioID2

The influence of Sestrins on STAT3, whether solely through PTPRD or via additional mechanisms, has yet to be fully elucidated. While our PTPRD reconstitution expressed the protein at roughly 2500-fold the levels of control and showed significant attenuation of p-STAT3 levels in SESN1&2 knockout, this finding does not preclude the possibility that Sestrin proteins may influence STAT3 through alternative mechanisms. While RNAseq allowed us to identify some possible regulators of STAT3 phosphorylation, this analysis was limited to identifying the changes in the transcription of these genes in stable growing cells. Whether Sestrins modulate the activity of STAT3 regulators through protein-protein interactions or influence the activity of certain transcription factors that promote STAT3 dephosphorylation remains to be investigated by other means.

While previous large-scale research discovered the binding partner of Sestrins in GATOR2 via mass spectrometry of tandem affinity purified complexes, a novel proximity labelling approach offers potential for uncovering weaker, transient interactants or proteins in the vicinity of SESN2. The BioID method employs a promiscuous biotin ligase to identify protein-protein interactions and nearby proteins within living cells. BioID2, derived from the biotin ligase of *A. aeolicus*, was engineered with a mutation in the biotin catalytic site (R40G) [352]. As demonstrated during the development of the original BioID, this mutation in the conserved region of the protein abolishes its substrate specificity, enabling it to constitutively biotinylate nearby proteins, including itself [353].

We have developed an A549 SESN1&2 knockout which expresses the fusion product of SESN2 to the BioID2. To enhance efficiency and extend the range of biotinylation to nearby proteins, the BioID2 designers recommend using a spacer sequence. The N-terminal tail of

SESN2 was chosen for the fusion, as it is long, disordered and loose. Furthermore, given that BioID2 is loosely connected to SESN2 via this tail, we anticipate that this design will minimize steric hindrance to SESN2's functional domains, such as the leucine-binding pocket and GATOR2 binding sites, without altering the overall conformation of SESN2. Figure B shows the hypothetical structure that this fusion product would form.

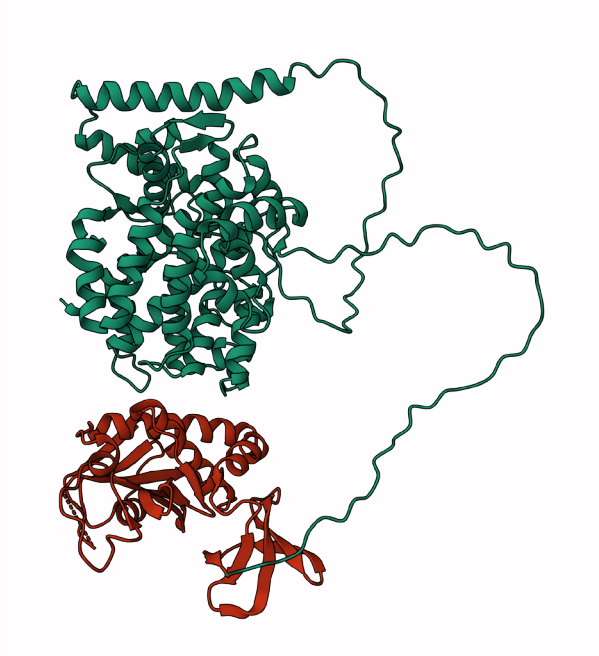

Figure B: The fusion of BioID2 to SESN2.
The figure shows the AlphaFold structure of SESN2 (AlphaFold ID: AF-P58004-F1) artificially fused to the crystal structure of BioID2 (PDB ID: 2EAY) using the programme Pymol. Green – SESN2. Red – BioID2.

3.12.3. The impact of leucine on SESN-STAT3

The influence of leucine on STAT3 has not been comprehensively evaluated. Although we conducted a few preliminary experiments, the results were not sufficiently convincing to confirm or refute leucine's effect on STAT3. While the mTORC1 signalling function of Sestrins seems not to be involved in this process, this does not exclude the possibility that Sestrin conformation is relevant to STAT3 phosphorylation. It is plausible that leucine modulates the conformational state of Sestrins, thereby linking leucine availability to STAT3 activity through a mechanism that remains to be determined. Given that our experiments were conducted under leucine-rich conditions, the primary difference between wild-type and SESN1&2 knockout cells is the reduced ability to sense leucine for the mTORC1 pathway. Additionally, this difference may extend to other pathways in which the role of Sestrins has not yet been determined.

3.12.3.1. *In Vivo* Studies

A core limitation of this research is the lack of evidence demonstrating that this cellular signalling has physiological implications. Despite the SESN-deficient cells growing faster *in vitro* and exhibiting greater resistance to chemotherapeutic drugs, this does not provide any insight into the importance of Sestrins *in vivo*. Previous studies have shown that A549 xenografts lacking SESN2 grew to a significantly larger volume compared to wild-type xenografts of the same cell line [254, 324]. To reinforce the findings presented here, we could employ a similar approach by studying xenografts of A549 cells with knockdown of STAT3, MCL1, and PTPRD to determine if this effect is ameliorated. Similarly, an *in vivo* approach to study the impact of SESNs on tumorigenesis was performed using the KrasLSL-G12D model, in which SESN2 was knocked out. This knockout did not show an effect on tumorigenesis, suggesting that SESNs may play a role in tumour progression rather than suppressing carcinogenesis [254]. The KrasLSL-G12D oncogene model precluded examining the late stages of carcinogenesis, as most mice died from asphyxia, and the tumours did not progress to the late metastatic stage. Therefore, investigating metastasis and late-stage progression of cancer *in vivo* could more accurately illustrate the role of SESNs in cancer.

3.12.4. Mutational studies

A structural and conservation-based approach could be employed to investigate the role of individual active domains of Sestrin in STAT3 signalling. We have shown that the reconstitution of SESN2 restores STAT3 phosphorylation to control levels. Using this same approach, we could examine the effect of site-specific mutations on STAT3 activity, attempting to relate these effects to Sestrin structure. Mutants of SESN2 are readily available from public plasmid repositories such as Addgene. Leucine-insensitive SESN2 mutants (E451A & L261A), GATOR2-binding-compromised mutants (S190W, D406A), antioxidantly compromised mutant (C125S), and others prepared as part of the Kim 2015 and Sabatini 2016 studies are available on Addgene. By combining knowledge from public databases and conservation analysis, as outlined in Appendix B of the introduction, we could identify crucial domains on SESN2 and prepare additional mutants, as well as acquire existing ones from Addgene. With a comprehensive panel of mutants, it would be possible to use the A549 SESN1&2 knockout cells to reconstitute various mutants and investigate their role in the effect on STAT3.

3.12.5. Therapeutic targeting of the SESN-STAT3 pathway

The knowledge that SESN deficiency can elevate the activity of the STAT3 pathway may be valuable in scenarios where a tumour can be genetically analysed for its signalling pathways. Our experiments, along with the consensus of existing publications, suggest that SESN deficiency correlates with a poor prognosis in cancer [278]. Therefore, if the STAT3 pathway is closely associated with SESN, targeting the SESN-STAT3 interaction could be a

therapeutic strategy for treating cancers where either pathway is impaired. As we have demonstrated, the inhibitor C188-9 and the knockdown of MCL1 can attenuate the cell death resistance conferred by SESN deficiency in cancer. Although there are currently no FDA-approved STAT3 or MCL1 inhibitors, inhibitors such as C188-9 are in clinical trials, and future pharmaceuticals may be pivotal in halting the progression of SESN-deficient cancers.

As Sestrins are targets of leucine, several efforts have been made to develop drugs targeting the leucine-binding pocket of Sestrins. Navitor Pharmaceuticals' NV-5138, a small molecule that acts as a leucine mimetic for SESN2, is currently in Phase 2 clinical trials for antidepressants [38]. Similarly, a small molecule that binds SESN2 without disrupting its GATOR2 binding could be developed, and a proof-of-concept was previously trialled by our lab. Modulating SESN2's activity may provide a therapeutic approach to enhance cancer treatment, potentially through co-treatment with these leucine mimetics and chemotherapeutic drugs.

As we have shown, p53 is essential in initiating the SESN-mediated cell death in response to cisplatin, and the absence of p53 confers resistance to cell death similar to that observed in SESN1&2 knockout cells (Figure 4). Enhancing SESN transcription by utilizing other transcription factors may be an avenue to restore cell death in p53-deficient cells. Sestrins respond to various transcription factors. For example, drugs such as metformin, which potentiates transcription factors ATF4 and FOXO3 [354, 355], could be used to upregulate Sestrins and improve cancer therapy in p53-deficient cells. Alternatively, attempts to restore mutant p53 activity could rely on Sestrins to mediate the reconstituted p53 activity [356].

3.13. Conclusion

At the beginning of this research project, we discovered that SESN1&2-deficient cells were markedly resistant to cisplatin. We determined that this cell death is apoptotic and dependent on p53. Our hypothesis was that Sestrins mediate the effects of p53-induced cell death via interaction with the mTORC1 pathway. As a result of this research, we have determined that abolishing Sestrin association with GATOR2, and thus its signalling on mTORC1, has no effect on cell death. In our search for an alternative mechanism, we have found that Sestrin protein levels have a direct correlation with levels of activated STAT3. We employed numerous methods to attenuate STAT3 and demonstrated that its controlled attenuation restores cell death to control levels. In an attempt to understand how Sestrin influences STAT3, we discovered that SESN2 protein levels correlate with the transcription of PTPRD. Consequently, we have learned that Sestrins may influence cancer via the control of STAT3 activation, potentially through mechanisms yet to be determined, one of which could involve PTPRD. Future research will focus on determining which structural features of Sestrins are responsible for their effect on STAT3. Additionally, we will examine the link between STAT3 and Sestrin leucine sensitivity. Finally, we aim to identify potential interactants of Sestrins that influence STAT3 signalling via BioID2 analysis and assess the physiological implications of this cellular signalling to determine its viability as a therapeutic avenue for combating cancer.

1. Buckbinder, L., et al., *Gene regulation by temperature-sensitive p53 mutants: identification of p53 response genes.* Proceedings of the National Academy of Sciences, 1994. **91**(22): p. 10640-10644.
2. McKeehan, W. and B. Hardesty, *The mechanism of cycloheximide inhibition of protein synthesis in rabbit reticulocytes.* Biochem Biophys Res Commun, 1969. **36**(4): p. 625-30.
3. Velasco-Miguel, S., et al., *PA26, a novel target of the p53 tumor suppressor and member of the GADD family of DNA damage and growth arrest inducible genes.* Oncogene, 1999. **18**(1): p. 127-137.
4. Budanov, A.V., et al., *Identification of a novel stress-responsive gene Hi95 involved in regulation of cell viability.* Oncogene, 2002. **21**(39): p. 6017-6031.
5. Peeters, H., et al., *PA26 is a candidate gene for heterotaxia in humans: identification of a novel PA26-related gene family in human and mouse.* Human Genetics, 2003. **112**(5): p. 573-580.
6. Lee, J.H., et al., *Sestrin as a Feedback Inhibitor of TOR That Prevents Age-Related Pathologies.* Science, 2010. **327**(5970): p. 1223-1228.
7. Yang, Y.-L., et al., *SESN-1 is a positive regulator of lifespan in Caenorhabditis elegans.* Experimental Gerontology, 2013. **48**(3): p. 371-379.
8. Edwards, A.C., et al., *Mutations in many genes affect aggressive behavior in Drosophila melanogaster.* BMC Biology, 2009. **7**(1): p. 29.
9. Lee, Jun H., et al., *Maintenance of Metabolic Homeostasis by Sestrin2 and Sestrin3.* Cell Metabolism, 2012. **16**(3): p. 311-321.
10. Lee, Jun H., Andrei V. Budanov, and M. Karin, *Sestrins Orchestrate Cellular Metabolism to Attenuate Aging.* Cell Metabolism, 2013. **18**(6): p. 792-801.
11. Bae, Soo H., et al., *Sestrins Activate Nrf2 by Promoting p62-Dependent Autophagic Degradation of Keap1 and Prevent Oxidative Liver Damage.* Cell Metabolism, 2013. **17**(1): p. 73-84.
12. Peng, M., N. Yin, and Ming O. Li, *Sestrins Function as Guanine Nucleotide Dissociation Inhibitors for Rag GTPases to Control mTORC1 Signaling.* Cell, 2014. **159**(1): p. 122-133.
13. Budanov, A.V., J.H. Lee, and M. Karin, *Stressin' Sestrins take an aging fight.* EMBO Mol Med, 2010. **2**(10): p. 388-400.
14. Fritz-Laylin, L.K., et al., *The Genome of Naegleria gruberi Illuminates Early Eukaryotic Versatility.* Cell, 2010. **140**(5): p. 631-642.
15. Madeira, F., et al., *Search and sequence analysis tools services from EMBL-EBI in 2022.* Nucleic acids research, 2022. **50**(W1): p. W276-W279.
16. Letunic, I. and P. Bork, *Interactive Tree Of Life (iTOL) v5: an online tool for phylogenetic tree display and annotation.* Nucleic Acids Research, 2021. **49**(W1): p. W293-W296.
17. Zhang, J., *Evolution by gene duplication: an update.* Trends in Ecology & Evolution, 2003. **18**(6): p. 292-298.
18. Kondrashov, F.A., *Gene duplication as a mechanism of genomic adaptation to a changing environment.* Proceedings of the Royal Society B: Biological Sciences, 2012. **279**(1749): p. 5048-5057.
19. Brown, C.J., K.M. Todd, and R.F. Rosenzweig, *Multiple duplications of yeast hexose transport genes in response to selection in a glucose-limited environment.* Molecular Biology and Evolution, 1998. **15**(8): p. 931-942.
20. Riehle, M.M., A.F. Bennett, and A.D. Long, *Genetic architecture of thermal adaptation in Escherichia coli.* Proc Natl Acad Sci U S A, 2001. **98**(2): p. 525-30.
21. Panchy, N., M. Lehti-Shiu, and S.-H. Shiu, *Evolution of Gene Duplication in Plants.* Plant Physiology, 2016. **171**(4): p. 2294-2316.
22. Lupski, J.R., J.R. Roth, and G.M. Weinstock, *Chromosomal duplications in bacteria, fruit flies, and humans.* Am J Hum Genet, 1996. **58**(1): p. 21-7.

23. Bayés, M., et al., *Mutational mechanisms of Williams-Beuren syndrome deletions.* Am J Hum Genet, 2003. **73**(1): p. 131-51.
24. Pavlicek, A., et al., *Traffic of genetic information between segmental duplications flanking the typical 22q11.2 deletion in velo-cardio-facial syndrome/DiGeorge syndrome.* Genome Res, 2005. **15**(11): p. 1487-95.
25. Lander, E.S., et al., *Initial sequencing and analysis of the human genome.* Nature, 2001. **409**(6822): p. 860-921.
26. Pace, J.K., 2nd and C. Feschotte, *The evolutionary history of human DNA transposons: evidence for intense activity in the primate lineage.* Genome Res, 2007. **17**(4): p. 422-32.
27. Leonova, K.I., et al., *p53 cooperates with DNA methylation and a suicidal interferon response to maintain epigenetic silencing of repeats and noncoding RNAs.* Proceedings of the National Academy of Sciences, 2013. **110**(1): p. E89-E98.
28. De Cecco, M., et al., *L1 drives IFN in senescent cells and promotes age-associated inflammation.* Nature, 2019. **566**(7742): p. 73-78.
29. Peze-Heidsieck, E., et al., *Retrotransposons as a Source of DNA Damage in Neurodegeneration.* Frontiers in Aging Neuroscience, 2022. **13**.
30. Gorbunova, V., et al., *The role of retrotransposable elements in ageing and age-associated diseases.* Nature, 2021. **596**(7870): p. 43-53.
31. Haidurov, A. and A.V. Budanov, *Sestrin family – the stem controlling healthy ageing.* Mechanisms of Ageing and Development, 2020. **192**: p. 111379.
32. Budanov, A.V., *Stress-responsive sestrins link p53 with redox regulation and mammalian target of rapamycin signaling.* Antioxid Redox Signal, 2011. **15**(6): p. 1679-90.
33. Budanov, A.V., et al., *Regeneration of peroxiredoxins by p53-regulated sestrins, homologs of bacterial AhpD.* Science, 2004. **304**(5670): p. 596-600.
34. Bryk, R., et al., *Metabolic Enzymes of Mycobacteria Linked to Antioxidant Defense by a Thioredoxin-Like Protein.* Science, 2002. **295**(5557): p. 1073-1077.
35. Budanov, A.V. and M. Karin, *p53 Target Genes Sestrin1 and Sestrin2 Connect Genotoxic Stress and mTOR Signaling.* Cell, 2008. **134**(3): p. 451-460.
36. Kim, H., et al., *Janus-faced Sestrin2 controls ROS and mTOR signalling through two separate functional domains.* Nature Communications, 2015. **6**(1): p. 10025.
37. Saxton, R.A., et al., *Structural basis for leucine sensing by the Sestrin2-mTORC1 pathway.* Science, 2016. **351**(6268): p. 53-58.
38. Sengupta, S., et al., *Discovery of NV-5138, the first selective Brain mTORC1 activator.* Scientific Reports, 2019. **9**(1): p. 4107.
39. Enright, A.J., et al., *Protein interaction maps for complete genomes based on gene fusion events.* Nature, 1999. **402**(6757): p. 86-90.
40. Ben-Neriah, Y., et al., *The chronic myelogenous leukemia-specific P210 protein is the product of the bcr/abl hybrid gene.* Science, 1986. **233**(4760): p. 212-4.
41. Parmigiani, A., et al., *Sestrins Inhibit mTORC1 Kinase Activation through the GATOR Complex.* Cell Reports, 2014. **9**(4): p. 1281-1291.
42. Hein, Marco Y., et al., *A Human Interactome in Three Quantitative Dimensions Organized by Stoichiometries and Abundances.* Cell, 2015. **163**(3): p. 712-723.
43. Valenstein, M.L., et al., *Structure of the nutrient-sensing hub GATOR2.* Nature, 2022. **607**(7919): p. 610-616.
44. Zou, X.-D., et al., *Genome-wide Analysis of WD40 Protein Family in Human.* Scientific Reports, 2016. **6**(1): p. 39262.
45. Ibarra, A. and M.W. Hetzer, *Nuclear pore proteins and the control of genome functions.* Genes Dev, 2015. **29**(4): p. 337-49.
46. Loïodice, I., et al., *The Entire Nup107-160 Complex, Including Three New Members, Is Targeted as One Entity to Kinetochores in Mitosis.* Molecular Biology of the Cell, 2004. **15**(7): p. 3333-3344.

47. Zuccolo, M., et al., *The human Nup107–160 nuclear pore subcomplex contributes to proper kinetochore functions.* The EMBO Journal, 2007. **26**(7): p. 1853-1864-1864.
48. Thannickal, V.J. and B.L. Fanburg, *Reactive oxygen species in cell signaling.* Am J Physiol Lung Cell Mol Physiol, 2000. **279**(6): p. L1005-28.
49. Essler, S., N. Dehne, and B. Brüne, *Role of sestrin2 in peroxide signaling in macrophages.* FEBS Letters, 2009. **583**(21): p. 3531-3535.
50. Itoh, K., J. Mimura, and M. Yamamoto, *Discovery of the negative regulator of Nrf2, Keap1: a historical overview.* Antioxid Redox Signal, 2010. **13**(11): p. 1665-78.
51. Ro, S.H., et al., *Sestrin2 promotes Unc-51-like kinase 1 mediated phosphorylation of p62/sequestosome-1.* Febs j, 2014. **281**(17): p. 3816-27.
52. Zhang, D.D. and M. Hannink, *Distinct cysteine residues in Keap1 are required for Keap1-dependent ubiquitination of Nrf2 and for stabilization of Nrf2 by chemopreventive agents and oxidative stress.* Mol Cell Biol, 2003. **23**(22): p. 8137-51.
53. Nguyen, T., P. Nioi, and C.B. Pickett, *The Nrf2-antioxidant response element signaling pathway and its activation by oxidative stress.* J Biol Chem, 2009. **284**(20): p. 13291-5.
54. Eid, A.A., et al., *Sestrin 2 and AMPK connect hyperglycemia to Nox4-dependent endothelial nitric oxide synthase uncoupling and matrix protein expression.* Mol Cell Biol, 2013. **33**(17): p. 3439-60.
55. Murphy, Michael P., *How mitochondria produce reactive oxygen species.* Biochemical Journal, 2008. **417**(1): p. 1-13.
56. Cui, H., Y. Kong, and H. Zhang, *Oxidative stress, mitochondrial dysfunction, and aging.* J Signal Transduct, 2012. **2012**: p. 646354.
57. Palikaras, K., E. Lionaki, and N. Tavernarakis, *Mechanisms of mitophagy in cellular homeostasis, physiology and pathology.* Nature Cell Biology, 2018. **20**(9): p. 1013-1022.
58. Kim, M.J., et al., *SESN2/sestrin2 suppresses sepsis by inducing mitophagy and inhibiting NLRP3 activation in macrophages.* Autophagy, 2016. **12**(8): p. 1272-91.
59. Kovaleva, I.E., et al., *Mitochondrial localization of SESN2.* PLoS One, 2020. **15**(4): p. e0226862.
60. Ding, B., et al., *Sestrin2 is induced by glucose starvation via the unfolded protein response and protects cells from non-canonical necroptotic cell death.* Scientific Reports, 2016. **6**(1): p. 22538.
61. Kumar, A. and C. Shaha, *SESN2 facilitates mitophagy by helping Parkin translocation through ULK1 mediated Beclin1 phosphorylation.* Scientific Reports, 2018. **8**(1): p. 615.
62. Kozlowski, L.P., *Proteome-pI: proteome isoelectric point database.* Nucleic Acids Research, 2017. **45**(D1): p. D1112-D1116.
63. Goutte-Gattat, D. *What's the average size of a human protein?* 2013 [cited 2024 17/03/2024]; Available from: https://web.archive.org/web/20240317092928/https://incenp.org/notes/2013/average-protein-size.html.
64. Eng, C.P., S.N. Sehgal, and C. Vézina, *Activity of rapamycin (AY-22,989) against transplanted tumors.* J Antibiot (Tokyo), 1984. **37**(10): p. 1231-7.
65. Martel, R.R., J. Klicius, and S. Galet, *Inhibition of the immune response by rapamycin, a new antifungal antibiotic.* Can J Physiol Pharmacol, 1977. **55**(1): p. 48-51.
66. Sabatini, D.M., *Twenty-five years of mTOR: Uncovering the link from nutrients to growth.* Proceedings of the National Academy of Sciences, 2017. **114**(45): p. 11818-11825.
67. Yang, H., et al., *Mechanisms of mTORC1 activation by RHEB and inhibition by PRAS40.* Nature, 2017. **552**(7685): p. 368-373.
68. Kim, D.-H., et al., *mTOR Interacts with Raptor to Form a Nutrient-Sensitive Complex that Signals to the Cell Growth Machinery.* Cell, 2002. **110**(2): p. 163-175.
69. Hara, K., et al., *Raptor, a Binding Partner of Target of Rapamycin (TOR), Mediates TOR Action.* Cell, 2002. **110**(2): p. 177-189.

70. Kim, D.H., et al., *GbetaL, a positive regulator of the rapamycin-sensitive pathway required for the nutrient-sensitive interaction between raptor and mTOR.* Mol Cell, 2003. **11**(4): p. 895-904.
71. Yang, H., et al., *mTOR kinase structure, mechanism and regulation.* Nature, 2013. **497**(7448): p. 217-223.
72. Guertin, D.A., et al., *Ablation in Mice of the mTORC Components raptor, rictor, or mLST8 Reveals that mTORC2 Is Required for Signaling to Akt-FOXO and PKCα, but Not S6K1.* Developmental Cell, 2006. **11**(6): p. 859-871.
73. Rogala, K.B., et al., *Structural basis for the docking of mTORC1 on the lysosomal surface.* Science, 2019. **366**(6464): p. 468-475.
74. Schalm, S.S., et al., *TOS Motif-Mediated Raptor Binding Regulates 4E-BP1 Multisite Phosphorylation and Function.* Current Biology, 2003. **13**(10): p. 797-806.
75. Nojima, H., et al., *The Mammalian Target of Rapamycin (mTOR) Partner, Raptor, Binds the mTOR Substrates p70 S6 Kinase and 4E-BP1 through Their TOR Signaling (TOS) Motif*.* Journal of Biological Chemistry, 2003. **278**(18): p. 15461-15464.
76. Sancak, Y., et al., *PRAS40 Is an Insulin-Regulated Inhibitor of the mTORC1 Protein Kinase.* Molecular Cell, 2007. **25**(6): p. 903-915.
77. Haar, E.V., et al., *Insulin signalling to mTOR mediated by the Akt/PKB substrate PRAS40.* Nature Cell Biology, 2007. **9**(3): p. 316-323.
78. Peterson, T.R., et al., *DEPTOR is an mTOR inhibitor frequently overexpressed in multiple myeloma cells and required for their survival.* Cell, 2009. **137**(5): p. 873-86.
79. Gao, D., et al., *mTOR Drives Its Own Activation via SCFβTrCP-Dependent Degradation of the mTOR Inhibitor DEPTOR.* Molecular Cell, 2011. **44**(2): p. 290-303.
80. Yip, C.K., et al., *Structure of the Human mTOR Complex I and Its Implications for Rapamycin Inhibition.* Molecular Cell, 2010. **38**(5): p. 768-774.
81. Aylett, C.H.S., et al., *Architecture of human mTOR complex 1.* Science, 2016. **351**(6268): p. 48-52.
82. Inoki, K., et al., *Rheb GTPase is a direct target of TSC2 GAP activity and regulates mTOR signaling.* Genes Dev, 2003. **17**(15): p. 1829-34.
83. Long, X., et al., *Rheb Binds and Regulates the mTOR Kinase.* Current Biology, 2005. **15**(8): p. 702-713.
84. Sancak, Y., et al., *The Rag GTPases Bind Raptor and Mediate Amino Acid Signaling to mTORC1.* Science, 2008. **320**(5882): p. 1496-1501.
85. Kim, E., et al., *Regulation of TORC1 by Rag GTPases in nutrient response.* Nature Cell Biology, 2008. **10**(8): p. 935-945.
86. Dibble, C.C. and B.D. Manning, *Signal integration by mTORC1 coordinates nutrient input with biosynthetic output.* Nature Cell Biology, 2013. **15**(6): p. 555-564.
87. Dibble, Christian C., et al., *TBC1D7 Is a Third Subunit of the TSC1-TSC2 Complex Upstream of mTORC1.* Molecular Cell, 2012. **47**(4): p. 535-546.
88. Garami, A., et al., *Insulin Activation of Rheb, a Mediator of mTOR/S6K/4E-BP Signaling, Is Inhibited by TSC1 and 2.* Molecular Cell, 2003. **11**(6): p. 1457-1466.
89. Sarbassov, D.D., S.M. Ali, and D.M. Sabatini, *Growing roles for the mTOR pathway.* Curr Opin Cell Biol, 2005. **17**(6): p. 596-603.
90. Valvezan, A.J. and B.D. Manning, *Molecular logic of mTORC1 signalling as a metabolic rheostat.* Nature Metabolism, 2019. **1**(3): p. 321-333.
91. Tee, A.R., et al., *Tuberous Sclerosis Complex Gene Products, Tuberin and Hamartin, Control mTOR Signaling by Acting as a GTPase-Activating Protein Complex toward Rheb.* Current Biology, 2003. **13**(15): p. 1259-1268.
92. Manning, B.D., et al., *Identification of the Tuberous Sclerosis Complex-2 Tumor Suppressor Gene Product Tuberin as a Target of the Phosphoinositide 3-Kinase/Akt Pathway.* Molecular Cell, 2002. **10**(1): p. 151-162.

93. Menon, S., et al., *Spatial Control of the TSC Complex Integrates Insulin and Nutrient Regulation of mTORC1 at the Lysosome.* Cell, 2014. **156**(4): p. 771-785.
94. Demetriades, C., N. Doumpas, and Aurelio A. Teleman, *Regulation of TORC1 in Response to Amino Acid Starvation via Lysosomal Recruitment of TSC2.* Cell, 2014. **156**(4): p. 786-799.
95. Carter-Su, C., J. Schwartz, and L.S. Argetsinger, *Growth hormone signaling pathways.* Growth Hormone & IGF Research, 2016. **28**: p. 11-15.
96. Wang, X., et al., *Epidermal growth factor receptor-dependent Akt activation by oxidative stress enhances cell survival.* J Biol Chem, 2000. **275**(19): p. 14624-31.
97. Park, C.S., I.C. Schneider, and J.M. Haugh, *Kinetic analysis of platelet-derived growth factor receptor/phosphoinositide 3-kinase/Akt signaling in fibroblasts.* J Biol Chem, 2003. **278**(39): p. 37064-72.
98. Eswarakumar, V.P., I. Lax, and J. Schlessinger, *Cellular signaling by fibroblast growth factor receptors.* Cytokine & Growth Factor Reviews, 2005. **16**(2): p. 139-149.
99. Harrington, L.S., et al., *The TSC1-2 tumor suppressor controls insulin-PI3K signaling via regulation of IRS proteins.* J Cell Biol, 2004. **166**(2): p. 213-23.
100. Shah, O.J., Z. Wang, and T. Hunter, *Inappropriate Activation of the TSC/Rheb/mTOR/S6K Cassette Induces IRS1/2 Depletion, Insulin Resistance, and Cell Survival Deficiencies.* Current Biology, 2004. **14**(18): p. 1650-1656.
101. Inoki, K., et al., *TSC2 Integrates Wnt and Energy Signals via a Coordinated Phosphorylation by AMPK and GSK3 to Regulate Cell Growth.* Cell, 2006. **126**(5): p. 955-968.
102. Lee, D.-F., et al., *IKKβ Suppression of TSC1 Links Inflammation and Tumor Angiogenesis via the mTOR Pathway.* Cell, 2007. **130**(3): p. 440-455.
103. Ma, L., et al., *Phosphorylation and Functional Inactivation of TSC2 by Erk: Implications for Tuberous Sclerosisand Cancer Pathogenesis.* Cell, 2005. **121**(2): p. 179-193.
104. Roux, P.P., et al., *Tumor-promoting phorbol esters and activated Ras inactivate the tuberous sclerosis tumor suppressor complex via p90 ribosomal S6 kinase.* Proceedings of the National Academy of Sciences, 2004. **101**(37): p. 13489-13494.
105. Brugarolas, J., et al., *Regulation of mTOR function in response to hypoxia by REDD1 and the TSC1/TSC2 tumor suppressor complex.* Genes Dev, 2004. **18**(23): p. 2893-904.
106. DeYoung, M.P., et al., *Hypoxia regulates TSC1/2-mTOR signaling and tumor suppression through REDD1-mediated 14-3-3 shuttling.* Genes Dev, 2008. **22**(2): p. 239-51.
107. Gwinn, D.M., et al., *AMPK Phosphorylation of Raptor Mediates a Metabolic Checkpoint.* Molecular Cell, 2008. **30**(2): p. 214-226.
108. Shaw, R.J., et al., *The LKB1 tumor suppressor negatively regulates mTOR signaling.* Cancer Cell, 2004. **6**(1): p. 91-99.
109. Inoki, K., T. Zhu, and K.-L. Guan, *TSC2 Mediates Cellular Energy Response to Control Cell Growth and Survival.* Cell, 2003. **115**(5): p. 577-590.
110. Morrison, A., et al., *Sestrin2 promotes LKB1-mediated AMPK activation in the ischemic heart.* The FASEB Journal, 2015. **29**(2): p. 408-417.
111. Buse, M.G., *In vivo effects of branched chain amino acids on muscle protein synthesis in fasted rats.* Horm Metab Res, 1981. **13**(9): p. 502-5.
112. Bassit, R.A., et al., *The effect of BCAA supplementation upon the immune response of triathletes.* Medicine and science in sports and exercise, 2000. **32**(7): p. 1214-1219.
113. Negro, M., et al., *Branched-chain amino acid supplementation does not enhance athletic performance but affects muscle recovery and the immune system.* J Sports Med Phys Fitness, 2008. **48**(3): p. 347-51.
114. Shimomura, Y., et al., *Exercise Promotes BCAA Catabolism: Effects of BCAA Supplementation on Skeletal Muscle during Exercise1.* The Journal of Nutrition, 2004. **134**(6): p. 1583S-1587S.
115. Hara, K., et al., *Amino Acid Sufficiency and mTOR Regulate p70 S6 Kinase and eIF-4E BP1 through a Common Effector Mechanism*.* Journal of Biological Chemistry, 1998. **273**(23): p. 14484-14494.

116. Blommaart, E.F.C., et al., *Phosphorylation of Ribosomal Protein S6 Is Inhibitory for Autophagy in Isolated Rat Hepatocytes (∗).* Journal of Biological Chemistry, 1995. **270**(5): p. 2320-2326.
117. Sekiguchi, T., et al., *Novel G proteins, Rag C and Rag D, interact with GTP-binding proteins, Rag A and Rag B.* J Biol Chem, 2001. **276**(10): p. 7246-57.
118. Sancak, Y., et al., *Ragulator-Rag Complex Targets mTORC1 to the Lysosomal Surface and Is Necessary for Its Activation by Amino Acids.* Cell, 2010. **141**(2): p. 290-303.
119. Bar-Peled, L., et al., *Ragulator Is a GEF for the Rag GTPases that Signal Amino Acid Levels to mTORC1.* Cell, 2012. **150**(6): p. 1196-1208.
120. Shen, K., A. Choe, and D.M. Sabatini, *Intersubunit Crosstalk in the Rag GTPase Heterodimer Enables mTORC1 to Respond Rapidly to Amino Acid Availability.* Molecular Cell, 2017. **68**(3): p. 552-565.e8.
121. Bar-Peled, L., et al., *A Tumor Suppressor Complex with GAP Activity for the Rag GTPases That Signal Amino Acid Sufficiency to mTORC1.* Science, 2013. **340**(6136): p. 1100-1106.
122. Shen, K., et al., *Arg-78 of Nprl2 catalyzes GATOR1-stimulated GTP hydrolysis by the Rag GTPases.* Journal of Biological Chemistry, 2019. **294**(8): p. 2970-5944.
123. Peng, M., N. Yin, and M.O. Li, *SZT2 dictates GATOR control of mTORC1 signalling.* Nature, 2017. **543**(7645): p. 433-437.
124. Wolfson, R.L., et al., *KICSTOR recruits GATOR1 to the lysosome and is necessary for nutrients to regulate mTORC1.* Nature, 2017. **543**(7645): p. 438-442.
125. Shen, K., et al., *Architecture of the human GATOR1 and GATOR1–Rag GTPases complexes.* Nature, 2018. **556**(7699): p. 64-69.
126. Chantranupong, L., et al., *The CASTOR Proteins Are Arginine Sensors for the mTORC1 Pathway.* Cell, 2016. **165**(1): p. 153-164.
127. Saxton, R.A., et al., *Mechanism of arginine sensing by CASTOR1 upstream of mTORC1.* Nature, 2016. **536**(7615): p. 229-233.
128. Rebsamen, M., et al., *SLC38A9 is a component of the lysosomal amino acid sensing machinery that controls mTORC1.* Nature, 2015. **519**(7544): p. 477-481.
129. Wang, S., et al., *Lysosomal amino acid transporter SLC38A9 signals arginine sufficiency to mTORC1.* Science, 2015. **347**(6218): p. 188-194.
130. Wyant, G.A., et al., *mTORC1 Activator SLC38A9 Is Required to Efflux Essential Amino Acids from Lysosomes and Use Protein as a Nutrient.* Cell, 2017. **171**(3): p. 642-654.e12.
131. Lei, H.-T., et al., *Crystal structure of arginine-bound lysosomal transporter SLC38A9 in the cytosol-open state.* Nature Structural & Molecular Biology, 2018. **25**(6): p. 522-527.
132. Shen, K. and D.M. Sabatini, *Ragulator and SLC38A9 activate the Rag GTPases through noncanonical GEF mechanisms.* Proceedings of the National Academy of Sciences, 2018. **115**(38): p. 9545-9550.
133. Zoncu, R., et al., *mTORC1 Senses Lysosomal Amino Acids Through an Inside-Out Mechanism That Requires the Vacuolar H+-ATPase.* Science, 2011. **334**(6056): p. 678-683.
134. Petit, C.S., A. Roczniak-Ferguson, and S.M. Ferguson, *Recruitment of folliculin to lysosomes supports the amino acid-dependent activation of Rag GTPases.* J Cell Biol, 2013. **202**(7): p. 1107-22.
135. Tsun, Z.-Y., et al., *The Folliculin Tumor Suppressor Is a GAP for the RagC/D GTPases That Signal Amino Acid Levels to mTORC1.* Molecular Cell, 2013. **52**(4): p. 495-505.
136. Gu, X., et al., *SAMTOR is an S-adenosylmethionine sensor for the mTORC1 pathway.* Science, 2017. **358**(6364): p. 813-818.
137. Chantranupong, L., et al., *The Sestrins interact with GATOR2 to negatively regulate the amino-acid-sensing pathway upstream of mTORC1.* Cell Rep, 2014. **9**(1): p. 1-8.
138. Kim, J.S., et al., *Sestrin2 inhibits mTORC1 through modulation of GATOR complexes.* Scientific Reports, 2015. **5**(1): p. 9502.
139. Wolfson, R.L., et al., *Sestrin2 is a leucine sensor for the mTORC1 pathway.* Science, 2016. **351**(6268): p. 43-48.

140. Lee, J.H., U.S. Cho, and M. Karin, *Sestrin regulation of TORC1: Is Sestrin a leucine sensor?* Sci Signal, 2016. **9**(431): p. re5.
141. Brunn, G.J., et al., *Phosphorylation of the Translational Repressor PHAS-I by the Mammalian Target of Rapamycin.* Science, 1997. **277**(5322): p. 99-101.
142. Gingras, A.C., et al., *Regulation of 4E-BP1 phosphorylation: a novel two-step mechanism.* Genes Dev, 1999. **13**(11): p. 1422-37.
143. Hara, K., et al., *Regulation of eIF-4E BP1 Phosphorylation by mTOR *.* Journal of Biological Chemistry, 1997. **272**(42): p. 26457-26463.
144. Hsieh, A.C., et al., *The translational landscape of mTOR signalling steers cancer initiation and metastasis.* Nature, 2012. **485**(7396): p. 55-61.
145. Thoreen, C.C., et al., *A unifying model for mTORC1-mediated regulation of mRNA translation.* Nature, 2012. **485**(7396): p. 109-113.
146. Burnett, P.E., et al., *RAFT1 phosphorylation of the translational regulators p70 S6 kinase and 4E-BP1.* Proceedings of the National Academy of Sciences, 1998. **95**(4): p. 1432-1437.
147. Ruvinsky, I., et al., *Ribosomal protein S6 phosphorylation is a determinant of cell size and glucose homeostasis.* Genes Dev, 2005. **19**(18): p. 2199-211.
148. Chauvin, C., et al., *Ribosomal protein S6 kinase activity controls the ribosome biogenesis transcriptional program.* Oncogene, 2014. **33**(4): p. 474-483.
149. Mieulet, V., et al., *S6 kinase inactivation impairs growth and translational target phosphorylation in muscle cells maintaining proper regulation of protein turnover.* Am J Physiol Cell Physiol, 2007. **293**(2): p. C712-22.
150. Pende, M., et al., *S6K1(-/-)/S6K2(-/-) mice exhibit perinatal lethality and rapamycin-sensitive 5'-terminal oligopyrimidine mRNA translation and reveal a mitogen-activated protein kinase-dependent S6 kinase pathway.* Mol Cell Biol, 2004. **24**(8): p. 3112-24.
151. Stoneley, M. and A.E. Willis, *Cellular internal ribosome entry segments: structures, trans-acting factors and regulation of gene expression.* Oncogene, 2004. **23**(18): p. 3200-3207.
152. Xue, S., et al., *RNA regulons in Hox 5′ UTRs confer ribosome specificity to gene regulation.* Nature, 2015. **517**(7532): p. 33-38.
153. Kim, J., et al., *AMPK and mTOR regulate autophagy through direct phosphorylation of Ulk1.* Nature Cell Biology, 2011. **13**(2): p. 132-141.
154. Hosokawa, N., et al., *Nutrient-dependent mTORC1 Association with the ULK1–Atg13–FIP200 Complex Required for Autophagy.* Molecular Biology of the Cell, 2009. **20**(7): p. 1981-1991.
155. Ganley, I.G., et al., *ULK1.ATG13.FIP200 complex mediates mTOR signaling and is essential for autophagy.* J Biol Chem, 2009. **284**(18): p. 12297-305.
156. Dikic, I. and Z. Elazar, *Mechanism and medical implications of mammalian autophagy.* Nature Reviews Molecular Cell Biology, 2018. **19**(6): p. 349-364.
157. Kim, Y.M., et al., *mTORC1 phosphorylates UVRAG to negatively regulate autophagosome and endosome maturation.* Mol Cell, 2015. **57**(2): p. 207-18.
158. Dazert, E. and M.N. Hall, *mTOR signaling in disease.* Current Opinion in Cell Biology, 2011. **23**(6): p. 744-755.
159. Sablina, A.A., et al., *The antioxidant function of the p53 tumor suppressor.* Nature Medicine, 2005. **11**(12): p. 1306-1313.
160. Wei, C.L., et al., *A global map of p53 transcription-factor binding sites in the human genome.* Cell, 2006. **124**(1): p. 207-19.
161. Shin, B.Y., et al., *Nrf2-ARE pathway regulates induction of Sestrin-2 expression.* Free Radical Biology and Medicine, 2012. **53**(4): p. 834-841.
162. Hetz, C., *The unfolded protein response: controlling cell fate decisions under ER stress and beyond.* Nature Reviews Molecular Cell Biology, 2012. **13**(2): p. 89-102.
163. Olson, N., et al., *Activation of hypoxia-inducible factor-1 protects airway epithelium against oxidant-induced barrier dysfunction.* American Journal of Physiology-Lung Cellular and Molecular Physiology, 2011. **301**(6): p. L993-L1002.

164. Seo, K., et al., *Sestrin2 inhibits hypoxia-inducible factor-1α accumulation via AMPK-mediated prolyl hydroxylase regulation.* Free Radical Biology and Medicine, 2016. **101**: p. 511-523.
165. Jegal, K.H., et al., *Activating transcription factor 6-dependent sestrin 2 induction ameliorates ER stress-mediated liver injury.* Biochimica et Biophysica Acta (BBA) - Molecular Cell Research, 2017. **1864**(7): p. 1295-1307.
166. Saveljeva, S., et al., *Endoplasmic reticulum stress-mediated induction of SESTRIN 2 potentiates cell survival.* Oncotarget; Vol 7, No 11, 2016.
167. Brüning, A., M. Rahmeh, and K. Friese, *Nelfinavir and bortezomib inhibit mTOR activity via ATF4-mediated sestrin-2 regulation.* Mol Oncol, 2013. **7**(6): p. 1012-8.
168. Garaeva, A.A., et al., *Mitochondrial dysfunction induces SESN2 gene expression through Activating Transcription Factor 4.* Cell Cycle, 2016. **15**(1): p. 64-71.
169. Byun, J.-K., et al., *A Positive Feedback Loop between Sestrin2 and mTORC2 Is Required for the Survival of Glutamine-Depleted Lung Cancer Cells.* Cell Reports, 2017. **20**(3): p. 586-599.
170. Zhang, X.-Y., et al., *Upregulation of sestrin 2 expression via JNK pathway activation contributes to autophagy induction in cancer cells.* Cellular Signalling, 2013. **25**(1): p. 150-158.
171. Nogueira, V., et al., *Akt Determines Replicative Senescence and Oxidative or Oncogenic Premature Senescence and Sensitizes Cells to Oxidative Apoptosis.* Cancer Cell, 2008. **14**(6): p. 458-470.
172. Chen, C.-C., et al., *FoxOs Inhibit mTORC1 and Activate Akt by Inducing the Expression of Sestrin3 and Rictor.* Developmental Cell, 2010. **18**(4): p. 592-604.
173. Hagenbuchner, J., et al., *FOXO3-induced reactive oxygen species are regulated by BCL2L11 (Bim) and SESN3.* Journal of Cell Science, 2012. **125**(5): p. 1191-1203.
174. Darnell, J.E., I.M. Kerr, and G.R. Stark, *Jak-STAT Pathways and Transcriptional Activation in Response to IFNs and Other Extracellular Signaling Proteins.* Science, 1994. **264**(5164): p. 1415-1421.
175. Stark, G.R., et al., *How cells respond to interferons.* Annu Rev Biochem, 1998. **67**: p. 227-64.
176. Dariya, B., et al., *Targeting STAT proteins via computational analysis in colorectal cancer.* Molecular and Cellular Biochemistry, 2021. **476**(1): p. 165-174.
177. Furqan, M., et al., *STAT inhibitors for cancer therapy.* Journal of Hematology & Oncology, 2013. **6**(1): p. 90.
178. Zou, S., et al., *Targeting STAT3 in Cancer Immunotherapy.* Molecular Cancer, 2020. **19**(1): p. 145.
179. Ziemiecki, A., A.G. Harpur, and A.F. Wilks, *JAK protein tyrosine kinases: their role in cytokine signalling.* Trends in Cell Biology, 1994. **4**(6): p. 207-212.
180. Kawamura, M., et al., *Molecular cloning of L-JAK, a Janus family protein-tyrosine kinase expressed in natural killer cells and activated leukocytes.* Proceedings of the National Academy of Sciences, 1994. **91**(14): p. 6374-6378.
181. Musso, T., et al., *Regulation of JAK3 expression in human monocytes: phosphorylation in response to interleukins 2, 4, and 7.* J Exp Med, 1995. **181**(4): p. 1425-31.
182. Tortolani, P.J., et al., *Regulation of JAK3 expression and activation in human B cells and B cell malignancies.* J Immunol, 1995. **155**(11): p. 5220-6.
183. Hofmann, S.R., et al., *Jak3-independent trafficking of the common gamma chain receptor subunit: chaperone function of Jaks revisited.* Mol Cell Biol, 2004. **24**(11): p. 5039-49.
184. Ragimbeau, J., et al., *The tyrosine kinase Tyk2 controls IFNAR1 cell surface expression.* Embo j, 2003. **22**(3): p. 537-47.
185. Velazquez, L., et al., *A protein tyrosine kinase in the interferon αβ signaling pathway.* Cell, 1992. **70**(2): p. 313-322.
186. Argetsinger, L.S., et al., *Identification of JAK2 as a growth hormone receptor-associated tyrosine kinase.* Cell, 1993. **74**(2): p. 237-244.

187. Witthuhn, B.A., et al., *JAK2 associates with the erythropoietin receptor and is tyrosine phosphorylated and activated following stimulation with erythropoietin.* Cell, 1993. **74**(2): p. 227-236.
188. Müller, M., et al., *The protein tyrosine kinase JAK1 complements defects in interferon-α/β and -γ signal transduction.* Nature, 1993. **366**(6451): p. 129-135.
189. Silvennoinen, O., et al., *Interferon-induced nuclear signalling by Jak protein tyrosine kinases.* Nature, 1993. **366**(6455): p. 583-585.
190. Chen, M., et al., *The amino terminus of JAK3 is necessary and sufficient for binding to the common gamma chain and confers the ability to transmit interleukin 2-mediated signals.* Proc Natl Acad Sci U S A, 1997. **94**(13): p. 6910-5.
191. Shimoda, K., et al., *Tyk2 Plays a Restricted Role in IFNα Signaling, Although It Is Required for IL-12-Mediated T Cell Function.* Immunity, 2000. **13**(4): p. 561-571.
192. Williams, N.K., et al., *Dissecting Specificity in the Janus Kinases: The Structures of JAK-Specific Inhibitors Complexed to the JAK1 and JAK2 Protein Tyrosine Kinase Domains.* Journal of Molecular Biology, 2009. **387**(1): p. 219-232.
193. Chrencik, J.E., et al., *Structural and Thermodynamic Characterization of the TYK2 and JAK3 Kinase Domains in Complex with CP-690550 and CMP-6.* Journal of Molecular Biology, 2010. **400**(3): p. 413-433.
194. Wallweber, H.J.A., et al., *Structural basis of recognition of interferon-α receptor by tyrosine kinase 2.* Nature Structural & Molecular Biology, 2014. **21**(5): p. 443-448.
195. Ferrao, R., et al., *The Structural Basis for Class II Cytokine Receptor Recognition by JAK1.* Structure, 2016. **24**(6): p. 897-905.
196. Zhang, D., A. Wlodawer, and J. Lubkowski, *Crystal Structure of a Complex of the Intracellular Domain of Interferon λ Receptor 1 (IFNLR1) and the FERM/SH2 Domains of Human JAK1.* Journal of Molecular Biology, 2016. **428**(23): p. 4651-4668.
197. McNally, R., A.V. Toms, and M.J. Eck, *Crystal Structure of the FERM-SH2 Module of Human Jak2.* PLoS One, 2016. **11**(5): p. e0156218.
198. Yamaoka, K., et al., *The Janus kinases (Jaks).* Genome Biology, 2004. **5**(12): p. 253.
199. Manning, G., et al., *The Protein Kinase Complement of the Human Genome.* Science, 2002. **298**(5600): p. 1912-1934.
200. Saharinen, P., K. Takaluoma, and O. Silvennoinen, *Regulation of the Jak2 tyrosine kinase by its pseudokinase domain.* Mol Cell Biol, 2000. **20**(10): p. 3387-95.
201. James, C., et al., *A unique clonal JAK2 mutation leading to constitutive signalling causes polycythaemia vera.* Nature, 2005. **434**(7037): p. 1144-1148.
202. Baxter, E.J., et al., *Acquired mutation of the tyrosine kinase JAK2 in human myeloproliferative disorders.* The Lancet, 2005. **365**(9464): p. 1054-1061.
203. Kralovics, R., et al., *A Gain-of-Function Mutation of JAK2 in Myeloproliferative Disorders.* New England Journal of Medicine, 2005. **352**(17): p. 1779-1790.
204. Ceccarelli, D.F.J., et al., *Crystal Structure of the FERM Domain of Focal Adhesion Kinase*.* Journal of Biological Chemistry, 2006. **281**(1): p. 252-259.
205. Lupardus, P.J., et al., *Structural snapshots of full-length Jak1, a transmembrane gp130/IL-6/IL-6Rα cytokine receptor complex, and the receptor-Jak1 holocomplex.* Structure, 2011. **19**(1): p. 45-55.
206. Radtke, S., et al., *The Jak1 SH2 domain does not fulfill a classical SH2 function in Jak/STAT signaling but plays a structural role for receptor interaction and up-regulation of receptor surface expression.* J Biol Chem, 2005. **280**(27): p. 25760-8.
207. Fu, X.Y., et al., *The proteins of ISGF-3, the interferon alpha-induced transcriptional activator, define a gene family involved in signal transduction.* Proceedings of the National Academy of Sciences, 1992. **89**(16): p. 7840-7843.

208. Schindler, C., et al., *Proteins of transcription factor ISGF-3: one gene encodes the 91-and 84-kDa ISGF-3 proteins that are activated by interferon alpha.* Proc Natl Acad Sci U S A, 1992. **89**(16): p. 7836-9.
209. Quelle, F.W., et al., *Cloning of Murine Stat6 and Human Stat6, Stat Proteins That Are Tyrosine Phosphorylated in Responses to IL-4 and IL-3 but Are Not Required for Mitogenesis.* Molecular and Cellular Biology, 1995. **15**(6): p. 3336-3343.
210. Mui, A.L., et al., *Interleukin-3, granulocyte-macrophage colony stimulating factor and interleukin-5 transduce signals through two STAT5 homologs.* The EMBO Journal, 1995. **14**(6): p. 1166-1175-1175.
211. Yamamoto, K., et al., *Stat4, a novel gamma interferon activation site-binding protein expressed in early myeloid differentiation.* Mol Cell Biol, 1994. **14**(7): p. 4342-9.
212. Zhong, Z., Z. Wen, and J.E. Darnell, Jr., *Stat3 and Stat4: members of the family of signal transducers and activators of transcription.* Proc Natl Acad Sci U S A, 1994. **91**(11): p. 4806-10.
213. Zhong, Z., Z. Wen, and J.E. Darnell, *Stat3: a STAT Family Member Activated by Tyrosine Phosphorylation in Response to Epidermal Growth Factor and Interleukin-6.* Science, 1994. **264**(5155): p. 95-98.
214. Benekli, M., et al., *Signal transducer and activator of transcription proteins in leukemias.* Blood, 2003. **101**(8): p. 2940-54.
215. Fu, X.Y., et al., *ISGF3, the transcriptional activator induced by interferon alpha, consists of multiple interacting polypeptide chains.* Proc Natl Acad Sci U S A, 1990. **87**(21): p. 8555-9.
216. Wegenka, U.M., et al., *Acute-phase response factor, a nuclear factor binding to acute-phase response elements, is rapidly activated by interleukin-6 at the posttranslational level.* Mol Cell Biol, 1993. **13**(1): p. 276-88.
217. Bromberg, J. and J.E. Darnell, *The role of STATs in transcriptional control and their impact on cellular function.* Oncogene, 2000. **19**(21): p. 2468-2473.
218. Baker, S.J., S.G. Rane, and E.P. Reddy, *Hematopoietic cytokine receptor signaling.* Oncogene, 2007. **26**(47): p. 6724-6737.
219. Minegishi, Y., et al., *Dominant-negative mutations in the DNA-binding domain of STAT3 cause hyper-IgE syndrome.* Nature, 2007. **448**(7157): p. 1058-1062.
220. Minegishi, Y. and H. Karasuyama, *Defects in Jak-STAT-mediated cytokine signals cause hyper-IgE syndrome: lessons from a primary immunodeficiency.* Int Immunol, 2009. **21**(2): p. 105-12.
221. Hou, T., et al., *The STAT3 NH2-terminal domain stabilizes enhanceosome assembly by interacting with the p300 bromodomain.* J Biol Chem, 2008. **283**(45): p. 30725-34.
222. Vogt, M., et al., *The role of the N-terminal domain in dimerization and nucleocytoplasmic shuttling of latent STAT3.* J Cell Sci, 2011. **124**(Pt 6): p. 900-9.
223. Liao, J., Y. Fu, and K. Shuai, *Distinct roles of the NH2- and COOH-terminal domains of the protein inhibitor of activated signal transducer and activator of transcription (STAT) 1 (PIAS1) in cytokine-induced PIAS1-Stat1 interaction.* Proc Natl Acad Sci U S A, 2000. **97**(10): p. 5267-72.
224. Hu, T., et al., *Impact of the N-Terminal Domain of STAT3 in STAT3-Dependent Transcriptional Activity.* Mol Cell Biol, 2015. **35**(19): p. 3284-300.
225. Zhang, T., et al., *The coiled-coil domain of Stat3 is essential for its SH2 domain-mediated receptor binding and subsequent activation induced by epidermal growth factor and interleukin-6.* Mol Cell Biol, 2000. **20**(19): p. 7132-9.
226. Liu, L., K.M. McBride, and N.C. Reich, *STAT3 nuclear import is independent of tyrosine phosphorylation and mediated by importin-α3.* Proceedings of the National Academy of Sciences, 2005. **102**(23): p. 8150-8155.
227. Sasse, J., et al., *Mutational analysis of acute-phase response factor/Stat3 activation and dimerization.* Mol Cell Biol, 1997. **17**(8): p. 4677-86.

228. Wen, Z., Z. Zhong, and J.E. Darnell, Jr., *Maximal activation of transcription by Stat1 and Stat3 requires both tyrosine and serine phosphorylation.* Cell, 1995. **82**(2): p. 241-50.
229. Haan, S., et al., *Characterization and binding specificity of the monomeric STAT3-SH2 domain.* J Biol Chem, 1999. **274**(3): p. 1342-8.
230. Chen, X., et al., *Crystal structure of a tyrosine phosphorylated STAT-1 dimer bound to DNA.* Cell, 1998. **93**(5): p. 827-39.
231. Feng, J., et al., *Activation of Jak2 catalytic activity requires phosphorylation of Y1007 in the kinase activation loop.* Mol Cell Biol, 1997. **17**(5): p. 2497-501.
232. Argetsinger, L.S., et al., *Autophosphorylation of JAK2 on tyrosines 221 and 570 regulates its activity.* Mol Cell Biol, 2004. **24**(11): p. 4955-67.
233. Kurzer, J.H., et al., *Tyrosine 813 is a site of JAK2 autophosphorylation critical for activation of JAK2 by SH2-B beta.* Mol Cell Biol, 2004. **24**(10): p. 4557-70.
234. Shuai, K., et al., *A single phosphotyrosine residue of Stat91 required for gene activation by interferon-gamma.* Science, 1993. **261**(5129): p. 1744-6.
235. Nakajima, K., et al., *A central role for Stat3 in IL-6-induced regulation of growth and differentiation in M1 leukemia cells.* The EMBO Journal, 1996. **15**(14): p. 3651-3658-3658.
236. Shuai, K., et al., *Interferon activation of the transcription factor Stat91 involves dimerization through SH2-phosphotyrosyl peptide interactions.* Cell, 1994. **76**(5): p. 821-8.
237. Schaefer, T.S., et al., *Functional Differences between Stat3α and Stat3β.* Molecular and Cellular Biology, 1997. **17**(9): p. 5307-5316.
238. Maritano, D., et al., *The STAT3 isoforms α and β have unique and specific functions.* Nature Immunology, 2004. **5**(4): p. 401-409.
239. Zammarchi, F., et al., *Antitumorigenic potential of STAT3 alternative splicing modulation.* Proc Natl Acad Sci U S A, 2011. **108**(43): p. 17779-84.
240. Yang, J., et al., *Novel Roles of Unphosphorylated STAT3 in Oncogenesis and Transcriptional Regulation.* Cancer Research, 2005. **65**(3): p. 939-947.
241. Yang, J., et al., *Unphosphorylated STAT3 accumulates in response to IL-6 and activates transcription by binding to NFkappaB.* Genes Dev, 2007. **21**(11): p. 1396-408.
242. Ireland, N.C.R., *Cancer in Ireland 1994-2021: Annual statistical report of the National Cancer Registry*. 2023, National Cancer Registry Ireland, NCRI, Cork, Ireland.
243. Ferlay, J., et al., *Cancer statistics for the year 2020: An overview.* International Journal of Cancer, 2021. **149**(4): p. 778-789.
244. Bray, F., et al., *Global cancer statistics 2018: GLOBOCAN estimates of incidence and mortality worldwide for 36 cancers in 185 countries.* CA: A Cancer Journal for Clinicians, 2018. **68**(6): p. 394-424.
245. Rotow, J. and T.G. Bivona, *Understanding and targeting resistance mechanisms in NSCLC.* Nature Reviews Cancer, 2017. **17**(11): p. 637-658.
246. Zappa, C. and S.A. Mousa, *Non-small cell lung cancer: current treatment and future advances.* Transl Lung Cancer Res, 2016. **5**(3): p. 288-300.
247. Vasan, N., J. Baselga, and D.M. Hyman, *A view on drug resistance in cancer.* Nature, 2019. **575**(7782): p. 299-309.
248. Greaves, M. and C.C. Maley, *Clonal evolution in cancer.* Nature, 2012. **481**(7381): p. 306-313.
249. Chiba, I., et al., *Mutations in the p53 gene are frequent in primary, resected non-small cell lung cancer. Lung Cancer Study Group.* Oncogene, 1990. **5**(10): p. 1603-10.
250. DuPage, M., A.L. Dooley, and T. Jacks, *Conditional mouse lung cancer models using adenoviral or lentiviral delivery of Cre recombinase.* Nat Protoc, 2009. **4**(7): p. 1064-72.
251. Fischer, M., *Census and evaluation of p53 target genes.* Oncogene, 2017. **36**(28): p. 3943-3956.
252. Park, S.-J., et al., *GENT2: an updated gene expression database for normal and tumor tissues.* BMC Medical Genomics, 2019. **12**(5): p. 101.

253. Chen, K.B., et al., *Sestrin2 expression is a favorable prognostic factor in patients with non-small cell lung cancer.* Am J Transl Res, 2016. **8**(4): p. 1903-9.
254. Ding, B., et al., *p53-inducible SESTRINs might play opposite roles in the regulation of early and late stages of lung carcinogenesis.* Oncotarget, 2019. **10**(65): p. 6997-7009.
255. Darnell, J.E., *Validating Stat3 in cancer therapy.* Nature Medicine, 2005. **11**(6): p. 595-596.
256. Johnson, D.E., R.A. O'Keefe, and J.R. Grandis, *Targeting the IL-6/JAK/STAT3 signalling axis in cancer.* Nature Reviews Clinical Oncology, 2018. **15**(4): p. 234-248.
257. Bromberg, J.F., et al., *Stat3 as an Oncogene.* Cell, 1999. **98**(3): p. 295-303.
258. Bowman, T., et al., *Stat3-mediated Myc expression is required for Src transformation and PDGF-induced mitogenesis.* Proceedings of the National Academy of Sciences, 2001. **98**(13): p. 7319-7324.
259. Zamo, A., et al., *Anaplastic lymphoma kinase (ALK) activates Stat3 and protects hematopoietic cells from cell death.* Oncogene, 2002. **21**(7): p. 1038-1047.
260. Koskela, H.L., et al., *Somatic STAT3 mutations in large granular lymphocytic leukemia.* N Engl J Med, 2012. **366**(20): p. 1905-13.
261. Yu, H., et al., *Revisiting STAT3 signalling in cancer: new and unexpected biological functions.* Nat Rev Cancer, 2014. **14**(11): p. 736-46.
262. Yu, H., M. Kortylewski, and D. Pardoll, *Crosstalk between cancer and immune cells: role of STAT3 in the tumour microenvironment.* Nat Rev Immunol, 2007. **7**(1): p. 41-51.
263. Igelmann, S., H.A. Neubauer, and G. Ferbeyre, *STAT3 and STAT5 Activation in Solid Cancers.* Cancers (Basel), 2019. **11**(10).
264. Hanahan, D. and R.A. Weinberg, *Hallmarks of cancer: the next generation.* Cell, 2011. **144**(5): p. 646-74.
265. Parmigiani, A. and A.V. Budanov, *Sensing the Environment Through Sestrins: Implications for Cellular Metabolism.* Int Rev Cell Mol Biol, 2016. **327**: p. 1-42.
266. Saxton, R.A. and D.M. Sabatini, *mTOR Signaling in Growth, Metabolism, and Disease.* Cell, 2017. **168**(6): p. 960-976.
267. White, E., *Deconvoluting the context-dependent role for autophagy in cancer.* Nat Rev Cancer, 2012. **12**(6): p. 401-10.
268. Oricchio, E., et al., *Genetic and epigenetic inactivation of SESTRIN1 controls mTORC1 and response to EZH2 inhibition in follicular lymphoma.* Sci Transl Med, 2017. **9**(396).
269. Nutt, S.L., et al., *EZH2 function in immune cell development.* Biol Chem, 2020. **401**(8): p. 933-943.
270. Easton, J.B. and P.J. Houghton, *mTOR and cancer therapy.* Oncogene, 2006. **25**(48): p. 6436-6446.
271. Ding, B., et al., *Sestrin2 facilitates death receptor-induced apoptosis in lung adenocarcinoma cells through regulation of XIAP degradation.* Cell Cycle, 2015. **14**(20): p. 3231-41.
272. Budanov, A.V., *SESN2 inactivation in mice causes decreased growth of liver tumours*.
273. Liu, Y., et al., *Sesn3 deficiency promotes carcinogen-induced hepatocellular carcinoma via regulation of the hedgehog pathway.* Biochim Biophys Acta Mol Basis Dis, 2019. **1865**(10): p. 2685-2693.
274. Tamura, K., et al., *Molecular features of hormone-refractory prostate cancer cells by genome-wide gene expression profiles.* Cancer Res, 2007. **67**(11): p. 5117-25.
275. Shan, J., et al., *Targeting Wnt/EZH2/microRNA-708 signaling pathway inhibits neuroendocrine differentiation in prostate cancer.* Cell Death Discovery, 2019. **5**(1): p. 139.
276. Zhao, B., et al., *Sestrin2 protein positively regulates AKT enzyme signaling and survival in human squamous cell carcinoma and melanoma cells.* J Biol Chem, 2014. **289**(52): p. 35806-14.
277. Zhao, B., et al., *Distinct Role of Sesn2 in Response to UVB-Induced DNA Damage and UVA-Induced Oxidative Stress in Melanocytes.* Photochem Photobiol, 2017. **93**(1): p. 375-381.

278. Wei, J.L., et al., *Decreased expression of sestrin 2 predicts unfavorable outcome in colorectal cancer.* Oncol Rep, 2015. **33**(3): p. 1349-57.
279. Ro, S.H., et al., *Tumor suppressive role of sestrin2 during colitis and colon carcinogenesis.* Elife, 2016. **5**: p. e12204.
280. Batlle, E. and H. Clevers, *Cancer stem cells revisited.* Nat Med, 2017. **23**(10): p. 1124-1134.
281. Shlush, L.I., et al., *Tracing the origins of relapse in acute myeloid leukaemia to stem cells.* Nature, 2017. **547**(7661): p. 104-108.
282. Kim, C.F., et al., *Identification of bronchioalveolar stem cells in normal lung and lung cancer.* Cell, 2005. **121**(6): p. 823-35.
283. Zakaria, N., et al., *Human non-small cell lung cancer expresses putative cancer stem cell markers and exhibits the transcriptomic profile of multipotent cells.* BMC Cancer, 2015. **15**: p. 84.
284. He, G., et al., *Identification of liver cancer progenitors whose malignant progression depends on autocrine IL-6 signaling.* Cell, 2013. **155**(2): p. 384-96.
285. Wang, N., et al., *Cancer stem cells in hepatocellular carcinoma: an overview and promising therapeutic strategies.* Ther Adv Med Oncol, 2018. **10**: p. 1758835918816287.
286. Munro, M.J., et al., *Cancer stem cells in colorectal cancer: a review.* J Clin Pathol, 2018. **71**(2): p. 110-116.
287. Zabierowski, S.E. and M. Herlyn, *Melanoma stem cells: the dark seed of melanoma.* J Clin Oncol, 2008. **26**(17): p. 2890-4.
288. Boumahdi, S., et al., *SOX2 controls tumour initiation and cancer stem-cell functions in squamous-cell carcinoma.* Nature, 2014. **511**(7508): p. 246-50.
289. Martinez-Climent, J.A., et al., *Lymphoma stem cells: enough evidence to support their existence?* Haematologica, 2010. **95**(2): p. 293-302.
290. Wen, Y., et al., *Role of EZH2 in cancer stem cells: from biological insight to a therapeutic target.* Oncotarget, 2017. **8**(23): p. 37974-37990.
291. Zakaria, N., et al., *Targeting Lung Cancer Stem Cells: Research and Clinical Impacts.* Front Oncol, 2017. **7**: p. 80.
292. Ke, J., et al., *A subpopulation of CD24$^+$ cells in colon cancer cell lines possess stem cell characteristics.* Neoplasma, 2012. **59**(3): p. 282-8.
293. Parmigiani, A., et al., *Sestrins inhibit mTORC1 kinase activation through the GATOR complex.* Cell Rep, 2014. **9**(4): p. 1281-91.
294. Budanov, A.V. and M. Karin, *p53 target genes sestrin1 and sestrin2 connect genotoxic stress and mTOR signaling.* Cell, 2008. **134**(3): p. 451-60.
295. Ding, B., et al., *Sestrin2 is induced by glucose starvation via the unfolded protein response and protects cells from non-canonical necroptotic cell death.* Sci Rep, 2016. **6**: p. 22538.
296. Solomon, D.A., et al., *Mutational inactivation of PTPRD in glioblastoma multiforme and malignant melanoma.* Cancer Res, 2008. **68**(24): p. 10300-6.
297. Wright, K., *Antibodies a Laboratory Manual: by E Harlow and D Lane. pp 726. Cold Spring Harbor Laboratory. 1988. $50 ISBN 0-87969-314-2.* Biochemical Education, 1989. **17**(4): p. 220.
298. Franken, N.A.P., et al., *Clonogenic assay of cells in vitro.* Nature Protocols, 2006. **1**(5): p. 2315-2319.
299. Bolger, A.M., M. Lohse, and B. Usadel, *Trimmomatic: a flexible trimmer for Illumina sequence data.* Bioinformatics, 2014. **30**(15): p. 2114-20.
300. Langmead, B. and S.L. Salzberg, *Fast gapped-read alignment with Bowtie 2.* Nat Methods, 2012. **9**(4): p. 357-9.
301. Dobin, A., et al., *STAR: ultrafast universal RNA-seq aligner.* Bioinformatics, 2013. **29**(1): p. 15-21.
302. Liao, Y., G.K. Smyth, and W. Shi, *featureCounts: an efficient general purpose program for assigning sequence reads to genomic features.* Bioinformatics, 2014. **30**(7): p. 923-30.

303. Robinson, M.D., D.J. McCarthy, and G.K. Smyth, *edgeR: a Bioconductor package for differential expression analysis of digital gene expression data.* Bioinformatics, 2010. **26**(1): p. 139-40.
304. Yu, G., et al., *clusterProfiler: an R package for comparing biological themes among gene clusters.* OMICS, 2012. **16**(5): p. 284-7.
305. Chen, J., *The Cell-Cycle Arrest and Apoptotic Functions of p53 in Tumor Initiation and Progression.* Cold Spring Harb Perspect Med, 2016. **6**(3): p. a026104.
306. Vousden, K.H., *p53: death star.* Cell, 2000. **103**(5): p. 691-4.
307. Meek, D.W., *Tumour suppression by p53: a role for the DNA damage response?* Nat Rev Cancer, 2009. **9**(10): p. 714-23.
308. Liu, X., et al., *p53 upregulates death receptor 4 expression through an intronic p53 binding site.* Cancer Res, 2004. **64**(15): p. 5078-83.
309. Lanna, A., et al., *A sestrin-dependent Erk-Jnk-p38 MAPK activation complex inhibits immunity during aging.* Nat Immunol, 2017. **18**: p. 354-63.
310. Rinaldi, L., et al., *Mitochondrial AKAP1 supports mTOR pathway and tumor growth.* Cell Death Dis, 2017. **8**(6): p. e2842.
311. Wei, J., et al., *Sestrin2 reduces cancer stemness via Wnt/beta-catenin signaling in colorectal cancer.* Cancer Cell Int, 2022. **22**(1): p. 75.
312. Budanov, A.V., *SESTRINs regulate mTORC1 via RRAGs: The riddle of GATOR.* Molecular & Cellular Oncology, 2015. **2**(3).
313. Bethune, G., et al., *Epidermal growth factor receptor (EGFR) in lung cancer: an overview and update.* J Thorac Dis, 2010. **2**(1): p. 48-51.
314. Gao, S.P., et al., *Mutations in the EGFR kinase domain mediate STAT3 activation via IL-6 production in human lung adenocarcinomas.* J Clin Invest, 2007. **117**(12): p. 3846-56.
315. Yao, Z., et al., *A Global Analysis of the Receptor Tyrosine Kinase-Protein Phosphatase Interactome.* Mol Cell, 2017. **65**(2): p. 347-360.
316. Moyer, J.D., et al., *Induction of apoptosis and cell cycle arrest by CP-358,774, an inhibitor of epidermal growth factor receptor tyrosine kinase.* Cancer Res, 1997. **57**(21): p. 4838-48.
317. O'Hare, T., et al., *In vitro activity of Bcr-Abl inhibitors AMN107 and BMS-354825 against clinically relevant imatinib-resistant Abl kinase domain mutants.* Cancer Res, 2005. **65**(11): p. 4500-5.
318. Shah, N.P., et al., *Dasatinib (BMS-354825) inhibits KITD816V, an imatinib-resistant activating mutation that triggers neoplastic growth in most patients with systemic mastocytosis.* Blood, 2006. **108**(1): p. 286-91.
319. Redell, M.S., et al., *Stat3 signaling in acute myeloid leukemia: ligand-dependent and -independent activation and induction of apoptosis by a novel small-molecule Stat3 inhibitor.* Blood, 2011. **117**(21): p. 5701-9.
320. Sancho, M., et al., *Understanding MCL1: from cellular function and regulation to pharmacological inhibition.* FEBS J, 2022. **289**(20): p. 6209-6234.
321. Beroukhim, R., et al., *The landscape of somatic copy-number alteration across human cancers.* Nature, 2010. **463**(7283): p. 899-905.
322. Ortiz, B., et al., *Loss of the tyrosine phosphatase PTPRD leads to aberrant STAT3 activation and promotes gliomagenesis.* Proc Natl Acad Sci U S A, 2014. **111**(22): p. 8149-54.
323. Leclerc, G.J., G.M. Leclerc, and J.C. Barredo, *Real-time RT-PCR analysis of mRNA decay: half-life of Beta-actin mRNA in human leukemia CCRF-CEM and Nalm-6 cell lines.* Cancer Cell Int, 2002. **2**(1): p. 1.
324. Sablina, A.A., et al., *The antioxidant function of the p53 tumor suppressor.* Nat Med, 2005. **11**(12): p. 1306-13.
325. Lee, J.H., et al., *Maintenance of metabolic homeostasis by Sestrin2 and Sestrin3.* Cell Metab, 2012. **16**(3): p. 311-21.

326. Bae, S.H., et al., *Sestrins activate Nrf2 by promoting p62-dependent autophagic degradation of Keap1 and prevent oxidative liver damage.* Cell Metab, 2013. **17**(1): p. 73-84.
327. Umemura, A., et al., *p62, Upregulated during Preneoplasia, Induces Hepatocellular Carcinogenesis by Maintaining Survival of Stressed HCC-Initiating Cells.* Cancer Cell, 2016. **29**(6): p. 935-948.
328. Lundberg, A.S. and R.A. Weinberg, *Functional inactivation of the retinoblastoma protein requires sequential modification by at least two distinct cyclin-cdk complexes.* Mol Cell Biol, 1998. **18**(2): p. 753-61.
329. Budanov, A.V., et al., *Identification of a novel stress-responsive gene Hi95 involved in regulation of cell viability.* Oncogene, 2002. **21**(39): p. 6017-31.
330. Tashiro, E., A. Tsuchiya, and M. Imoto, *Functions of cyclin D1 as an oncogene and regulation of cyclin D1 expression.* Cancer Sci, 2007. **98**(5): p. 629-35.
331. Martindale, J.L. and N.J. Holbrook, *Cellular response to oxidative stress: signaling for suicide and survival.* J Cell Physiol, 2002. **192**(1): p. 1-15.
332. Coppo, P., et al., *BCR-ABL activates STAT3 via JAK and MEK pathways in human cells.* Br J Haematol, 2006. **134**(2): p. 171-9.
333. Huynh, J., et al., *The JAK/STAT3 axis: A comprehensive drug target for solid malignancies.* Semin Cancer Biol, 2017. **45**: p. 13-22.
334. Peyser, N.D., et al., *Loss-of-Function PTPRD Mutations Lead to Increased STAT3 Activation and Sensitivity to STAT3 Inhibition in Head and Neck Cancer.* PLoS One, 2015. **10**(8): p. e0135750.
335. Chan, T.A. and A. Heguy, *The protein tyrosine phosphatase receptor D, a broadly inactivated tumor suppressor regulating STAT function.* Cell Cycle, 2009. **8**(19): p. 3063-4.
336. Lin, Y., et al., *Protein tyrosine phosphatase receptor type D gene promotes radiosensitivity via STAT3 dephosphorylation in nasopharyngeal carcinoma.* Oncogene, 2021. **40**(17): p. 3101-3117.
337. Meng, Q., et al., *Protein tyrosine phosphatase receptor type delta (PTPRD) suppresses the expression of PD-L1 in human hepatocellular carcinoma by down-regulating STAT3.* Transl Cancer Res, 2020. **9**(9): p. 5574-5584.
338. Ashrafizadeh, M., et al., *Dual relationship between long non-coding RNAs and STAT3 signaling in different cancers: New insight to proliferation and metastasis.* Life Sci, 2021. **270**: p. 119006.
339. Zhu, S., et al., *PTPLAD2 is a tumor suppressor in esophageal squamous cell carcinogenesis.* FEBS Lett, 2014. **588**(6): p. 981-9.
340. Saferali, A., et al., *Immunomodulatory function of the cystic fibrosis modifier gene BPIFA1.* PLoS One, 2020. **15**(1): p. e0227067.
341. Kovaleva, I.E., et al., *Mitochondrial localization of SESN2.* PLoS One, 2020. **In press**.
342. Tomasovic, A., et al., *Sestrin 2 protein regulates platelet-derived growth factor receptor beta (Pdgfrbeta) expression by modulating proteasomal and Nrf2 transcription factor functions.* J Biol Chem, 2015. **290**(15): p. 9738-52.
343. Singh, A., et al., *Dysfunctional KEAP1-NRF2 interaction in non-small-cell lung cancer.* PLoS Med, 2006. **3**(10): p. e420.
344. Shih, P.C. and K.C. Mei, *Role of STAT3 signaling transduction pathways in cancer stem cell-associated chemoresistance.* Drug Discov Today, 2021. **26**(6): p. 1450-1458.
345. Spitzner, M., et al., *STAT3: A Novel Molecular Mediator of Resistance to Chemoradiotherapy.* Cancers (Basel), 2014. **6**(4): p. 1986-2011.
346. Morelli, A.P., et al., *STAT3 contributes to cisplatin resistance, modulating EMT markers, and the mTOR signaling in lung adenocarcinoma.* Neoplasia, 2021. **23**(10): p. 1048-1058.
347. Rebe, C. and F. Ghiringhelli, *STAT3, a Master Regulator of Anti-Tumor Immune Response.* Cancers (Basel), 2019. **11**(9).
348. Liu, G.Y. and D.M. Sabatini, *mTOR at the nexus of nutrition, growth, ageing and disease.* Nat Rev Mol Cell Biol, 2020.

349. Alas, S. and B. Bonavida, *Inhibition of constitutive STAT3 activity sensitizes resistant non-Hodgkin's lymphoma and multiple myeloma to chemotherapeutic drug-mediated apoptosis.* Clin Cancer Res, 2003. **9**(1): p. 316-26.
350. Huynh, J., et al., *Therapeutically exploiting STAT3 activity in cancer - using tissue repair as a road map.* Nat Rev Cancer, 2019. **19**(2): p. 82-96.
351. Saxton, R.A., et al., *Structural basis for leucine sensing by the Sestrin2-mTORC1 pathway.* Science, 2016. **351**(6268): p. 53-8.
352. Kim, D.I., et al., *An improved smaller biotin ligase for BioID proximity labeling.* Molecular Biology of the Cell, 2016. **27**(8): p. 1188-1196.
353. Cronan, J.E., *Targeted and proximity-dependent promiscuous protein biotinylation by a mutant Escherichia coli biotin protein ligase.* The Journal of Nutritional Biochemistry, 2005. **16**(7): p. 416-418.
354. Queiroz, E.A.I.F., et al., *Metformin Induces Apoptosis and Cell Cycle Arrest Mediated by Oxidative Stress, AMPK and FOXO3a in MCF-7 Breast Cancer Cells.* PLOS ONE, 2014. **9**(5): p. e98207.
355. Kim, K.H., et al., *Metformin-induced inhibition of the mitochondrial respiratory chain increases FGF21 expression via ATF4 activation.* Biochemical and Biophysical Research Communications, 2013. **440**(1): p. 76-81.
356. Lambert, J.M.R., et al., *PRIMA-1 Reactivates Mutant p53 by Covalent Binding to the Core Domain.* Cancer Cell, 2009. **15**(5): p. 376-388.